Valorization of waste biomass derived chemicals via supercritical water hydrolysis and continuous flow ozonolysis

by

Sphurti Prakash Kulkarni
20EE18J26016

A thesis submitted to the
Academy of Scientific & Innovative Research
for the award of the degree of
DOCTOR OF PHILOSOPHY
in
Engineering

Under the supervision of
Dr. Amol A. Kulkarni & Dr. Sunil S. Joshi

CSIR-National Chemical Laboratory, Pune.

Academy of Scientific and Innovative Research
AcSIR Headquarters, CSIR-HRDC campus
Sector 19, Kamla Nehru Nagar,
Ghaziabad, U.P.–201 002, India
July-2023

CERTIFICATE

This is to certify that the work incorporated in this Ph.D. thesis entitled "*Valorization of waste derived chemicals via supercritical water hydrolysis and continuous flow ozonolysis*" submitted by *Ms. Sphurti Prakash Kulkarni* to Academy of Scientific and Innovative Research (AcSIR) in fulfillment of the requirements for the award of the Degree of **Doctor of Philosophy** *in* **Engineering**, embodies original research work under our guidance. We further certify that this work has not been submitted to any other university or institution in part or full for the award of any degree or diploma. Research material obtained from other sources has been duly acknowledged in the thesis. Any text, illustration, table etc., used in the thesis from other sources, have been duly cited and acknowledged.

It is also certified that this work done by the student, under our supervision, is plagiarism free.
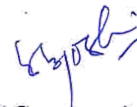
(Student)
Ms. Sphurti P. Kulkarni,
CEPD Division,
CSIR-NCL, Pune

(Supervisor)
Dr. Amol A. Kulkarni,
Senior Principal Scientist,
CEPD Division,
CSIR-NCL, Pune

(Co-supervisor)
Dr. Sunil S. Joshi,
Senior Principal Scientist,
CEPD Division,
CSIR-NCL, Pune

Date : 07/07/2023

Place : Pune

STATEMENTS OF ACADEMIC INTEGRITY

I , **Sphurti Prakash Kulkarni** a Ph.D. student of the Academy of Scientific and Innovative Research (AcSIR) with Registration No. **20EE18J26016** hereby undertake that, the thesis entitled "**Valorization of waste biomass derived chemicals via supercritical water hydrolysis and continuous flow ozonolysis**" has been prepared by me and that the document reports original work carried out by me and is free of any plagiarism in compliance with the UGC Regulations on *"Promotion of Academic Integrity and Prevention of Plagiarism in Higher Educational Institutions (2018)"* and the CSIR Guidelines for *"Ethics in Research and in Governance (2020)"*.
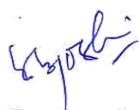
Sphurti Prakash Kulkarni
Date   : 07/07/2023
Place   : Pune

It is hereby certified that the work done by the student, under my/our supervision, is plagiarism-free in accordance with the UGC Regulations on *"Promotion of Academic Integrity and Prevention of Plagiarism in Higher Educational Institutions (2018)"* and the CSIR Guidelines for *"Ethics in Research and in Governance (2020)"*.

Dr. Sunil S. Joshi
Co-supervisor
Date   : 07/07/2023
Place : Pune

Dr. Amol A. Kulkarni
Supervisor
Date   :07/07/2023
Place : Pune

Dedicated to my parents "Aai and Baba"!

Acknowledgement

Ph.D. is not just a degree; it is an experience of lifetime in a very short span of time. It is my deepest pleasure to acknowledge my humble and warm appreciation to each and every one who supported, guided, and encouraged me to during my testing time. I consider myself ultimately fortunate to have got guidance from many experienced persons during my Ph.D.

First and foremost, I express my deepest gratitude to my research supervisors Dr. Amol A. Kulkarni and Dr. Sunil S. Joshi. I am grateful to my guide Dr. Sunil S. Joshi for providing me with the opportunity to work on the difficult problem, for his constant moral support and motivation.

I am extremely grateful to my mentor Dr. Amol A. Kulkarni, without whose support it was impossible for me to accomplish this journey. I consider myself the luckiest to have received his guidance, technical inputs, moral and all the support. The toughest times makes you toughest nuts, true. I will always be thankful to him for showing trust in me, believing in my potential and guiding me through toughest phase of my Ph.D. life. I shall be ever grateful to him for assisting me in returning to the subject of chemical engineering, which I greatly appreciate. I will always strive to attain his practical approach towards problem solving, thinking like a scientist more like a chemical engineer, to imagine and do big things, simplifying complex problems with determination to solve, team work, technical excellence and patience. While it is true that the bar he sets is high and I am truly aware of how short I fall when it comes to his expectations. There will forever be a share for him in the credit for whatever I achieve in my professional life.

I am also grateful to the members of Doctoral Advisory Committee (DAC) members, Dr. GVN Rathna, Dr. Rahul Bhambure and Dr. Nilesh Mali for their sincere comments, suggestions and constant support. I thank all my teachers at NCL Dr. Ahsish Orpe, Dr. Ram Rup Sarkar, Dr. Mugdha Gadgil, Dr. Rahul Bhambure and Dr. Nilesh Mali who once again exposed me to the wonderful subjects of Chemical Engineering. I take this opportunity to thank Mr. Kiran Pandare and other laboratory members including Dr. Reddy's lab members and Dr. Utpal Das's lab members for helping me out in my chemistry and analysis related experimentation and queries.

I am grateful to Dr. Ashwini Kumar Nangia and Dr. Ahish Lele, Directors, CSIR-NCL, Pune for allowing me to carry out my research work in India's most prestigious, well-equipped and biggest chemical laboratory. I am grateful for the GATE-JRF Research Fellowship provided by CSIR-HRDG. I am also thankful to the AcSIR coordination office, Student Academic office, PP-I workshop, and the various sections of NCL establishment for their continued support.

<div style="text-align: right">

Sphurti Prakash Kulkarni
CSIR-National Chemical Laboratory, Pune.

</div>

Synopsis Report

	Synopsis of the Thesis to be submitted to the Academy of Scientific and Innovative Research for Award of the Degree of Doctor of Philosophy in Engineering
Name of the Candidate	Sphurti Prakash Kulkarni
Degree Enrollment No. & Date	20EE18J26016 & 17/09/2019
Laboratory	CSIR-National Chemical Laboratory, Pune.
Title of the Thesis	Valorization of waste biomass derived chemicals via supercritical water hydrolysis and continuous flow ozonolysis
Research Supervisor/ Co-supervisor	Dr. Amol A. Kulkarni / Dr. Sunil S. Joshi

Introduction

With the emergence of the concept of circular bio-economy, the efficient utilisation of wastes and residues has gained immense importance.[1] The conversion of waste biomass, in particular, is an inherent part of circular bio-economy strategies. The majority of biomass waste is generated from various sectors including agricultural waste, forest waste, seafood waste and plant oils, etc. The lignocellulosic biomass with constructing components viz. lignin, cellulose and hemicellulose is being extensively studied.[2] Seafood waste and plant oils are other abundant waste biomass resources generated in several million tons every year, however, surprisingly remain under explored compared to lignocellulosic biomass. The conversion of such materials to value-added chemicals can solve issues of the disposal of these wastes and bring back the material to carbon chain, thus, promoting the bio-economy cycle.

Around 6–8 million tons of seafood waste is generated annually.[3] The properties of these materials such as high thermal and mechanical stability help marine animals sustain the harsh environmental conditions while alive, also pose serious disposal problems when discarded as seafood waste. Chitin is one of the major constituents (20–50 %) of the seafood waste, representing almost 50 % of the total marine biomass. Chitin is a polysaccharide composed of monosaccharide viz. *N*-acetyl-D-glucosamine (NAG). Any process that converts chitin biopolymer to chemicals proceeds via depolymerisation followed by conversion of NAG to the chemicals. On the other hand, NAG is efficiently obtained by acid or enzymatic hydrolysis of chitin. Due to the abundance of NAG along with structural similarity to that of glucose , NAG derived form seafood waste has become a strong candidate for production of valuable chemicals.

Another chemical Cardanol is a major fraction of Cashew Nut Shell Liquid (CNSL), a byproduct of Cashew industry, generated in several million tons every year. [4] Cardanol forms around 60-65 % of technical CNSL with remaining Anacardic acid and Cardol. Cardanol is structurally a phenol with an aliphatic carbon chain (C15) attached at the meta position with one or two double bonds at C7 or C9. Due to the rich structural properties i.e. aromatic group with long aliphatic chains cardanol has emerged as the goldfield of functional monomers for synthesis of various polymers. The synthesis of Liquid Crystal Polymers (LCPs) is one of such atrractive appications of cardanol. As LCPs find tremendous appications such as ultra-high-strength and lightweight fibers and cables, bulletproof vests and as as functional materials in all kinds of optic and optoelectronic devices, their synthesis from biobased resources has gained importance. [5] Cardanol, with structural similarity, is a potential candidate for synthesis of monomers used for synthesis of LCPs naturally.

In this thesis, the valorization of two waste biomass-derived chemicals viz. *N*-acetyl-D-glucosamine (NAG) and caradnol have been investigated via sub- and supercritical water hydrolysis and continuous flow ozonolysis, respectively.

Statement of the problem

The processing of real biomass is complex owing to the complex structures and diverse compositions. The understanding of mechanism of constituent compounds of biomass solves the complexity and assists in the understanding of overall conversion processes of biomass e.g. in order to understand the possible product distribution and kinetics of cellulose hydrolysis it is imperative to understand the hydrolysis of its monomer glucose. Though lignocellulosic biomass is widely explored, plant oils and animal based biomass are underexplored, comparatively. Herein, two such waste biomass derived chemicals NAG and Cardanol, derived from seafood waste and cashew nut shell liquid respectively are investigated for the potential generation of valuable chemicals.

The so far reported methods for conversion of NAG to valuable products employ ionic liquids, metal salts, etc. along with volatile solvents. Inorder to develop a greener process, it is desirable to avoid the usage of toxic chemicals as much as possible. Water, at subcritical (SubCW) and supercritical (SCW) conditions, acts as a tunable reaction medium with tunable solvent properties e.g. low ionic product at SubCW (acidic water) and low dielectric constant at SCW (non-polar water). Owing to these properties and the fact that NAG is fairly soluble in water than any other organic solvent, SubCW and SCW hydrolysis can be a potential greener method for valorization of NAG and chitininuous biomass consequently. However, there is little to no knowledge available on the transformations and challenges associated with the NAG hydrolysis using SubCW and SCW. Hence, the primary objectives were to develop the understanding of hydrolysis of NAG in SubCW and SCW in terms of mechanism, reaction pathways and reaction kinetics in order to produce valuable chemicals from NAG using this method.

In case of the Cardanol valorization, the previous methods of oxidation use conventional catalyst $KMnO_4$ to yield 8-(3-hydroxyphenyl)octanoic acid.[6] The method requires primary protection of phenol by acetylation followed by oxidation and deprotection. Other studies reported the oxidation of cardanol using catalyst Pd/C to yield 8-(3-hydroxyphneyl)octanal at -78 ^{o}C.[7] The methods reported for oxidation of cardanol are multistep and require reductive work up to yield desired monomers. Ozonolysis of cardanol is a simple single step method for synthesis of aldehydes or acids, however, conventional batch ozonolysis is problematic in terms of control and safety associated with ozone. Hence, a continuous flow method is needed for addressing these issues and producing functional monomers from cardanol in a simple manner at mild conditions.

Methodology, results and their interpretation

The thesis is divided in five chapters. ***Chapter 1*** :Introduction; ***Chapter 2***: Valorization of N-acetyl-D-glucosamine (NAG) via subcritical water hydrolysis; ***Chapter 3***: Valorization of NAG via supercritical water (SCW) hydrolysis : Kinetics using flow reactor; ***Chapter 4***: Valorization of Cardanol via continuous flow ozonolysis; ***Chapter 5***:Conclusion and future directions

Chapter 2: Valorization of *N*-acetyl-D-glucosamine (NAG) via subcritical water (SubCW) hydrolysis

The hydrolysis of NAG in SubCW in absence of any oxidative reagent or external catalyst was investigated initially. The SubCW hydrolysis of NAG was studied initially by varying temperature in the range of 70–200 ∘C, reaction time in the range of 60–180 min and pressure in the range of 1-15 MPa using a high pressure and temperature batch reactor.A detailed analysis of product distribution was carried out by using HPLC, GC, GC-MS and HR-MS. It was found that the minimum temperature required for hydrolysis of NAG was 170 ^{o}C; as there was practically no conversion of NAG at temperatures less than 170 ^{o}C but almost 100 % conversion at all temperatures higher than 170 ∘C irrespective of the reaction time. A wide product distribution including products lactic acid, formic acid, acetic acid, glucose, fructose and solids characterized as humins were obtained during non-catalytic hydrolysis of NAG. At 200 ^{o}C and 10 MPa, the yield of acetic acid and humins increased with time from 60 to 180 min, however, the variation in the yields of other products was insignificant. The product distribution is least affected by the pressure in the tested pressure range at subcritical temperatures. Approximately 80 % yield (20 % on mass) of acetic acid was obtained at almost all operating conditions of temperature higher than 170 ^{o}C.
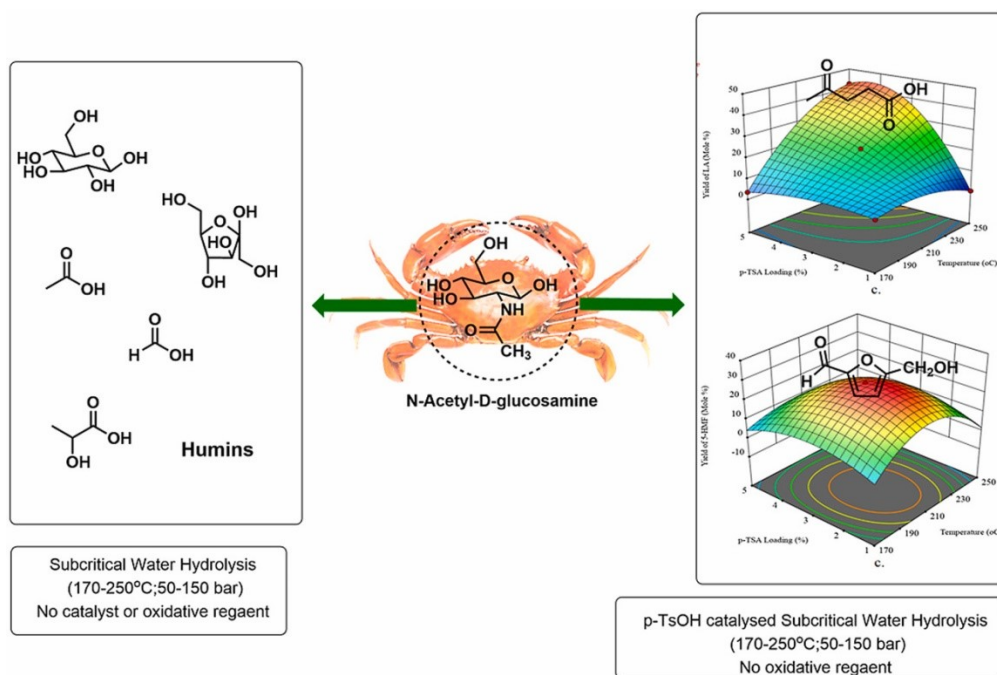
Fig. 1. Subcritical water hydrolysis of NAG

The products of NAG obtained during SubCW hydrolysis could be varied by employing different condtions, as shown in fig. 1. In order to synthesize the valuable chemicals viz. 5-HMF and LA , an acid catalyst *p*-toluenesulfonic acid (*p*-TsOH) was employed during SubCW hydrolysis of NAG. Based on the primary experiments, the product distribution, reaction pathways and ranges of sensitive operating conditions were elucidated. The major products of the reactions were LA, acetic acid, formic acid along with traces of 5-HMF, lactic acid, glucose, etc. A statistical approach of response surface methodology was adopted to optimize the process coditions to obtain maximum yields of 5-HMF and LA. A remarkable yield of 27 % and 57 mol % of 5-HMF and LA were obtained at optimized conditions. The yield of humins was drastically dropped compared to that of non-catalytic reactions. Yield of 5-HMF was favored at high NAG loading and low *p*-TsOH concentration at temperature 210 $^{\circ}$C in time shorter than 30 min. For maximizing the yield of LA, higher temperatures and high *p*-TsOH to NAG ratios should be employed for enough long reaction times.The reaction pathways proposed based on the identified products is shown in fig. 2.
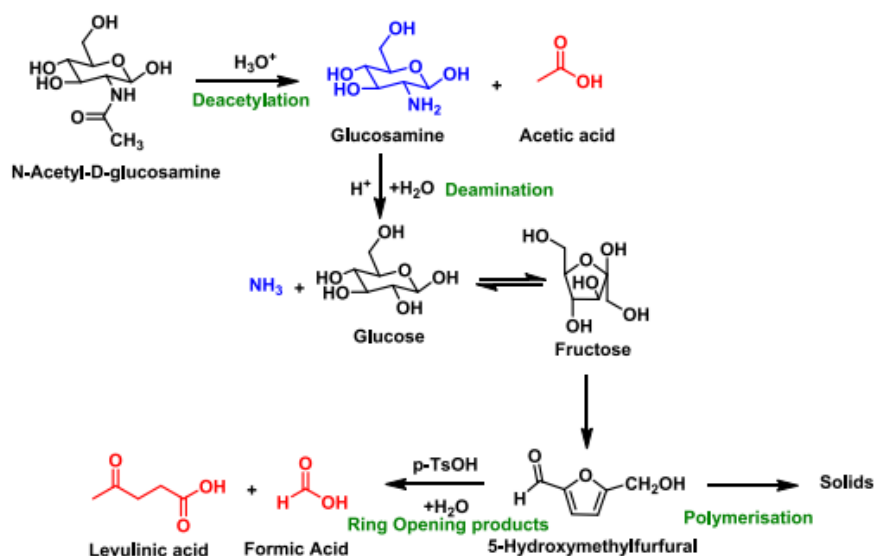
Fig 2. Proposed reaction pathway of *p*-TsOH-catalyzed subcritical water hydrolysis of NAG

Chapter 3: Valorization of NAG via supercritical water (SCW) hydrolysis : Kinetics using flow reactor

As the conversions of NAG in SubCW and SCW were instantaneous, a continuous flow reactor was developed to investigate the immediate transformations NAG undergoes in SubCW and SCW. NAG was almost always consumed completely at all temperatures (200 to 400 $^{\circ}$C at 25 MPa) even at lowest reaction time of 2 s. The products with diverse nature were obtained during hydrolysis of NAG at the tested hydrothermal conditions including solids, gases and majorly aqueous compounds. Aqueous products were always the dominant fractions with minute solids or gases (< 1%). The most commonly identified products of NAG hydrolysis in water at both subcritical (250-350 $^{\circ}$C) and supercritical temperatures (400 $^{\circ}$C) were glycolic acid, formic acid, acetic acid, 5-HMF and acetamide. Other identified products were furfural, pyrazole, 3-pyrdine carboxyldehyde, piperidine, 1-methyl pyrrolidine, pyridine, 2-acetyl pyrazine, piperidine, pyrrole. These products were specific to reaction conditions as were not seen over the entire reaction temperature and residence time ranges. Due to the excessive formation of solids in SubCW (250 $^{\circ}$C and 350 $^{\circ}$C) resulting in the blockage of the reactor, the influence of the residence time was explored mainly in SCW at 400 $^{\circ}$C and 25 MPa, where more products were identified and no solids were formed.
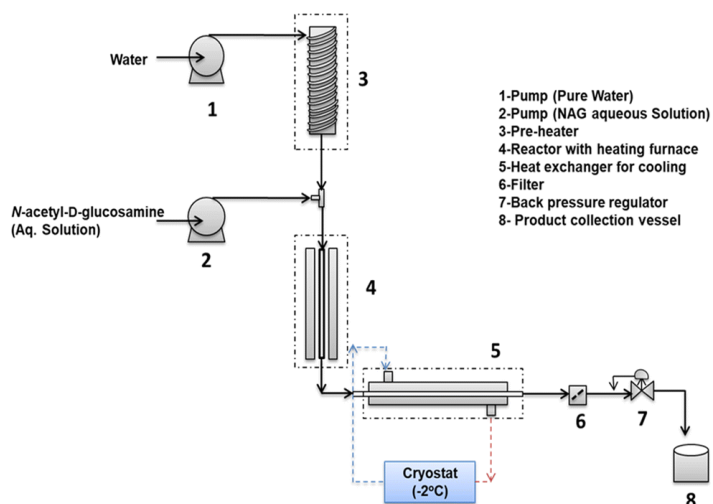
Fig. 3. Schematic of the experimental set-up used for hydrolysis of NAG in subcritical and supercritical water

A simplified kinetic model is developed to predict the yields of acetic acid (AA), glycolic acid(GA) and formic acid (FA).Though the rate constants for the reactions involved in the NAG hydrolysis were influenced by the temperature, the rates do not necessarily increase with temperature. The rates of both AA and GA formation increased with temperature at subcritical conditions (250 and 350 ^{o}C) but dropped in SCW at 400 ^{o}C. As previously reported, formation of AA by deacetylation is acid catalysed reaction whereas the GA is an oxidation product. The reduction in the rate of formation of AA and GA was presumably caused by the reduction in the concentration of the ions H^+ and OH^- catalysing individual glucose hydrolysis reactions forming these stable products in SCW; as the ionic product of water increases with temperature at subcritical temperatures and drops in SCW. The rates of formation of FA and intermediates increased with temperature, on the contrary, formation of decomposition products from both, directly from NAG and from other intermediates decreased with increase in the temperature. This simplified model accurately predicts the different product concentrations obtained at different temperatures (250 ^{o}C, 350 ^{o}C and 400 ^{o}C) at constant pressure of 25 MPa. Complexity of the reaction network and number of possible reaction paths under highly ionic conditions makes this process extremely fast, which does not allow monitoring the reaction under real conditions at such small time scales. The model helps to understand the same to some extent in a systematic manner.

Chapter 4: Valorization of Cardanol via continuous flow ozonolysis

The ozonolysis of caradnol is a simple and single stage oxidation technique to synthsize desired aldehyde 8-(3-hydroxyphenyl)octanal (HPOA). The primary investigation of ozonolysis of cardanol to check the feasibility for synthesis was carried out using semi-batch reactor. The products were characterized by NMR and GC-MS. The conditions were optimized and it was found that the 5 min was enough time for HPOA synthesis at 0 ^{o}C. The longer times reduced selectivity and resulted in generation of waxy compounds. It was also seen that a control over contact time is required to utilize ozone efficiently and avoid further degaradation of phenolic moiety in caradnol.

1. Liquid pump (Cardanol Solution)
2. Ozone Generator
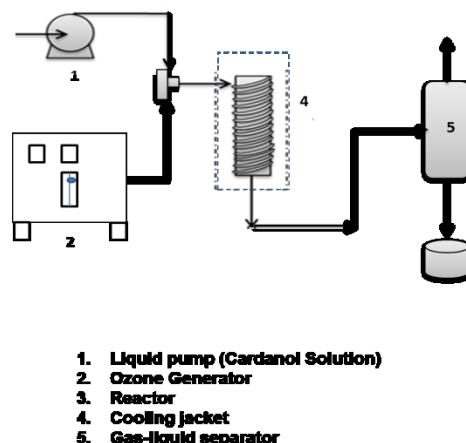3. Reactor
4. Cooling Jacket
5. Gas-liquid separator

Fig. 4. Schematic of the experimental set-up used for continuous flow ozonolysis of Cardanol

The ozonolysis of cardanol was carried out in a continuous manner by using a helical coil reactor for improved control and safety, using set up shown in fig 4. The major identified products were HPOA and heptanal. Around 33-40 % yield of HPOA was obtained at 0 $^{\circ}$C in 9 s at 54.3 % conversion of cardanol. The other products included 8-(3-hydroxyphenyl)octanoic acid, heptanoic acid and phenolic derivatives. The yield of aldehydes increased with temperature and time upto 9-10 s and dropped further.As high gas to liquid ratios were employed, high mass transfer rates were obtained. The overall volumetric mass transfer coefficient of the helical coil reactor, measured by using dissolved oxygen method, was in the range of 0.05 to 6 s^{-1}.The mean residence times at various gas and liquid flow rates were estimated by using residence time distribution.The conversion of cardanol increased with temperature in the tested range of temperatures (-10 to 20 $^{\circ}$C) and also with the increase in ozone to cardanol ratio. The complete conversion of cardanol was obtained at ratio of 2. Liquid residence time had significant influence on yield of HPOA as at higher liquid flowartes (short residence times) the yields were higher, but at low flowrates the yield dropped, which is attributed to the further oxidation of HPOA to acids. Owing to high mass transfer rates, a simple kinetic model was developed by considering reactions in liquid phase, governing the formation of aldehydes.The predictions show good agreement with the experimental yields of aldehydes and cardanol conversion at various temperatures.

Conclusions

Concluding the results of NAG valorization by SubCW hydrolysis it was found that the various value added chemicals can be synthesized via SubCW and SCW hydrolysis. The value-added chemicals 5-HMF and LA were selectively produced by employing a catalyst that significantly suppresses humin formation. SCW hydrolysis of NAG using a flow reactor demonstrated that NAG can be transformed to various compounds with control over product distribution. The analysis of complete products is needed to develop more understanding and a detailed kinetic model. The issues such as myriad product formation during NAG

hydrolysis by SubCW and SCW, the instantaneous transformations of NAG (difficult to control), the solid formation during hydrolysis and costs must be addressed for further development.

A simple and safe synthesis of functional monomers by ozonolysis of cardanol using a flow reactor was demonstrated. However, the efficient utilization of ozone and enhancement of selectivity still remains challenging.

In this chapter the major findings, insights generated and future directions are discussed.

References

1.   Ubando, A. T., Felix, C. B. & Chen, W. H. Biorefineries in circular bioeconomy: A comprehensive review. *Bioresour. Technol.* **299**, (2020).

2.   Haq, I. U. *et al.* Advances in valorization of lignocellulosic biomass towards energy generation. *Catalysts* **11**, 1–26 (2021).

3.   Yan, N. & Chen, X. Don't waste seafood waste: Turning cast-off shells into nitrogen-rich chemicals would benefit economies and the environment. *Nature* **524**, 155–157 (2015).

4.   Buckner, C. A. *et al.* Cashew Nut Shell Oil — A Renewable and Reliable Petrochemical Feedstock. *Intech* **11**, 13 (2016).

5.   Liu, D. & Broer, D. J. Liquid crystal polymer networks: Preparation, properties, and applications of films with patterned molecular alignment. *Langmuir* **30**, 13499–13509 (2014).

6.   C. K. S. Pillai, D. C. S. and A. S. Therrnotropic liquid crystalline copolyester based on 8-(3-hydroxyphenyl) octanoic acid and p-hydroxybenzoic acid C. *Polym. Commun. Guildf.* **27**, 2–5 (1986).

7.   Graham, M. B. & Tyman, J. H. P. Ozonization of phenols from Anacardium occidentale (cashew). *JAOCS, J. Am. Oil Chem. Soc.* **79**, 725–732 (2002).

Publications

1. Kulkarni, S. P., Dure, S. N., Joshi, S. S., Pandare, K. V., & Mali, N. A. (2022). Subcritical water hydrolysis of *N*-acetyl-D-glucosamine: Hydrolysis mechanism, reaction pathways and optimization for selective production of 5-HMF and levulinic acid. *Carbohydrate Research*, *516*, 108560.DOI: 10.1016/j.carres.2022.108560

2. Kulkarni, S. P., Joshi, S. S., & Kulkarni, A. A. (2023). Reaction pathways and kinetics of *N*-acetyl-D-glucosamine hydrolysis in sub-and supercritical water. *Reaction Chemistry & Engineering*. DOI: 10.1039/d3re00046j

Sphurti Prakash Kulkarni

Student Name and signature

Dr. Amol A. Kulkarni

Guide Name and Signature

Dr. Sunil S. Joshi

Co-guide Name and Signature

Table of contents

List of Figures

List of Tables

Chapter 1

Introduction

Circular Bio-economy

1.1 General Introduction

The current world population is around 8 billion people which are expected to reach to 10 billion by 2050.[1] With this explosive increase in world population, the energy demand is also expected to increase exponentially. Currently, society's demand of energy, chemicals and materials is largely met by deriving energy from fossil resources i.e. oil, gas and coal. Based on the modified Klass model,[2] it is estimated that the timelines for the depletion of fossil fuel reserves of oil, coal and gas are approximately 35, 107 and 37 years, respectively. The another global concern is the alarming levels of CO_2 emissions. Following a decline in 2020 owing to pandemic restrictions, CO_2 emission levels again increased by 4.8 % in 2021. If the current trend follows, the earth's total carbon budget will be consumed completely in 9.5 years.[3] Hence, some urgent actions need to be taken to tackle the challenges of reducing dependence from rapidly depleting fossil resources and increasing CO_2 emissions to preserve the earth and the eco-system. A solution to these problems lies in the scrutiny of current energy infrastructure. The traditional linear model of production and consumption relies on finite energy resources and generates large amounts of waste. In stark contrast to this, an economy paradigm which is circular in nature and utilizes renewable bio-based resources is one of the most promising endeavors to tackle environmental challenges and generate energy in a sustainable fashion.[4] The circular bio-economy (CBE) has become an increasingly important concept in recent years as a way to both address climate change and reduce waste. It aims at using renewable resources and waste to create products that can be reused and recycled, thus creating a closed-loop system of production and consumption.

1.2 Introduction to waste biomass

Every year around 1.2 to 1.3×10^{11} ton of natural resources are consumed generating a massive amount of waste along with it.[5] According to the World Bank's report,[6] with the current trajectory, the global waste generation will increase by 70% from current levels in 2050. With traditional attitude of disposing waste, waste management is a challenging problem, environmentally and financially, however, with promotion of CBE, waste has well defined role as potential renewable feedstock.

Waste biomass is a carbon-rich resource. Any organic matter derived from living and recently living organism can be defined as biomass. As illustrated in figure 1.1, there are numerous sources of waste biomass formation. The major sectors are agricultural waste, food processing waste,

industrial waste, municipal solid waste, animal derived waste, wood residues and sewage waste. Waste can also be separated into lignocellulosic and non-lignocellulosic categories. Waste composed of cellulose, hemicellulose, and lignin is called lignocellulosic waste and is widely available. One of the most researched types of waste biomass is lignocellulosic waste. Lignocellulosic materials have the potential to be transformed into high-value goods including chemicals, biofuels, particularly bioethanol, bio-oil.[5,7–11] For the conversion of lignocellulosic biomass, a variety of conversion technologies are available that use thermal, thermochemical, chemical and biological processes.[10] While lignocellulosic biomass is tremendously studied, non lignocellulosic biomass still remains under explored. The exploration of valorization of food processing wastes, Crustaceans shell waste and cashew nut shell liquid, is discussed in this thesis.

Figure 1.1 Waste biomass from various sources

1.3 Crustaceans shell waste

Every year, millions of tons of waste containing crustacean shells are generated worldwide, creating a serious environmental issue. Not only do this waste end up in landfills and other waste sites, but they also become part of the ocean's micro-plastic (MP) problem as the MP contaminated organs are often discarded as waste. It is estimated that around 4 million tons of crustacean shell waste are generated each year, most of which come from shrimp, crab, and lobster shells. This waste is typically generated through the fishing and aquaculture industries, as well as through the consumption of crustaceans as food. When dumped as waste, the properties of these materials, such as excellent thermal and mechanical resilience, which allow marine creatures to endure the

environment while living, provide significant disposal challenges. Converting this waste into value-added chemicals can address the issue of waste disposal while simultaneously returning the material to the carbon chain, thereby promoting the bio-economy cycle as shown in figure 1.2. Chitin is a significant component (20-50%) of seafood waste, accounting for around half of all marine biomass waste, as shown in figure 1.3. Chitin is a polymer composed of the monosaccharide *N*-acetyl-D-glucosamine (NAG). Any technique that converts chitin biopolymer to chemicals first depolymerizes it before converting it to NAG; nonetheless, NAG can be easily generated through acid or enzymatic hydrolysis of chitin as shown in figure1.5. Hence, NAG represents major fraction of crustaceans shell waste, hence, valorization of NAG becomes significant to valorize crustacean shell waste.
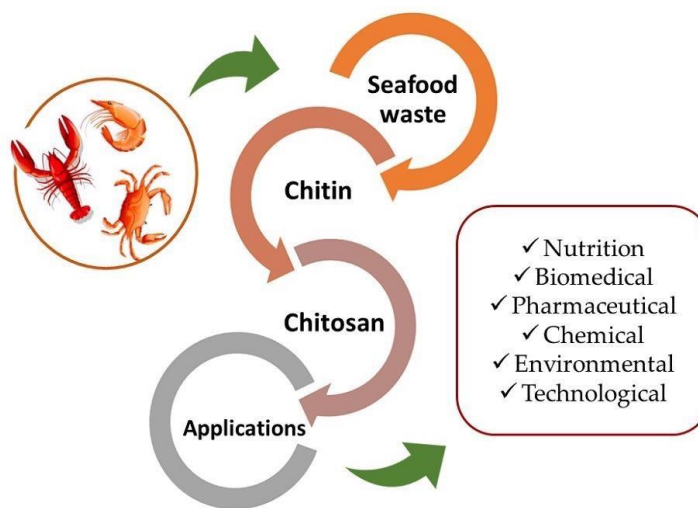
Figure 1.2 Value chain from seafood waste[12]

Crustacean shell waste	Chitin	Calcium Carbonate	Protein
	• 15-40 % • Biopolymer of sugar monomer • Insoluble in common solvents	• 20-50 % • Salt • Pharmaceutical, agricultural and many more applications	• 20-50 % • Biopolymer of amino acids • Pharmaceutical, agricultural and many more applications

Figure 1.3 Composition of crustacean shell waste

1.3.1 *N*-acetyl-D-glucosamine
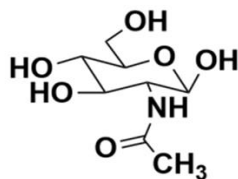
Figure 1.4 Structure of *N*-acetyl-D-glucosamine

Structurally, *N*-acetyl-D-glucosamine (NAG) is a glucose derivative in which an acetyl amino group takes the place of the hydroxyl group at the C2 position of glucose, shown in figure 1.4. There are typically three different methods for producing NAG. The first involves converting a nitrogen-free substrate (such as glucose) to NAG by adding nitrogen-containing functional groups using the Haber process. This approach typically uses a lot of energy and produces a large amount of byproducts. The second method is selecting and modifying microbes in order to use them in fermentation to create NAG. The third method involves directly releasing NAG units from nitrogen-containing material, such as chitin. For the conversion of chitin to NAG, both chemical and enzyme catalysts have been developed.

Recently, NAG has been explored as potential starting material for synthesis of value-added products. Different organic acids, furan derivatives, nitrogen containing compounds were synthesized from NAG. Man Qi and co-workers reported that around 33% and 30% of acetic acid is produced from NAG and chitin respectively using catalyst V_2O_5 under 0.5 MPa pressure of oxygen at 200 ºC in 2-3 h.[13] Various organic acids were synthesized from chitin and NAG using base catalysts, among which $Ba(OH)_2$ showed best results at moderate oxygen pressure by Jingwei Wu and group. Though a total yield of organic acids was 53.1 %, the yield of acetic acid obtained was as low as 16%.[14] The platform chemicals 5-Hydroxymethylfurfural (5-HMF) and Levulinic Acid (LA) are listed as the top ten molecules derived from biomass with versatility and ability to bridge the gap between petroleum based processes and bio-based processes.[15] Recently, the metal salt catalysts $FeCl_2$, $ZnCl_2$ etc. have been explored for the production of 5-HMF and LA from NAG or chitin along with using various volatile organic solvents.[16] Among the various combinations of different dipolar aprotic solvents with water, DMSO-Water favored the 5-HMF formation where DMSO promoted the breaking of intra-molecular hydrogen bonding of water molecules and thus pushing reaction towards formation of 5-HMF as reported by Yu et al.[17] Y. Wang et al.[16] used concentrated $ZnCl_2$ aqueous solution for conversion of chitin biomass to 5-HMF along with the

co-catalysts. Recently, Wuxin Hou and co-workers[18] reported the production of LA from chitin using ionic liquids (ILs). At 180 °C, the 56.7% yield of LA was obtained from chitin using ([C$_3$SO$_3$Hmim]HSO$_4$) in 5 h. The LA yield increased with the acidity of IL, therefore, acid catalyst has essential role in the formation of LA from chitin. Zang et al.[19] showed that ionic liquid [Hmim] [HSO$_4$] effectively catalyzed the conversion of NAG to 5-HMF in a DMSO-Water mixture. The cation [Hmim] promotes the NAG conversion whereas the anion [HSO$_4$] selectively catalyzes the conversion to 5-HMF. Though the ILs gave promising yields, their intricate and expensive synthesis procedures are main challenges for the practical use of ILs for large scale. [20] A wide product distribution obtained from NAG by various treatments is shown in figure 1.6. The methods reported so far use volatile solvents and toxic catalysts for the synthesis of valuable chemicals from NAG which hinders the development of a complete green process. Pyrolysis or hydrolysis in presence of ammonia gives nitrogen containing compounds including Pyrrole, Pyrrolidine, Pyrazole and their derivatives.[21,22] Only replacing the feedstock does not ensure an ecological process, the process itself should consider the greener solvent and catalysts for a sustainable production. In this thesis, water, at subcritical and supercritical conditions, is explored as a greener medium for synthesis of value added chemicals from NAG.
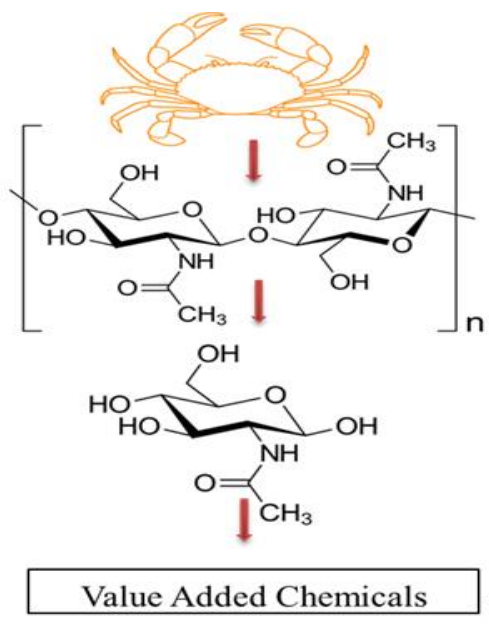
Figure 1.5 Chitinous biomass to value added products
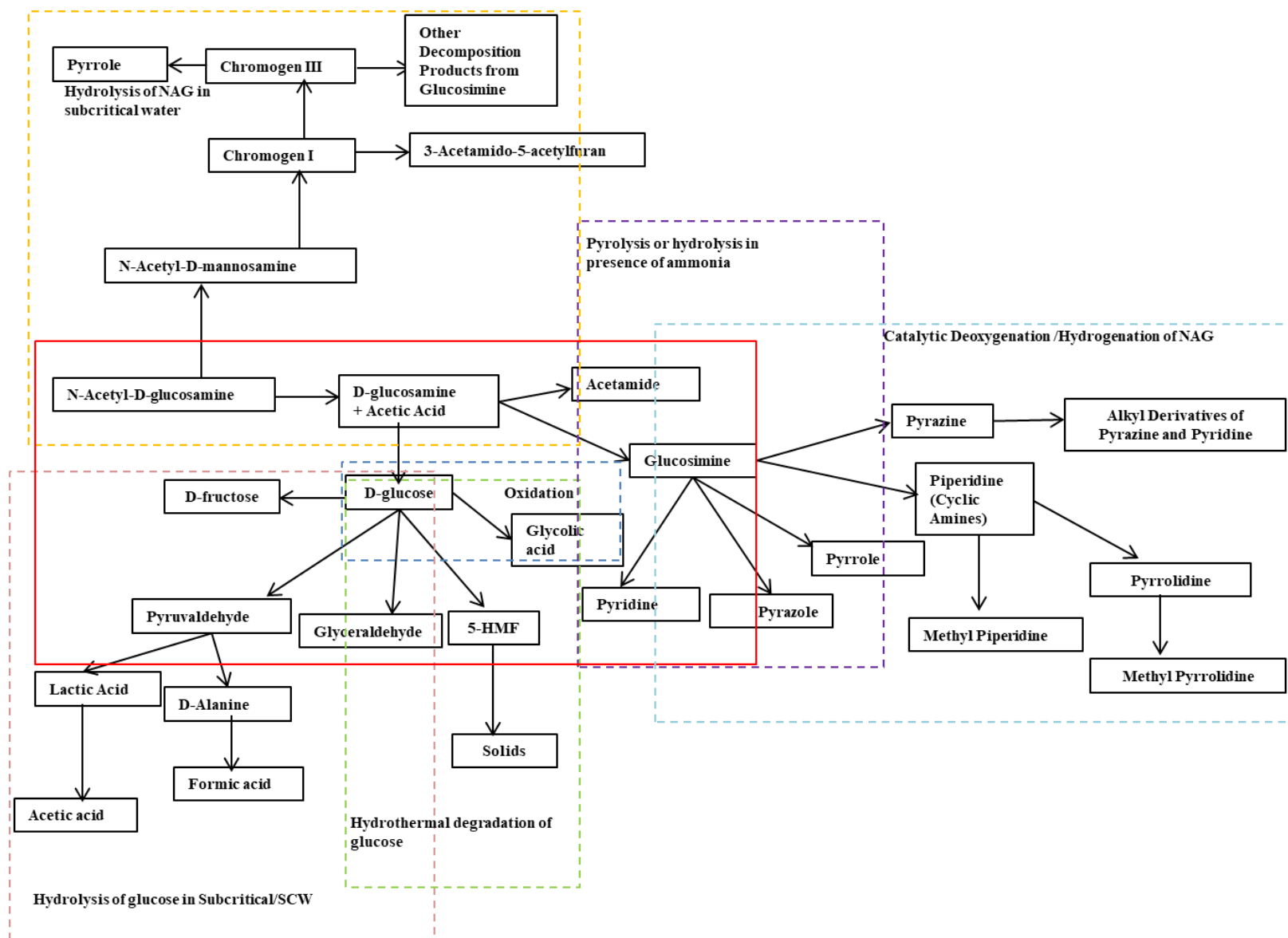
Figure 1.6 Various transformations of NAG and reported product distribution [21–31]
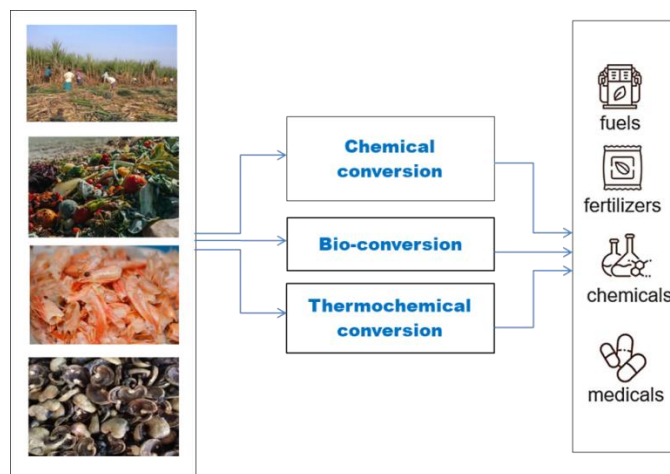
Figure 1.7 Common routes for waste conversion to value added chemicals

1.4 Cashew nut shell liquid (CNSL)

The cashew tree (*Anacardium occidentale*) is indigenous to many countries. The Amazon basin, Brazil, India, Tanzania, and Srilanka few countries producing cashews at large. While cashew apple is served as the food, the nut that covers the cashew apple is discarded as waste. An oil obtained from this waste i.e. cashew nutshell liquid (CNSL) has emerged as a potential feedstock.[32,33] A variety of phenolic substances with aliphatic side chains, including 70% anacardic acid, 5 % cardanol, and 18 % cardol, make up natural CNSL, shown in figure 1.8. Hot oil process, solvent extraction, mechanical extraction, vacuum distillation, or supercritical fluids procedures are some of the ways to extract CNSL.[34]

1.4.1 Cardanol

Cardanol is a major component of CNSL. Around 1 million MT of cardanol is generated every year.[35] Structurally, Cardanol is a phenolic ring with hydroxyl group and C15 carbon change. This structural attribute makes cardanol an interesting feedstock for synthesis of various value-added products which can be synthesized either by functionalization of phenolic ring, hydroxyl group or unsaturated carbon in alkyl chain. Different diacids, dialdehydes, diamines, diols, diacylhydrazide, etc. can be synthesized from cardanol, which on condensation produces polymers with polyamides, polymimides, polyoxadiazoles, etc.[36]

Cardanol–formaldehyde resins produced by polymerization of cardanol are used as protective varnishes in food industry.[37] Various surfactants are prepared from cardanol by sulphonation of cardanol using sulfuric acid. [38] A number of epoxy resins are produced by co-polymerization of

cardanol used as auto primers, potting and encapsulation of electrical and electronic components, electrical laminates and protective coating materials.[39,40] Efficient (means?) plasticizers were synthesized by derivatizing cardanol added to PVC for improving its properties. Lubricating oil additives i.e. antioxidants are produced by preparing metal salts of cardanol thiophosphate and sulphonated ethers following hydrogenation of cardanol.[41]

Flexible thermoset polymers can also be obtained from the monomers synthesized by base catalyzed reactions of cardanol.[42] The oxygenated monomers are one of the simplest yet valuable monomers that can be synthesized from cardanol. Potential monomers for the manufacture of liquid crystal polymers include 8-(3-hydroxyphenyl) octanal or 8-(3-hydroxyphenyl) octanoic acid (HPOAc), which are generated by the oxidation of cardanol. Liquid crystal polymers are high performance polymers with expanding global market applications in electrical and electronic devices, telecommunication, fibre optics, and optical storage devices. Chapter 3 of this thesis discusses oxidation of cardanol for synthesis of monomers in batch and continuous flow mode.

C$_{15}$H$_{31-n}$ =

1-4 %

30-35 %

15-20 %

40-50 %

n= 0; fully saturated alkyl chain
1; unsaturated alkyl chain with double bond at C$_8$
2; unsaturated alkyl chain with double bond at C$_8$ and C$_{11}$
3; unsaturated alkyl chain with double bond at C$_8$, C$_{11}$ and C$_{14}$
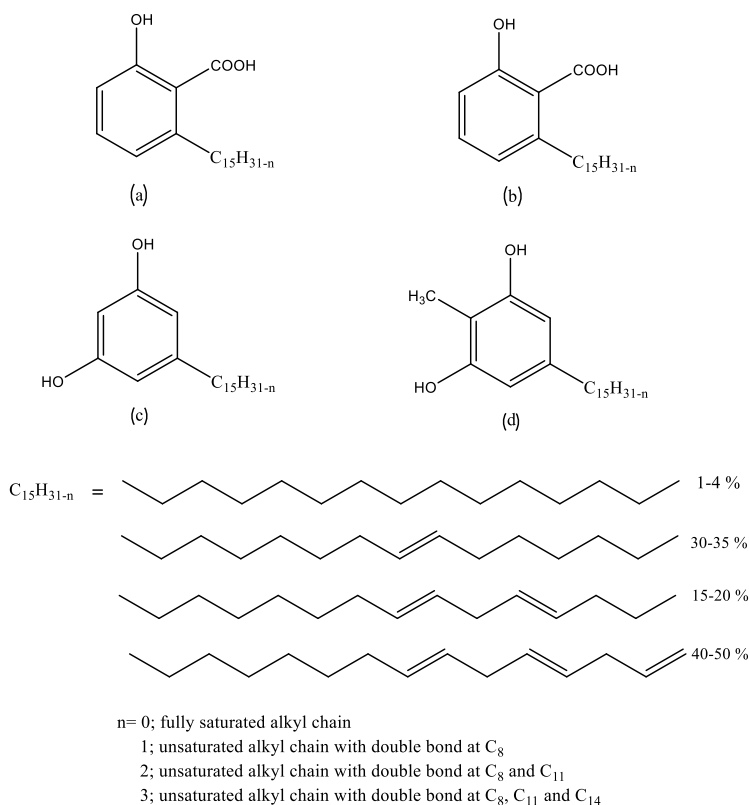
Figure 1.8 Composition of CNSL (a) Anacardic acid (b) Cardanol (c) Cardol (d) 2-methyl cardol

1.5 Techniques for biomass valorization

There are numerous techniques to valorize biomass majorly classified as biological, chemical and thermochemical or hydrothermal methods, shown in figure 1.7. The selection of method always depends on the composition and nature of biomass. Thermochemical or hydrothermal methods are suitable to recalcitrant biomass processing, while, chemical and biological methods are appropriate for biomass which is easily degradable.[43] While any one technique is scarcely proven to be efficient, it is always an integration of techniques that enhances process efficiency.[44] Pretreatment or direct treatment, the methods broadly can be classified as biological, thermochemical, hydrothermal and chemical as discussed further.

1.5.1 Biological methods

Various biological methods including enzymatic hydrolysis, anaerobic digestion, or composting and fermentation, etc. are employed for valorization of biomass. Aerobic and anaerobic digestion is generally employed for bio-methane production from lignocellulosic biomass, while the targeted

product is gaseous fuel, the efficiency achieved from waste biomass through aerobic or anaerobic digestion is low.[45] Another technique used for producing bioenergy from waste is fermentation. Utilizing yeast or bacteria, this technique uses microorganisms to break down organic materials. The end products include biofuel or chemicals, which can be utilized as an energy source or as a fuel for vehicles. Lactic acid is the prime product obtained by fermentation of lignocellulosic biomass from sugars.[46] Hydrolysis of biomass for separation and synthesis of constituent monomers using enzymes is the most simple but sensitive method. Enzymatic hydrolysis as pretreatment enhances material treatability and yield of products consequently. Enzymatic hydrolysis of waste biomass is often employed to produce second generation bio-ethanol. Pretreatment or hydrolysis, development of enzymatic process is limited by high cost of enzymes and sensitivity of process to process conditions.[46]

1.5.2 Thermochemical methods

Thermochemical methods for biomass valorization are majorly classified as dry method and wet method.[47] Dry thermochemical methods involve pyrolysis, gasification and carbonization in absence of air and water. The aim of these methods is to produce fuels such as bio-fuel, bio-char and synthesis gas, etc. Based on the temperature and heating rate, dry thermochemical methods are classified as pyrolysis (slow fast pyrolysis and flash pyrolysis), torrefaction, gasification etc. as shown in figure 1.11a. Pyrolysis and torrefaction are similar methods involving biomass heating in absence of air low heating rate except that pyrolysis takes place at high temperature and torrefaction at low temperature.[48] Gasification occurs when biomass is heated to a very high temperature at a high heating rate producing combustible gases like H_2, CH_4, CO, etc.[49] While these methods are the oldest the high energy requirement, low yields and need of drying biomass are key problems. Alongside, high energy costs, capital cost, and total product costs limit the scalability of these processes for biomass valorization. A classification is shown in figure 1.9.
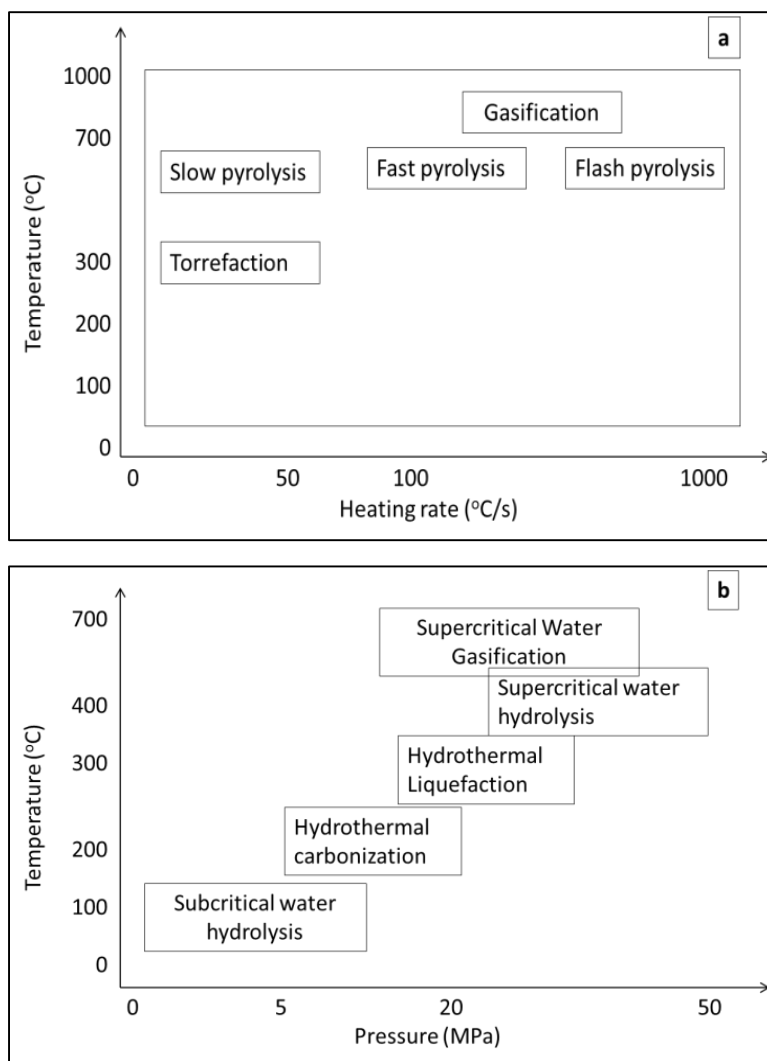
Figure 1.9 Biomass valorization techniques a) Thermochemical processes b) Hydrothermal processes

1.5.3 Hydrothermal methods

Hydrothermal processes are similar to dry thermochemical processes, except that it has many degrees of freedom as solvent water is used to process biomass. Usage of water offers many advantages to a high temperature biomass valorization process like the control over product distribution, precise control over process conditions, elimination of drying step of biomass.[9,50–52] On the basis of temperature and pressure, hydrothermal processes are classified as subcritical water hydrolysis at low temperature and pressure and supercritical water hydrolysis and gasification at higher temperature and pressure. At moderate process temperature and pressure carbonization of biomass and liquefaction occurs. Above critical point of water, biomass is either hydrolyzed or

gasified. The basis of every hydrothermal process is water and its properties that is water at subcritical and supercritical conditions possessing advantageous properties discussed further in detail.

Fundamentals of Sub and Supercritical water as reaction medium for biomass
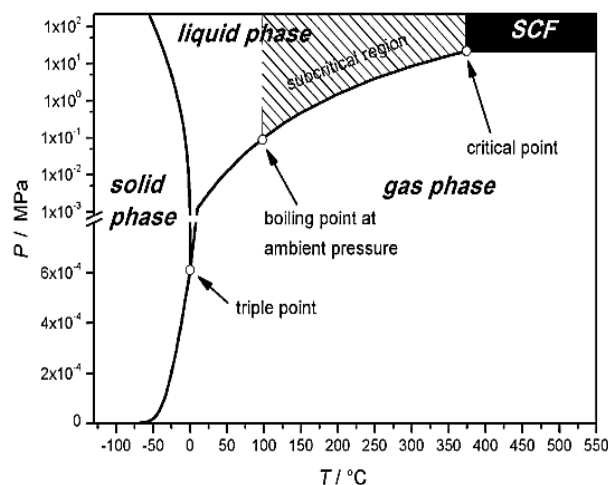
Figure 1.10 Phase diagram of water[53]

Supercritical water (SCW) is a thermodynamic state achieved by simultaneous heating and pressurizing water above its critical temperature ($T_c = 374$°C) and pressure ($P_c = 22$ MPa). Subcritical water (SubCW) is simply the compressed hot water state that is water at temperatures above boiling temperature but below critical temperature at pressure high enough to maintain liquid state of water.[54] At supercritical conditions, water is neither liquid nor gas but possess the thermo-physical properties having values ranging in between to liquid or gas.
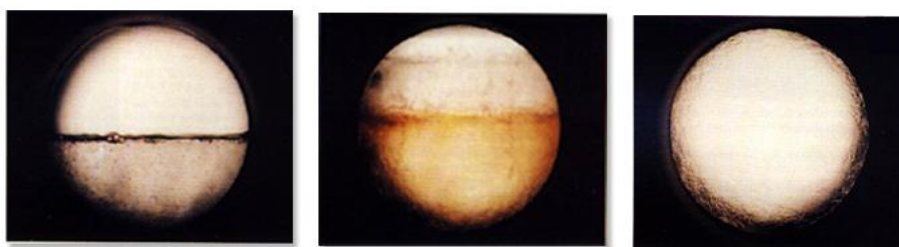
Figure 1.11 Photograph of supercritical CO_2 at normal, subcritical and supercritical conditions (from left to right)[55]

The supercritical state of any fluid is characterized by following attributes

1. *Disappearance of difference between vapor and liquid*

The phases, liquid and vapor, becomes indistinguishable and another plasma like state is attained. At this state, the intermolecular forces of attraction are less than liquid (high T) but more than gases (high P) resulting in a gas and liquid like properties tunable with pressure and temperature.

Table 1.1 Thermo-physical properties of water[55]

Phase	Normal Water	Sub-critical water	Supercritical water		Superheated water
T(^{o}C)	25	250	400	400	400
P(MPa)	0.1	5	25	50	0.1
ρ(g/ml)	0.997	0.8	0.17	0.58	0.0003
ε	78.5	27.1	5.9	10..5	1
pk$_w$	14	11.2	19.4	11.9	-
C$_p$(kJ/kg/K)	4.22	4.86	13	6.8	2.1
η(mPa.s)	0.89	0.11	0.03	0.07	0.02
k(W/m/K)	0.608	0.620	0.160	0.438	0.055
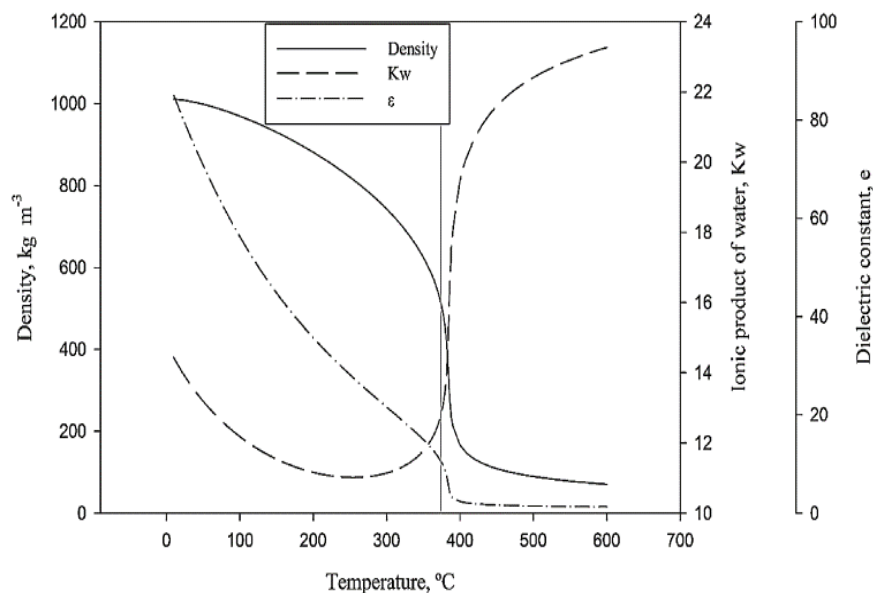
Figure 1.12 Properties of subcritical and supercritical water. Density (kg/m^3) (solid line), dielectric constant (dotted-dashed line), and ionic product of water (pK$_w$) (dashed line)[56]

2. *The divergence of the compressibility*

At supercritical state, fluid achieves infinite compressibility such that the fluid compresses under its own weight.

 3. *Critical Opalescence*

The visual changes in the state of fluid are observed as the meniscus separating fluids disappears, as shown in figure 1.11. This is well explained as the critical opalescence and is attributed to density fluctuations having range comparable wavelength of light, far exceeding molecular dimensions.

The thermo-physical properties of water such as dielectric constant, ionic product, density, viscosity and diffusivity at such conditions are highly dominated by the process temperature and pressure so the desired reaction environment can be maintained by selecting appropriate reaction conditions, as shown in figure 1.12. The dielectric constant and hydrogen bonding of water increases with density and decreases with temperature, hence, high temperature promotes solubility of those solutes in sub- and/or supercritical state that are sparingly or insoluble in ambient water, particularly, bio-polymers like cellulose, lignin, hemicellulose etc. The highest ionic product of water i.e. 10^{-11} is observed at temperatures of around 300 °C, indicating the significant increase in the acidity of water.[56] Water at these thermodynamic conditions is proven to catalyze few reactions involving glucose and glucosamine. Due to these fascinating attributes of SubCW and SCW i.e. improved solvency, tunability of properties and faster reactions, SubCW and SCW has emerged as the potential reaction medium wherein water can act as solvent, catalyst or reactant as well depending on the reaction suitable for processing of biomass with different chemical composition in a greener manner.

1.5.4 Chemical methods

Chemical methods refer to the direct and simple chemical transformations of biomass. Various new solvents and catalysts are emerging for value up-gradation of waste biomass.[57] While ionic liquids and deep eutectic solvents are extensively being explored as solvents and catalyst, conventional homogenous and heterogeneous catalysts still remains the essential for development of efficient processes.[58] Chemical methods are specifically employed to produce chemicals from biomass.[59] Oxidation in this context has gained importance as pretreatment or direct treatment. Ozonolysis is the simplest yet efficient oxidation method for valorization of biomass including

lignin, fats and oils etc. In this context, ozonolysis for biomass pre-treatment or treatment is discussed in next section.
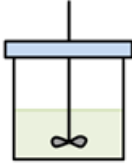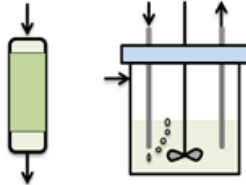
1.6 Ozonolysis of biomass and bio derived chemicals

As pretreatment, Ozonolysis is a well-known method for delignification of lignocellulosic biomass. Ozonation has been proven as an efficient technique in degrading the lignin polymer, but also helps to oxidize carbohydrates concurrently although the rate of reaction with the latter is slower.[60] This increases the accessibility of cellulose and hemicellulose for hydrolysis resulting in higher sugar yields. Cheng et.al.[61] investigated the effect of particle size and moisture content of Maize Stover on the ozonolysis employed to improve the enzymatic digestibility of maize Stover. The ozonolysis treatment increased the glucose yield to 80 % from 18.5 % and around 75 % delignification was achieved at small particle size of 300 mesh with 60 % moisture content. Almomani et. al.[62] employed ozonation as intermediate step to enhance biogas production from animal dung and agricultural waste mixed substrates. It was found that the oxidation of fatty acids formed in first stage improved the methane production and efficiency of anaerobic digestion significantly. Travini et. al.[63] reported the ozonolysis of sugarcane bagasse in a fixed bed reactor. High yields of glucose (41 %) and xylose (52 %) were obtained, however, other inhibitory compounds including xylitol, lactic, formic and acetic acid were detected. Recently, Travaini et al.[64] reviewed the progress of ozonolysis as lignocellulosic biomass pretreatment with emphasis on pathways of ozone –biomass chemical reaction, the compositional and structural changes in the ozonated biomass, the formation of inhibitory products and factors influencing its biofuel production capacity. While a variety of biomass can be treated via this method, several challenges in terms of the ozone utilization and safety prevail.

As synthetic technique, ozonolysis is widely adopted to produce valuable diacids, aldehydes or hydroxyacids from fatty acids derived from renewable vegetable oils.[65] The unsaturated bonds in fatty acids are cleaved leading to formation of ozonide and trioxane which necessitates the additional step of oxidative or reductive up. The ozonolysis of canola oil containing oleic (~62 %), linoleic (~22 %) and α-linolenic (~10 %) acids produced a variety of products including propanal, 1,3-propanedial, hexanal and nonanal.[66] The aldehyde nonanal widely used in perfume industry was synthesized by ozonolysis of canola oil free fatty acid, the ozonolysis resulted in comparable yields of aldehydes to that of commercial hydroforrmylation process.[67] The synthesis

of adhesives from cashew nut shell liquid by ozonolysis was demonstrated by khan et. al. implying need for exploration of ozonolysis for production of commodity chemicals.[68]

Table 1.2 Comparison of reactors for ozonolysis of lignin or ligno-cellulosic biomass

	Batch	Flow-through (Solid bed or gas sparged in liquid)	Continuous
Purpose	Delignification of real biomass	Delignification of real biomass	Synthesis of value-added product from extracted lignin or lignin model compound
Feeding	Manual	Manual (Loading and unloading of solid biomass)	Automatic
Design	Easy	Difficult as reactant and product composition is changing with time	Moderate (More degrees of freedom)
Control	No control	Poor control over ozone concentration profile	Better control over flow of gas and liquid
Real biomass handling	Easy	Moderately easy	Difficult
Mixing	Mechanical stirring	No mechanical stirring (control over gas flow)	Mixing can be enhanced in various ways (Control over gas-liquid flows, flow patterns, reactor geometry)
Efficiency	Moderate	Comparable but depends on ozone profile in the flow-through	Comparable but depends on reactor design
Scalability	Easy but uneconomical	Difficult and uneconomical	Simpler and economical
Safety	Risky (accumulation of ozonides and high pressure ozone may lead to explosion)	Moderately safe	Safer

As pretreatment or as synthetic technique, the major challenges pertinent to development of an effective ozonolysis process are high cost of ozone generation and safety related to unstable nature of ozone and formation of potentially explosive ozonide intermediates.[69,70] A proper process

design aiming at efficient use of ozone and safe handling of compounds can overcome these challenges. Conventional batch reactors are widespread as simple reactors for ozonolysis, however, are certainly a poor choice for such gas-liquid reactions due to requirement of ozone at high pressure and generation of products inside a closed chamber that can lead to accumulation and explosion.[69] Recently, the fixed bed reactor has been employed by many researchers in which ozone gas passes through bed of solid biomass, however, manual loading and unloading, control over gas flow and change in bed length with time makes this type of operation difficult for scale-up.[71] It is now well recognized that continuous flow reactors are advantageous from scalability and safety point of view.[72] The volumes handled at any time in the continuous flow are smaller making it inherently safer. Moreover, the precise control over reaction conditions, mixing and liberty to select the reactor for enhanced performance makes the continuous flow enviable technique for safe and effective ozonolysis. A conceptual comparison of reactors particularly for lignin valorization via ozonolysis is given in table 1.2.
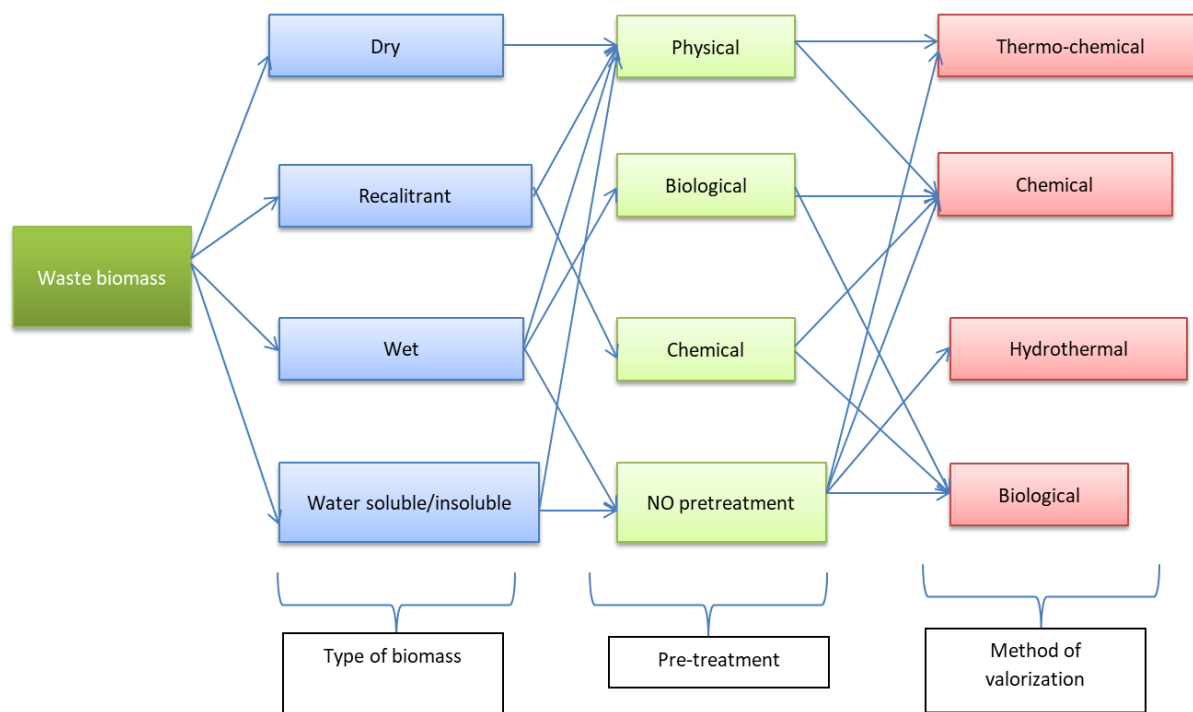
Figure 1.13 Techniques for waste biomass valorization

1.7 Process selection and research need

Out of many valorization techniques being extensively explored, the selection of method always depends on the type of biomass and the desired product. Figure 1.13 illustrates the methods briefly. In this thesis, two waste biomass based molecules were investigated for potential synthesis of chemicals. *N*-acetyl-D-glucosamine represents recalcitrant chitinuous biomass. Its polymers are insoluble in water or any other solvent, however, supercritical water a distinct state of water may have potential to solubilize chitin or similar polymers as demonstrated that for cellulose and lignin. Hence, subcritical and supercritical water can be a greener hydrolysis and valorization technique for chitin valorization. However, during the extensive literature survey it was found that such method is not explored yet. Moreover, there was little to no information available on transformations, mechanism and kinetics of NAG imperative for development of such process. Hence, subcritical water and supercritical water hydrolysis of NAG was selected to explore the potential valorization of NAG and chitin consequently.

Cardanol, on the other hand, compound obtained from cashew nut shell, is a reactive molecule owing to hydroxyl phenolic group and unsaturation in the alkyl chain. Many transformations of cardanol to various value added products mainly via polymerization are reported, however, oxidation is less reported. Moreover, the reported methods for cardanol valorization are scarcely intensified. In this thesis, the development of continuous flow ozonolysis of cardanol was undertaken to valorize cardanol in a more intensified way.

1.4 Research objectives

The work reported in this thesis focuses on the following major aspects:

- Understanding process chemistry and mechanism of hydrolysis of chitin model compound *N*-acetyl-D-glucosamine using subcritical and supercritical water
- Synthesis of value added chemicals from *N*-acetyl-D-glucosamine via subcritical and supercritical water
- Understanding hydrolysis kinetics of *N*-acetyl-D-glucosamine in subcritical and supercritical water
- Development of continuous flow method for ozonolysis of cardanol
- Systematic characterization of reactor and kinetic modelling of cardanol ozonolysis

1.5 Organization of thesis

The thesis is organized into five chapters. A basic introduction to need for waste biomass valorization, waste biomass sources and fundamentals of techniques sub/supercritical water hydrolysis and ozonolysis in the context of biomass conversion are discussed in **chapter 1.**

In **chapter 2**, subcritical water hydrolysis of *N*-acetyl-D-glucosamine (NAG) is described. The transformations NAG undergoes during subcritical water hydrolysis with and without acid catalyst is illustrated in this chapter. A systematic optimization of process conditions to synthesize 5-hydroxymethylfurfural (5-HMF) and Levulinic acid (LA) from NAG is described. The influence of process conditions on yields of 5-HMF and LA are studied using response surface methodology. The reaction pathways and mechanism of NAG hydrolysis in subcritical and supercritical water are devised in **chapter 3.** The process chemistry of NAG and reaction network of several transformations is discussed based on the results of subcritical and supercritical water hydrolysis using a continuous flow reactor. Various approaches for modeling of kinetics of several series and parallel reactions occurring during hydrolysis of NAG are discussed. A kinetic model for acid formation is devised and the unconventional Arrhenius behavior of few reactions is investigated.

In **chapter 4**, ozonolysis of cardanol is investigated. Semi-batch ozonolysis for reaction feasibility and product identification was performed. The batch to continuous flow ozonolysis of cardanol is illustrated. The mass transfer and residence time distribution inside the reactor was investigated. A kinetic model incorporating non-ideality to predict cardanol conversion is developed.

Finally, **chapter 5** is a brief conclusion of this thesis, a summary of challenges and outcomes of the research work and future scope. A list of publications emanating from the research is attached in this thesis.

1.6 References

1   *Ppopulaation Ref. Burau*, 2017.

2   S. Shafiee and E. Topal, *Energy Policy*, 2009, **37**, 181–189.

3   Z. Liu, Z. Deng, S. J. Davis, C. Giron and P. Ciais, *Nat. Rev. Earth Environ.*, 2022, **3**, 217–219.

4   S. Venkata Mohan, S. Dahiya, K. Amulya, R. Katakojwala and T. K. Vanitha, *Bioresour. Technol. Reports*, 2019, **7**, 100277.

5   W. Dessie, X. Luo, M. Wang, L. Feng, Y. Liao, Z. Wang, Z. Yong and Z. Qin, *Appl. Microbiol. Biotechnol.*, 2020, **104**, 4757–4770.

6   S. Goulette, *Proc. Inst. Civ. Eng. Munic. Eng.*, 2000, **139**, 167–169.

7   M. Alherech, S. Omolabake, C. M. Holland, G. E. Klinger, E. L. Hegg and S. S. Stahl, *ACS Cent. Sci.*, 2021, **7**, 1831–1837.

8   K. Alper, K. Tekin, S. Karagöz and A. J. Ragauskas, *Sustain. Energy Fuels*, 2020, **4**, 4390–4414.

9   M. Kumar, A. Olajire Oyedun and A. Kumar, *Renew. Sustain. Energy Rev.*, 2018, **81**, 1742–1770.

10   A. Asghar, S. Sairash, N. Hussain, Z. Baqar, A. Sumrin and M. Bilal, *Biofuels, Bioprod. Biorefining*, 2022, **16**, 1478–1494.

11   S. Maina, V. Kachrimanidou and A. Koutinas, *Curr. Opin. Green Sustain. Chem.*, 2017, **8**, 18–23.

12   B. E. Teixeira-Costa and C. T. Andrade, *Biomolecules*, 2021, **11**, 1–19.

13   M. Qi, X. Chen, H. Zhong, J. Wu and F. Jin, *ACS Sustain. Chem. Eng.*, 2020, **8**, 18661–18670.

14   J. Wu, M. Qi, G. Gozaydln, N. Yan, Y. Gao and X. Chen, *Ind. Eng. Chem. Res.*, 2021, **60**, 3239–3248.

15   T. Werpy and G. Petersen, *Us Nrel*, 2004, Medium: ED; Size: 76 pp. pages.

16   Y. Wang, C. M. Pedersen, T. Deng, Y. Qiao and X. Hou, *Bioresour. Technol.*, , DOI:10.1016/j.biortech.2013.06.024.

17   S. Yu, H. Zang, S. Chen, Y. Jiang, B. Yan and B. Cheng, *Polym. Degrad. Stab.*, 2016, **134**, 105–114.

18   W. Hou, Q. Zhao and L. Liu, *Green Chem.*, 2020, **22**, 62–70.

19   H. Zang, S. Yu, P. Yu, H. Ding, Y. Du, Y. Yang and Y. Zhang, *Carbohydr. Res.*, 2017, **442**, 1–8.

20   G. Cevasco and C. Chiappe, *Green Chem.*, 2014, **16**, 2375–2385.

21   L. Zeng, C. Qin, L. Wang and W. Li, *Carbohydr. Polym.*, 2011, **83**, 1553–1557.

22   Z. X. Xu, J. H. Cheng, Z. X. He, Q. Wang, Y. W. Shao and X. Hu, *Bioresour. Technol.*, 2019, **278**, 311–317.

23   S. Xie, C. Jia, S. S. Go Ong, Z. Wang, M. jun Zhu, Q. Wang, Y. Yang and H. Lin, *iScience*, 2020, **23**, 101096.

24   X. Gao, X. Chen, J. Zhang, W. Guo, F. Jin and N. Yan, *ACS Sustain. Chem. Eng.*, 2016, **4**, 3912–3920.

25   Y. Huang, C. Pathirana, Q. Ye and V. Palaniswamy, *Tetrahedron Lett.*, 2015, **56**, 4516–4519.

26   B. M. Kabyemela, T. Adschiri, R. M. Malaluan and K. Arai, *Ind. Eng. Chem. Res.*, 1999, **38**, 2888–2895.

27   K. Li, C. Zhu, L. Zhang and X. Zhu, *Bioresour. Technol.*, 2016, **209**, 142–147.

28   F. W. Lichtenthaler, *Acc. Chem. Res.*, 2002, **35**, 728–737.

29   M. R. Park, H. S. Kim, S. K. Kim and G. T. Jeong, *Fuel Process. Technol.*, 2018, **172**, 115–124.

30   A. T. Quitain, N. Sato, H. Daimon and K. Fujie, *Ind. Eng. Chem. Res.*, 2001, **40**, 5885–5888.

31   A. L. Weber, *J. Mol. Evol.*, 1985, **21**, 351–355.

32   C. A. Buckner, R. M. Lafrenie, J. A. Dénommée, J. M. Caswell, D. A. Want, G. G. Gan, Y. C. Leong, P. C. Bee, E. Chin, A. K. H. Teh, S. Picco, L. Villegas, F. Tonelli, M. Merlo, J. Rigau, D. Diaz, M. Masuelli, S. Korrapati, P. Kurra, S. Puttugunta, S. Picco, L. Villegas, F. Tonelli, M. Merlo, J. Rigau, D. Diaz, M. Masuelli, M. Tascilar, F. A. de Jong, J. Verweij and R. H. J. Mathijssen, *Intech*, 2016, **11**, 13.

33   2019.

34   D. C. Ike, M. U. Ibezim-Ezeani and O. Akaranta, *Green Chem. Lett. Rev.*, 2021, **14**, 618–631.

35   S. Caillol, *Curr. Opin. Green Sustain. Chem.*, 2018, **14**, 26–32.

36   C. Voirin, S. Caillol, N. V. Sadavarte, B. V. Tawade, B. Boutevin and P. P. Wadgaonkar,

Polym. Chem., 2014, **5**, 3142–3162.

37   W. Guo, X. Wang, J. Huang, X. Mu, W. Cai, L. Song and Y. Hu, *Chem. Eng. J.*, 2021, **423**, 130192.

38   I. Faye, V. Besse, G. David and S. Caillol, *Green Mater.*, 2017, **5**, 144–152.

39   W. J. Lee, S. H. Cha and D. H. Kim, *Polymers (Basel).*, , DOI:10.3390/polym14235205.

40   E. Manarin, F. Corsini, S. Trano, L. Fagiolari, J. Amici, C. Francia, S. Bodoardo, S. Turri, F. Bella and G. Griffini, *ACS Appl. Polym. Mater.*, , DOI:10.1021/acsapm.2c00335.

41   A. Greco and A. Maffezzoli, *Polym. Degrad. Stab.*, 2016, **132**, 213–219.

42   S. Mitra and C. K. S. Pillai, *J. Appl. Polym. Sci.*, 2008, **107**, 778–783.

43   C. Nzeteu, F. Coelho, E. Davis, A. Trego and V. O'Flaherty, *Fermentation*, , DOI:10.3390/fermentation8090445.

44   H. Amiri, M. Aghbashlo, M. Sharma, J. Gaffey, L. Manning, S. M. Moosavi Basri, J. F. Kennedy, V. K. Gupta and M. Tabatabaei, *Nat. Food*, 2022, **3**, 822–828.

45   N. Xu, S. Liu, F. Xin, J. Zhou, H. Jia, J. Xu, M. Jiang and W. Dong, *Front. Bioeng. Biotechnol.*, 2019, **7**, 1–12.

46   Y. Ren, X. Wang, Y. Li, Y. Y. Li and Q. Wang, *Sustain.*, 2022, **14**, 1–18.

47   L. Leng, L. Yang, J. Chen, Y. Hu, H. Li, H. Li, S. Jiang, H. Peng, X. Yuan and H. Huang, *J. Clean. Prod.*, 2021, **294**, 126238.

48   G. Wang, Y. Dai, H. Yang, Q. Xiong, K. Wang, J. Zhou, Y. Li and S. Wang, *Energy and Fuels*, 2020, **34**, 15557–15578.

49   S. Mishra and R. K. Upadhyay, *Mater. Sci. Energy Technol.*, 2021, **4**, 329–340.

50   S. S. Toor, L. Rosendahl and A. Rudolf, *Energy*, 2011, **36**, 2328–2342.

51   H. Di Domenico Ziero, L. S. Buller, A. Mudhoo, L. C. Ampese, S. I. Mussatto and T. F. Carneiro, *J. Environ. Chem. Eng.*, , DOI:10.1016/j.jece.2020.104406.

52   J. A. Okolie, R. Rana, S. Nanda, A. K. Dalai and J. A. Kozinski, *Sustain. Energy Fuels*, 2019, **3**, 578–598.

53   M. Möller, P. Nilges, F. Harnisch and U. Schröder, *ChemSusChem*, 2011, **4**, 566–579.

54   M. Möller, P. Nilges, F. Harnisch and U. Schröder, *ChemSusChem*, 2011, 4, 566–579.

55   D. Bröll, C. Kaul, A. Krämer, P. Krammer, T. Richter, M. Jung, H. Vogel and P. Zehner, *Angew. Chemie - Int. Ed.*, 1999, **38**, 2998–3014.

56   D. A. Cantero, M. Dolores Bermejo and M. José Cocero, *J. Supercrit. Fluids*, 2015, **96**, 21–

35.

57   S. R. Collinson and W. Thielemans, *Coord. Chem. Rev.*, 2010, **254**, 1854–1870.

58   E. S. Morais, M. Costa, M. G. Freire, C. S. R. Freire, A. P. Coutinho and A. J. D. Silvestre,

       .

59   Y. Jiang, X. Wang, Q. Cao and L. Dong, *Chemical Conversion of Biomass to Green Chemicals*, .

60   N. S. Ab Rasid, M. M. Zainol and N. A. S. Amin, in *Refining Biomass Residues for Sustainable Energy and Bioproducts: Technology, Advances, Life Cycle Assessment, and Economics*, Elsevier Inc., 2019, pp. 303–336.

61   C. Li, L. Wang, Z. Chen, Y. Li, R. Wang, X. Luo, G. Cai, Y. Li, Q. Yu and J. Lu, *Bioresour. Technol.*, 2015, **183**, 240–247.

62   F. Almomani, M. Shawaqfah, R. R. Bhosale, A. Kumar and M. A. M. Khraisheh, *Int. Biodeterior. Biodegrad.*, 2017, **119**, 176–187.

63   R. Travaini, M. D. M. Otero, M. Coca, R. Da-Silva and S. Bolado, *Bioresour. Technol.*, 2013, **133**, 332–339.

64   R. Travaini, J. Martín-Juárez, A. Lorenzo-Hernando and S. Bolado-Rodríguez, *Bioresour. Technol.*, 2016, **199**, 2–12.

65   R. G. Kadesch, *Prog. Chem. Fats Other Lipids*, 1963, **6**, 291–312.

66   T. S. Omonov, E. Kharraz and J. M. Curtis, *JAOCS, J. Am. Oil Chem. Soc.*, 2011, **88**, 689–705.

67   T. S. Omonov, E. Kharraz, P. Foley and J. M. Curtis, *RSC Adv.*, 2014, **4**, 53617–53627.

68   2004, 1, 0–4.

69   J. Kula, *Chem. Heal. Saf.*, 1999, **6**, 21–22.

70   S. G. Van Ornum, R. M. Champeau and R. Pariza, *Chem. Rev.*, 2006, **106**, 2990–3001.

71   E. M. Anderson, M. L. Stone, R. Katahira, M. Reed, G. T. Beckham and Y. Román-Leshkov, *Joule*, 2017, **1**, 613–622.

72   M. Movsisyan, E. I. P. Delbeke, J. K. E. T. Berton, C. Battilocchio, S. V. Ley and C. V. Stevens, *Chem. Soc. Rev.*, 2016, **45**, 4892–4928.

Chapter 2

Subcritical water hydrolysis of *N*-acetyl-D-glucosamine
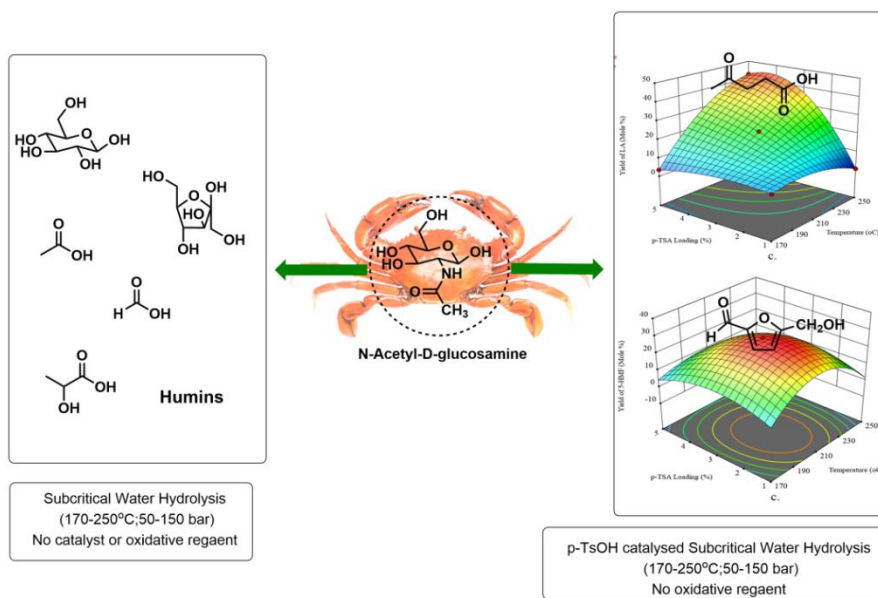
This chapter is based on:

2.1 Introduction

The efficient utilization of wastes and residues has grown in relevance since the notion of circular bio-economy emerged. Waste biomass conversion, in particular, is an essential component of circular bio-economy goals.[1,2] Every year, around 6-8 million tonnes of seafood waste are produced.[3] These materials' qualities, such as strong thermal and mechanical stability, aid marine species in surviving extreme climatic conditions. However, when discarded as seafood waste, these properties pose serious disposal issues.[4] The conversion of such materials to value-added chemicals can address the issue of waste disposal while also returning the material to the carbon chain, so promoting the bio-economy cycle. Chitin is a substantial ingredient (20-50 %) of seafood trash, accounting for about half of total marine biomass. Chitin is a polymer made up of *N*-acetyl-D-glucosamine (NAG), a monosaccharide. Any technique that converts chitin biopolymer to chemicals first depolymerizes it, and then converts NAG to the chemicals. NAG, on the other hand, is easily produced through acid or enzymatic hydrolysis of chitin. [5,6,7] As a result, NAG has emerged as a viable candidate for the manufacture of important compounds alongside glucose. Chitin and NAG have previously been examined for as feedstock for synthesis of organic acids such as acetic acid, formic acid, glyceric acid, and lactic acid in the presence of water using oxidative reagents. Qi and colleagues found that 33 % and 30 % of acetic acid is generated from NAG and chitin, respectively, in 2-3 hours using V_2O_5 as a catalyst under 0.5 MPa oxygen pressure at 200 ºC.[8] Wu and colleagues synthesized several organic acids from chitin and NAG using base catalysts, with $Ba(OH)_2$ producing the best results at moderate oxygen pressure. Although the overall organic acid yield was 53.1 %, the acetic acid yield was as low as 16 %.[9]

The top ten compounds with adaptability and ability to bridge the gap between petroleum-based processes and bio-based processes include 5-hydroxymethylfurfural (5-HMF) and levulinic acid (LA). [10] Metal salt catalysts such as $FeCl_2$, $ZnCl_2$, and others have recently been investigated for the manufacture of 5-HMF and LA from NAG or chitin utilizing various volatile organic solvents.[11] The highest yields of 5-HMF from chitin (19.3 %) and NAG (37.9 %) were produced in the presence of $FeCl_2.4H_2O$ at 180 ºC for a prolonged reaction period of 5 h. According to Yu et al., among the numerous combinations of different dipolar aprotic solvents with water, DMSO-water favored the synthesis of 5-HMF because DMSO increased the breaking of intramolecular hydrogen bonding of water molecules, thus pushing the reaction towards the formation of 5-HMF.[12] Wang et al.[11] used an aqueous solution of $ZnCl_2$ with co-catalysts to convert chitin to 5-

HMF. Chitin was dissolved in a 67 % aqueous $ZnCl_2$ solution after swelling for 48 h, although the yields of chitin and its monomer NAG were very low (10 and 2.8 %), which was attributed to the weak interaction of -NHAc with Zn^{2+} caused by the steric hindrance of the -Ac group. However, a significant amount of humins were formed. Hou and colleagues[13] recently reported the use of ionic liquids to produce LA from chitin. In 5 h at 180 °C, chitin yielded 56.7 % LA using ($[C_3SO_3Hmim]HSO_4$). Considering that the acidity of the ionic liquid (IL) increased the yield of LA, the acid catalyst plays an important role in the formation of LA from chitin. The process of chitin hydrolysis varies from that of cellulose and chitosan in that the -N acetyl group prevents acid catalysts from accessing the glycosidic linkage by establishing strong inter- and intramolecular hydrogen bonds.

Zang et al.[14] recently demonstrated that IL [Hmim][HSO4] efficiently catalyzed the conversion of NAG to 5-HMF in a DMSO-water combination. The anion [HSO4] selectively catalyzes the conversion to 5-HMF while the cation [Hmim] favors the conversion to NAG. At atmospheric pressure, the yield of 5-HMF was only 3 %, but it increased to 44 % under hydrothermal conditions, indicating the importance of pressure in the conversion of NAG to 5-HMF. Though the ILs produced promising results, the difficult and costly synthesis techniques are the main obstacles to the practical application of ILs on a large scale.[15] Szabolcs and co-workers[16] employed microwave activation for conversion of simple carbohydrates to LA. Microwave heating reduced the time of conversion of NAG to LA and resulted in LA yield of 22.1 % in the presence of HCl and 20.6 % in the presence of H_2SO_4 in 10 min. However, the extensive humin formation could not be avoided which is generally known to occur in strong acidic environment by self- condensation of 5-HMF. For the synthesis of useful compounds from NAG, the methods reported thus far require volatile solvents and toxic catalysts, which impede the development of a green approach. Only switching the feedstock does not ensure an environmentally friendly process; the process itself should incorporate greener solvents and catalysts for long-term production.

Due to its unique solvent qualities, subcritical water, that is, water at a temperature above its boiling point and at a pressure sufficient to retain the liquid state, has emerged as a green solvent. As indicated in Table 2.1, the ionic product of water at subcritical conditions, i.e. at 150-250 °C and 1-10 MPa, increases from 10^{-14} to 10^{-11}, showing a larger concentration of H^+ and OH^- ions at subcritical conditions than at normal conditions. [17] As a result, by eliminating the necessity for an acid-base catalyst, subcritical water as a solvent can bring out the reactions. Furthermore, the

solubility of carbohydrates in water is greater than in any other volatile solvent; water can solubilize the greatest amount of NAG of any solvent, which can be further enhanced by increasing the temperature.[18]

Table 2.1 Physical and chemical properties of reaction medium [17]

Reaction medium	Temperature (°C)	Pressure (MPa)	State	Density (g/mL)	Ionic Product (k_w)	Dielectric Constant (ε)
Ambient Water	0-100	1	Liquid	0.99 (25 °C)	10^{-14}	78.5
Subcritical Water	170-250	50	Hot Compressed Liquid	0.90 (170 °C)-0.80 (250 °C)	10^{-12} to 10^{-11}	27.1 (250 °C and 5 MPa)

 In the study reported by Rongchuna and co-workers, the degradation of both D-glucosamine and NAG in subcritical water was investigated, wherein the kinetics of the degradation of both D-glucosamine and NAG was reported. It was found that D-glucosamine forms minute quantities of 5-HMF, however, no details concerning the products obtained from NAG were provided [19]. Considering the interactions, between NAG molecule and subcritical water, it is imperative to form some organic acids like acetic acid. However, to best of our knowledge, no previous study has reported the non-catalytic synthesis of acetic acid from NAG. There is limited information available on product distribution of NAG at such hydrothermal conditions, which is necessary for developing a process using chitinous feedstock.

The transformations of NAG during non-catalytic and catalytic subcritical water hydrolysis are studied in this chapter. The studies on understanding of the non-catalytic efficient deacetylation of NAG to acetic acid using only subcritical water and no extra oxidative reagent supported by a detailed product distribution and reaction mechanism are discussed. Further a combination of the catalyst *p*-Toluenesulfonic acid (*p*-TsOH) and subcritical water was investigated for more environmentally friendly selective synthesis of platform chemicals such as 5-HMF and LA. [20,21] A multi response optimization based on Box-Behnken Design is carried out for estimating the optimum process conditions for maximizing yields of 5-HMF and LA during *p*-TsOH catalysed subcritical water hydrolysis of NAG. The influence of process variables and their interactions on

the yields is studied using response surface methodology. The models are developed by regression analysis of experimental data for predicting yield of both 5-HMF and LA during hydrolysis.

2.2 Materials and methods

2.2.1 Chemicals

N-Acetyl-D-glucosamine (purity > 99 %) was purchased from HiMedia Laboratories, Mumbai, India. 5-Hydroxymethylfurfural (purity > 99 %) and levulinic acid (purity 98%) were purchased from Sigma Aldrich. Acetic acid (purity > 99 %) and *p*-toluenesulfonic acid monohydrate (purity 98 %) were obtained from Loba Chemie Pvt.Ltd.. Formic Acid (purity > 98 %) and lactic Acid (purity > 90 %) were purchased from Avra Chemicals and Merck Specialities, respectively. All chemicals were used as received. The deionized water obtained from LabQ apparatus was used in all the experiments.

2.2.2 Subcritical water hydrolysis

In a typical experiment, the reactor was loaded with the reaction mixture and filled with inert gas followed by heating to the required temperature at a constant stirring speed of 600 rpm, maintaining the operating conditions for the stipulated time, followed by quick cooling to stop the reaction. The reactant NAG (1-5 g) and catalyst *p*-TsOH (0-5 g) were added to deionized water (90-95 g) in a batch autoclave reactor of volume 300 mL (Hast C, Parr Instruments, Moline, IL, USA), designed for maximum operating pressure of 2500 psi. The pressure in the reactor (5 MPa) was maintained by using argon. The initial pressure was estimated considering the expansion of argon gas with reaction temperature. The reactor was heated to the required temperature (170-250 °C) using the electrical heating mantle. The temperature and stirring speed of 600 rpm were maintained by using a PID controller. After the stipulated time (30-90 min), the reactor was quickly cooled down to the room temperature by passing cold water through dip U tube placed inside the reactor. In case of the solid formation during the reaction, the solid and liquid products were separated by vacuum filtration and analyzed without any further treatment.

2.2.3 Qualitative and quantitative analysis of products

The filtered aqueous reaction mixture was further diluted and analyzed using HPLC and Mass Spectroscopy. The identification of the products was done by LC-MS and HR-MS (Figures A1-A3) and also by injecting standard compounds for confirmation to HPLC. For quantitative analysis of products, the aqueous reaction mixture obtained by filtration was analyzed using HPLC. The black coloured solid residue was dried in a vacuum oven at 75 °C / 25 mmHg for 3 h and vacuum and analyzed using ATR-FTIR.

The aqueous product mixture obtained in the reaction was analyzed using HPLC equipped with the Aminex-87H column (Bio-Rad, USA) and Shodex Refractive Index detector. The analysis of sample was done using 5 mM sulfuric acid as mobile phase at a flow rate of 0.6 mL/min while keeping column at a constant temperature of 50 °C. The samples were filtered using 0.22 micron filter before injecting for the analysis; the chromatograms are shown in figures A4-A6. The calibration curves for each compound were generated for quantification using HPLC.

The conversion of NAG and yield of 5-HMF and LA are calculated using following equations

$$Conversion\ of\ NAG\ (\%) = \frac{(Initial\ moles\ of\ NAG - Moles\ of\ NAG\ after\ the\ reaction)}{Initial\ moles\ of\ NAG} * 100$$

$$Yield\ of\ Product\ (\%) = \frac{Moles\ of\ Product}{Initial\ Moles\ of\ NAG} * 100$$

2.2.4 Design of Experiments

The Box Behnken Design (BBD) method is an efficient method for design of experiments in order to find out the optimum operating conditions and the effect of interactions of the reaction variables on the reaction yield as it uses fewer experiments for predicting the results. Recently, BBD has been extensively used to optimize for complex reactions like biomass processing where systematic optimization becomes difficult as the number of influential operating parameters is almost always higher than two. [22,23] The preliminary reactions of NAG in presence of *p*-TsOH in subcritical water were conducted to determine the key variables and their ranges affecting yield of 5-HMF and LA. Further, the catalytic reactions of NAG were designed using BBD method for determining the optimum operating conditions. A method comprising three levels and four factors that is total 27 experiments was designed using the software Design Expert 13.0 (Stat-Ease, Inc., Minneapolis, MN, USA). In this study, four variables x_1 -Temperature (170-250 °C), x_2 -Time (30-

90 min), x_3 -NAG concentration (1-5 % w/w) and x_4 -p-TsOH loading (1- 5 % w/w) were varied in the specified ranges for optimizing yield of y_1-HMF and y_2- LA, as given in table 2.2.

The empirical models for the yield of 5-HMF and yield of LA were developed by fitting the experimental data for the value of the regression coefficient of approximately 1. Further, the quality of model was assessed by analysis of variance (ANOVA).

Table 2.2 Range and levels of key parameters (at a fixed operating pressure of 5 MPa) selected for optimization using BBD method

Factor	Reaction Parameters	Unit	Range and Level		
			Minimum (-1)	Middle (0)	Maximum (+1)
x_1	Temperature	ºC	170	210	250
x_2	Time	Min	30	60	90
x_3	NAG Loading	% (w/w)	1	3	5
x_4	p-TsOH Loading	% (w/w)	1	3	5

2.3 Results and Discussion

2.3.1 Non-catalytic subcritical water hydrolysis of NAG

The subcritical water hydrolysis of NAG was studied initially by varying temperature in the range of 70-200 ºC, reaction time in the range of 60-180 min and pressure in the range of 1-15 MPa. There was practically no conversion of NAG at temperatures less than 170 ºC; on the contrary NAG was almost always consumed 100 % at all temperatures higher than 170 ºC irrespective of the reaction time. Hence, the hydrolysis of NAG is instantaneous and controlled by the temperature. It was interesting to see the formation of some products identified to be lactic acid, formic acid, acetic acid, glucose, fructose and solids characterized as humins during non-catalytic

hydrolysis of NAG, as the formation of these products requires either acid or base catalysts. Based on moles, 80 % yield (20 % on mass) of acetic acid was obtained at almost all operating conditions of temperature higher than 170 ^{o}C. Thus, it can be stated that NAG undergoes almost complete deacetylation forming acetic acid and glucosamine. Glucosamine was not detectable using HPLC method mentioned in 2.2.3, however, the formation of the other compounds like glucose, fructose and large amount of humins indicates that the glucosamine undergoes deamination which further gets converted to glucose followed by formation of fructose and lactic acid. The only plausible pathway for formation of lactic acid is by the conversion of glucose which requires a basic catalyst. The presence of traces of lactic acid and formic acid in product mixture of non-catalytic subcritical hydrolysis of NAG confirms that water at subcritical conditions acts as an acid-base catalyst. However, the concentration of dissociated water ions catalyzing reaction is not enough for selective formation of the particular acid. A reaction pathway of NAG hydrolysis in subcritical water is shown in figure 2.1.

Figure 2.1 Reaction pathways for hydrolysis of NAG in subcritical water in absence of external catalyst

Table 2.3 summarizes the product distribution of non-catalytic hydrolysis of NAG in water at various subcritical temperatures and pressures. The previously reported TGA-DSC analysis of NAG shows that it starts decomposing at temperatures near 180 ^{o}C, as the mass of NAG drastically drops even before NAG melts completely.[18] Simultaneously, the neutral reaction medium becomes

acidic as the value of ionization constant of water drops from 14 at 25 °C to 11.2 at 170 °C at constant 10 MPa, indicating the increased concentration of H^+ and OH^- ions at the higher temperature.[24] This temperature conditional behavior of NAG deacetylation can be attributed to the combined effect of thermal instability of NAG and properties of subcritical water. The subcritical temperature provides the activation energy while the dissociated ions of water catalyze the transformation; hence, NAG undergoes efficient and instantaneous deacetylation at 170 °C. There was less pronounced effect of pressure on the product yields of NAG hydrolysis in the operating pressure range (5-10 MPa) at a temperature of 200 °C and time of 60 min. The value of the ionic product of water is in the range of 11.2 to 11.5 at tested temperature and pressure combinations; increasing pressure from 2-15 MPa does not change ionic product significantly, hence, the product distribution is least affected by the pressure in the tested pressure range at subcritical temperature. [24] The product distribution was significantly influenced by the reaction time during the subcritical water hydrolysis of NAG. At 200 °C and 10 MPa, the yield of acetic acid and humins increased with time from 60 to 180 min, however, the variation in the yields of other products was insignificant. Against previously reported systems [8,9], the comparable or even higher yield of acetic acid was obtained at shorter reaction time and even in the absence of catalyst or oxidative reagents such as oxygen.

Acetic acid, the deacetylation product of NAG, was one of the major products amongst all identified compounds with almost 80 % yield on mol basis and maximum 20 % on weight basis. As per the previous reports, the deacetylation of NAG is an acid-catalyzed reaction, which requires strong mineral acids such as HCl, H_2SO_4 etc.[25] Recently, solid acid catalysts such as the cation exchange resins are used for deacetylation.[26] Recent studies have also showed that the role of oxidative reagent, oxygen gas in particular, is crucial in facilitating breakage of acetamide bond which is least affected by the presence of catalyst or temperature.[8,9] Herein, the efficient deacetylation of NAG using water at subcritical conditions in the absence of any external catalyst and/or an oxidative reagent is investigated. Water at the temperature and pressure ranges maintained here becomes acidic as the ionic product of water drops to 11.2-11.5, engendering the formation of hydronium ion responsible for deacetylation of NAG. A plausible mechanism is shown in figure 2.2. The protonation of oxygen of carbonyl group by hydronium ion present in subcritical water forms a carbocation. The carbocation is then attacked by the nucleophilic water molecule forming an oxonium intermediate. Another attack of hydroxyl ion results in the addition

of one water molecule and removal of the acetic acid from glucosamine ring followed by the regeneration of another water molecule. [25]

2.3.2 p-TsOH catalyzed subcritical water hydrolysis of NAG

The previous results of non-catalytic hydrolysis show that after deacetylation some of the transformations of NAG proceed *via* formation of glucose. A stronger catalyst is required to further convert the glucose to 5-HMF and LA by avoiding the formation of solid humin products. An acid catalyst viz. *p*-TsOH was employed to produce 5-HMF and LA from NAG. The preliminary reactions were carried out to investigate the catalytic performance of *p*-TsOH towards selectively converting NAG to LA in subcritical water. The temperature and time varied in the range of 170-250 ^{o}C and 5-180 min, respectively for a constant pressure of 5 MPa. The pressure of 5 MPa was selected to maintain acidity of water at all temperatures, as the ionic product varies from 11.2-10.90 at 170-250 ^{o}C at 5 MPa. [24]

The major products of the reactions were LA, acetic acid, formic acid along with traces of 5-HMF, lactic acid, glucose, etc. A remarkable yield of 57 mol % of LA was obtained from 5 % (w/w) NAG at 250 ^{o}C and 5 MPa in 60 min using *p*-TsOH 5% (w/w) in subcritical water. The yield of LA was even higher (~53.46 %) than that obtained from glucosamine (~49.9 %) using methanesulfonic acid at 200 ^{o}C in 30 min. [27] The yield of humins was drastically dropped than that observed in non-catalytic reactions. During *p*-TsOH-catalyzed hydrolysis of NAG the yield of solids was less than 10 % whereas during non-catalytic hydrolysis the yield of humins was almost always more than 20 % at all subcritical operating conditions. As shown in figure 2.13, FT-IR analysis of the solids formed during *p*-TsOH-catalyzed hydrolysis showed that there may be structural difference between the solids formed during non-catalytic and catalytic hydrolysis of NAG subcritical water. The solids formed in presence of *p*-TsOH might constitute sulfonated products as has been reported previously.[28] However, the detailed structural analysis of humins was not undertaken in the present study.

Table 2.3 Product distribution of non-catalytic subcritical water hydrolysis of NAG (based on identified products)

Experiment	Temperature (ºC)	Pressure (MPa)	Time (min)	Initial NAG Concentration (%)	Conversion of NAG (%)	Product Distribution (weight of product/weight of NAG) *100						Accountability # (%)
						Glucose	Fructose	Lactic acid	Formic acid	Acetic acid	Humins	
1	70	10	60	5.0	0	0	0	0	0	0	0	100
2	170	10	60	5.0	91.00	0.0	0.30	0.14	0.35	5.85	33.64	40.28
3	200	10	60	5.0	99.64	0.12	0.40	0.35	1.16	15.82	29.61	47.46
4	200	1.5	60	5.0	98.60	0.12	0.33	0.42	1.13	18.17	39.60	59.78
5	200	5	60	5.0	99.62	0.14	0.55	0.89	5.57	15.72	31.50	49.30
6	200	10	120	5.0	100	0.10	0.00	0.04	0.80	15.94	29.91	46.71
7	200	10	180	5.0	100	0.37	0.14	0.34	0.95	21.47	38.90	62.18

#(Total weight of identified products/Initial weight of NAG) *10
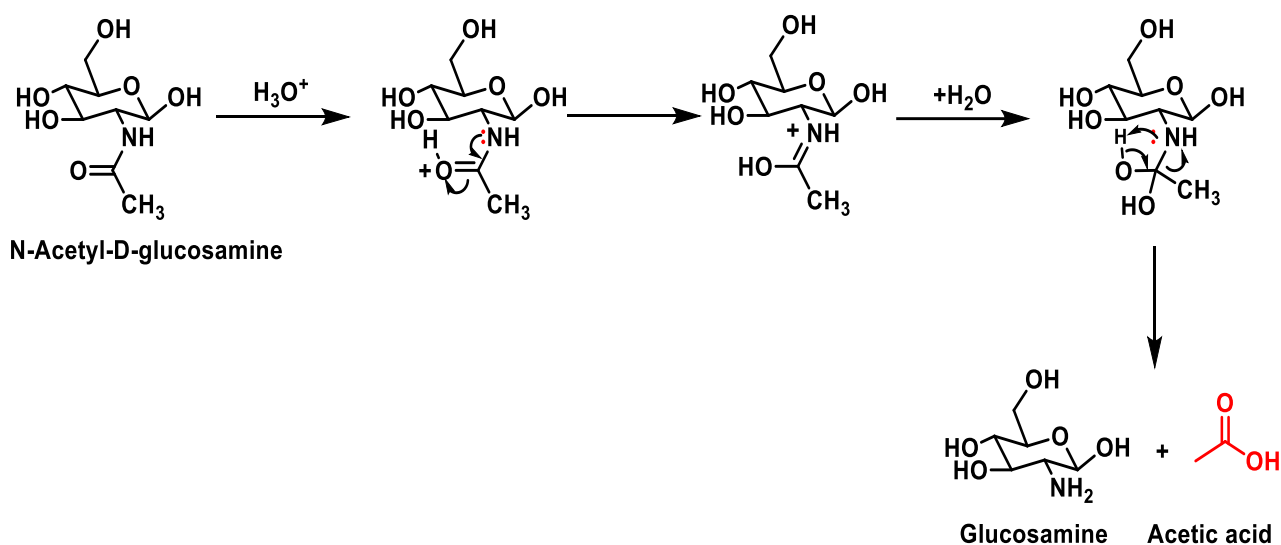
Figure 2.2 Plausible mechanism of NAG deacetylation in subcritical water in absence of any external catalyst

Nevertheless, it was confirmed that *p*-TsOH shows a significant catalytic activity by suppressing solid humin formation and selectively transforming NAG to LA which is discussed in 2.3.3.

The sensitive range of operating conditions was identified based on the results of the preliminary experiments carried out to optimize 5-HMF and LA yield using BBD method. As observed in non-catalytic reactions, the minimum temperature required for conversion of NAG is 170 ºC at which low yield of LA (~5 %) was obtained even in the presence of *p*- TsOH (Figure 2.3a). It was found that the yield of LA was increased with increasing temperature at lower reaction time of 60 min. For longer reaction times, the yield of LA and formic acid was highest at 210 ºC and was lowest at 170 ºC. However,the yield of LA was highest at 210 ºC than that at tempertures of 170 ºC and 250 ºC. The yield of acetic acid was least affected by the operating temperature and time, as shown in Figure 2.4, however, on comparison with non-catalytic reaction,the complete deacetylation of NAG with 100 % yield of acetic acid was observed in the presence of *p*-TsOH .

Figure 2.3 Effect of temperature and time on yield of LA [NAG aqueous concentration 1% (w/w); pressure-5 MPa; *p*-TsOH:NAG-5:1(w/w))]

Figure 2.4 Effect of temperature and time on yield of acetic acid [NAG aqueous concentration 1% (w/w); pressure-5 MPa; *p*-TsOH:NAG-5:1(w/w))]

Figure 2.5 Effect of temperature and time on yield of 5-HMF [NAG aqueous concentration 1 % (w/w); pressure-5 MPa; p-TsOH: NAG-5:1(w/w))]

As shown in Figure 2.5, though small but the yield of 5-HMF was favored by short reaction time at low temperature (170 ^{o}C) and by longer reaction time at 210 ^{o}C. The presence of minute quantity of 5-HMF and its response to the changes in the operating conditions shows that even 5-HMF can be obtained in significant amount during same process. However, it is imperative to find out the suitable conditions. In order to find out if the lower or higher reaction time favors yield of LA and 5-HMF at low and high temperatures at different conentrations of *p*-TsOH catalyst and initial NAG ,a multi response optimization study was carried out along with a detailed analysis of the response surfaces of yields of compounds obatined by response surface methodology (RSM).The initial ranges of factors for optimization were fixed based on preliminary observations and the range of studied temperature, time, *p*-TsOH loading and NAG cocnentration are shown in table 2.2.

2.3.3 Reaction pathway and catalytic mechanism of LA formation
The reaction pathway for the formation of LA is proposed based on the product distribution of *p*-TsOH catalyzed conversion of NAG in subcritical water. Similar to the non-catalytic reactions, the subcritical water facilitates the deacetylation of NAG to form glucosamine and acetic acid as the equal moles of acetic acid were obtained from initial moles of NAG in both

the cases (figure 2.4). Glucosamine undergoes deamination forming glucose and ammonia. The isomerization of glucose to fructose is accelerated in presence of *p*-TsOH. Further, *p*-TsOH catalyzes the dehydration of fructose to form 5-HMF, upon rehydration 5-HMF forms LA along with formic acid as by-product. The mechanism of formation of 5-HMF is presumed to be similar to that of conversion of fructose to 5-HMF as reported previously.[29]

The solid products are characterised to be humins, having similar functional groups to that of products reported previously in subcritical water (figure 2.13). The solids are a polymerisation product of the compounds formed during subcritical water hydrolysis of 5-HMF and glucose.[30] Hence, the formation of solids during NAG hydrolysis was accounted to 5-HMF. In the absence of any strong acid, 5-HMF undergoes self-condensation wherein it's own nucleophilic oxygen of hydroxyl group attacks aldehyde group removing water and forming polymers, which may further combine with glucose and undergo polymerisation to produce solid humins.On the contrary, in presence of *p*-TsOH, alcoholic oxygen of 5-HMF acts as a base instead of nucleophile which leads to ring opening by protonation rather than self-condensation. Hence, the solid formation is avoided, causing the ring opening followed by the formation of LA and formic acid, as shown in figure 2.5. A quantitative comparison of catalytic and non-catalytic subcritical water hydrolysis of NAG was done by carrying out reactions under similar operating conditions with and without *p*-TsOH. The results summarised in table 2.7 supports the mechanism proposed above, as around 60 % (mass basis) of solids were formed during non-catalytic reactions from NAG at similar temperature, pressure and reaction time,whereas, only 8.4 % (mass basis) of solids were obatined in *p*-TsOH-catalysed reaction with highest LA yield.
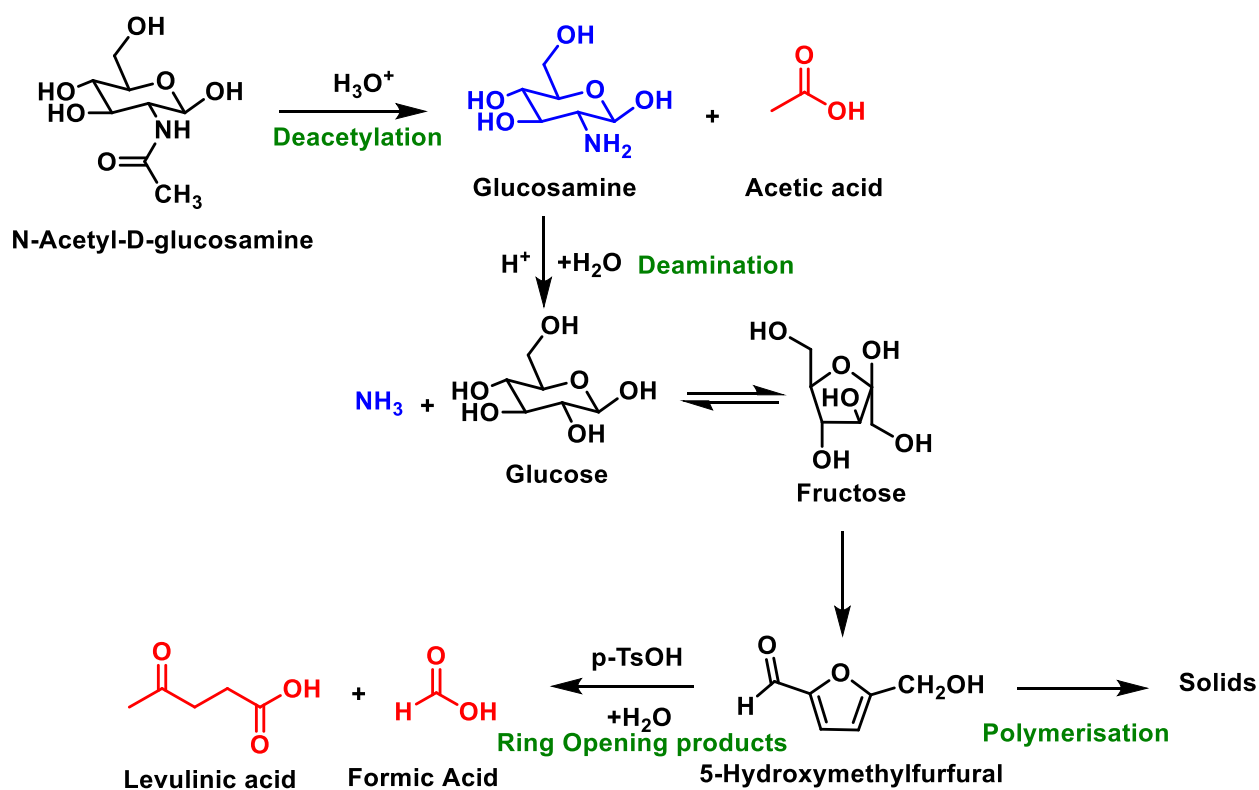
Figure 2.6 Proposed reaction pathway of *p*-TsOH-catalyzed subcritical water hydrolysis of NAG
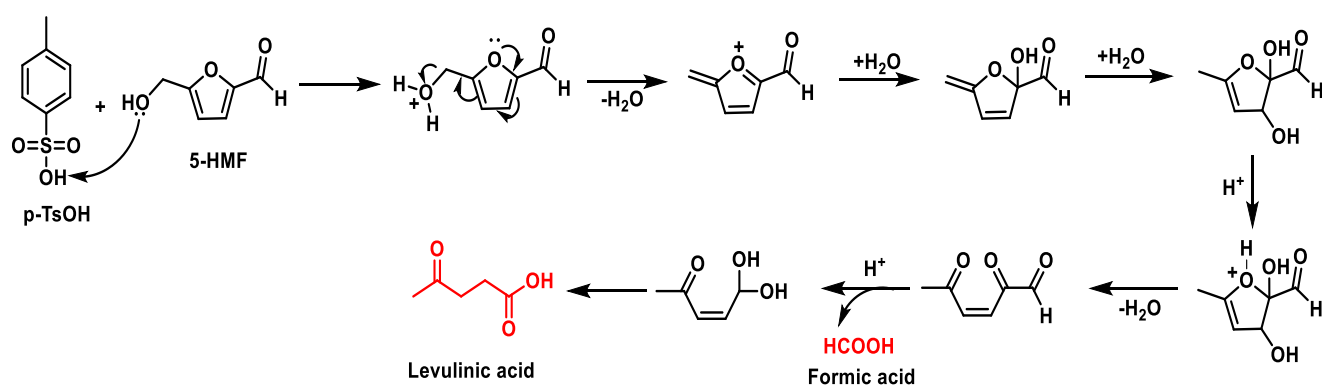
Figure 2.7 Proposed reaction mechanism of *p*-TsOH catalyzed subcritical water hydrolysis of NAG

Table 2.4 Box-Behnken Design reaction matrix with actual response of yield of 5-HMF and LA

Run	Temperature (ºC)	Time (min)	NAG Concentration %(w/w)	p-TsOH Loading % (w/w)	Yield of 5-HMF (% on mol basis)	Yield of LA (% on mol basis)
	x_1	x_2	x_3	x_4	y_1	y_2
1	210	90	1	3	1.69	38.69
2	170	60	1	3	3.01	3.64
3	170	60	5	3	7.26	2.98
4	250	60	3	5	0.49	42.45
5	250	30	3	3	0.45	33.95
6	170	60	3	5	3.03	3.47
7	170	90	3	3	6.83	3.19
8	210	60	5	1	13.05	3.82
9	210	30	1	3	5.17	19.84
10	210	30	3	5	3.61	17.61
11	210	30	3	1	21.79	4.58
12	210	90	3	1	19.89	1.69
13	250	60	3	1	8.04	0.08
14	210	90	5	3	22.15	9.14
15	170	60	3	1	12.16	7.54
16	250	60	1	3	0.00	46.07

17	210	60	5	5	2.40	24.16
18	250	60	5	3	1.39	8.64
19	210	60	3	3	7.38	22.82
20	210	60	3	3	7.38	22.82
21	170	30	3	3	3.89	3.41
22	210	60	1	1	23.70	13.46
23	210	30	5	3	27.14	2.88
24	210	90	3	5	1.37	34.66
25	210	60	3	3	7.38	22.19
26	210	60	1	5	2.60	36.14
27	250	90	3	3	0.00	32.97

Table 2.5 ANOVA for the regression model of yield of 5-HMF

Source	Sum of Squares	DF	Mean Square	F-value	p-value	
Yield of 5-HMF						
Model	1713.24	23	74.49	923.47	< 0.0001	Significant
x_1:Temperature (ºC)	45.83	1	45.83	568.22	0.0002	
x_2:Time (min)	1.55	1	1.55	19.16	0.0221	
x_3:NAG Concentration (% w/w)	450.16	1	450.16	5580.85	< 0.0001	
x_4:*p*-TsOH Loading (% w/w)	336.78	1	336.78	4175.27	< 0.0001	
x_1x_2	2.87	1	2.87	35.59	0.0094	
x_1x_3	2.05	1	2.05	25.4	0.0151	
x_1x_4	0.6237	1	0.6237	7.73	0.0689	
x_2x_3	0.5622	1	0.5622	6.97	0.0777	
x_2x_4	0.0291	1	0.0291	0.3612	0.5902	
x_3x_4	27.33	1	27.33	338.83	0.0003	
x_1^2	227.98	1	227.98	2826.31	< 0.0001	
x_2^2	39.38	1	39.38	488.24	0.0002	
x_3^2	42.34	1	42.34	524.91	0.0002	
x_4^2	1.96	1	1.96	24.35	0.016	
$x_1^2x_3$	169.24	1	169.24	2098.15	< 0.0001	
$x_1^2x_4$	50.12	1	50.12	621.38	0.0001	

$x_1x_4^2$	1.42	1	1.42	17.66	0.0246	
$x_2x_3^2$	15.01	1	15.01	186.03	0.0009	
$x_2x_4^2$	5.49	1	5.49	68.1	0.0037	
$x_3^2x_4$	3.06	1	3.06	37.96	0.0086	
$x_3x_4^2$	354.87	1	354.87	4399.44	< 0.0001	
$x_1^2x_4^2$	29.04	1	29.04	360.07	0.0003	
$x_3^2x_4^2$	1.81	1	1.81	22.43	0.0179	
Residual	0.242	3	0.0807			
Cor Total	1713.48	26				
R^2	0.9999					

Table 2.6 ANOVA for the regression model of yield of LA

Source	Sum of Squares	DF	Mean Square	F-value	p-value	
Yield of LA						
Model	5551.28	23	241.36	526.83	0.0001	Significant
x_1:Temperature(^{o}C)	909.52	1	909.52	1985.28	< 0.0001	
x_2:Time(min)	157.68	1	157.68	344.17	0.0003	
x_3:NAG Concentration (% w/w)	540.78	1	540.78	1180.4	< 0.0001	
x_4:*p*-TsOH Loading (% w/w)	990.72	1	990.72	2162.52	< 0.0001	
x_1x_2	0.146	1	0.146	0.3186	0.6119	
x_1x_3	338.23	1	338.23	738.27	0.0001	
x_1x_4	538.92	1	538.92	1176.34	< 0.0001	
x_2x_3	39.64	1	39.64	86.52	0.0026	
x_2x_4	99.35	1	99.35	216.87	0.0007	
x_3x_4	1.37	1	1.37	2.99	0.182	
x_1^2	0.7825	1	0.7825	1.71	0.2824	
x_2^2	87.43	1	87.43	190.84	0.0008	
x_3^2	0.0421	1	0.0421	0.0919	0.7816	
x_4^2	35.66	1	35.66	77.83	0.0031	
$x_1^2x_2$	86.59	1	86.59	189	0.0008	
$x_1^2x_3$	8.87	1	8.87	19.37	0.0218	

$x_1^2x_4$	6.44	1	6.44	14.05	0.0331	
$x_1x_3^2$	18.69	1	18.69	40.79	0.0078	
$x_1x_4^2$	103.62	1	103.62	226.19	0.0006	
$x_2x_4^2$	15.01	1	15.01	32.76	0.0106	
$x_3x_4^2$	77.42	1	77.42	169	0.001	
$x_1^2x_3^2$	60.94	1	60.94	133.01	0.0014	
$x_1^2x_4^2$	45.6	1	45.6	99.54	0.0021	
Residual	1.37	3	0.4581			
Cor Total	5552.65	26				
R^2	0.9998					

2.4 Response surface methodology (RSM) study for 5-HMF and LA production from NAG

2.4.1 Model Analysis

The results of the various experiments designed according to the BBD (27 runs) for studying the effect of four variables viz. temperature, time, feed concentration and catalyst loading on yield of two important compounds 5-HMF and LA obtained by p-TsOH catalyzed subcritical water hydrolysis of NAG are shown in the table 2.4. The linear, 2 FI, quadratic and cubic polynomial models were inadequate for predicting the response of the yield of 5-HMF and LA, indicated either by high p-values or by small R^2 or F-values. Therefore, it was imperative to employ the reduced quartic models for prediction of both, the yield of 5-HMF and the yield of LA, as in eq. 1 and 2.

$Y_{5-HMF} = 368.705 - 2.7356x_1 - 0.5732x_2 - 142.134x_3 - 186.093x_4 - 0.0007x_1x_2 + 1.1984x_1x_3 + 1.4424x_1x_4 + 0.1307x_2x_3 + 0.0814x_2x_4 + 6.6896x_3x_4 + 0.0065x_1^2 + 0.0036x_2^2 + 0.9956x_3^2 + 41.4959x_4^2 - 0.0028x_1^2x_3 - 0.0034x_1^2x_4 - 0.3490x_1x_4^2 - 0.0228x_2x_3^2 - 0.0138x_2x_4^2 + 0.6590x_3^2x_4 - 1.1606x_3x_4^2 + 0.0008x_1^2x_4^2 - 0.0840598x_3^2x_4^2$ **…………….. equation 1**

$$Y_{LA} = -506.849 + 4.9137x_1 - 5.4509x_2 + 356.763x_3 + 182.09x_4 + 0.0574x_1x_2 - 3.3504x_1x_3 - 2.040x_1x_4 - 0.0524x_2x_3 + 0.2200x_2x_4 - 4.8128x_3x_4 - 0.0123x_1^2 - 0.0054x_2^2 - 49.804x_3^2 - 38.8256x_4^2 - 0.0001x_1^2x_2 + 0.0079x_1^2x_3 + 0.00584x_1^2x_4 + 0.4931x_1x_3^2 + 0.3981x_1x_4^2 - 0.02282x_2x_4^2 + 0.7777x_3x_4^2 - 0.00121x_1^2x_3^2 - 0.00105x_1^2x_4^2$$

.……………….. **equation 2**

Where x_1, x_2, x_3 and x_4 are reaction temperature (°C), reaction time (min) , NAG concentration (% w/w) and catalyst p-TsOH loading (% w/w) respectively. The value of R^2 for HMF model and LA model were 0.9999 and 0.9998, respectively that is very close to 1 which indicates that the models can adequately predict the response of the experiments in the prescribed range of operating conditions. Table 2.5 and 2.6 describe the analysis of variance (ANOVA) for the models with F-values and p-Values. Both the models were significant with small p-values (<0.05) and high F-values. For 5-HMF yield the analysis revealed that the all the model terms except the interaction model terms x_1x_4, x_2x_3 and x_2x_4 were highly significant, as the p-values of these terms x_1x_4, x_2x_3, and x_2x_4 were higher than 0.05 the yield of 5-HMF has least effect of interaction between temperature and catalyst loading, time and feed concentration and time, catalyst loading, etc. On the other hand, the interaction terms of LA model x_1x_2, x_3x_4 , quadratic terms x_1^2, x_3^2 were insignificant with p-values higher than 0.05, indicating the less significance of interaction between temperature-time, feed loading-catalyst loading and the increase in the temperature and feed loading itself on LA yield, all other model terms were highly significant. The parity plots (figure 2.14 and 2.15) of both the models demonstrated the competence of both the models developed for predicting the yield of 5-HMF and LA in the investigated range of operating conditions.

2.4.2 Response Surface Analysis of 5-HMF yield

The effect of interaction of four factors is more complex as the yield is governed by both the formation and consumption of 5-HMF. Therefore, it is essential to study the interaction carefully to obtain the optimum yield of 5-HMF. The contour plots 2.8a-f represents the effect of the parameters on yield of 5-HMF within the limited range of operating conditions that is temperature from 170-250 °C, reaction time from 30-90 min, NAG concentration 1-5% (w/w) and p-TsOH loading 1-5% (w/w) at zero levels of the constant parameters.

As shown in figure 2.8a, 5-HMF yield does not vary with the proportion of change in temperature and time, a certain combination of these parameters must be maintained to get the high yield of 5-HMF. The temperature around 210 °C and time either short 30 min or high 90 min resulted in higher yield of 5-HMF. As discussed in the previous sections, 5-HMF

undergoes rehydration to form LA and formic acid. Low temperature does not suffice the energy of formation of 5-HMF and that at 210 ºC the energy is just sufficient for formation of 5-HMF. On the other hand, longer reaction time allows degradation of 5-HMF to other compounds explaining the high yield of 5-HMF at medium temperature and low time. When the interaction between the temperature and NAG concentration is considered, as shown in figure 2.8b, similar to the previous discussion moderate temperature and a high NAG loading resulted in the high yield of 5-HMF at 3 % *p*-TsOH loading. The effect of feed concentration on yield gives an idea about the order of the reaction that the reaction rate is not first order unlike the reaction of glucose to 5-HMF.

The circular nature of contour plot 2.8c showed that the maximum yield is obtained near 210 ºC and 1 % (w/w) *p*-TsOH loading. Any further increase in temperature and *p*-TsOH concentration leads to further reactions like rehydration which consumes 5-HMF resulting in lower yields of 5-HMF. There was strong interaction between NAG loading and time, as in figure 2.8d, where the yield was highest at maximum NAG loading obtained in time shorter than 30 min, at 210 ºC and 3 % *p*-TsOH loading. The yield of 5-HMF increases by decreasing time than 30 min and maintaining 3 % *p*-TsOH loading, as shown in figure 2.8e, clearly increasing *p*-TsOH loading alone does not improve 5-HMF yield. According to the contour plot 2.8f, low *p*-TsOH to NAG ratios favored the formation of 5-HMF. In general, the yield of 5-HMF can be maximized by using high NAG loading and low *p*-TsOH concentration at temperature 210 ºC in time shorter than 30 min.

2.4.3 Response surface analysis of LA yield

The four reaction variables viz. reaction temperature, time, NAG loading and *p*-TsOH concentration has conspicuous effect on the yield of LA in the investigated region of the variables. Figures 2.9a-f show the interaction effects of variables on LA yield at subcritical pressure of 5 MPa when remaining variables are maintained at the zero levels. The elliptical nature of contours in figure 2.9a indicates that the temperature and time have significant interaction on LA yield, where, the temperature dominates the yield; as the yield of LA is high at high temperature irrespective of the time at 1:1 ratio of NAG and *p*-TsOH. Figure 2.9b shows that the low NAG concentration favours the formation of LA from 5-HMF at sufficient *p*-TsOH loading of 3 % (w/w) in an hour at higher temperatures around 250 ºC.
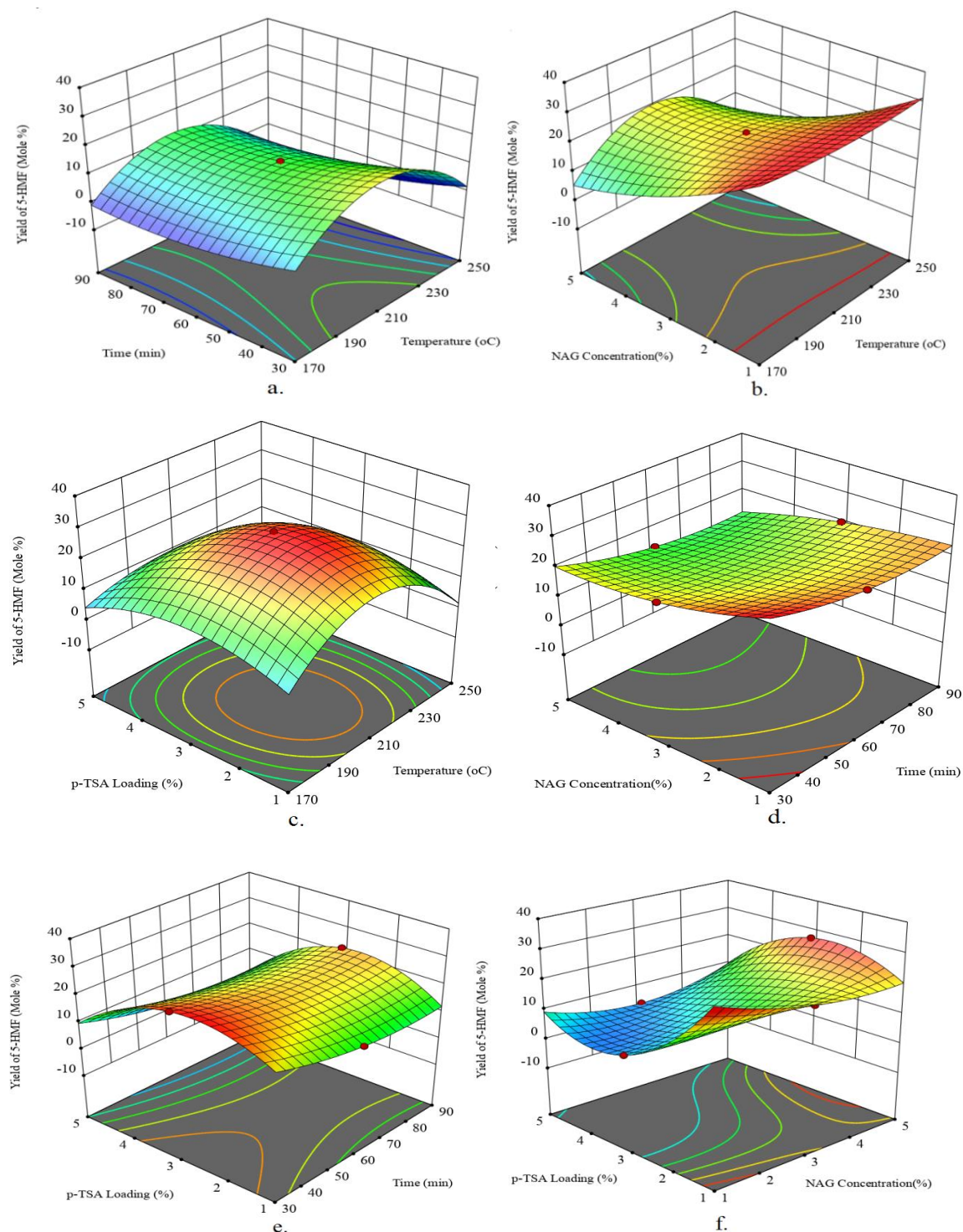
Figure 2.8 Response surfaces of 5-HMF yield

The increase in the initial concentration of NAG is probably introducing mass transfer limitations causing the drop in the yield and conversion. High *p*-TsOH loading favors the formation of LA from 5-HMF, as discussed in reaction pathway section, *p*-TsOH catalyzes both fructose to 5-HMF conversion and 5-HMF to LA conversion, hence, for obtaining high yields of LA, high concentration of *p*-TsOH is required, as shown in figure 2.9c. The nature of

2.9d plot indicates that time and NAG loading have less interaction and to achieve the maximum LA yield for the longer reaction times are required at low NAG loading, which can further increase when NAG concentration in increased. Figure 2.9e, shows that the interaction between time and catalyst loading is moderately significant due to the elliptical curvature, increasing both the *p*-TsOH concentration and time simultaneously can improve the yield of LA. Unlike the case 5-HMF, higher *p*-TsOH to NAG ratio would favor the formation of LA. The surface plot 6f shows increasing both concentrations of *p*-TsOH and NAG leads to poor yield of LA. However at low NAG concentration of 1% (w/w) high LA yield upto 46% was obtained at *p*-TsOH loading of 4% (w/w). It is interesting to note that the further increase in the *p*-TsOH loading could not improve LA yield which could be ascribed to the side reactions leading to the formation of humins. In nutshell, for maximizing the yield of LA, higher temperatures and high *p*-TsOH to NAG ratios should be employed for sufficiently longer reaction times.

2.4.4 Optimization Study

The operating conditions for obtaining highest yield of 5-HMF and LA using *p*-TsOH-catalyzed subcritical water hydrolysis were identified. A numerical optimization based on the model and the analysis of response surfaces were performed using design expert 13 where the criteria for 5-HMF yield was maximization of 5-HMF and minimization of LA and that in case of LA yield was the minimization of 5-HMF and maximization of LA. The maximum yield of 5-HMF was obtained by subcritical water hydrolysis of NAG at 210 $^{\circ}$C for 30 min with 5% (w/w) NAG concentration and 3 % (w/w) *p*-TsOH loading with desirability of 1, The maximum yield of LA could be achieved from hydrolysis at 238 $^{\circ}$C, 1%(w/w) NAG concentration, 4 % (w/w) *p*-TsOH loading in 83 min with desirability of 0.971, where desirability describes the closeness of response to ideal value based on desirability function analysis available in software. The solid yield of the reaction carried out at optimum temperature, time and pressure without catalyst was 60 % unlike 8.4 % to that of catalytic showing significant suppression of humin formation by *p*-TsOH.

The yield of 5-HMF and LA obtained by performing the reactions at the predicted optimum conditions were 27.13 and 53.21% with error less than 1% and is within 5% significance level, as shown in table 2.7 The obtained yields of LA are comparable to that of obtained from glucose[31].
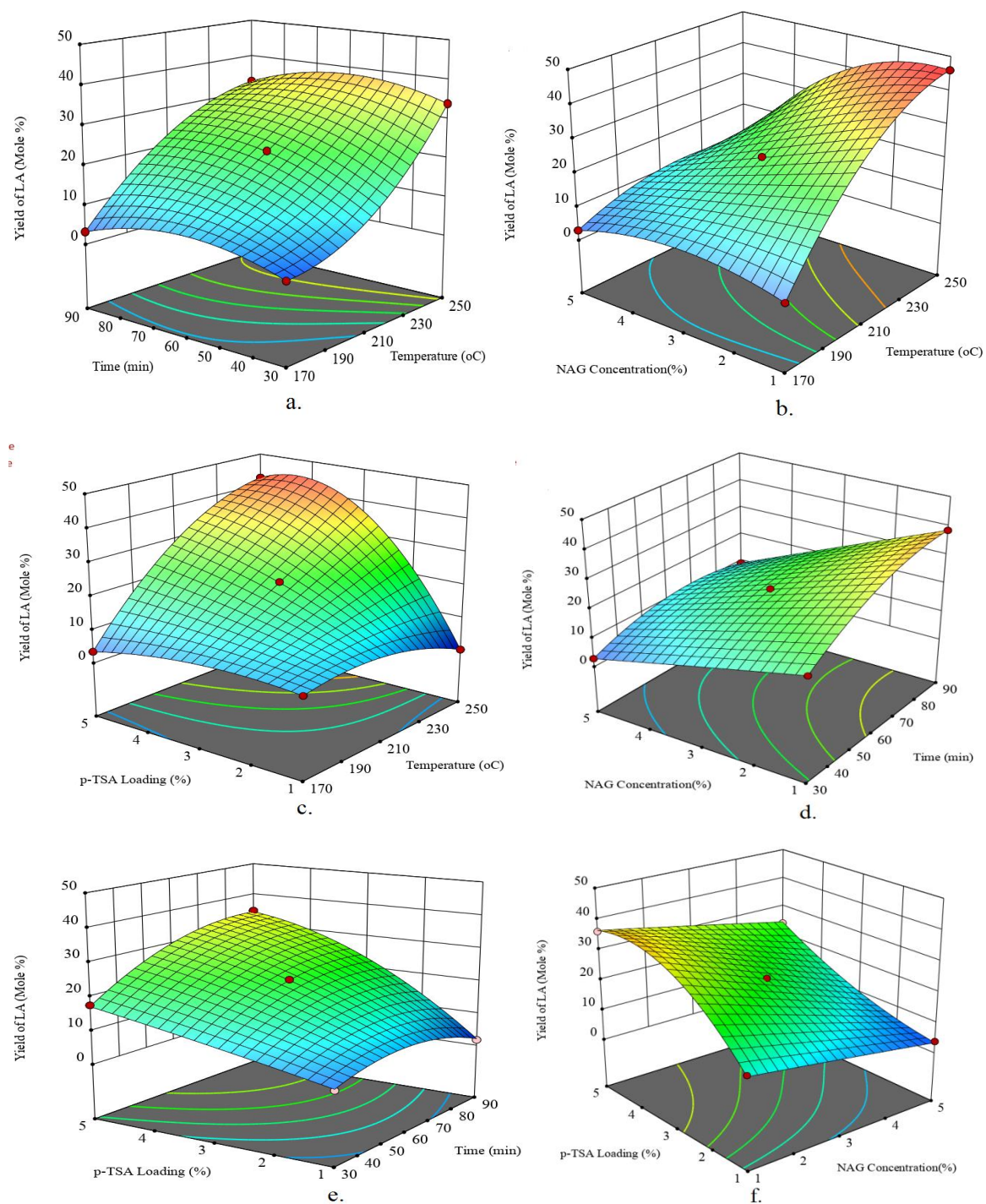
Figure 2.9 Response surfaces of LA yield

Table 2.7 Optimized conditions for 5-HMF and LA yield- prediction and validation

Experiment	Reaction Temperature (ºC)	Reaction Pressure (bar)	Reaction Time (min)	NAG concentrations (%)	*p*-TsOH Loading (%)	Yield % (mol basis)		Error[a]	Solid Yield (% w/w of NAG)
						Predicted	Obtained		
5-HMF yield optimization	210	50	30	5	3	27.02	27.13	0.40	9.7
LA yield optimization	238	50	83	1	4.09	53.21	53.46	0.46	8.4
Non-catalytic reaction	238	50	90	1	-	-	-	NA	60

[a]Error= [(Experimental value – Predicted value) /Predicted value] *100

2.5 Conclusion

The efficient deacetylation of NAG to produce acetic acid could be achieved by using water at subcritical conditions in the absence of any external catalyst or oxidative reagent. Further, a catalytic activity of subcritical water was observed which was confirmed by presence of lactic acid and formic acid in product mixture. However, the humin formation by self-aldol condensation of 5-HMF followed by polymerization was the dominating reaction during hydrolysis of NAG. The overall reactions occurring during hydrolysis of NAG at subcritical conditions are complex, instantaneous and temperature dependent, as NAG was always completely consumed as the temperature reached minimum 170 $^\circ$C which was unaffected by the presence of catalyst.

LA was selectively produced by employing *p*-TsOH as a catalyst during hydrolysis of NAG in subcritical water. *p*-TsOH significantly suppressed humin formation by favoring the ring opening of 5-HMF. The process conditions viz. temperature, reaction time, NAG concentration and *p*-TsOH loading were optimized using BBD coupled with RSM. A maximum 27.02 % yield of 5-HMF was obtained at 210 $^\circ$C for a NAG to *p*-TsOH ratio of 5:3 in 30 min whereas maximum 53.21 % yield of LA was achieved at 238 $^\circ$C for a 1:4 ratio of NAG to *p*-TsOH in 83 min, at constant 5 MPa, with desirability of 0.97 and 1, respectively. The control over selectivity of 5-HMF and LA can be achieved by tuning the process conditions during subcritical water hydrolysis of NAG ascertained by multi-response optimization technique.

2.6 Experimental section and supporting information

2.6.1 Identification of LA
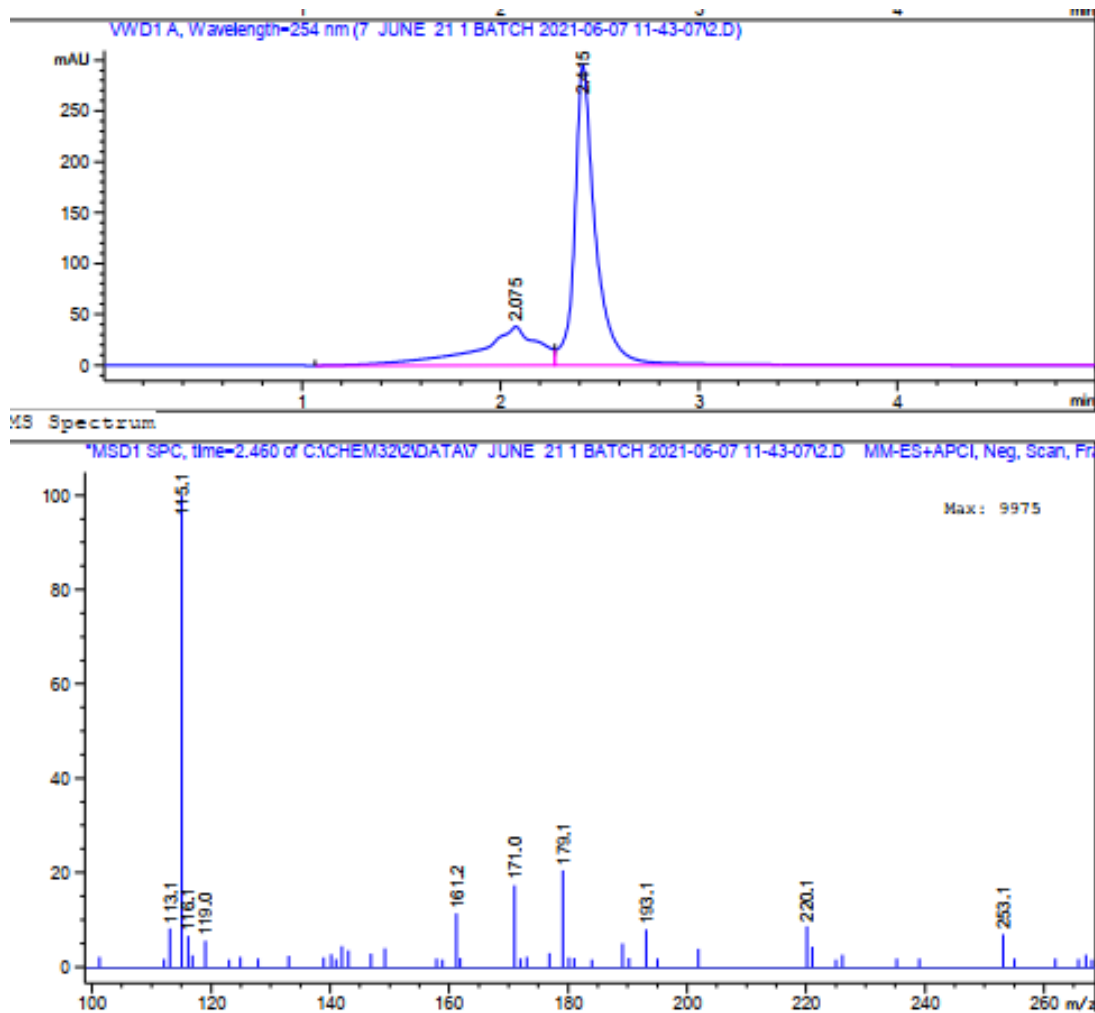
Figure 2.10 Mass spectrum of reaction mixture [Reaction Conditions- Temperature-238 °C; Time-83 min; NAG Concentration-1 % (w/w); p-TsOH loading-4.09 %(w/w), yield of LA 53.4% (mol basis)]

2.6.2 Identification of LA and HMF by HR-MS (positive mode)

BRX-14 #608 RT: 3.30 AV: 1 NL: 3.72E6
T: FTMS + p ESI Full ms [50.0000-750.0000]

117.0544
R=104907
$C_5 H_9 O_3 = 117.0546$
-1.7755 ppm

115.0751
R=104002

116.0704
R=100302

118.0860
R=103902

119.0187
R=100702

120.0194
R=86700

121.0646
R=101802
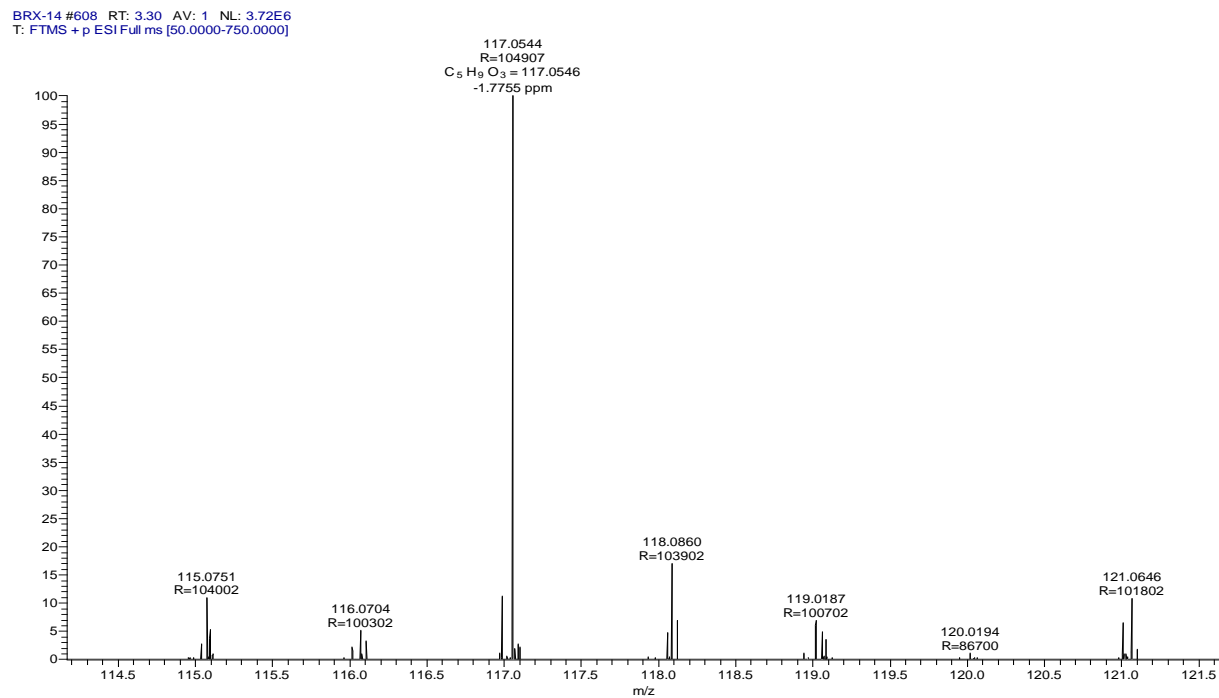
Figure 2.11 HR-Mass spectra at reaction Conditions- Temp-238 °C; Time-83 min; NAG Concentration-1 % (w/w); *p*-TsOH loading-4.09%(w/w) yield of LA 53.4% (mole basis)
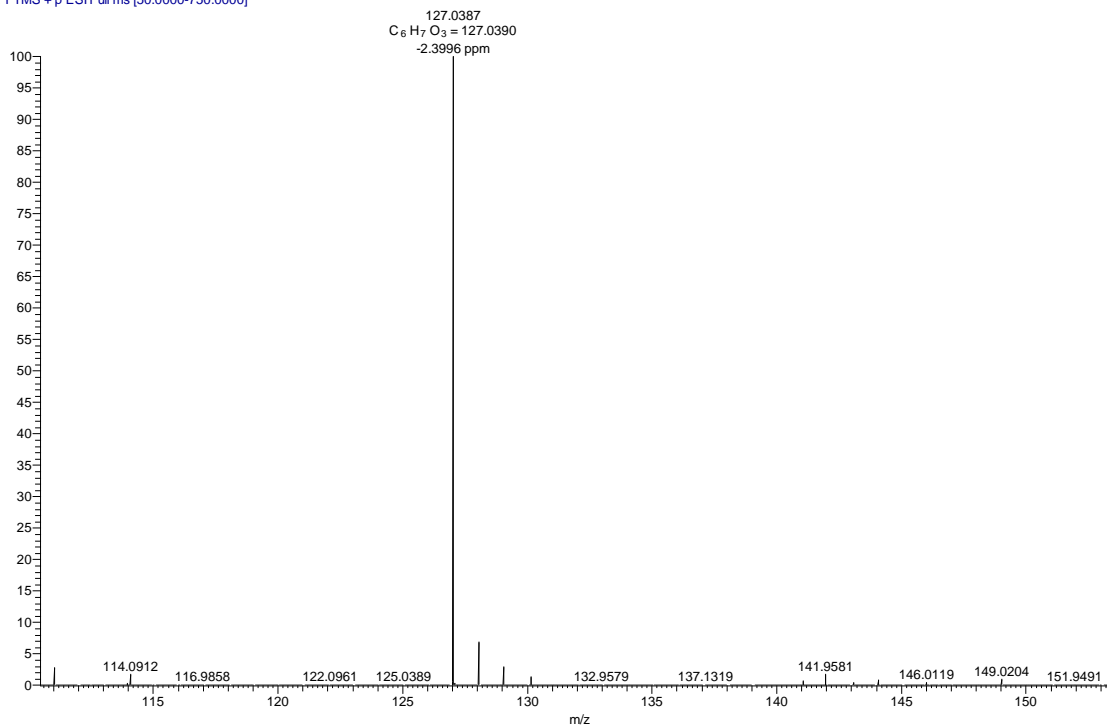
Figure 2.12 HR-Mass spectra at reaction Conditions- Temp-210 $^{\circ}$C; Time-30 min; NAG Concentration-5% (w/w);*p*-TsOH loading-3%(w/w) yield of 5-HMF 27.12% (mole basis)

2.6.3 Quantification of products

The aqueous product mixture obtained by the reaction was analyzed using HPLC equipped with the Aminex-87H 121 column (Bio-Rad, USA) and Shodex Refractive Index detector. The analysis of sample was done using 5mM sulfuric acid as mobile phase at a flow rate of 0.6 ml/min while keeping column at constant temperature of 50 $^{\circ}$C. The samples were filtered using 0.22 micron filters before injecting for the analysis. The calibration curves for each compound were generated using standard compounds commercially available for quantification using HPLC.
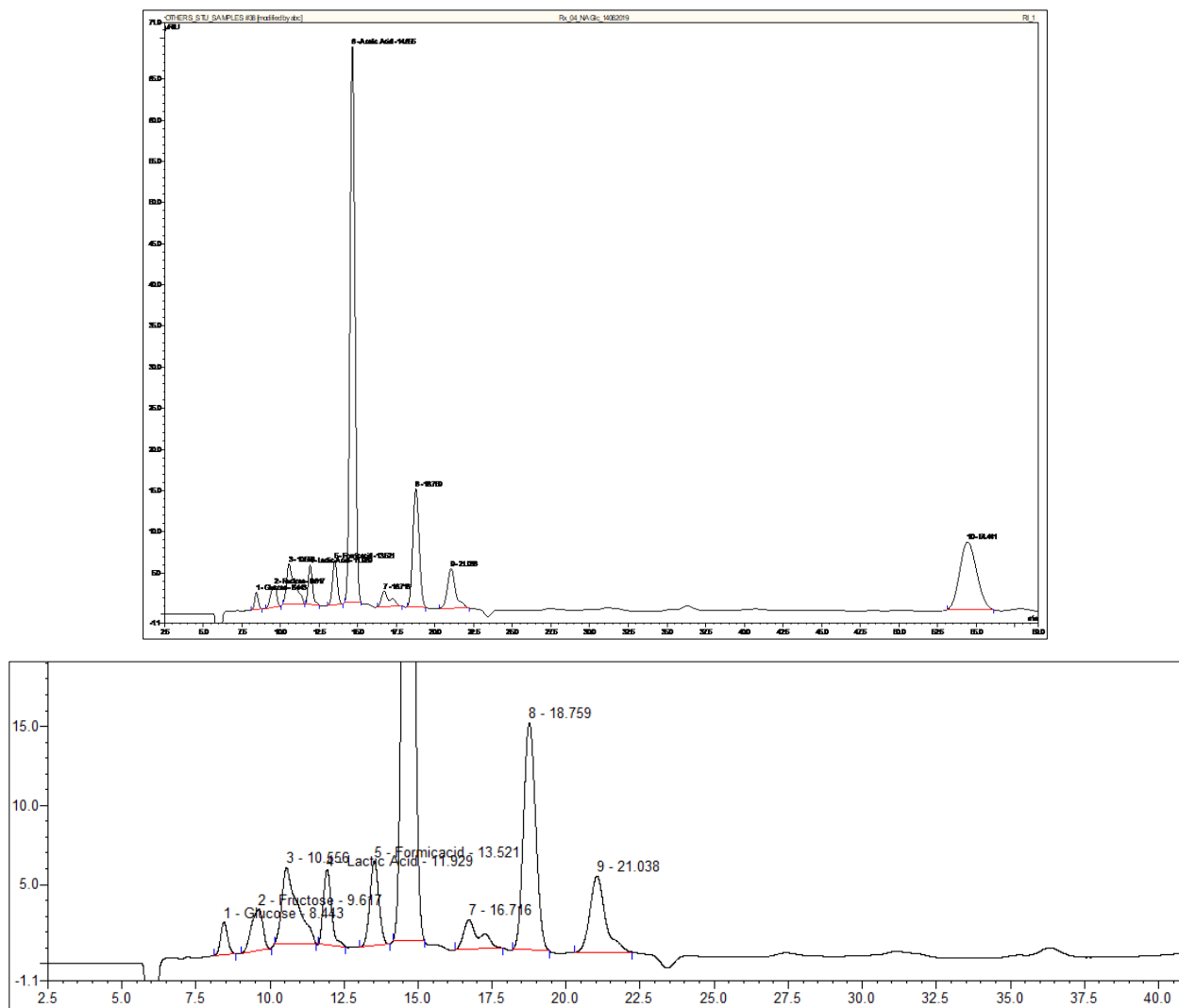
Figure 2.13 HPLC trace of product mixture obtained by non-catalytic subcritical water hydrolysis of NAG (200 ^{o}C,10 MPa and 5 %(w/w) of NAG)(Zoomed-in HPLC trace is shown at the bottom)
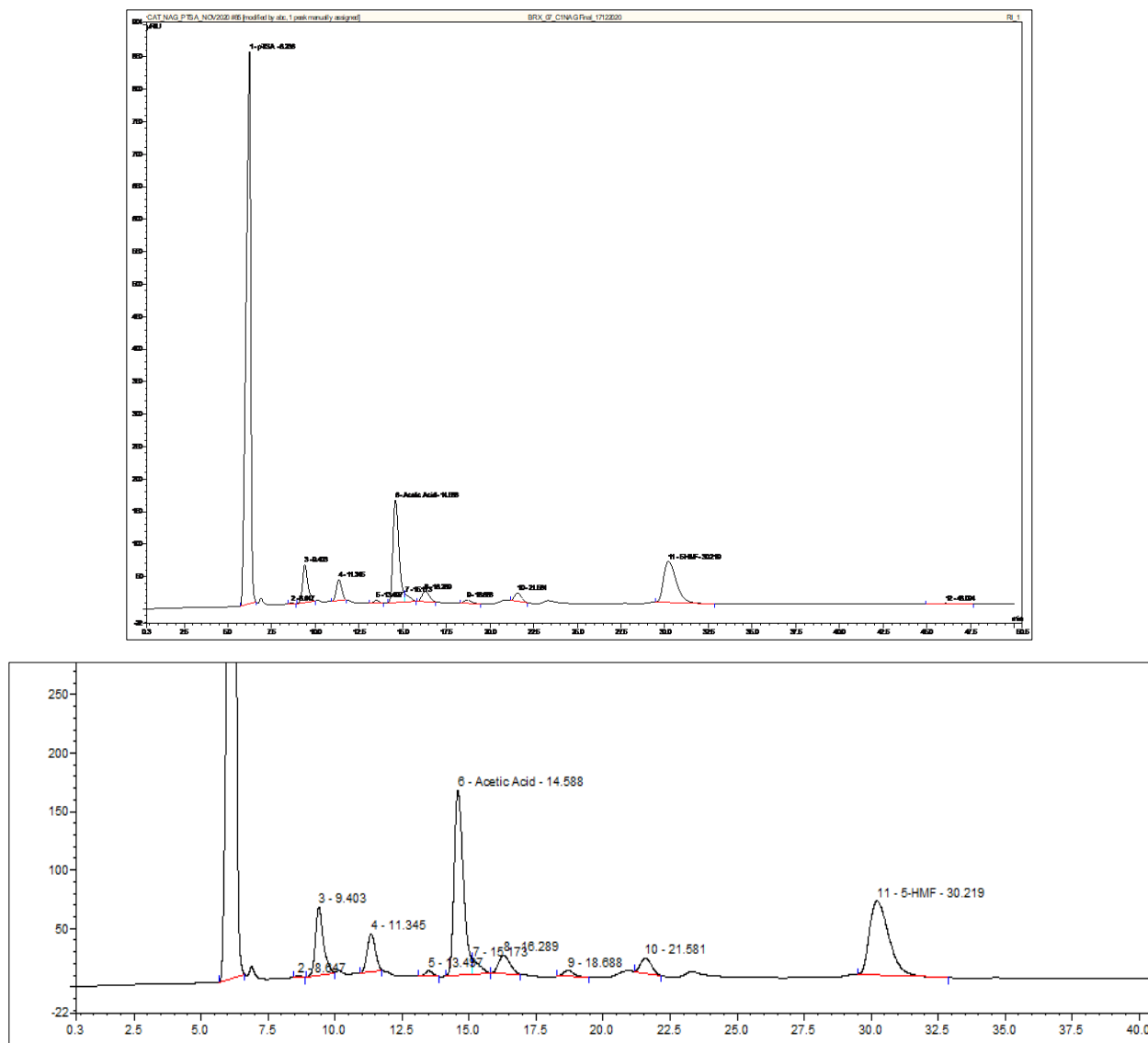
Figure 2.14 HPLC chromatogram of *p*-TsOH catalyzed subcritical water hydrolysis of NAG ;Reaction Conditions- Temp-210 ℃; Time-30 min; NAG Concentration-5% (w/w);p-TsOH loading-3 %(w/w) yield of 5-HMF 27.12% (mole basis)

Figure 2.15HPLC chromatogram of *p*-TsOH catalyzed subcritical water hydrolysis of NAG ; Reaction Conditions- Temp-238 °C; Time-83 min; NAG Concentration-1% (w/w);*p*-TsOH loading-4.09%(w/w) yield of LA 53.4% (mole basis)

2.6.4 Characterization of solids
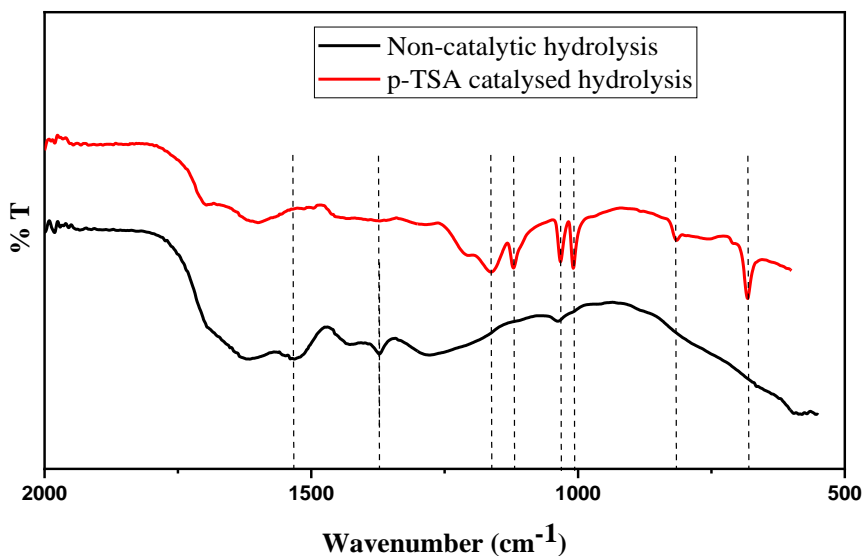
Figure 2.16 FT-IR of solids formed during catalytic and non-catalytic subcritical water hydrolysis of NAG

2.6.5 Parity plots for models developed for prediction of yield of 5-HMF and LA
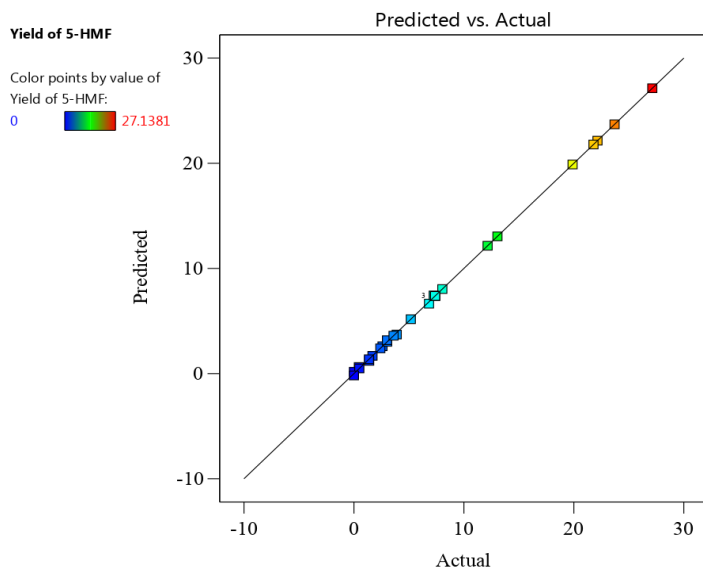
Figure 2.17 Parity plot for model for yield of 5-HMF
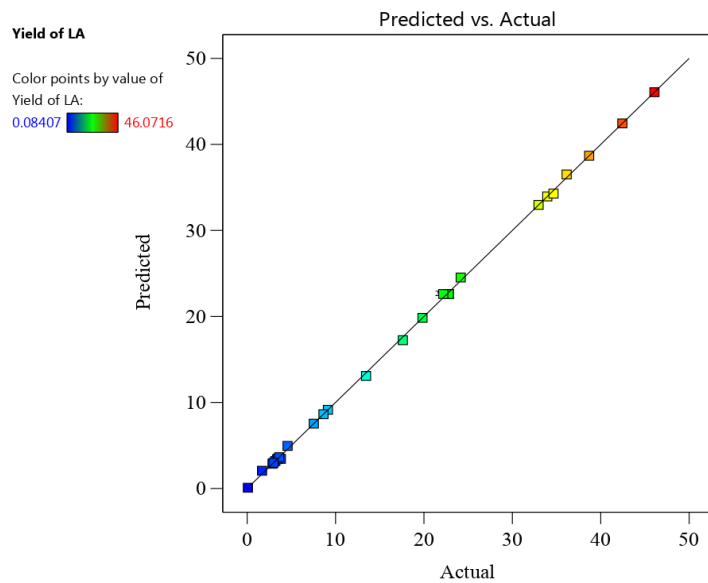
Figure 2.18 Parity plot for model for yield of LA

2.7 References

1   P. Stegmann, M. Londo and M. Junginger, *Resour. Conserv. Recycl. X*, 2020, **6**, 100029.

2   Y. Li, S. S. Bhagwat, Y. R. Cortés-Penã, D. Ki, C. V. Rao, Y. S. Jin and J. S. Guest, *ACS Sustain. Chem. Eng.*, 2021, **9**, 1341–1351.

3   N. Yan and X. Chen, *Nature*, 2015, **524**, 155–157.

4   S. Islam, M. A. R. Bhuiyan and M. N. Islam, *J. Polym. Environ.*, 2017, **25**, 854–866.

5   D. N. Poshina, S. V. Raik, A. N. Poshin and Y. A. Skorik, *Polym. Degrad. Stab.*, 2018, **156**, 269–278.

6   V. Y. Novikov, *Russ. J. Appl. Chem.*, 2004, **77**, 490–493.

7   A. Zhang, G. Wei, X. Mo, N. Zhou, K. Chen and P. Ouyang, *Green Chem.*, 2018, **20**, 2320–2327.

8   M. Qi, X. Chen, H. Zhong, J. Wu and F. Jin, *ACS Sustain. Chem. Eng.*, 2020, **8**, 18661–18670.

9   J. Wu, M. Qi, G. Gozaydln, N. Yan, Y. Gao and X. Chen, *Ind. Eng. Chem. Res.*, 2021, **60**, 3239–3248.

10   T. Werpy and G. Petersen, *Us Nrel*, 2004, Medium: ED; Size: 76 pp. pages.

11   Y. Wang, C. M. Pedersen, T. Deng, Y. Qiao and X. Hou, *Bioresour. Technol.*, , DOI:10.1016/j.biortech.2013.06.024.

12   S. Yu, H. Zang, S. Chen, Y. Jiang, B. Yan and B. Cheng, *Polym. Degrad. Stab.*, 2016, **134**, 105–114.

13   W. Hou, Q. Zhao and L. Liu, *Green Chem.*, 2020, **22**, 62–70.

14   H. Zang, S. Yu, P. Yu, H. Ding, Y. Du, Y. Yang and Y. Zhang, *Carbohydr. Res.*, 2017, **442**, 1–8.

15   G. Cevasco and C. Chiappe, *Green Chem.*, 2014, **16**, 2375–2385.

16   Á. Szabolcs, M. Molnár, G. Dibó and L. T. Mika, *Green Chem.*, 2013, **15**, 439–445.

17   M. Möller, P. Nilges, F. Harnisch and U. Schröder, *ChemSusChem*, 2011, 4, 566–579.

18   W. Fang, K. Chen, L. Ji, J. Zhu, B. Wu and Y. Wu, *Phys. Chem. Liq.*, 2019, **57**, 587–599.

19   R. Wang, T. Kobayashi and S. Adachi, *Food Sci. Technol. Res.*, 2011, **17**, 273–278.

20   N. Azizi, A. K. Amiri, R. Baghi, M. Bolourtchian and M. M. Hashemi, *Monatshefte fur Chemie*, 2009, **140**, 1471–1473.

21   B. Baghernejad, *Curr. Org. Chem.*, 2011, **15**, 3091–3097.

22   N. A. S. Ramli and N. A. S. Amin, *Bioenergy Res.*, 2017, **10**, 50–63.

23   S. Varala, B. Dharanija, B. Satyavathi, V. V. Basava Rao and R. Parthasarathy, *Chem. Eng. J.*, 2016, **302**, 786–800.

24   A. V. Bandura and S. N. Lvov, *J. Phys. Chem. Ref. Data*, 2006, **35**, 15–30.

25   N. V Dolgopyatova, V. Y. Novikov, I. N. Konovalova and N. M. Putintsev, *Russ. J. Appl. Chem.*, 2013, **86**, 986–991.

26   2005, 1.

27   M. R. Park, H. S. Kim, S. K. Kim and G. T. Jeong, *Fuel Process. Technol.*, 2018, **172**, 115–124.

28   S. Kang, G. Zhang, X. Yang, H. Yin, X. Fu, J. Liao, J. Tu, X. Huang, F. G. F. Qin and Y. Xu, *Energy and Fuels*, 2017, **31**, 2847–2854.

29   H. Pawar and A. Lali, *RSC Adv.*, 2014, **4**, 26714–26720.

30   A. Chuntanapum and Y. Matsumura, *Ind. Eng. Chem. Res.*, 2009, **48**, 9837–9846.

31   K. S. Lau, S. X. Chin, S. N. S. Jaafar and C. H. Chia, *Tetrahedron Lett.*, 2021, **80**, 153330.

Chapter 3

Supercritical water hydrolysis of *N*-acetyl-D-glucosamine: Kinetics using flow reactor
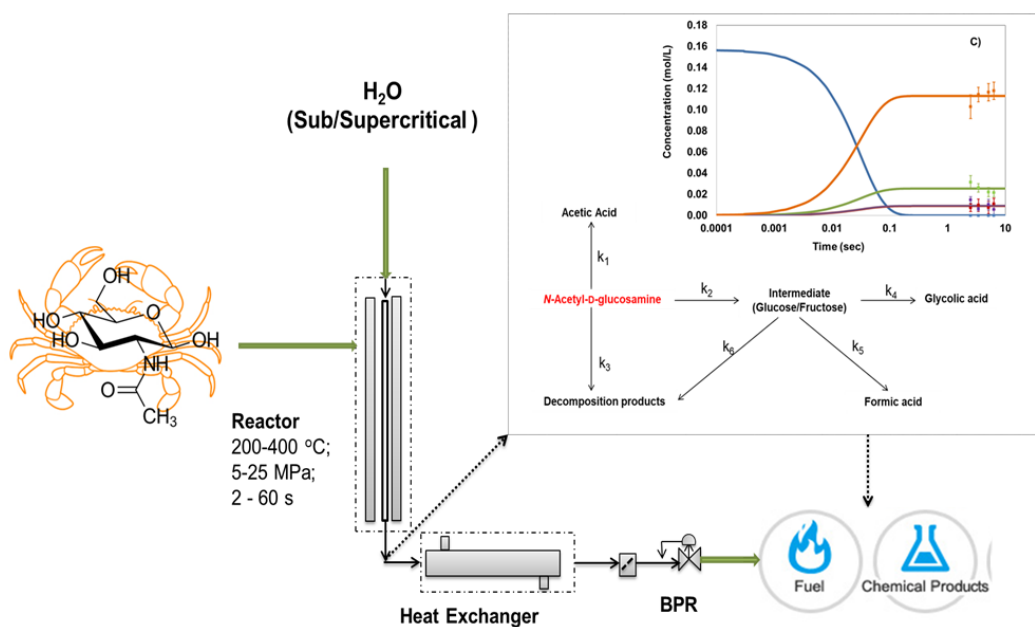
This chapter is based on:

Kulkarni, S. P., Joshi, S. S., & Kulkarni, A. A. (2023). Reaction pathways and kinetics of N-acetyl-D-glucosamine hydrolysis in sub-and supercritical water. Reaction Chemistry & Engineering. DOI: 10.1039/d3re00046j

3.1 Introduction

With rapid depletion in fossil fuels and increased global demand of energy, the need for the development of sustainable circular bio-economy is arisen. The efficient utilization of wastes and residues is a crucial step in the development the circular bio-economy.[1] With around 6-8 million tonnes of global annual production, seafood waste is an abundant and cost effective resource of carbon and nitrogen rich material and energy. Given the fact that it does not compete with the food chain, chitinous seafood waste has emerged as a potential feedstock to produce various chemicals and bring the carbon and nitrogen from oceanic biomass waste back to the energy cycle.[2] Along with protein and calcium carbonate, chitin is a major component representing almost 40 % of seafood shell waste.

Chitin is a biopolymer composed of linear chains of monomer *N*-acetyl-D-glucosamine (NAG). The direct conversion of chitin to value-added chemicals is inherently a two-step reaction involving depolymerisation of chitin to NAG followed by conversion of NAG to various compounds. Hence, NAG has a pivotal role in chitin chemistry and valorisation of chitinous biomass. Structurally, NAG is an amide derivative of glucose, however, unlike glucose NAG is still understudied specifically due to complexity introduced by nitrogen atom and the amide linkage. Owing to the presence of natural nitrogen in the molecule, NAG can be a natural resource for greener production of N-containing heterocyclic compounds. NAG has been previously explored for the synthesis of various compounds such as organic acids (viz. acetic acid, formic acid, levulinic acid, etc.) and platform chemicals (viz. 5-hydroxymethylfurfural (5-HMF), 3-acetamido-5-acetylfuran (3A5AF), and nitrogen containing heterocyclic compounds like Pyrrole, Pyrrolidine, etc.)[3].

Omari and co-workers[4] have reported one-pot synthesis of 3A5AF from NAG using boric acid (B(OH)$_3$) and sodium chloride (NaCl) in dimethyl acetamide. Under microwave irradiation, around 62 % of 3A5AF was obtained in 15 min at 220 °C from NAG. The use of mineral acids especially sodium and chloride ions need to be eliminated in order to develop an environmentally benign process. Drover and co-workers[5] employed ionic liquids (ILs) along with boric acid replacing NaCl to synthesize 3A5AF, 60 % yield of 3A5AF was obtained in a shorter time of 3 min under microwave irradiation. In another study, Chen and co-workers[6] found that the presence of chloride ion is essential in ILs to produce high yields of 3A5AF. At 180 °C, along with the additives boric acid and hydrochloric acid (HCl), the IL 1-Butyl-3-methylimidazolium chloride

([BMIm]Cl) resulted in the highest yield at the prevailing conditions. However, the overall yield reported was lower for ILs than for organic solvents and was in general lower than other reported processes. Wang et al.[7] have used greener IL system based on amino acids and

Table 3.1 Reaction conditions and properties of reaction medium [8–10]

Reaction medium	State	Temperature $^{\circ}$C	Pressure MPa	Time s	Density of water kg/m^3	pk$_w$	Dielectric constant (ε)
Subcritical water	Hot compressed liquid	250	25	1 - 60	820	-11.05	~78.5
Near critical water	Hot compressed liquid	350	25	1 – 60	620	-11.55	~15
Supercritical water	Supercritical state	400	25	1 – 15	160	-16.57	~5.9

obtained ~53 % yield of 3A5AF in 10 min from NAG without using boron based catalysts. Higher yield is attributed to the introduction of the chloride ions in the form of CaCl$_2$. Padovan et al.[11] showed that the comparable yields of 3A5AF could be achieved in a relatively simple process by employing AlCl$_3$.6H$_2$O, wherein 30 % yield was obtained at 120 $^{\circ}$C in N,N-dimethylformamide (DMF) solvent in 30 min. Zang et al.[12] employed Pyridinium salt based IL for converting NAG to 3A5AF, however, the need of additives, B$_2$O$_3$ and CaCl$_2$, along with IL 1-carboxymethyl pyridinium chloride could not be avoided to achieve higher 67 % yield of 3A5AF at 180 $^{\circ}$C in 20 min. Another platform chemical 5-HMF was synthesized from NAG using N-methylimidazolium hydrogen sulfate ([Hmim][HSO$_4$]) in a solvent mixture of water/dimethyl sulfoxide wherein 64 % yield of 5-HMF was obtained at 180 $^{\circ}$C, however, it required a longer reaction time of 6 h.[13] Some organic acids viz. acetic acid, formic acid and glyceric acid were produced from NAG at room

temperature using NaOH as a catalyst in the presence of oxidative reagents like hydrogen peroxide.[14] Though the obtained yields of formic acid (57 %), acetic acid and glyceric acid (total 42 %) were higher when compared at the milder conditions reported so far, the use of oxidants and sodium hydroxide poses various challenges in order to develop a complete green process. Thus, the so far reported methods for conversion of NAG to a variety of products use ILs or metal salts and organic volatile solvents. The intricate and expensive synthesis of ILs, disposal problems of metal and chloride containing waste and the use of organic volatile solvents poses various environmental challenges. There is a need for the development of newer and greener method to convert NAG to more valuable compounds, which not only eliminates the usage of these compounds but also reduces number of steps and is more universal for both monomer NAG and polymer chitin.

Subcritical (SubCW) and supercritical water (SCW) is being extensively explored as a potential green reaction medium for a number of reactions.[15–18] Thermodynamically, SubCW refers to a state of water at the temperatures higher than its boiling point but below critical temperature (100 ^{o}C < T < 374 ^{o}C) at a pressure high enough to maintain compressed liquid state. On the other hand, supercritical water (SCW) is a distinct state of water (T > T_c= 374 ^{o}C ; P > P_c= 22 MPa) wherein the distinction between liquid and vapour disappears and water becomes non-polar. The thermo-physical properties of water at such hydrothermal conditions can be tuned by varying temperature and pressure conditions. SCW is a more suitable medium for processing of chitin biopolymer as it can overcome the challenges associated with chitin such as solubility and crystallinity.[19] SCW hydrolysis has already been reported to be an effective pre-treatment for the enzymatic depolymerisation of chitin, wherein, the hydrolysis efficiency was significantly increased as the crystallinity of chitin was significantly reduced in SCW.[19–21] During our previous study we found that the NAG undergoes instantaneous reactions in SubCW.[22] Hence, during hydrothermal pre-treatment of chitin if even a small quantity of NAG is formed, its exposure to such conditions even for a fraction of time may produce the undesirable products. The presence of such compound can even affect the enzymatic depolymerisation of chitin if not separated. Thus, it is imperative to investigate the reactions of NAG at such conditions in order to develop processes using chitin and NAG. Osada et al. reported that NAG undergoes dehydration to form Chromogen I and III which further forms 3A5AF in water at subcritical

conditions.[23,24] Wang et al.[25] investigated the degradation behaviour of NAG in SubCW; however, they did not report the products in SCW condition. In our previous study, it was demonstrated that NAG forms organic acids such as acetic acid, formic acid and lactic acid in SubCW, however, longer reaction times and lower heating rates resulted in the excessive formation of solids.[22]

In this chapter, more insights into the hydrolysis of chitin model compound, NAG, in SubCW and SCW has been generated. Detailed analysis of conversion of NAG to various compounds was done to understand the underlying mechanism and the kinetics of acid formation are elucidated using a compact continuous flow reactor enabling short residence times and high heating rates. This manuscript reports for the first time the synthesis of valuable chemicals from NAG via SubCW and SCW hydrolysis without using any external catalyst or oxidant.
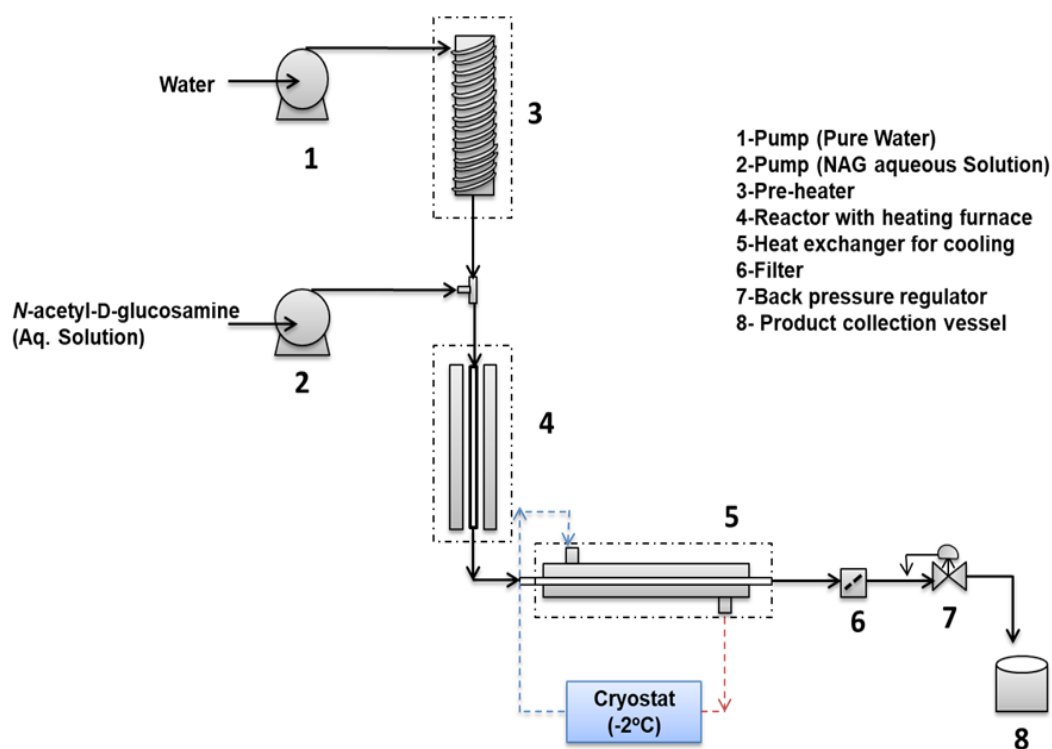
Figure 3.1 Schematic of the experimental set up used for hydrolysis of NAG in subcritical and supercritical water

3.2 Experimental

3.2.1 Chemicals

NAG was purchased from HiMedia Laboratories (India). Glycolic acid and acetamide was obtained from Merck Specialities. Acetic acid and formic acid were purchased from Loba Chemie Pvt. Ltd. and Avra Chemicals Pvt. Ltd., respectively. The standards for 5-HMF, 3-pyridine carboxyldehyde, Piperidine, Pyrrole, N-methyl pyrrolidine, pyridine, 2-acetyl pyrazine were obtained from sigma Aldrich. The deionized water (LabQ) was used in all the experiments. Analytical grade solvents were used for analysis purpose.

3.2.2 Hydrolysis of NAG in SubCW and SCW using a continuous flow reactor

Experiments were carried out using an experimental set up designed for operation of continuous flow high pressure and high temperature reactions (figure 3.1). In a typical continuous hydrolysis experiment, water was pumped using high pressure pump 1 (Gilson 305) to a helical coil preheater at the flow rates in the range of 8 to 25 mL/min, where the water was heated to temperatures (250 to 420 °C) higher than what is desired in the reactor using the electrical heater (1 kW, Yog Electronics, India) placed inside the brass rod around which the preheater helical coil is wrapped, as shown in figure 3.9. The aqueous solution of NAG (1-10 %) was fed to the tee mixer using another high pressure pump 2 (Gilson, 305) at the flow rate of 0.8 to 2.5 mL/min, where it was instantly mixed with SubCW or SCW, which further entered a 5.5 mL tubular reactor (SS 316) tube (Sandvik 3R60; OD = 6.35 mm and thickness = 1.24 mm). The reactor was heated to the reaction temperatures of 250 °C to 400 °C using the electrical furnace (500 W). Temperature was monitored by using thermocouples at the inlet and outlet of the reactor and a PID controller (KLB instruments). The reaction mixture was quickly cooled down to the room temperature using a sequence of the heat exchangers placed at the immediate exit of the reactor using the external cooling jacket through which coolants are passed using the chilling unit (Thermo HAAKE DC 30). All the experiments were carried out at the constant pressure of 25 MPa maintained by using back pressure regulator (Tescom, model 26) placed after the heat exchanger and a

filter of 7 micron mounted inline to avoid flow of any solids to the regulator. A range of operating conditions was selected, given in table 3.1.

The residence time (τ) was calculated considering the variation in the density with temperature and pressure, using following formula,

$$\tau = \frac{V}{[F * (\rho_I / \rho_{RxT})]}$$

where V is the volume of the reactor, F is the total flow rate, ρ_I and ρ_{RxT} are densities of pure water at room temperature and at reaction temperature, respectively. Since, the reaction mixture was a dilute aqueous solution of NAG (<1 % (w/w)), the influence of density variation on residence time is accounted by considering density of pure water (99 % (w/w)), similar to the approach adopted by several researchers previously.[24,26–29] Corresponding values of densities were obtained from National Institute of Standard and Technology (NIST) database.

3.2.3 Design of reaction set up and reaction matrix for flow of SubCW and SCW

Unlike constant property flow of fluids, the design of flow reaction set up and reaction matrix for SubCW and SCW is not straight forward, as the governing thermo-physical properties vary continuously with variation in temperature and pressure. Especially the maximum achievable temperature and minimum residence time for this particular reactor set up was dependent on the i) minimum/critical mass for achieving higher temperature and ii) heat transfer limitations and the minimum residence time. The specific heat capacity of water goes through maxima with highest value at pseudo critical point (76 J/gK at 385 °C and 25 MPa and 13.2 J/gK at 400 °C and 25 MPa), hence, the flow rate required to achieve particular temperature using the pre-heater (1 KW) was different at different temperatures. Thermodynamically, SubCW is a hot compressed state, whereas, SCW does not undergo phase change, hence, no latent heat was considered. The approximately flow rates were calculated simply by sensible heat balance across pre-heater,

$$Q = \dot{m} C_{pRxT} [T_{RxT} - T_I]$$

where Q is the heat provided by external heater, $\dot{m}$ is mass flow-rate, T_{RxT} is desired reaction temperature, T_I is reactor inlet temperature (25 °C) and C_{pRxT} corresponds to specific heat capacity of water at T_{RxT} temperature. It should be noted that the C_{pRxT} is a function of

temperature; however, for a generic idea of flow ranges the maximum value at reaction temperature was considered. The shorter residence times were required to analyse the primary products of NAG hydrolysis. One of the ways to achieve short residence times was by using high flow-rates, however, heat transfer limitations posed challenges in achieving shorter times (<2 s). Considering, this transient state unidirectional heat transfer from reactor wall to the fluid, the estimation of minimum residence time (i.e. maximum mass flow rate) was done. The major problem with this method is the unknown values of h, heat transfer coefficient, at SubCW and SCW. There are several modified correlations, which considers the continuous change in density, viscosity, thermal conductivity and overall thermal diffusivity, however, till date no accurate correlation has been proposed.[30] Nevertheless, from the experimental observation and theoretical calculations, it was understood that in order to have a practical reactor configuration for reactions with flow of SCW providing required shorter reaction times (s), the reactor should be designed to provide maximum heat transfer coefficient by means of either high heat transfer area and low volume or by improving heat transfer by mixing during the flow. In this study, the reactor configuration described in section 3.2.2 is used; a small tubular reactor with a helical coil preheater of almost double volume was used to achieve high temperatures at 25 MPa. NAG hydrolysis was explored in the range of shortest possible residence times achieved by the current reaction set up.

3.2.4   Hydrolysis of NAG in SubCW using a batch reactor

Initially, batch reactions were carried out in a batch autoclave of volume 300 mL (Hast C, Parr Instruments, Moline, IL, USA), designed for maximum operating pressure of 17.5 MPa (2500 psi). In a typical experiment, the reactor was loaded with the aqueous reaction mixture of NAG (0.1 to 5 % w/w). Pressure in the reactor was maintained at 5 MPa under argon. The initial pressure was estimated considering the expansion of argon gas with reaction temperature. The reactor was heated to the required temperature (170 to 250 °C) using the electrical heating mantle. The temperature and stirring speed of 600 rpm were maintained by using a PID controller. After the stipulated time (30-90 min), the reactor was quickly cooled down to room temperature by passing cold water through dip U tube placed

inside the reactor. In case of solid formation during the reaction, the solid and liquid products were separated by vacuum filtration and analysed without any further treatment.

3.2.5 Analytical techniques

The qualitative analysis of the products is done by using High Resolution Mass Spectrochem (HR-MS) (Q-exactive orbitap spectrometer; Thermo Scientific Acela 1250 Pump) equipped with ODS C18 (Hypersil™ ODS C18) and Electrospray Ionisation Mass Spectrometry (ESI) detector. High performance liquid chromatography (HPLC) (Agilent 1260 Infinity II). The solids formed during the reaction were filtered and analysed using Attenuated Total Reflection- Fourier transform infrared spectroscopy (ATR-FTIR) (Perkin Elmer Spectrum 65). The quantitative analysis of NAG, glycolic acid, formic acid, acetic acid, acetamide was done using HPLC equipped with the Aminex-87H column (Bio-Rad, USA) and Shodex Refractive Index detector. A mobile phase of 5 mM sulfuric acid was passed at the flow rate of 0.6 mL/min through the column maintained at 50 $^{\circ}$C. The calibration curves for each compound were generated for quantification using HPLC. In another method, the HPLC (Agilent 1260 Infinity II) equipped with ODS C18 (Hypersil™ ODS C18) column and UV detector was used to qualitatively investigate the products of reaction mixture. A mobile phase of 90:10 Water: Methanol was used to separate the products passed through column at the flow rate of 0.5 mL/min.Based on previous reports on products of NAG hydrolysis and pyrolysis, the number of products were compared and analyzed. There were several of unknown peaks in the chromatogram the identified peaks were confirmed by comparing retention times with standard compounds and/or by spiking standard compounds to the samples. Solids were analyzed using ATR-FTIR. Owing to very small formation of non-condensable gaseous products at particular reaction conditions, no gaseous products were analysed. Total reactant conversion, product selectivity and yield of products are estimated on basis of mass balance and mole balance.

3.3 Results and discussion

3.3.1 Product distribution and reaction pathways of NAG hydrolysis in SubCW and SCW

The conversion of NAG in SubCW and SCW is instantaneous as NAG was almost always consumed completely at all temperatures (200 to 400 ^{o}C) even at lowest reaction time of 2 s. The products with diverse nature were obtained during hydrolysis of NAG at the tested hydrothermal conditions including solids, gases and majorly aqueous compounds, given in table 3.2. As liquid products were always the dominant fractions with minute solids or gases (< 1 %), no attempts were made to quantify solid and gaseous products. The most commonly identified products of NAG hydrolysis in water at both subcritical (250 to 350 ^{o}C) and supercritical temperatures (400 ^{o}C) were glycolic acid, formic acid, acetic acid, 5-HMF and acetamide. Other identified products were furfural, pyrazole, 3-pyrdine carboxyldehyde, piperidine, 1-methyl pyrrolidine, pyridine, 2-acetyl pyrazine, piperidine, pyrrole. These products were found to be present in reaction product mixture at supercritical conditions but were not seen over the entire reaction temperature and residence time ranges. There were several other unidentified products in product mixture indicated by the unknown peaks in the chromatogram as shown in Figure 3.10-3.14, these are suspected to be the nitrogen containing compounds, which are predominantly heterocyclic, few compounds were identified by HR-MS, shown in figure 3.15-3.21.

Figure 3.2 shows the plausible reaction pathways for the formation of the identified compounds from NAG in SubCW and SCW. The presence of wide number of products of diverse nature confirmed that during SubCW or SCW hydrolysis of NAG, it undergoes rapid decomposition forming several compounds which further undergo secondary degradation. The products identified from such sequence of reactions are the most stable compounds at the tested hydrothermal conditions. NAG first undergoes deacetylation to form acetic acid and glucosamine, which is an acid catalysed reaction and/or requires oxidative reagent.[31] The pk_w of water decreases from 14 at ambient conditions to 11.2 at subcritical and/or supercritical conditions providing enough acidity for reaction medium to catalyse the NAG deacetylation, refer table 3.1.

Table 3.2 Product distribution of by continuous flow hydrolysis of NAG in SubCW and SCW (% yield for various products: (1) Glycolic Acid, (2) Formic Acid, (3) Acetic Acid, (4) 5-HMF, (5) Furfural, (6) Acetamide, (7) Pyrazole, (8) 1-Methyl pyrrolidine, (9) 3-Pyridine carboxyldehyde, and (10) 2-Acetyl Pyrazine)

Temperature (°C)	Pressure (MPa)	Residence Time (s)	Initial NAG† (% w/w)	% yield										Accountability* %
				1	2	3	4	5	6	7	8	9	10	
400	25	3-10	0.7-0.9	20.64 ±1.99	3.68 ±2.12	5.43 ±2.0	0.142 ±0.07	0.124 ±0.1	7.29 ±0.95	0.29 ±0.16	4.86 ±0.09	0.36 ±0.08	0.76 ±0.32	40.58 ±2.09
250	25	24-30.5	0.9-1	11.97 ±2.13	1.19 ±0.07	5.34 ±0.26	0.733 ±0.38	0.1 ±0.01	3.25 ±0.29	0	0	0	0	22.59 ±1.61

*Accountability=(weight of total identified products*100 / initial weight of NAG) †Concentration of NAG after mixing with hot water at reactor inlet

Moreover, the dissociation of water is an endothermic reaction, hence, with increase in temperature more dissociation of water molecules occurs which can also provide an oxidative environment under these conditions. At these conditions water can act as both mild catalyst as well as an oxidant. However, the phase of water that is, subcritical or supercritical, has a significant effect on dominating reaction mechanism. A few products such as nitrogen containing heterocyclic compounds identified as pyrazole, 3-pyrdine carboxyldehyde, piperidine, 1-methyl pyrrolidine, pyridine, 2-acetyl pyrazine, piperidine, pyrrole were detected only in SCW at 400 $^{\circ}$C and 25 MPa. This can happen if glucosamine further reacts in two competing ways; (i) either it undergoes deamination forming glucose or (ii) gets protonated to form ammonium salt which further undergoes cyclization to form distinct cyclic products. The only pathway to form glycolic acid and formic acid is by oxidation of glucose, which is also reported to happen at hydrothermal liquefaction of cellulose previously.[32,33] Hence, the reaction medium is favouring both oxidation and reduction. Another important compound 5-HMF was believed to be formed by dehydration of glucose. The presence of acetamide indicated that the acetic acid undergoes amidation by reacting with ammonia formed by deamination of glucosamine. There may be other pathways by which amides can be generated as decomposition products.[34] The phase of reaction medium has significant influence on product composition, which is discussed in detail in section 3.3.2.

3.3.2 Effect of state of water or reaction temperature

Water is a unique reaction medium owing to its tunable thermo physical properties which can be tuned by varying temperature and pressure. Water at subcritical state exists as a hot compressed liquid. At these conditions, the dissociation of water molecules is highest as indicated by highest ionization constant value 10^{-11} (at 200 to 350 $^{\circ}$C), hence, water turns acidic at subcritical conditions.[10]As shown in figure 3.3, the phase of water had influence on the nature of products. In SubCW at 250 $^{\circ}$C and 25 MPa, the products among identified were glycolic acid, formic acid, acetic acid, 5-HMF, furfural and acetamide. Glycolic acid was the major product with a yield of 13 % on mass basis along with 3 to 7 % yield of acetic acid and acetamide along with traces of formic acid, 5-HMF and furfural. At these

conditions, the flow reactor often choked due to excessive formation of solids and it is not easy to remove the charred products that get stuck to the reactor wall. The FT-IR characterization of solids revealed that the solids are humins and have structural similarity as that of solids formed during batch reactions of NAG in subcritical water. Solids, in absence of any other strong catalyst, are formed by the self-aldol condensation and polymerization of glucose and 5-HMF.[35] Hence, it could be concluded that NAG undergoes immediate deacetylation followed by deamination and several other degradation reactions leading to the formation of solids by polymerization of 5-HMF and other degradation products.

On the contrary no solids were formed during the hydrolysis of NAG in SCW i.e. at 400 °C and 25 MPa. Nevertheless, the presence of foam and bubbles coming from the outlet indicated the gasification of products. The reactions in SCW were carried out smoothly in the flow reactor without choking. At these conditions, the maximum yield of glycolic acid i.e. 23.2 % on mass basis was obtained along with 5.4 % acetic acid and 3.6 % formic acid. No 5-HMF and furfural were detected at these conditions. Interestingly, some distinct heterocyclic compounds viz. pyrazole, 3-pyrdine carboxyldehyde, piperidine, 1-methyl pyrrolidine, pyridine, 2-acetyl pyrazine were identified in the product mixture of SCW hydrolysis of NAG. While all the heterocyclic products could not be quantified using our analysis method, the total yield of pyrazole, 1-methyl pyrrolidine, 3-pyridine carboxyldehyde and 2-acetyl pyrazine was around 6 % (w/w of NAG). The formation of exactly these compounds was not observed during SubCW hydrolysis of NAG, however, the chromatogram had several peaks nearby the retention time of these compounds, hence, there is possibility that some other similar heterocyclic products are formed during hydrolysis of NAG in both SubCW and SCW. Water under subcritical conditions is a hot-compressed liquid state with higher acidity (pk_w~11.05) which is a favourable reaction medium for ionic reactions. On the other hand, at supercritical conditions, water, with density 160 kg/m^3, lower dielectric constant and ionic product values, loses its liquid-like characteristics and behaves as gas like fluid promoting free radical reactions.[36] Therefore, such a change in product distribution observed during hydrolysis of NAG can be attributed to the change in the phase of water and consequently the properties of reaction medium. This dramatic change in solvent properties and consequently in the product distribution can

act as a control factor for tuning the product distribution, especially beneficial in case of molecules containing nitrogen like NAG as the distinct N-heterocyclic compounds viz. pyrazole, 3-pyrdine carboxyldehyde, piperidine, 1-methyl pyrrolidine, pyridine, 2-acetyl pyrazine, pyrrole are formed at supercritical conditions.[37]
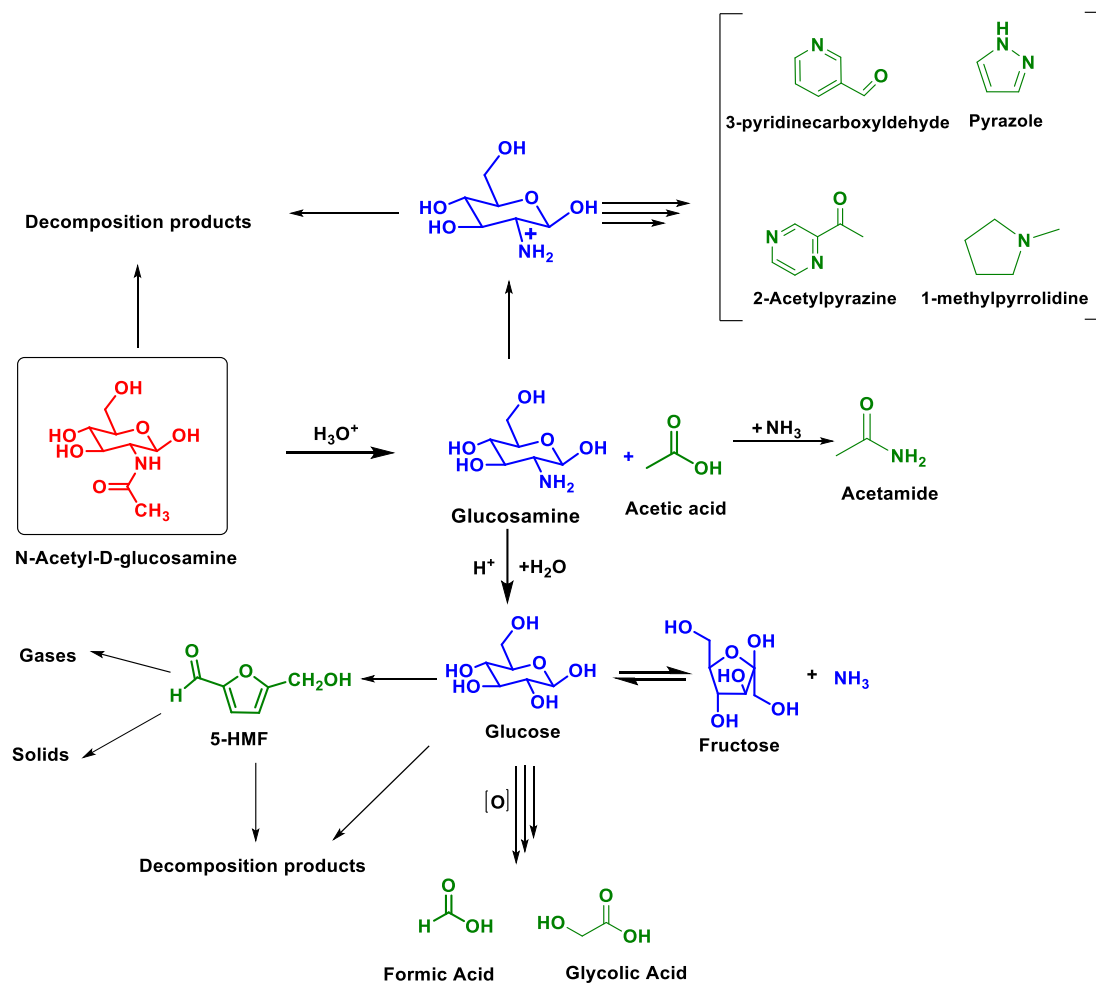
Figure 3.2 Plausible reaction pathways of products formation during SubCW/SCW hydrolysis of NAG

3.3.3 Effect of pressure

There was no significant effect of pressure on composition of aqueous products in the range of pressure investigated here, however, the pressure had role in suppressing gas formation during SCW hydrolysis and solid suppression during SubCW hydrolysis. Due to the very low concentration of gaseous and solid products, the effect of pressure could not be

quantitated, figure 3.22, shows the visual changes observed during NAG hydrolysis in SubCW at 250 °C at 5 MPa, 12.5 MPa and 25 MPa, respectively. The reaction mixture was found to be cloudy at 5 MPa which turned dark at 12.5 MPa and turned clear brown at 25 MPa indicating the compositional change.

Table 3.3 Rate constants obtained from the model for NAG hydrolysis in SubCW and SCW

Temperature (°C)	$k_1(s^{-1})$	$k_2(s^{-1})$	$k_3(s^{-1})$	$k_4(s^{-1})$	$k_5(s^{-1})$	$k_6(s^{-1})$
	NAG† to Acetic acid	NAG to Intermediates	NAG to DP†	Glycolic acid formation	Formic acid formation	Intermediates to DP
250	15.9	64.9	180.1	124.1	9.8	139.2
350	22.0	81.2	162.9	130.3	18.5	129.0
400	14.8	99.7	152.3	126.1	48.5	118.6

† [NAG]: *N*-acetyl-D-glucosamine; [DP]: Decomposition Products
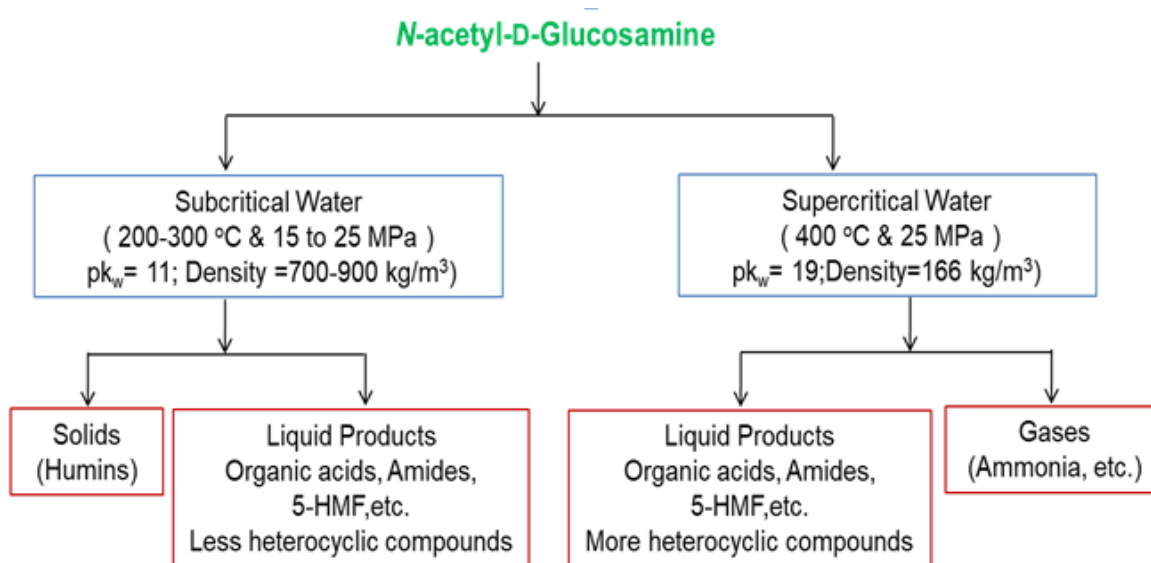
Figure 3.3 Effect of state of water on product distribution during NAG hydrolysis in SubCW and SCW

3.3.4 Effect of residence time

Due to the excessive formation of solids in SubCW (250 ^{o}C and 350 ^{o}C) resulting in the blockage of the reactor, the influence of the residence time was explored mainly in SCW at 400 ^{o}C and 25 MPa, where more products were identified and no solids were formed. The effect of time was studied by varying the flow rates of pure water and aqueous NAG solution in a constant ratio. The residence time was varied in the range of 3 to 10 s. Above 10 s, there was almost no change in the product yields. The yields of glycolic acid and 3-pyridine carboxyldehyde were seen to be higher at 5 s and decreased further, which can be attributed to their further degradation to other compounds. On the contrary, 1-methyl pyrrolidine formed only after 5 s, whereas the yield of formic acid decreased with residence time. The yields of all other products identified were less influenced by this range of residence time in this time range as shown in figure 3.4.

3.3.5 Effect of heating rate

The heating rate was observed to have a significant effect on the product distribution of hydrolysis of NAG. In general, the heating rate of batch reactor was around 2.5 ^{o}C/min, which means that at least 58 min were required to achieve 170 ^{o}C from room temperature of 25 ^{o}C. Few batch reactions were carried out to understand the effect of time during heating period, by allowing reaction mixture to achieve the temperature and then cooling it quickly. It was observed that the major products formed during the heating periods were solids, which were similar to the compounds obtained in batch reactions, carried out at various subcritical conditions. The yield of solids during the batch experimentation in SubCW was not much affected by the changes in the operating temperature and pressure, but it increased with increase in the reaction time. Another experiment was carried out to check the minimum time required for the complete conversion of NAG, it was observed that the NAG was completely converted during heating period only. Hence it was evident that the higher heating rates are required for investigation of immediate transformations NAG is undergoing in SubCW and SCW. The higher heating rates of around 150-190 ^{o}C/s were obtained using continuous reaction set up developed as shown in figure 3.1, wherein the desired temperature is reached in <1 to 8 s depending on the temperature set point (due to density variation, discussed previously).

Few batch reactions were carried out to understand the effect of time during heating period, by allowing reaction mixture to achieve the temperature and then cooling it quickly. It was observed that the major products formed during the heating periods were solids, which were similar to the compounds obtained in batch reactions, carried out at various subcritical conditions. The yield of solids during the batch experimentation in SubCW was not much affected by the changes in the operating temperature and pressure, but it increased with increase in the reaction time. Another experiment was carried out to check the minimum time required for the complete conversion of NAG, it was observed that the NAG was completely converted during heating period only. Hence it was evident that the higher heating rates are required for investigation of immediate transformations NAG is undergoing in SubCW and SCW. The higher heating rates of around 150-190 ^{o}C/s were obtained using continuous reaction set up developed as shown in figure 1, wherein the desired temperature is reached in <1 to 8 s depending on the temperature set point (due to density variation, discussed previously).
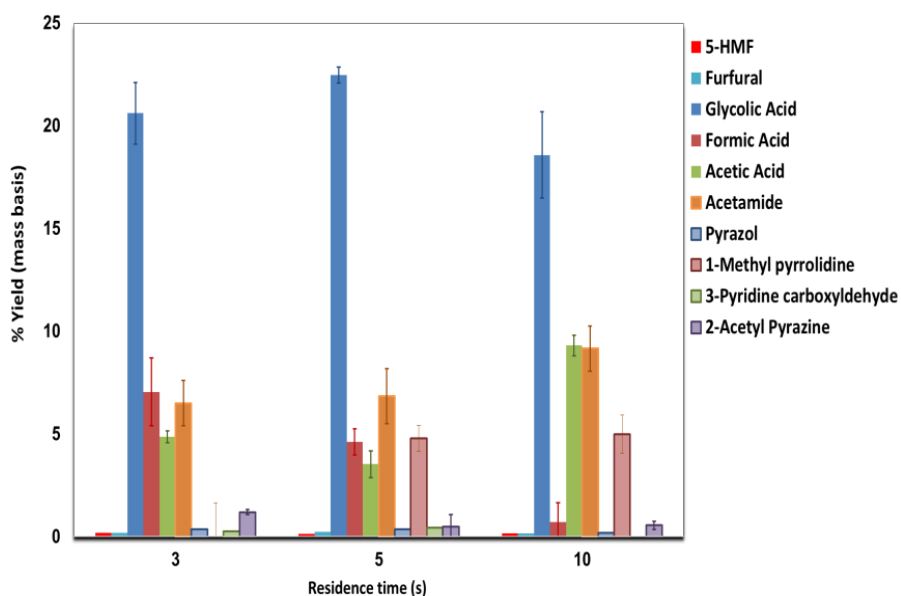
Figure 3.4 Effect of residence time on yields of the products at NAG concentration 1 % (w/w); 400 ^{o}C; 25 MPa

3.3.6   Kinetics of formation of organic acids

During hydrolysis of NAG by SubCW and SCW, several key chemicals were formed. In particular, the oxidation products carboxylic acids acetic acid (AA), glycolic acid (GA) and formic acid (FA), etc. are key platform chemicals finding wide applications. Here, in order to understand the decomposition of NAG and formation of oxidation products i.e. carboxylic acids AA, GA and FA, etc. during SubCW and

SCW hydrolysis, the kinetics of the reactions was investigated. Since, the hydrolysis of NAG involved several series and parallel reactions, speculated based on the identified products; few approaches were adopted in order to come out with an appropriate reaction model. The decomposition products were defined to account all unknown products majorly including the cyclic products and the reduction products. Initially, the conventional approach of the detailed stoichiometric reactions and net rate laws was tested as shown in Figure 3.5a. It was difficult to have a precise stoichiometry or mole balance for formation of GA, FA, acetamide and other unknown products as these compounds were the secondary degradation products of primary products. Moreover, the lack of information on concentration of Glucosamine, ammonia and other unidentified compounds would have resulted in the poor predictions of yields of the model developed using this scheme. Hence, another approach of lumping was adopted to describe the hydrolysis of NAG in SubCW and SCW. Two different lumping schemes, Figure 3.5b and 3.5c, were proposed using two different criteria. In the first scheme, the products were grouped together considering the type of reactions of their formation e.g. deacetylation, oxidation, amidation, decomposition, etc. Another scheme was developed by grouping the products of similar functional groups e.g. organic acids, amides, furfurals, sugars, decomposition products, etc. Based on these schemes, assuming each step to be first order, the kinetic equations were deduced. The system of equations was solved using the least square fit and *fminsearch* solvers in the MatLab to find out the values of k. The two models developed using the two lumping schemes resulted in poor prediction of compounds. The values of predicted concentrations of the products were either higher or lower. It was attributed to the unknown fraction of the converted NAG. Nevertheless, the model was further simplified by considering only known reaction pathways.

Amidation products
(Acetamide,etc.)

c.

Oxidation products (GA,FA etc.)

Deacetylation products
(AA ,etc.)

N-acetyl-D-glucosamine   **Sugars**
(Glucose/Fructose,etc.)

DP
(Other hydrolysis products, cyclic
products,solids,gases,etc)   **Dehydration products (5-HMF,etc.)**
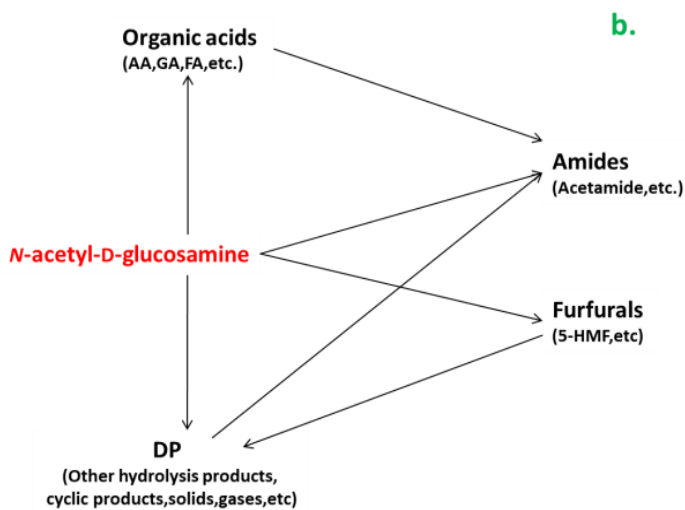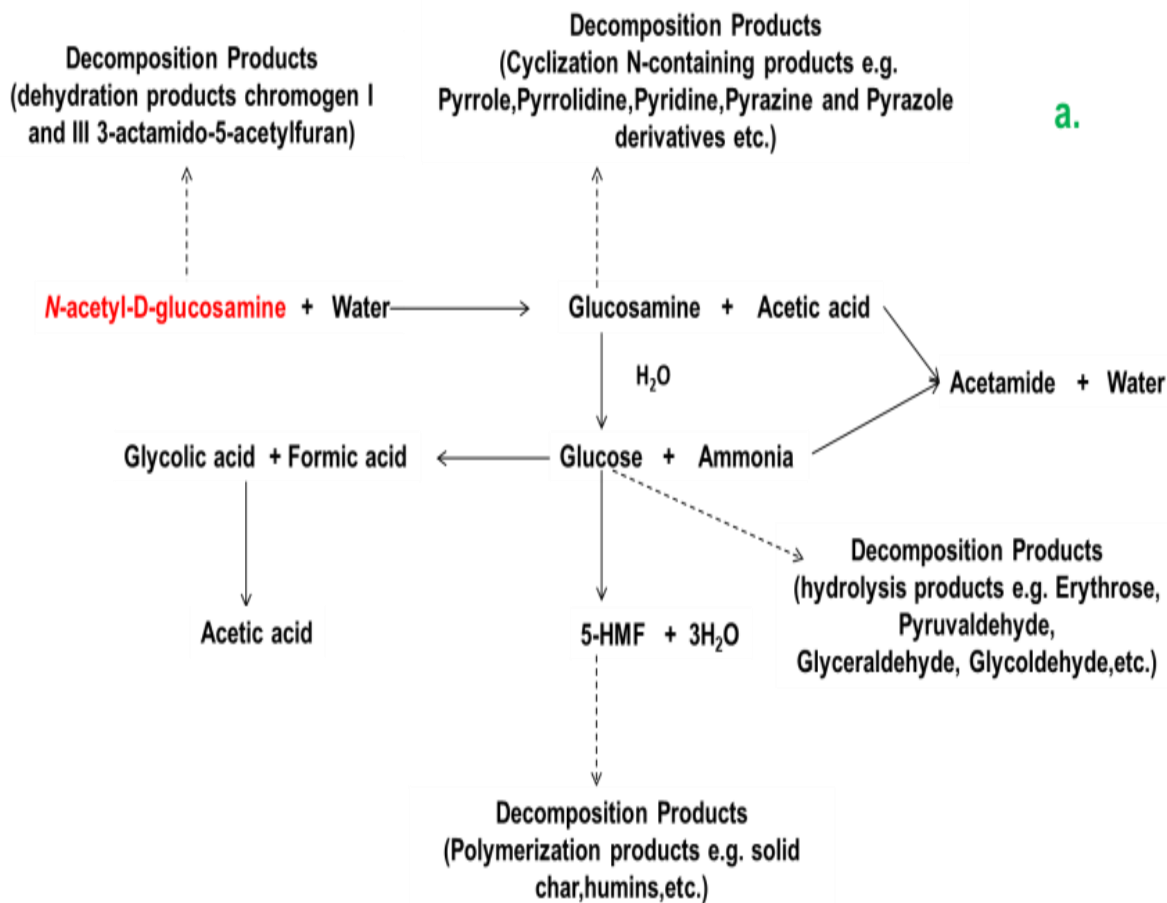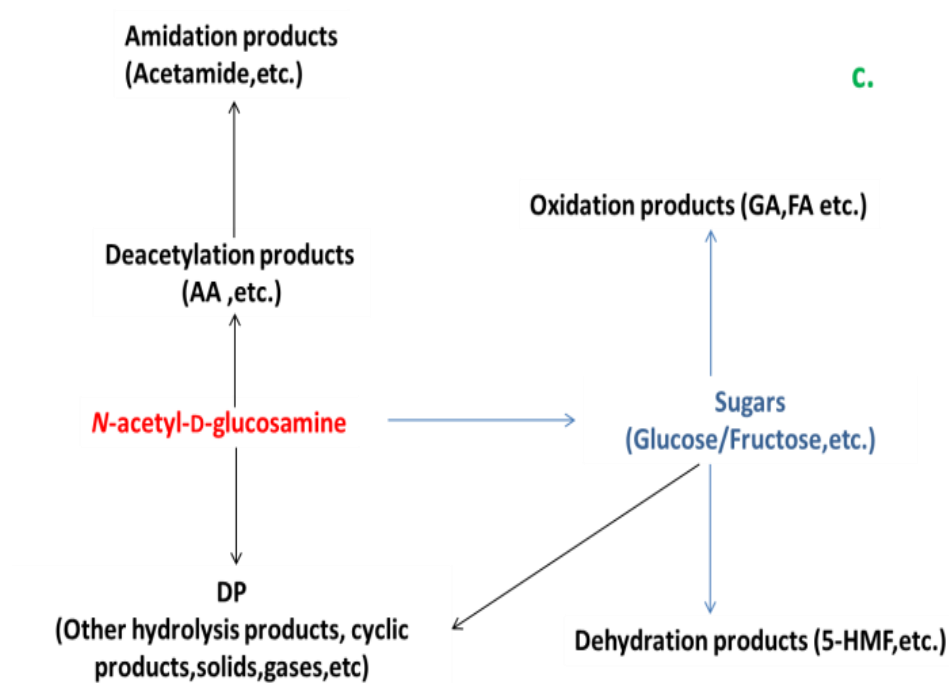
Figure 3.5 Schemes for lumping of products of NAG hydrolysis in subcritical and supercritical water a) Individual reaction pathways b) Lumping of reaction schemes /paths on basis of functional groups; c) Lumping on basis of type of reaction products

A wide product distribution is obtained during NAG hydrolysis in SubCW and SCW. In particular, the oxidation products carboxylic acids viz. acetic acid (AA), glycolic acid (GA) and formic acid (FA) are key platform chemicals finding wide applications.[38–40] The formation of myriad compounds and complex reactions complicates the understanding of the mechanism and kinetics of NAG hydrolysis. Similar complexity in developing kinetic model in case of hydrothermal liquefaction, pyrolysis or gasification of biomass, have been simplified by adopting the lumping approach.[41]

A simplified kinetic model is developed to predict the yields of AA, GA and FA as shown in figure 3.6. While developing the scheme it was assumed that the AA is directly formed from NAG in the first step during deacetylation. An intermediate 'I' was introduced representing the lumping of all the products involved in the formation of GA and FA such as glucose, fructose, glycoldehyde, erythrose, pyruvaldehyde, etc. The 'I' intermediates the formation of GA, FA and also forms unknown products termed as decomposition products (DP). As 'I' was hypothetically representing glucose and similar compounds, it was

considered to form and react instantaneously as there were no traces of glucose in product mixture as discussed previously. As the total yield of identified N-containing products including cyclic products is less than 10 %, it is proposed that DP mostly represents the polymerization products i.e. solids and few other secondary products. The model equations to estimate the rate parameters of reactions involved in acids formation during SubCW and SCW hydrolysis of NAG are given below. All the reactions were assumed to be pseudo-first order with reference to individual components, as the water was always in excess. The temperature and density were assumed to be constant along the length of the reactor.
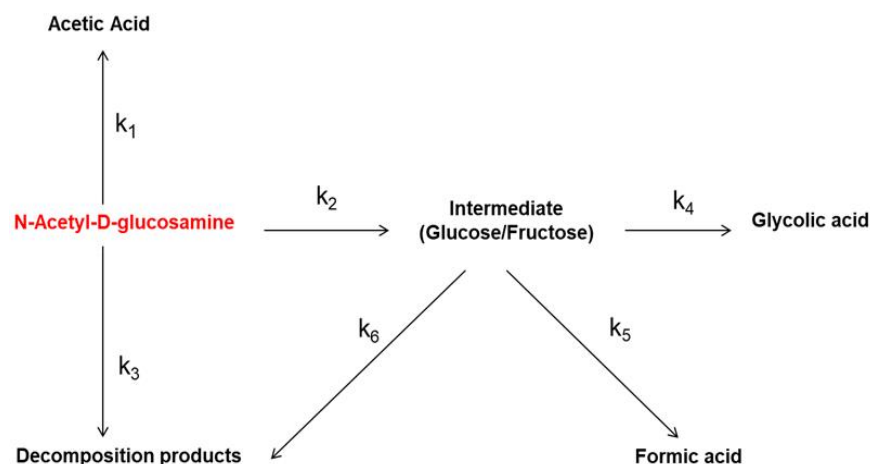
Figure 3.6 Proposed model for estimation of kinetics of acid formation during hydrolysis of NAG in SubCW and SCW

The reaction was considered homogenous and the mass transfer limitations are neglected. The intermediate 'I' was considered to be the instantaneous reaction intermediate forming and disappearing in fraction of time, hence, the net rate of 'I' was considered zero. The net rate equations for other molecules were developed considering the quantitative concentration of the compounds. The expression for concentration of 'I' was determined given in equations 1-3 and replaced in the final differential equations 4-8,

$$\frac{d[I]}{dt} = k_2[NAG] - (k_4 + k_5 + k_6)[I] \tag{1}$$

$$r_I = \frac{d[I]}{dt} = 0 \tag{2}$$

$$[I] = k_2[NAG]/(k_4 + k_5 + k_6)[I] \tag{3}$$

$$\frac{d[NAG]}{dt} = -(k_1 + k_2 + k_3)[NAG] \tag{4}$$

$$\frac{d[AA]}{dt} = k_1[NAG] \tag{5}$$

$$\frac{d[GA]}{dt} = k_4[I] \tag{6}$$

$$\frac{d[FA]}{dt} = k_5[I] \tag{7}$$

$$\frac{d[DP]}{dt} = k_3[NAG] + k_6[I] \tag{8}$$

Where [NAG], [I], [AA], [GA], [FA] and [DP] are concentrations of NAG, intermediates, acetic acid, glycolic acid, formic acid and decomposition products, respectively. The rate constants of individual steps calculated by solving ODEs (equations 4-8) using matlab ODE45 solver and *fminsearch* method, are given in table 3.3. The figure 3.7(a-c), compares the experimental data with model predictions at three temperatures 250 ºC, 350 ºC and 400 ºC at 25 MPa. The plots on normal scale are shown in figure 3.24. The model can accurately predict the concentrations of NAG and other products, evident by 0.85-0.99 values of R^2 estimated by comparing model predictions and experimental yields at same residence times. It was seen that the time required to completely consume NAG and formation of the products is far less (<0.1 s) than the minimum experimental reaction time (2.5 s). The consumption of NAG itself is instantaneous at those conditions (time shorter than 0.1 s at 400 ºC and 25 MPa).

This simplified model accurately predicts the different product concentrations obtained at different temperatures (250 ºC, 350 ºC and 400 ºC) at constant pressure of 25 MPa. Though the rate constants for the reactions involved in the NAG hydrolysis were influenced by the temperature, the rates do not necessarily increase with temperature. Complexity of the reaction network and number of possible reaction paths under highly ionic conditions makes this process extremely fast, which does not allow monitoring the reaction under real conditions at such small time scales. The model helps to understand the same to some extent

in a systematic manner. The rates of both AA and GA formation increased with temperature at subcritical conditions (250 and 350 °C) but dropped in SCW at 400 °C. As previously reported, the formation of AA by deacetylation is an acid catalyzed reaction whereas GA is an oxidation product.[42] The ions formed by dissociation of water i.e. H^+ and OH^- catalyze these reactions during hydrolysis using only water. The ionic product of water increases at subcritical conditions but drops in SCW resulting in reduced ion concentration. The reduction in the rate of formation of AA and GA was presumably caused by this reduction in the concentration of the ions H^+ and OH^- while shifting from subcritical to supercritical conditions.[10,43]

The rates of formation of FA and intermediates increased with temperature, on the contrary, formation of DP from both, directly from NAG and from other intermediates decreased with increase in the temperature. This can be explained by correlating this behaviour with experimental observations. As discussed previously, during the experiments it was observed that the solid formation at subcritical conditions was unavoidable and it blocked the reactor, on the contrary, the hydrolysis of NAG in SCW could be carried out smoothly with almost no formation of solids. As previously reported, solids are formed by polymerization of 5-HMF and other furfurals.
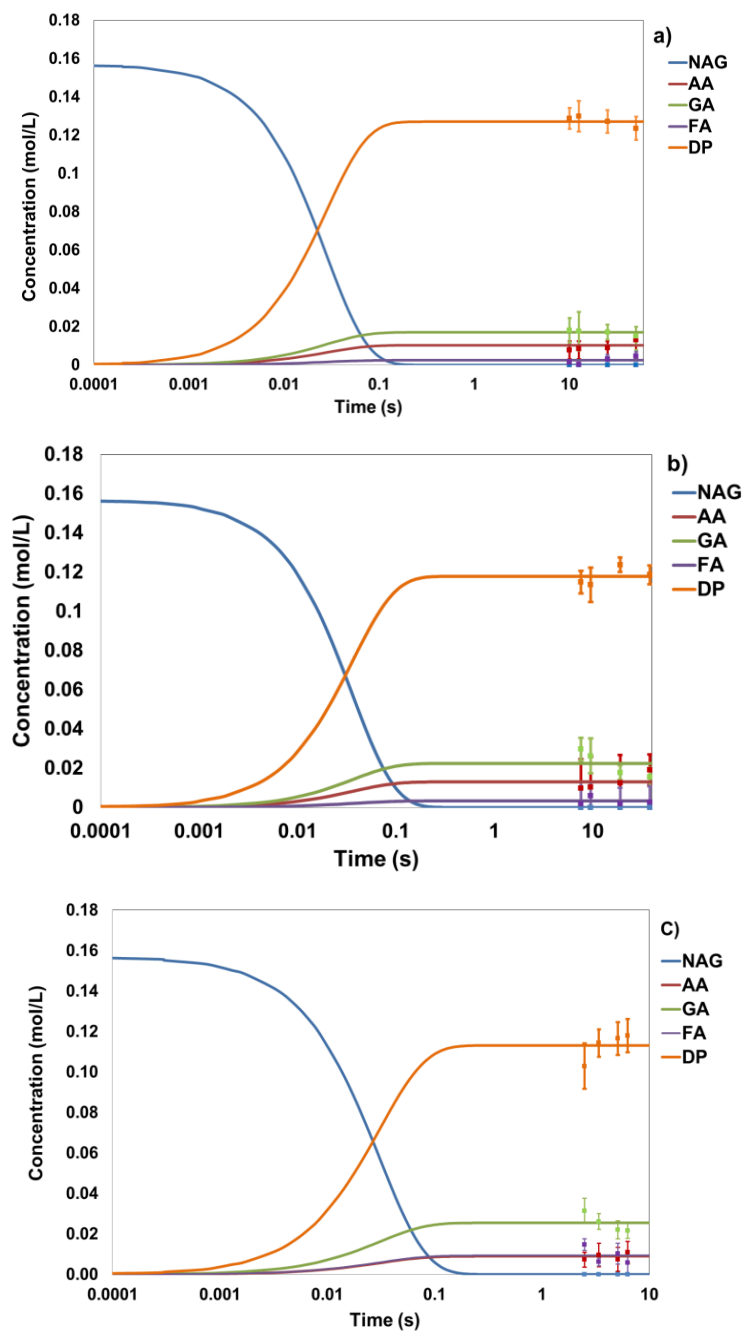
Figure 3.7 Kinetics of NAG hydrolysis in sub- and supercritical water: concentration of compounds with reaction time (a) 250 ℃ (b) 350 ℃ (c) 400 ℃ at 25 MPa; NAG: N-acetyl-D-glucosamine; AA: Acetic Acid; GA: Glycolic Acid; FA: Formic Acid; DP: Decomposition products

Promdej et al.[10] and few other researchers[44] reported that the decomposition of 5-HMF to such solids in water suddenly decreases in SCW and a similar negative temperature effect is an classical observation in such cases. Referring to our definition of DP (solids and few other secondary degradation products), the reduction of rate of formation of DP with temperature is attributed to change in reaction environment that is from ionic in SubCW to radical in SCW causing the change in solid formation. The decomposition of NAG to 'I' leading to acid formation follows the Arrhenius behaviour with activation energy of 7.3 kJ/mol and pre-exponential factor of 394.17 s^{-1}. The Arrhenius plots of the rate constants are shown in figures 3.7(a-c). The formation of AA and GA showed Arrhenius behaviour in SubCW; however, overall, it could not be described by the Arrhenius law, as shown in the figure 3.7b.
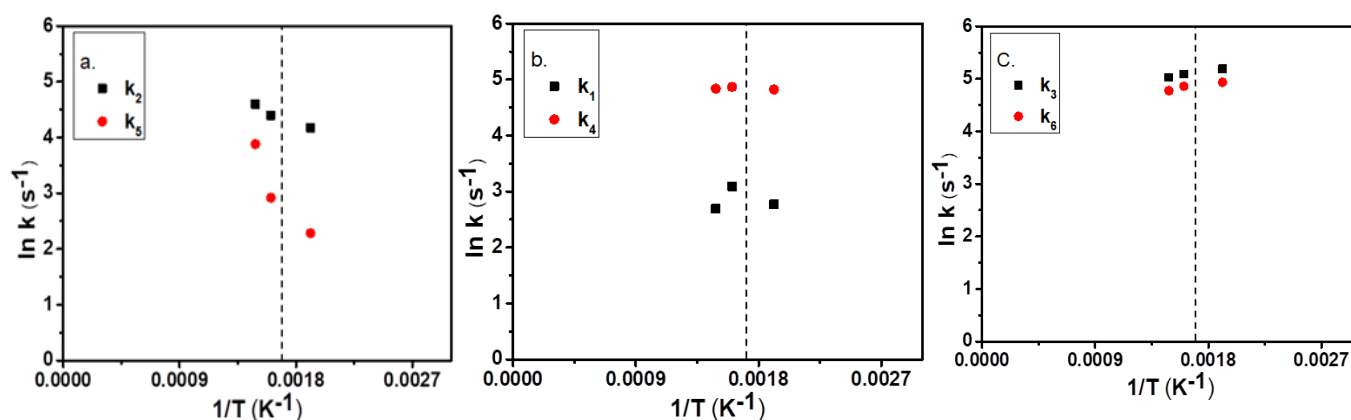
Figure 3.8 Arrhenius plots of rate constants of reactions during NAG hydrolysis in SubCW and SCW(a) NAG to I (k_2) and Formation of FA (k_5) (b) NAG to AA (k_1) and GA formation (k_4) (c) NAG to DP (k_3) and I to DP (k_6); NAG: *N*-acetyl-D-glucosamine, I: intermediates, FA: formic acid, AA: acetic acid, GA: glycolic acid, DP: decomposition products.

It is speculated that the behaviour is observed due to influence of water properties on the unknown pathways of AA and GA formation. On the other hand, the FA formation showed positive temperature effect, figure 3.8a, it is suggested that FA forms majorly by C-C cleavage of glucose as reported earlier, along with oxidation of glucose.[32] The formation of DP from both the reactions showed non-Arrhenius behaviour. As the lumped terms 'I' and 'DP' takes into account the combined unknown reactions occurring during NAG

hydrolysis, a deviation from ideal Arrhenius behaviour also suggests that the few of these reactions can be reversible.[45] The results agree with well-known observations of sugar degradation in SubCW and SCW and with our experimental observations.[44]

The overall rate constant for disappearance of NAG takes into account the three reactions NAG to acetic acid, NAG to intermediates and NAG to DP. These three reactions show different temperature dependence which is attributed to the change in the reaction medium properties. As the temperature effect is compensated by the change in the mechanism of three individual reactions, the apparent change in overall rate constant is not significant. However, there is an effect of temperature on the mechanism of NAG disappearance resulting into more intermediate products and less DP with higher temperature, whereas the acetic acid formation from NAG rate increases in SubCW and comparatively drops in SCW. Unlike single step reaction, the temperature effect on overall NAG hydrolysis can be accounted by using apparent activation energy, which can be estimated in different ways by considering all elementary steps. A detailed discussion on apparent activation energy is given by Mao et. al.[46]

The present approach assists in understanding the acid formation mechanism and kinetics during NAG hydrolysis in SubCW and SCW. A lumped kinetic model for predicting overall product distribution can be developed by quantitative understanding of the complete product distribution. Owing to very rapid reactions occurring during hydrolysis of NAG, for carrying out a detailed study, a reactor that is able to provide short residence time (i.e. low volumes) with sufficient heating and mixing should be employed. Monitoring of reaction using inline measurement can assist in studying the kinetics; however, the process temperature and pressure should be considered while designing the system. Nevertheless, the present model accurately predicts the yields of AA, GA and FA produced by NAG hydrolysis during SubCW and SCW hydrolysis, which can be used to design a system for selective production of these key chemicals from NAG.

3.4 Conclusion

The hydrolysis of NAG, a monomer of abundant biopolymer chitin, in water at sub- and supercritical conditions (250 to 400°C; 25 MPa; 2-60 s) was investigated using a continuous flow tubular reactor. The product distribution was varied with reaction conditions. The liquid products along with solids were main products formed during hydrolysis of NAG in SubCW, whereas liquid and gaseous products were obtained in SCW. The main identified products present in liquid fractions were glycolic acid (10-23 %), acetic acid (5-10%), formic acid (2-7 %) , 5-HMF (0.1-2%), and acetamide (3-8 %), etc. For the first time it is reported that the acetic acid, glycolic acid and formic acid can be obtained by SubCW/SCW of NAG without addition of any external catalyst or oxidant. The distinct nitrogen containing heterocyclic compounds (viz. Pyrazole, 3-Pyrdine carboxyldehyde, Piperidine, 1-Methyl pyrrolidine, Pyridine, 2-acetyl pyrazine, Piperidine, Pyrrole) were also observed, however, with significantly lower yields. The excessive solid formation from NAG hydrolysis in SubCW could be overcome in the SC conditions.

A first order kinetic model based on the reaction network of NAG conversions in SubCW and SCW was used to estimate the rate constants of the reactions. The overall hydrolysis reactions of NAG followed Arrhenius behaviour; however, individual reactions largely deviated from Arrhenius behaviour. These reactions believed to lead to the formation of solids in SubCW and gases in SCW; the shift in product distribution was attributed to change in dominating reaction mechanism from ionic in SubCW to radical in SCW, accelerating and suppressing known or unknown reactions during NAG hydrolysis.
The obtained product distribution and results of kinetic modelling of NAG hydrolysis demonstrates that the sub- and supercritical water are excellent reaction media for the production of valuable chemicals from chitinous biomass.

3.5 Experimental and supporting information

3.5.1 Experimental
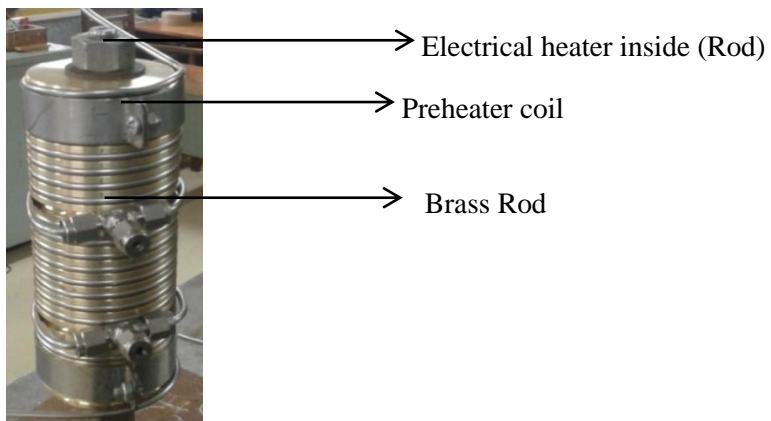
Figure 3.9 Actual photograph of preheater used to heat water to Subcritical and Supercritical temperatures

3.5.2 Identification and quantification of compounds using HPLC

Method: HPLC equipped with Biorad Aminex HPX-87H column (300 x 7.8 mm) and RI detector; Mobile phase: 5 mM aqueous sulphuric acid; Flow rate: 0.6 mL/min; Column Temperature: 50 $^{\circ}$C
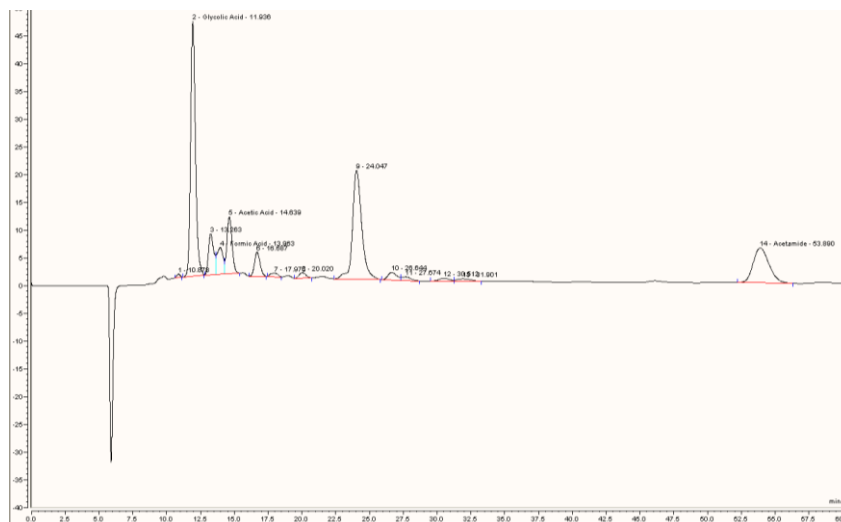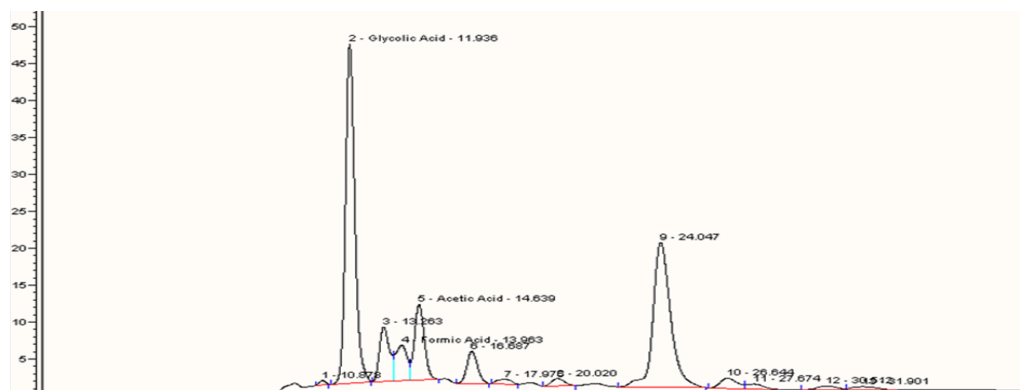
Figure 3.10 HPLC chromatogram of reaction mixture
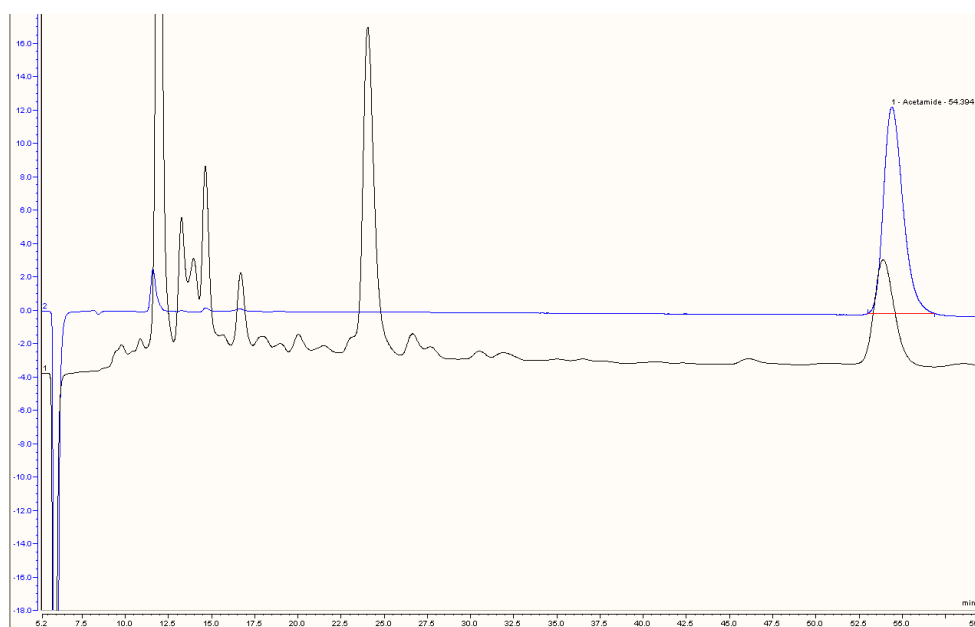
Figure 3.11 HPLC chromatogram of reaction mixture confirming Acetamide (Temperature : 400 °C ; Pressure: 25 MPa; NAG concentration: 1% (w/w); Residence time: 8 s)
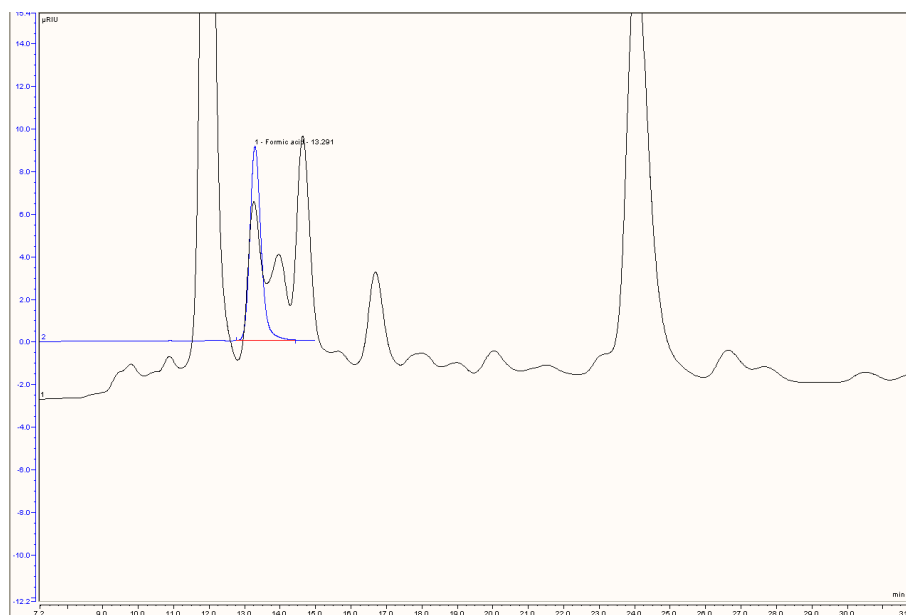
Figure 3.12 HPLC chromatogram of reaction mixture confirming Formic acid

(Temperature: 400 ºC ; Pressure-25 MPa ; NAG concentration: 1 % (w/w); Residence time: 8 s)
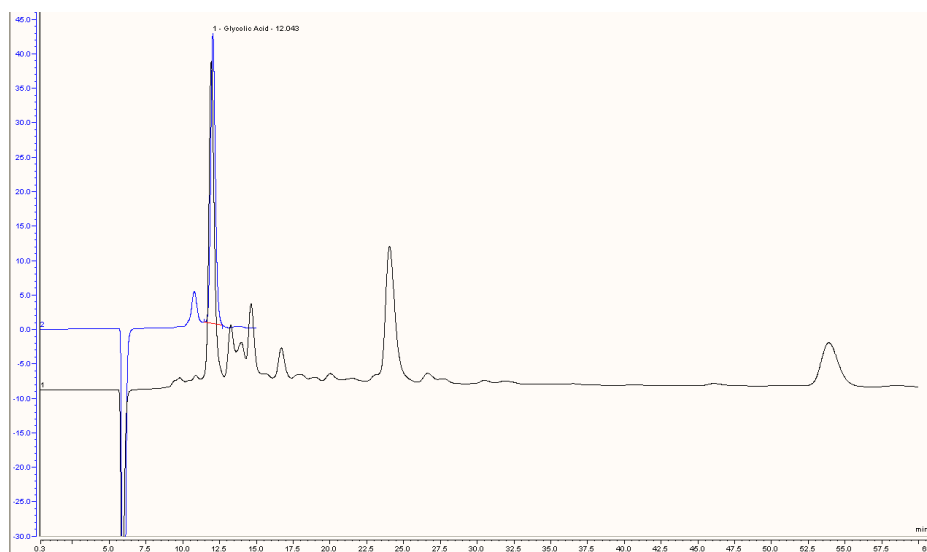
Figure 3.13 HPLC chromatogram of reaction mixture confirming Glycolic acid

(Temperature: 400 ºC; Pressure: 25 MPa; NAG concentration: 1 % (w/w); Residence time: 8 s)
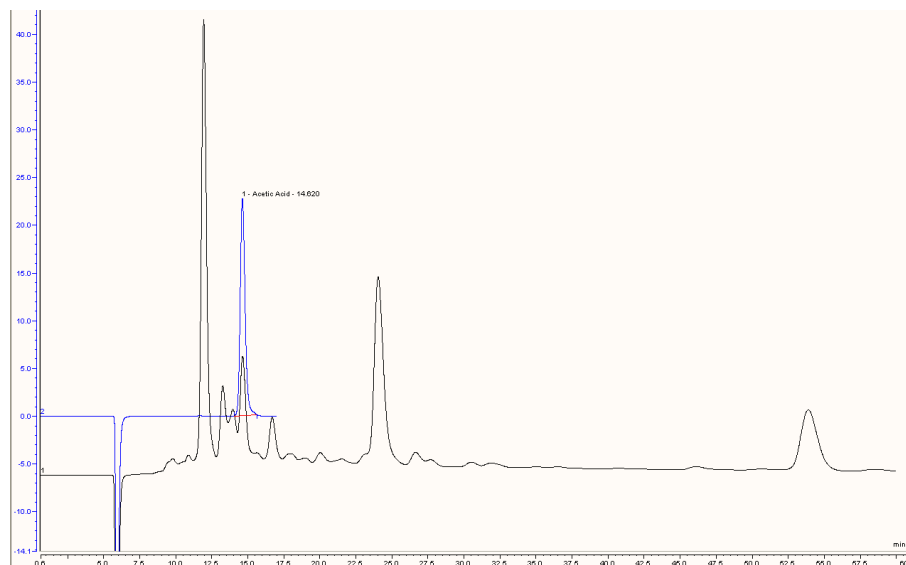
Figure 3.5 HPLC chromatogram of reaction mixture confirming Acetic acid

(Temperature: 400°C; Pressure: 25 MPa; NAG concentration: 1 % (w/w); Residence time: 8 s)

3.5.3 HR-MS of compounds present in reaction mixture during SCW hydrolysis

There were several unknown peaks present in the reaction chromatogram. Most of these compounds were collected separately. The confirmation of the products was done by HR-MS and standards. The possible products were identified based on the literature reported.
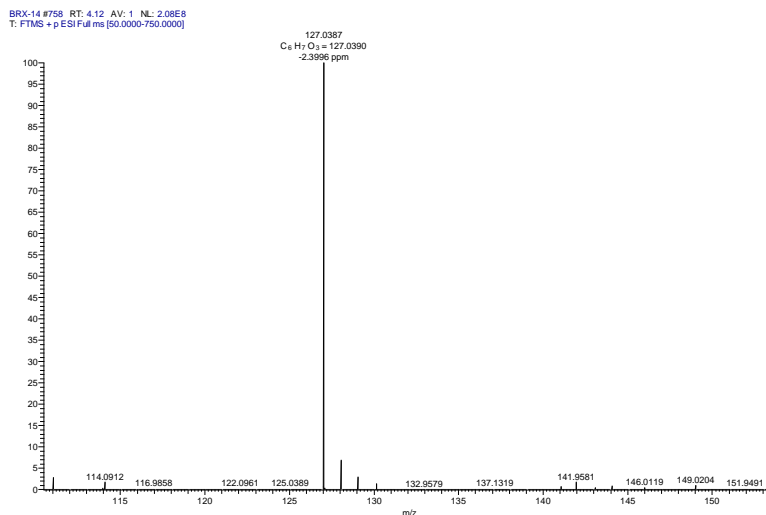
Figure 3.6 HR-MS of separated reaction mixture confirming 5-Hydroxymethylfurfural (126+1)

(Temperature: 400 °C; Pressure: 25 MPa ; NAG concentration: 1 % (w/w); Residence time: 8 s)

KCRX-Aq-01 #472 RT: 2.56 AV: 1 NL: 3.34E5
T: FTMS + p ESI Full ms [50.0000-750.0000]
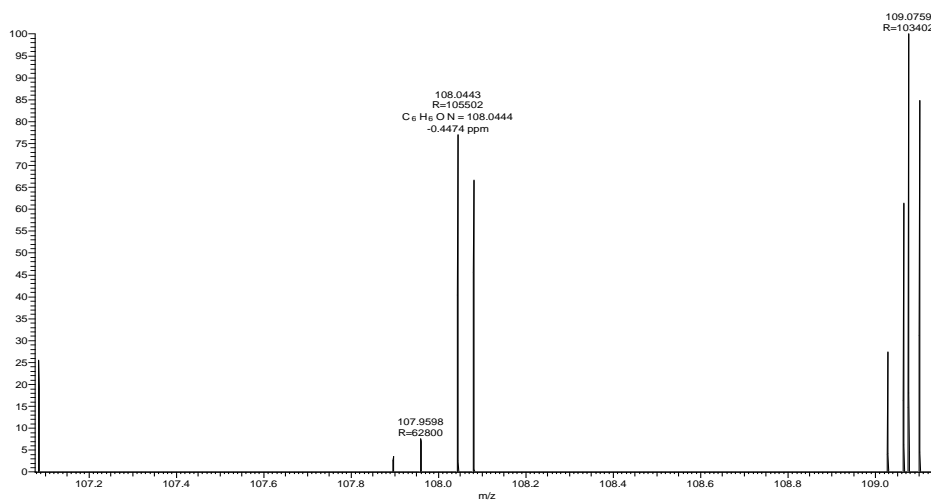
Figure 3.7 HR-MS of separated reaction mixture confirming 3-Pyridine carboxyldehyde

(107+1) (Temperature: 400 ºC; Pressure: 25 MPa; NAG concentration: 1% (w/w);

Residence time: 8 s)

KCRX-Aq-01 #350 RT: 1.90 AV: 1 NL: 2.68E6
T: FTMS + p ESI Full ms [50.0000-750.0000]
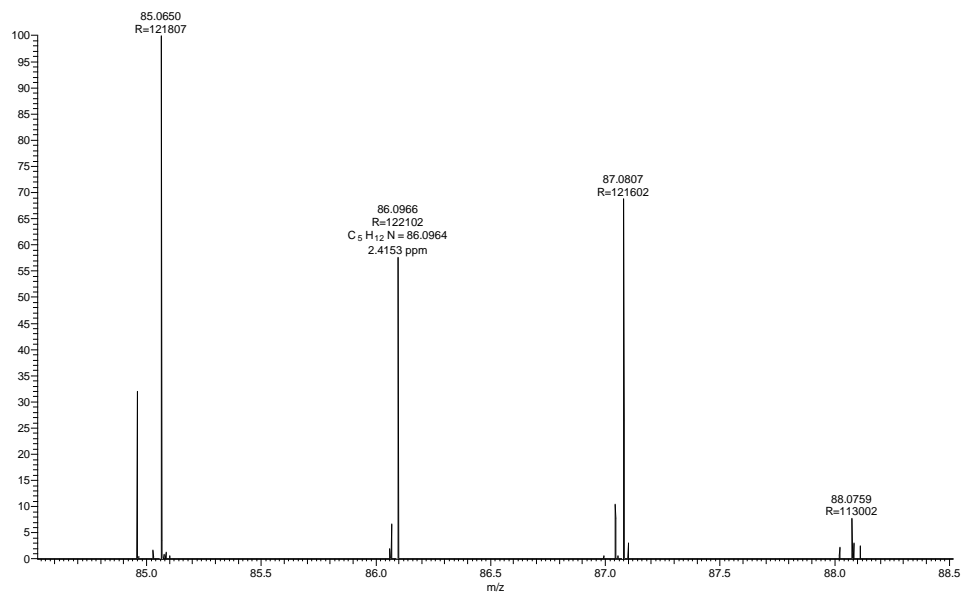
Figure 3.17 HR-MS of separated reaction mixture confirming Piperidine (85+1)

(Temperature: 400 ºC; Pressure: 25 MPa; NAG concentration: 1 % (w/w); Residence time: 8 s)

KCRX-Aq-01 #351 RT: 1.91 AV: 1 NL: 2.40E4
T: FTMS + p ESI Full ms [50.0000-750.0000]
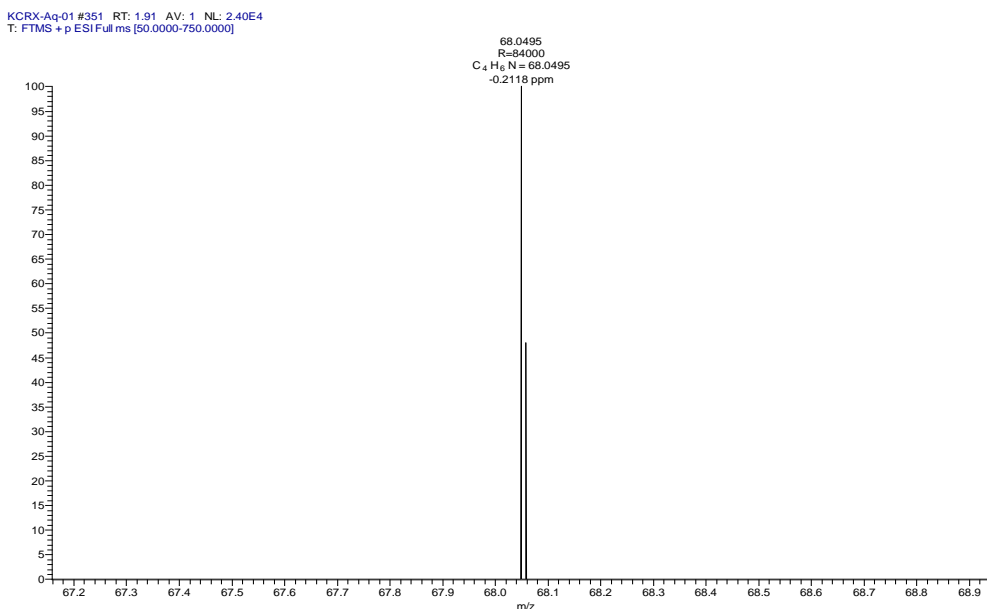
Figure 3.8 HR-MS of separated reaction mixture confirming Pyrrole (67+1)

(Temperature: 400 ºC; Pressure: 25 MPa; NAG concentration: 1 % (w/w); Residence time: 8 s)

KCRX-Aq-01 #387 RT: 2.10 AV: 1 NL: 2.69E6
T: FTMS + p ESI Full ms [50.0000-750.0000]
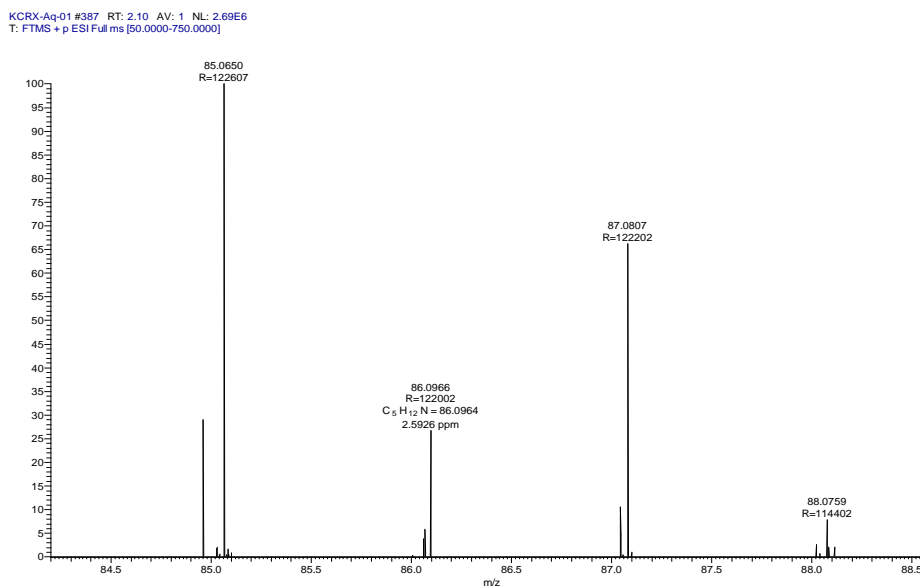
Figure 3.9 HR-MS of separated reaction mixture confirming *N*-methyl pyrrolidine (85+1)

(Temperature: 400 ºC; Pressure: 25 MPa; NAG concentration: 1 % (w/w); Residence time: 8 s)
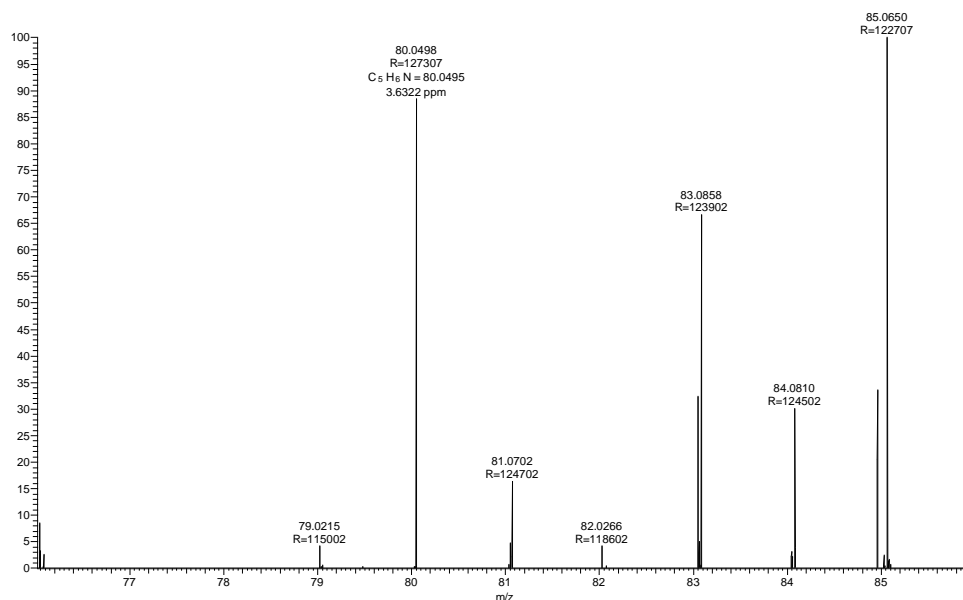
Figure 3.20 HR-MS of separated reaction mixture confirming Pyridine (79+1)

(Temperature: 400 °C; Pressure: 25 MPa; NAG concentration: 1% (w/w); Residence time: 8 s)
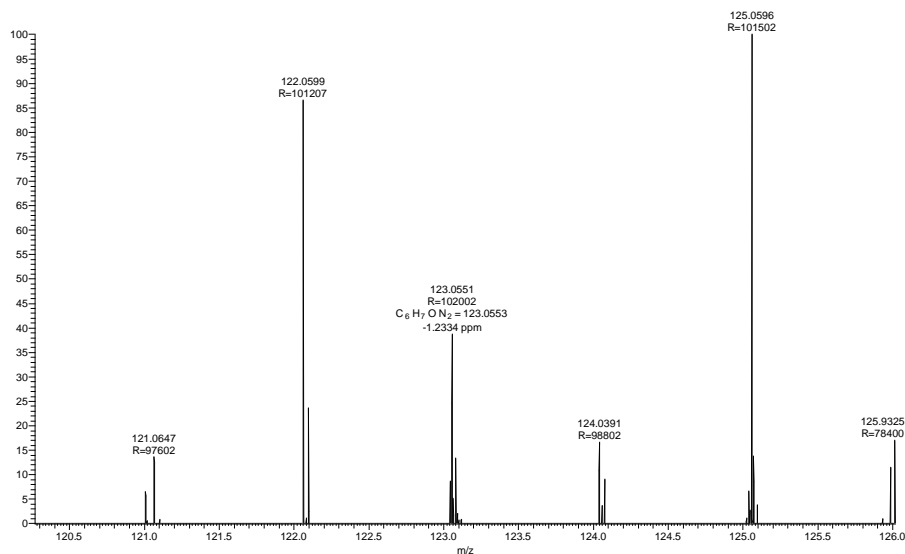
Figure 3.21 HR-MS of separated reaction mixture confirming 2-acetyl pyrazine (122+1)

(Temperature: 400 °C; Pressure: 25 MPa; NAG concentration: 1 % (w/w); Residence time: 8 s)

3.5.4   Effect of pressure

Figure 3.22 Reaction mixture of NAG hydrolysis in subcritical water at 250 $^{\circ}$C at 5 MPa, 12.5 MPa and 25 MPa (from left to right)

3.5.5 Characterization of solids
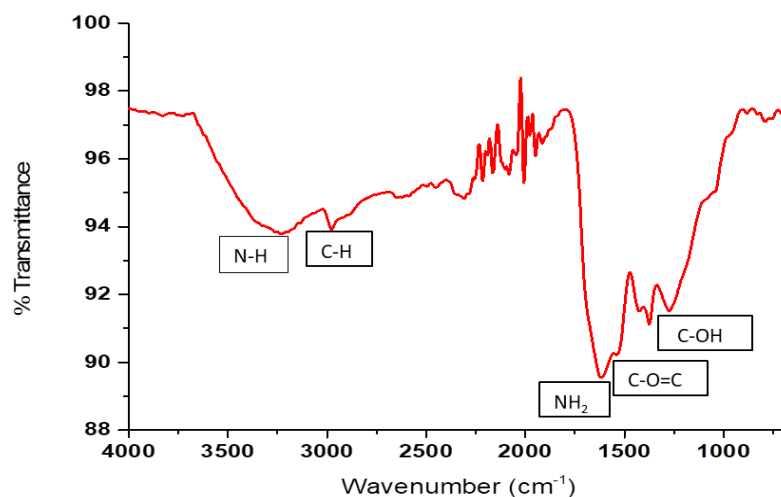
Figure 3.103 FT-IR spectra of solids formed during continuous flow hydrolysis of NAG in subcritical conditions (250 $^{\circ}$C; 25 MPa; 1 % NAG (w/w))

3.5.6 Kinetic plots of NAG hydrolysis on normal scale

The kinetic plots (figure 3.7a-c) are plotted on a log x-axis to capture the change in concentration. Followings are the plots on normal x-axis.
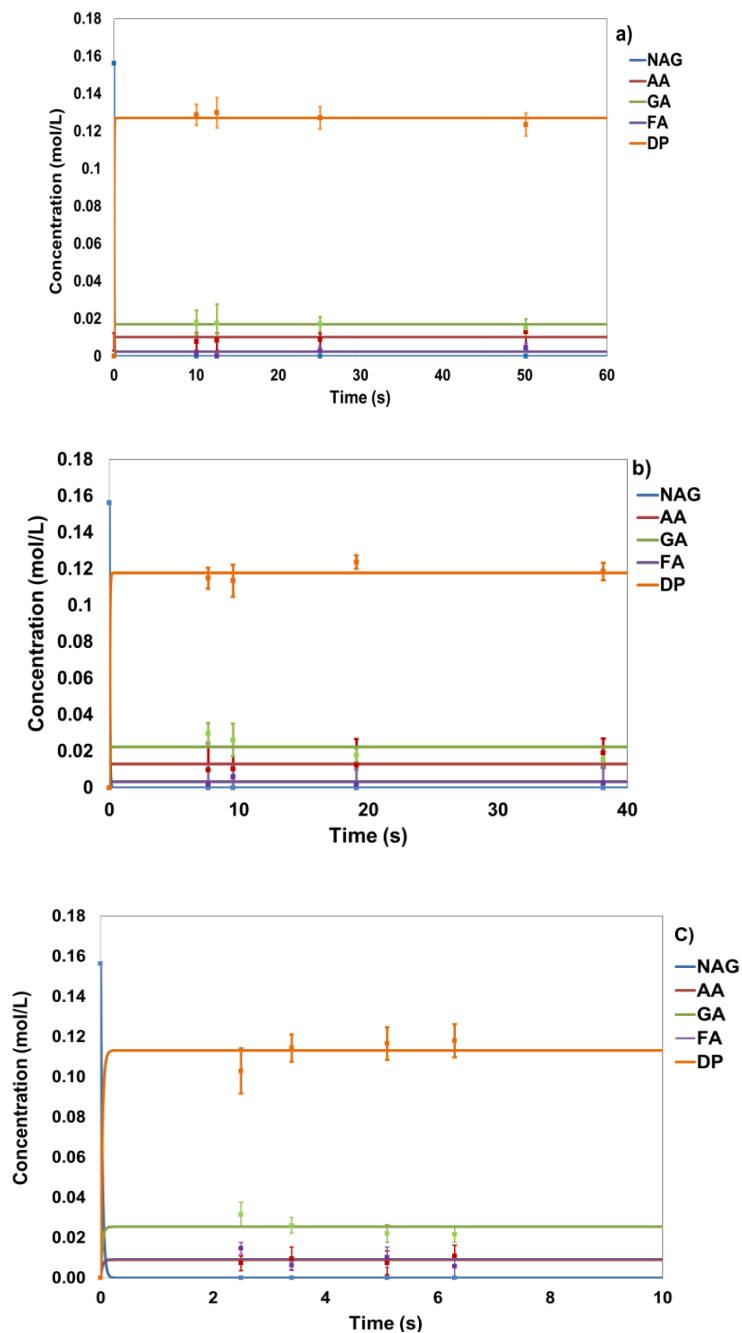
Figure 3.24 Kinetics of NAG hydrolysis in sub- and supercritical water: concentration of compounds with reaction time (a) 250 ºC (b) 350 ºC (c) 400 ºC at 25 MPa

3.6 References

1   P. Stegmann, M. Londo and M. Junginger, *Resour. Conserv. Recycl. X*, 2020, 6, 100029.

2   N. Yan and X. Chen, *Nature*, 2015, **524**, 155–157.

3   S. Cao, Y. Liu, L. Shi, W. Zhu and H. Wang, *Green Chem.*, 2022, **24**, 493–509.

4   K. W. Omari, L. Dodot and F. M. Kerton, *ChemSusChem*, 2012, **5**, 1767–1772.

5   M. W. Drover, K. W. Omari, J. N. Murphy and F. M. Kerton, *RSC Adv.*, 2012, **2**, 4642–4644.

6   X. Chen, Y. Liu, F. M. Kerton and N. Yan, *RSC Adv.*, 2015, **5**, 20073–20080.

7   J. Wang, H. Zang, S. Jiao, K. Wang, Z. Shang, H. Li and J. Lou, *Sci. Total Environ.*, 2020, **710**, 136293.

8   M. Möller, P. Nilges, F. Harnisch and U. Schröder, *ChemSusChem*, 2011, **4**, 566–579.

9   H. Yoshida, S. Izhar, E. Nishio, Y. Utsumi, N. Kakimori and S. A. Feridoun, *Detritus*, 2018, **4**, 98–103.

10   A. V. Bandura and S. N. Lvov, *J. Phys. Chem. Ref. Data*, 2006, **35**, 15–30.

11   D. Padovan, H. Kobayashi and A. Fukuoka, *ChemSusChem*, 2020, **13**, 3594–3598.

12   H. Zang, J. Lou, S. Jiao, H. Li, Y. Du and J. Wang, *J. Mol. Liq.*, 2021, **330**, 115667.

13   H. Zang, S. Yu, P. Yu, H. Ding, Y. Du and Y. Yang, *Carbohydr. Res.*, 2017, **442**, 1–8.

14   J. Wu, M. Qi, G. Gozaydln, N. Yan, Y. Gao and X. Chen, *Ind. Eng. Chem. Res.*, 2021, **60**, 3239–3248.

15   P. E. Savage, *Chem. Rev.*, 1999, **99**, 603–622.

16   Wahyudiono, S. Machmudah and M. Goto, *Eng. J.*, 2013, **17**, 1–12.

17   D. A. Cantero, M. Dolores Bermejo and M. José Cocero, *J. Supercrit. Fluids*, 2015, **96**, 21–35.

18   P. E. Savage, S. Gopalan, T. I. Mizan, C. J. Martino and E. E. Brock, *AIChE J.*, 1995, **41**, 1723–1778.

19   T. Michael, K. Oshima, C. Abe, R. Maruta, M. Iguchi, M. Watanabe and R. L. Smith, *Carbohydr. Polym.*, 2014, **106**, 172–178.

20   M. Osada, C. Miura, Y. S. Nakagawa, M. Kaihara, M. Nikaido and K. Totani, *Carbohydr. Polym.*, 2013, **92**, 1573–1578.

21   M. Osada, C. Miura, Y. S. Nakagawa, M. Kaihara, M. Nikaido and K. Totani, *Carbohydr. Polym.*, 2015, **134**, 718–725.

22   S. P. Kulkarni, S. N. Dure, S. S. Joshi, K. V. Pandare and N. A. Mali, *Carbohydr. Res.*, 2022, **516**, 108560.

23   M. Osada, S. Shoji, S. Suenaga and M. Ogata, *Fuel Process. Technol.*, 2019, **195**, 106154.

24   M. Osada, K. Kikuta, K. Yoshida, K. Totani, M. Ogata and T. Usui, *Green Chem.*, 2013, **15**, 2960–2966.

25   R. Wang, T. Kobayashi and S. Adachi, *Food Sci. Technol. Res.*, 2011, **17**, 273–278.

26   B. M. Kabyemela, T. Adschiri, R. M. Malaluan and K. Arai, *Ind. Eng. Chem. Res.*, 1997, **36**, 1552–1558.

27   X. Chen, Y. Liu, F. M. Kerton and N. Yan, *RSC Adv.*, 2015, **5**, 20073–20080.

28   S. Chern, H. Tu and A. Materials, *Eng. Technol. Int. J. Chem. Mol. Eng.*, 2017, **11**, 98–102.

29   C. Yan, J. Fraga-Dubreuil, E. Garcia-Verdugo, P. A. Hamley, M. Poliakoff, I. Pearson and A. S. Coote, *Green Chem.*, 2008, **10**, 98–10.

30   E. Shitsi, S. K. Debrah, V. Y. Agbodemegbe and E. Ampomah-Amoako, *World J. Eng. Technol.*, 2018, **06**, 241–267.

31   N. V Dolgopyatova, V. Y. Novikov, I. N. Konovalova and N. M. Putintsev, *Russ. J. Appl. Chem.*, 2013, **86**, 986–991.

32   R. He, T. Ma, J. Cheng, B. Jin and J. Xu, *ACS Omega*, 2021, **6**, 11260–11265.

33   N. Shimizu, B. Zeng and K. Kushima, *SN Appl. Sci.*, 2021, **3**, 1–15.

34   J. Chen, M. Wang and C. T. Ho, *J. Agric. Food Chem.*, 1998, **46**, 3207–3209.

35   Z. Xu, Y. Yang, P. Yan, Z. Xia, X. Liu and Z. C. Zhang, *RSC Adv.*, 2020, **10**, 34732–34737.

36   Antal, A. Brittain, C. DeAlmeida, S. Ramayya and J. C. Roy, in *ACS Symposium Series*, 1987, pp. 77–86.

37   C. A. Eckert, C. L. Liotta, D. Bush, J. S. Brown and J. P. Hallett, *J. Phys. Chem. B*, 2004, **108**, 18108–18118.

38   C. Cotellessa, K. Peris and S. Chimenti, *J. Eur. Acad. Dermato. Venereol.*, 1995, **5**, 215–217.

39   K. Shah and S. Consultant, *Indian Petrochem Conf.*, 2014, 1–23.

40   X. Liu, S. Li, Y. Liu and Y. Cao, *Chinese J. Catal.*, 2015, **36**, 1461–1475.

41   R. Kumar, *Energy Nexus*, 2022, **5**, 100042.

42   N. V. Dolgopyatova, V. Y. Novikov, I. N. Konovalova and N. M. Putintsev, *Russ. J. Appl. Chem.*, 2013, **86**, 986–991.

43   D. A. Cantero, M. D. Bermejo and M. J. Cocero, *ChemSusChem*, 2015, **8**, 1026–1033.

44   A. Chuntanapum, T. L. K. Yong, S. Miyake and Y. Matsumura, *Ind. Eng. Chem. Res.*, 2008, **47**, 2956–2962.

45   L. E. Revell and B. E. Williamson, *J. Chem. Educ.*, 2013, **90**, 1024−1027.

46   Z. Mao and C. T. Campbell, *ACS Catal.*, 2019, **9**, 9465–9473.

Chapter 4

Ozonolysis of cardanol in a continuous flow tubular reactor
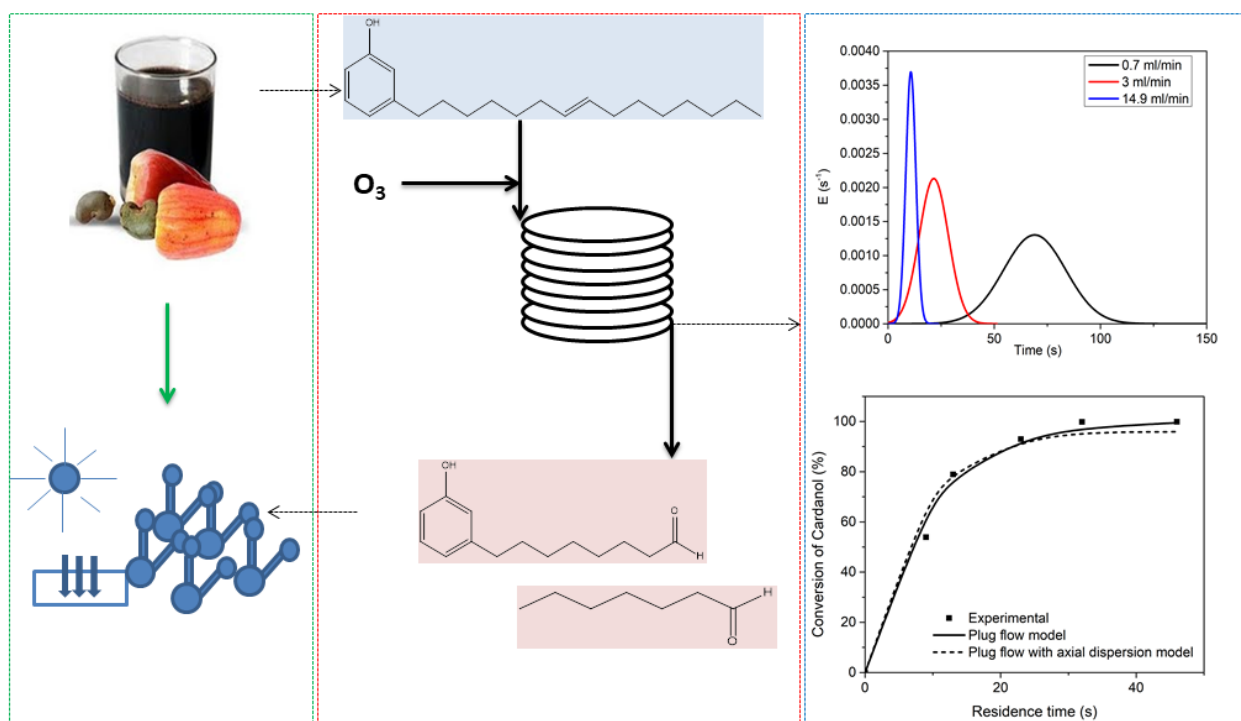
This chapter is based on:

4.1 Introduction

Polymers, synthetic or natural, are essential macromolecules playing indispensable role in every aspect of modern life. Owing to low cost, low density, resistance to corrosion, resistance to most chemicals, and easier manufacturing designs, polymers have entered in almost every field of engineering solutions.[1] The attribute of polymers that they can be synthesized according to the required applications (dictated by the molecular weight or chain length and functional groups), have enabled their usage in new engineering applications e.g. aircraft engineering, space studies, packaging, smart biomaterials and electronics.[2] The global polymers market size of USD 713.9 billion in 2021 is expected to achieve USD 1078.5 billion by 2030. The current polymer industry is mainly dependent on the chemicals that are derived from the fossil based resources. The depletion of fossil resources and increasing demand of the consumer goods has fuelled the research in the field of green bio-based polymer synthesis. While several bio-based feed stocks are being explored for the synthesis of new monomers and polymers, each material is considered for their inherent specific chemical structures required in the monomer to provide specific properties to the polymer. Cardanol, a phenolic lipid obtained from the cashew nut shell liquid as a byproduct of cashew production industry from cashew tree, *Anacardium occidentale*, finds many applications in chemical industry itself as resins, surfactant, coating, etc.[3,4] Cardanol has the specific structure characterized by both aromatic compounds and aliphatic compounds.[5,6] This structure provides the high temperature resistance, good flexibility, excellent hydrophobicity, etc. Moreover, the available double bonds and hydroxyl groups offer the simple chemical modification for the specific monomer synthesis. Previously, cardanol has been explored for the synthesis of several monomers e.g. the monomers Cardanyl acrylate or 3-pentadecenyl phenyl acrylate finding application as flexible thermoset polymer production were synthesized by base catalyzed reaction of cardanol. The difunctional condensation monomers including diamines, diacids, diols, dialdehydes, diacylhydrazide, etc. used for production various high performance polymers using cardanol.

Conventional approach is through different chemical modifications at either alkyl chain or phenolic group.[7] The monomers 8-(3-hydroxyphenyl) octanal or 8-(3-hydroxyphenyl) octanoic acid (HPOAc) obtained from oxidation of cardanol are potential monomers for synthesis of liquid crystal polymers. Liquid crystal polymers are high performance polymers used for specific applications in the areas of electrical devices and electronics, telecommunication, fiber optics, and optical storage devices with increasing global market.[8] The structural requirements of monomers

i.e. aromatic group for rigidity with flexible carbon chain for synthesis of liquid crystal polymers, similar to that of cardanol structure, shown in Figure 4.1, have intrigued researchers to synthesize the monomers specifically aldehydes or acids those can provide functional sites for polymer synthesis.

OH

Aromatic group-rigid kink   Aliphatic group-flexible spacers
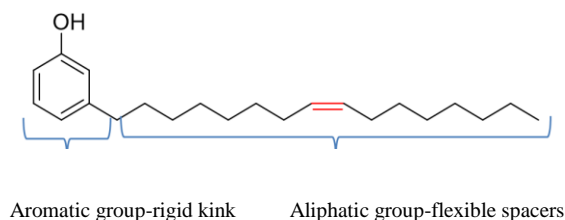
Figure 4.1 Structure of cardanol (monoene)

Pillai et. al.[9] reported the synthesis of thermotropic liquid crystal polyesters synthesis from the self and copolymerization of HPOAc and *p*-hydroxybenzoic acid. The monomer HPOAc was synthesized by the oxidation of cardanol using potassium permanganate. As the direct oxidation of cardanol with potassium permanganate always resulted in the cleavage of the phenolic moiety, a three stage batch protocol was developed; initially the hydroxyl group of cardanol was protected by acetylation, followed by oxidation and deacetylation to synthesize HPOAc. In another study, Pillai and group synthesized thermotropic terpolymers by a melt poly-condensation reaction of 2,6-naphthalenedicarboxylic acid, hydroquinone, and HPOAc.[10] The semi flexible random thermotropic polyesters were obtained by polymerization of HPOAc with 3-chloro-4-hydroxy benzoic acid/3,5-dibromo-4-hydroxy benzoic acid.[11] During all these studies, oxidation of cardanol was performed by conventional method using potassium permanganate. This conventional oxidation method necessitates three steps of protection, reaction and deprotection as well as the separation of substrates from homogenous phase. Ozonolysis i.e. oxidation using clean oxidant ozone has been employed by few researchers for cardanol functionalization. The monomer 8-(3-hydroxyphenyl) octanal (HPOA) was synthesized by ozonation of cardanol following catalytic hydrogenation of ozonides in which around 92.6 % yield of HPOA was obtained using Pd/C in 4.5 h at -78 °C. [12] The synthesis of HPOAc and HPOA by ozonolysis is intermediated by formation of ozonide followed by oxidative or reductive quenching. These ozonides and ozone itself are highly unstable moieties and require safe handling. Although the usage of monomers HPOA and HPOAc is well demonstrated for synthesis of special types of liquid crystal polymers,

the typical synthetic batch procedures are inefficient to address the safety related issues which might be a limiting factor for their commercial use. In this context, a continuous flow process looks advantageous in several terms. The basic operation that ensures replenishing of reaction mass in the reactor makes this process inherently safer for handling ozone and ozonides by diminishing accumulation of these compounds inside the reactor. Previously, continuous flow ozonolysis has been employed for conversion of renewable materials to value added products with the focus to explore reactor designs for such gas-liquid reaction.[13–16] However, the systematic studies of reactor performance and kinetics of oxidation of materials is scarcely done. Herein, we report a continuous flow process for ozonolysis of cardanol for exploring the potential to synthesize valuable monomers using a simple helical coil reactor. The influence of temperature, molar flow rates of ozone and cardanol and liquid residence time on cardanol conversion is investigated. The systematic characterization of gas-liquid mass transfer and residence time distribution was undertaken to understand its effects on cardanol consumption kinetics. The experimental results of reaction and flow characterizations experiments along with modeling of cardanol kinetics are presented in this contribution.

4.2 Experimental

4.2.1 Chemicals

Cardanol (NX-2021) was obtained from Cardolite Specialty Chemicals India LLP. Acetone was purchased from Merck Specialities. Heptanal and heptanoic acid were purchased from Sigma Aldrich. The deionized water (LabQ) was used in all the experiments. All solvents used for work up and analysis were analytical grade solvents. The compound 8-(3-hydroxyphenyl) octanal (HPOA) was synthesized in the laboratory by ozonolysis, purified by chromatography, spectroscopically pure compound was used as the internal standard for analysis.

4.2.2 Semi-batch reactions

Ozonolysis of cardanol was initially investigated using a semi-batch reactor. A 200 mL two necked round bottom flask was initially loaded with the solution of cardanol (0.5-3 % w/w) in a mixture of solvents acetone: water (90:10). A gas stream containing mixture of ozone and oxygen emanating from an ozone generator (Ozonics Pvt. Ltd, India) connected to oxygen generator (Invacare Pvt. Ltd.) was passed through the reaction mixture at a flow

rate of 1.5 L/min. The temperature of the reactor was maintained at 0 °C using an ice bath. After the stipulated time of the semi-batch reactions, the extractive work up was done using ethyl acetate or dichloromethane. The organic solvent from extracted reaction mixture was further evaporated. The progress of the reaction was initially monitored by thin layer chromatography (TLC) using Merck silica gel 60-F254 coated 0.25 mm plates and detected by UV. The separation of reaction compounds was done using the flash chromatography (Combiflash, Agilent Inc.) using solvents and silica gel (particle size 0.064−0.210 mm). The products were identified by using ^{1}H and ^{13}C NMR spectra recorded on a Bruker 200 MHz instrument with DMSO as the internal standard, which are given in the Supporting Information (Figure 4.12-4.15).

4.2.3 Continuous flow ozonolysis of cardanol

A schematic of continuous flow reactor used for carrying out ozonolysis of Cardanol is shown in Figure 4.2. An 8 mL helical coil of SS316 was used as reactor. In a typical ozonolysis experiment, a solution of cardanol (5 % (w/w)) in acetone: water (90:10) mixture was pumped to the reactor at flow rate 0.3 to 14.9 mL/min using HPLC pump (Teledyne LS class SSI Pump). The stream of gas with Ozone/Oxygen mixture emanating from ozone generator was introduced to liquid stream at a fixed flow rate of 1.5 L/min at reactor inlet using a three way valve. A SS316 vessel was used as the jacked for the reactor in which the reactor was tightly placed. A chiller (Julabo FP50) was used to maintain low temperatures of the reactor by passing coolant through the jacket. The gas and liquid streams were separated using a gas-liquid separator connected to the reactor outlet. The liquid reaction mixture was collected and analysed.
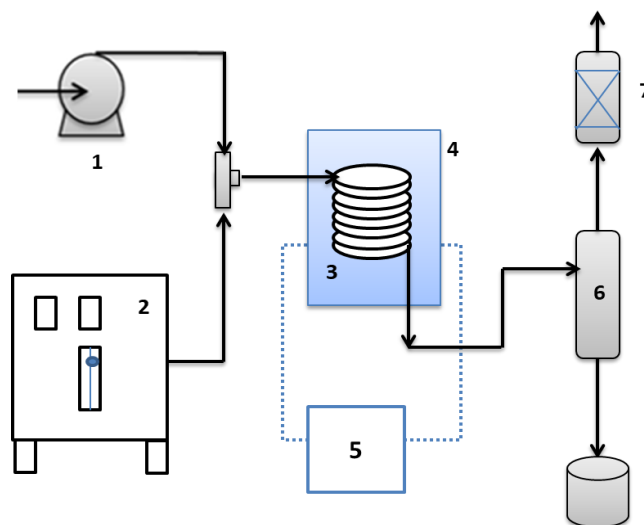
1. **Liquid pump (Cardanol Solution)**
2. **Ozone Generator**
3. **Reactor**
4. **Cooling jacket**
5. **Chiller**
6. **Gas-liquid separator**
7. **Scrubber**

Figure 4.2 Schematic of continuous flow reactor configuration

4.2.4 Analysis

The structural identification of the reaction mixture was done by ^{1}H and ^{13}C NMR on a Bruker 400 and 500 MHz instrument with Dimethyl sulfoxide as the internal standard. The qualitative analysis was done by gas chromatography- mass spectroscopy (Agilent 7890 B) equipped with Agilent HP-5 column (30 m x 2.5 m x 0.25 μm) and electron ionization detector using nitrogen as carrier gas. The oven temperature program was set as follows: 80°C for 1 min; then 10 °C/min ramps to 150 °C and holding for 5 min; then 5 °C/min to 250 °C holding for 1 min followed by 5 °C ramp to 280 °C holding for 1 min. The reaction mixture was extracted using dichloromethane and the quantitative analysis of the organic phase was done using gas chromatography (Agilent 7890 A) furnished with Agilent HP-5 column and flame ionization detector (FID) using same temperature ramping method as above.

4.2.5 Residence time distribution (RTD)

The residence time distribution of the reactor was studied at various liquid flow rates in the range 0.3 mL/min to 14.9 mL/min at constant gas flow rate of 1.5 L/min. A pulse input of tracer salt solution was injected to the reactor after three way valve. The concentration of salt in the solvent at reactor outlet was monitored by using an inline conductivity meter (Contech CC-01, India). The data obtained from the RTD experiments was processed as given in the section 4.4.5. Considering the dispersion model validity, Peclet numbers were calculated.

4.2.6 Volumetric mass transfer co-efficient

The liquid side volumetric mass transfer coefficient of the reactor was estimated by using method of dissolved oxygen (DO). The liquid solvent mixture containing acetone-water without cardanol was pumped to the reactor at different flow rates in the range from 0.3 mL/min to 14.9 mL/min, while oxygen gas was flowing at the rate of 1.5 L/min. The dissolved oxygen of the solvent before passing through the reactor was measured using DO analyzer (HANNA instruments) and the DO of the liquid sample collected from the outlet of gas-liquid separator was measured. Assuming film theory, the mass transfer coefficients were estimated at various flow rates using following equation,

$$\frac{dC}{d\tau} = k_{\mathrm{L}}a(C^* - C)$$

, wherein, k_La is liquid-phase volumetric mass transfer coefficient, C^*, C_0 and C are equilibrium oxygen concentration, initial DO and final DO of liquid samples. The value of C^* was 2.37 mM, solubility of oxygen in acetone.[17]

4.3 Results and discussions

4.3.1 Ozonolysis of cardanol

Ozonolysis of cardanol was initially investigated using a semi-batch reactor to characterize the products by varying reaction time from 5 min to 1 h using method described in section 2.2. Monitored by TLC, cardanol, at any initial concentration varied between 1 to 5 %, was completely converted within 5 min which was also confirmed by the visible changes in the reactor mixture turning from colourless to pale yellow (Figure 4.16). The ^{1}H NMR spectra

of the first isolated fraction, as shown in figure 4.13, confirmed the formation of the aldehyde HPOA. For a typical case, around 20.8 % isolated yield of HPOA was obtained by ozonolysis of 3 % cardanol solution within 5 min at 0 °C at 1.5 L/min of ozone flow rate. A plausible reaction pathway based on criegee mechanism for formation of various products including HPOA, heptanal and corresponding carboxylic acids is shown in Figure 4.3.[18]

It was observed that the time longer than 30 min resulted in waxy products which is attributed to the formation of various products by breakage or oxidation of phenol, which has also been reported by Trablesi and co-workers for the case of electrochemical oxidation of phenol.[19] The excessive time and exposure of ozone led to formation of these products, hence, it was asserted that the short times and better control over mole ratio of cardanol and ozone is required.
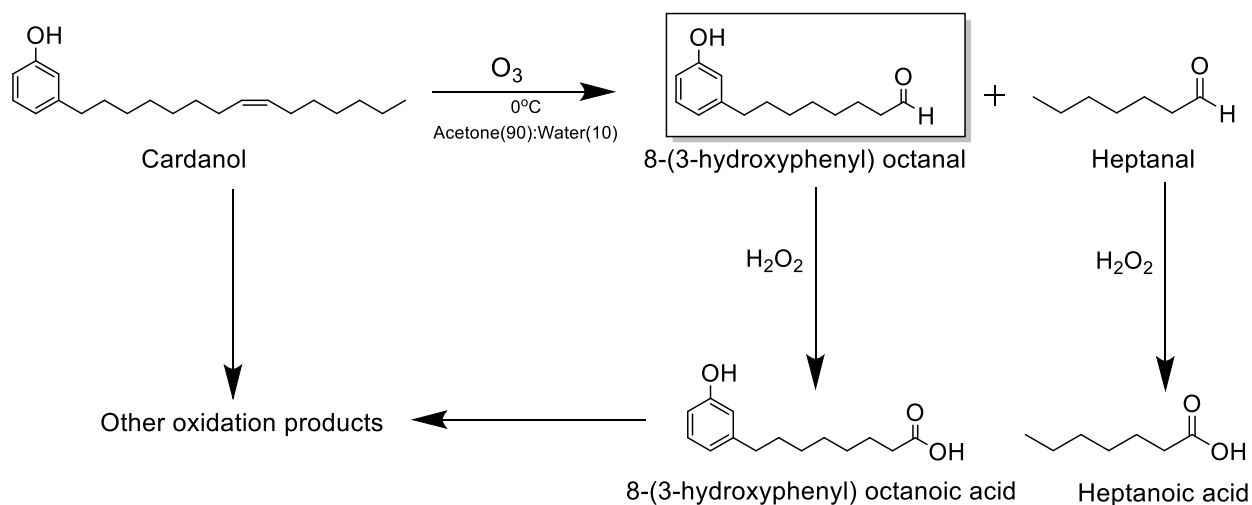
Figure 4.3 Plausible reaction pathways of cardanol (monoene) ozonolysis[18,20]

4.3.2 Continuous flow ozonolysis of cardanol

The continuous flow ozonolysis of cardanol was studied by using a simple helical coil reactor by varying various reaction conditions including temperature, gas-liquid flow rates and consequently molar flow rates of ozone to cardanol and liquid residence time. At ozone

to cardanol mole ratio of 2, the conversion of cardanol increases with temperature (Figure 4.4) however, for higher mole ratios (>2) cardanol was completely consumed at all temperatures. As the molar flow ratio was varied by varying liquid flow rates the trend could be attributed to either starvation of ozone at low ozone to cardanol ratio (~2) or short residence time of cardanol inside the reactor. As highlighted in Figure 4.5, the conversion of cardanol increased from 47 % to 80 % with temperature from -10 ºC (263 K) to 20 ºC (293 K), respectively, at constant mole ratio of 2.
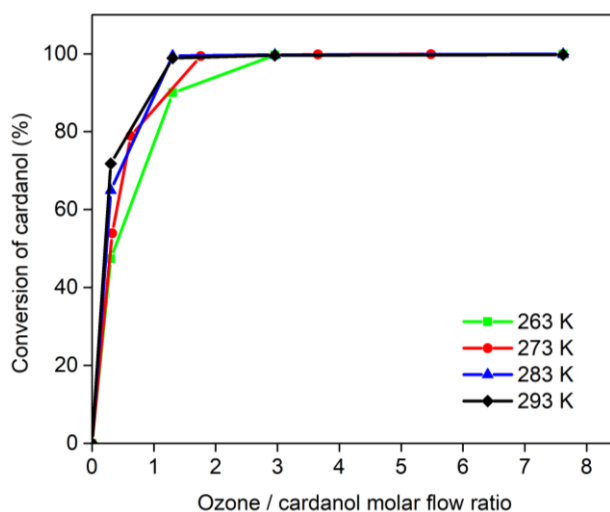
Figure 4.4 Effect of molar flow ratio on conversion of cardanol
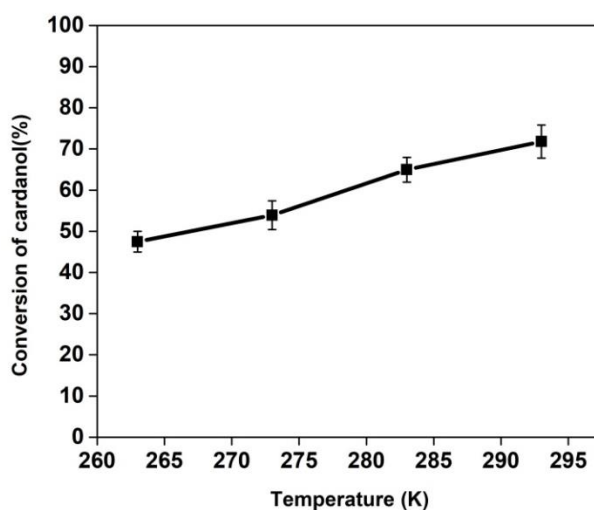
Figure 4.5 Effect of temperature on conversion of cardanol at ozone to cardanol mole ratio of 2

Figure 4.6 shows the variation in the yield of products and conversion of cardanol with ozone to molar flow ratio. As discussed previously, cardanol undergoes oxidation to produce primary oxidation products aldehydes viz. HPOA and heptanal, while at higher mole ratio of ozone to cardanol further oxidation products are seen, which reduce the yield of the desired product. Though acidic and other products could not be quantified using the analytical method mentioned in Section 4.2.4, the presence of acidic compounds was confirmed by ^{1}H NMR (figure 4.15). While the cardanol is completely converted the low yields of identified compounds suggests that there are other pathways by which cardanol is oxidized. While ozone is prone to attack the double bond at alkyl chain, the usage of solvent mixture acetone and water may promote formation of hydrogen peroxide.[20] The peroxide can oxidize the phenol group and result in breakage of phenol ring and thus lead to undesired product formation. The mass spectra of the reaction mixtures (Figure 4.17-4.21) show the difference in the product distribution at mole ratio of ~2 and ~12 respectively.
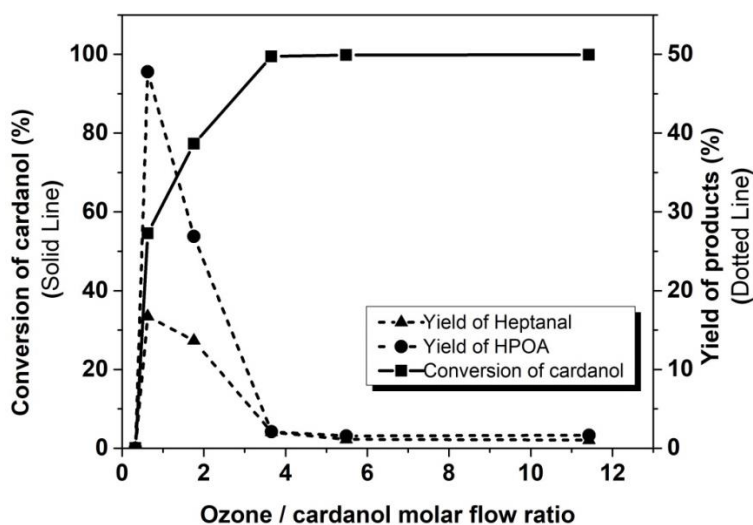
Figure 4.6 Effect of gas to liquid flow ratios on conversion of cardanol and yield of products
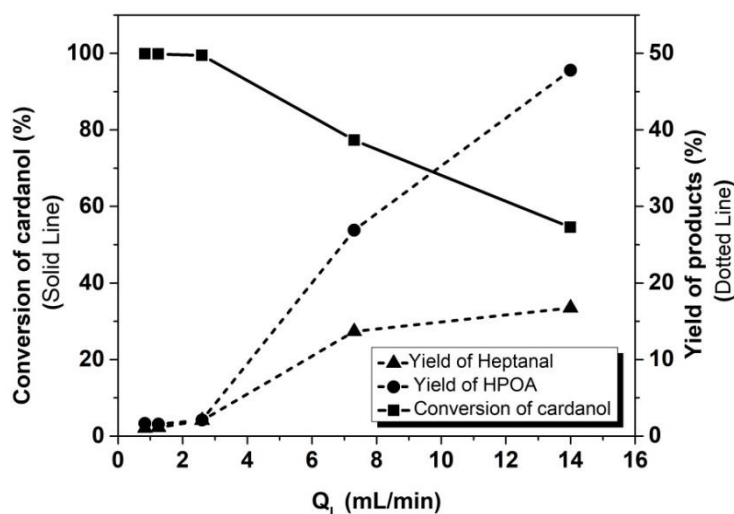
Figure 4.7 Effect of liquid flow rate on conversion of cardanol and yield of products

Figure 4.7 shows the effect of liquid flow rate on yield of the aldehydes and conversion of cardanol. As the flow rate increased from 0.7 to 14.9 mL/min at constant gas flow rate of 1.5 L/min, while cardanol conversion was dropped the yield of aldehydes increased, this could be attributed to insufficient concentration of ozone to drive the reaction further from aldehydes to acid. As high liquid flow rates facilitated shorter residence times, the further oxidation of these products and oxidation of cardanol via other methods was suppressed.

Nevertheless, optimization of the reaction conditions could give significant yields of desired monomers. A mechanistic understanding cardanol conversion and its kinetics are essential to optimize and design the reactor for conversion of cardanol via ozonolysis using this two phase flow reactor.

4.3.3 Kinetics of cardanol ozonolysis

Ozonolysis of cardanol in helical coil reactor is a typical example of two phase gas-liquid reaction. In order to predict the kinetics of conversion of cardanol during flow reaction, a systematic approach was followed. Initially, the liquid side volumetric mass transfer coefficient was determined by the method described in section 4.2.4. The values of mass transfer coefficient were in the range of 0.02 to 0.1 s^{-1} as flow rate was increased from 0.7 to 14.9 mL/min (Figure 4.22). The values of mass transfer coefficient for this reactor were high enough that allowed sufficient transfer of ozone from gas to liquid phase. Moreover, very high gas flow rate (1.5 L/min) compared

to liquid flow rates (<14.9 mL/min) also ensured the excess of ozone to liquid phase (> 2). Hence, the interphase mass transfer limitations were negligible and the ozonolysis of cardanol was assumed to be homogenous in liquid phase.

The superficial velocity of gas was in the range of 9.8 to 16.4 m/s whereas the liquid superficial velocity varied in the range 0.02 to 0.2 m/s. Clearly, liquid was pushed by the gas which accelerated the liquid flow by shortening residence time by many folds. In order to determine the mixing in the liquid flow that might hinder the reaction progress, the flow of liquid inside the reactor was characterized by residence time distribution (RTD) by the method given in section 4.4.5. Figure 4.8 shows RTD curves at various flow rates, which indicate that the dispersion was higher at lower liquid flow rate, whereas, at high flow rate the flow approached the near plug flow behavior. The RTD of the reactor was fitted to the axial dispersion model and the estimated values of peclet number, residence time and cardanol conversion are given in the Table 4.1.
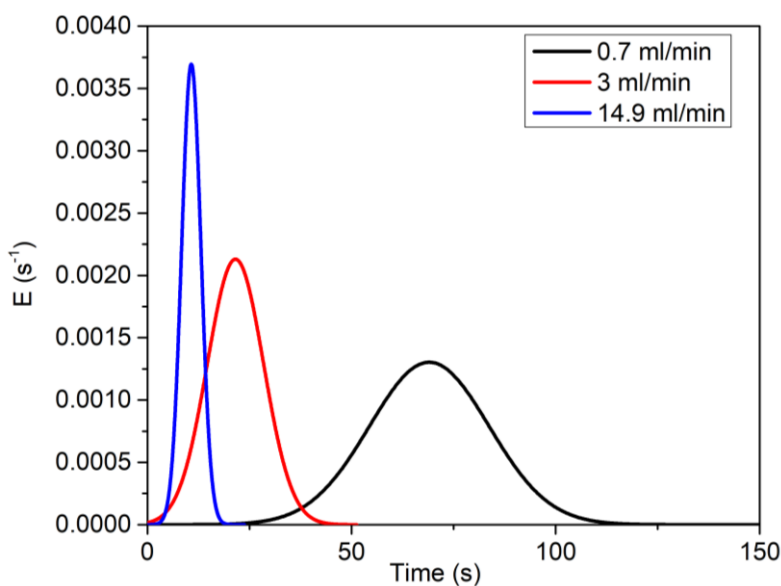
Figure 4.8 RTD curves for liquid in gas-liquid flow through helical coil reactor

Table 4.1 Mean liquid residence time, Peclet number and conversion of cardanol at various flow rates

Entry	Liquid flow rate Q_l (mL/min)	Mean liquid residence time (s) τ_l	Peclet number Pe	Conversion (x_{exp})
1	0	0	0	0.0
2	14.9	9	29	53.9
3	7.0	13	20	78.9
4	3.0	23	13	93.0
5	1.5	32	8	99.8
6	0.7	46	2	99.9

To estimate the intrinsic rate constants of overall cardanol consumption via ozonolysis reaction, two basic models for tubular reactor were tested. Assuming the first order reaction and plug flow behavior, the rate constants were estimated by minimizing the error between predicted and experimental conversion. The conversions could very well be predicted by this equation with value of rate constant at 0 ℃ was found to be 0.107 s⁻¹. As the dispersion was significant, the axial dispersion model was also employed to estimate kinetics of cardanol conversion.

$$x = 1 - e^{-k\tau}$$ ……………… (1)

where x is conversion, k is rate constant and τ is mean residence time (s). The mass balance equation for tubular reactor considering the dispersion in terms of Peclet number for first order reaction is given in equation 2.

$$x = 1 - \frac{4\,a\,e^{\left(\frac{Pe}{2}\right)}}{(1+a)^2\,e^{\left(\frac{a\,Pe}{2}\right)} - (1-a)^2 e^{\left(-\frac{a\,Pe}{2}\right)}}$$ ……………… (2)

$$a = \sqrt{1 + \left(\frac{4k\tau}{Pe}\right)}$$ ……………… (3)

where Pe is reactor Peclet number. Similar to approach followed previously reported, the value of rate constant was estimated by fitting this equation to experimental conversions at different Peclet numbers at various flow rates.[21,22] The predictions of both the models and experimental conversions are shown in Figure 4.9. The value of rate constant obtained was 0.096 s^{-1}, which was close to the previous values determined by plug flow model.
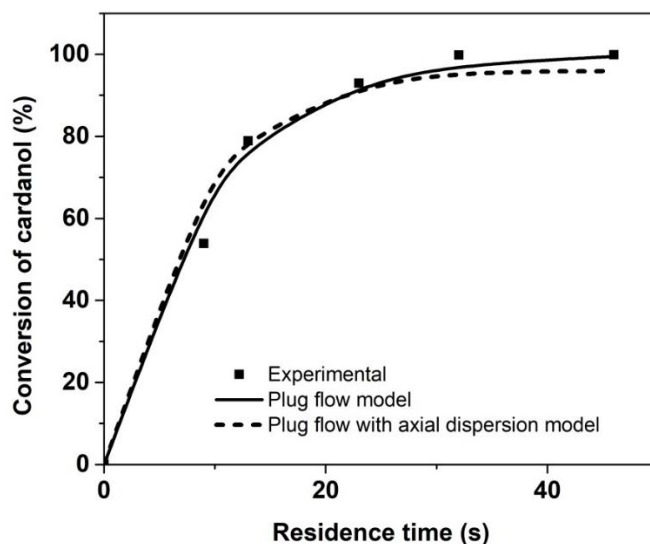
Figure 4.9 Kinetics of cardanol ozonolysis kinetics at 0 °C

Thus, it was concluded that reaction of cardanol oxidation is too fast and the dispersion has negligible effect on conversion at prevailing conditions. The only controlling factor was the residence time of liquid that is liquid flow rate of cardanol mixture. Hence, a simple plug flow model is appropriate to describe the kinetics of the cardanol ozonolysis at present conditions. Figure 4.10 shows cardanol conversion predictions and experimental values at different temperatures. The rate constants determined by plug flow model are given in Table 4.2. Based on the Arrhenius plot for cardanol conversion given in Figure 11, the activation energy and pre-exponential factors were estimated to be 16.17 kJ/mol and 136.67 s^{-1}, respectively

Table 4.2 Rate constants of cardanol ozonolysis

Entry	Temperature (^oC)	Overall cardanol consumption rate constants k (s^{-1})
1	-10	0.087
2	0	0.107
3	10	0.132
4	20	0.189
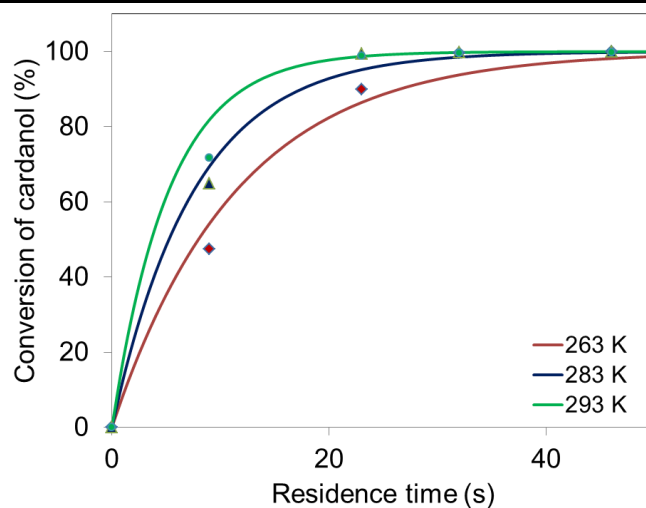
Figure 4.10 Kinetics of cardanol ozonolysis at various temperatures
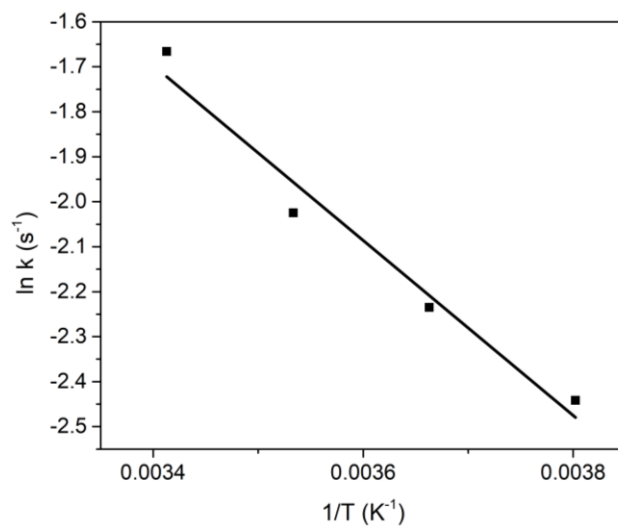
Figure 4.11 Arrhenius plot for conversion of cardanol via ozonolysis

A detailed model for prediction of monomer yields requires complete analysis and identification of products, the development of such model is underway. The current approach is simplified way to determine the intrinsic kinetics of gas-liquid reaction, herein, kinetics of cardanol ozonolysis using the continuous flow reactor.

4.4 Conclusion

Continuous flow ozonolysis of cardanol, a bio-based feedstock, for oxygenated functional monomer synthesis was studied. Unlike previous studies, a monomer 8-(3-hydroxyphenyl) octanal was synthesized along with many other oxidation products using acetone and water mixture as solvent. Though 47 % yield of HPOA lower compared to previous two/three step oxidation methods, the selective synthesis can be achieved by optimizing reaction conditions, hence, work up step can be eliminated. The yield of aldehydes HPOA and heptanal was maximum at 54.3 % conversion of cardanol at 0 °C and 9 s of liquid residence time, at an ozone to cardanol molar flow ratio of 2. Further, increase in mole ratio resulted in decrease of yield of products, however, conversion of cardanol was almost 99% at all mole ratios above 2. The positive effect of temperature on cardanol conversion was evident at low ozone to cardanol mole ratio.

The volumetric liquid mass transfer coefficient of the reactor was in the range of 0.02 to 0.1 s^{-1}. Owing to these values and high gas to liquid flow rates, the interphase mass transfer limitations on reaction kinetics were neglected. The dispersion in the liquid phase was characterized by RTD, the non-ideality in the flow was modeled using axial dispersion model. Two models, ideal plug flow and plug flow with axial dispersion, were evaluated for prediction of cardanol ozonolysis reaction kinetics. Despite prevailing dispersion, it was found that plug flow model was sufficiently predicting the conversion.

The results of the current study suggests that the perilous ozonolysis of cardanol for synthesis of valuable monomers can be carried out using a simple continuous flow technique in much more safer manner compared to the previous batch methods. While solvents and products can be recovered by coupling continuous distillation with flow reactors, optimization and design of continuous flow reactor for selective synthesis of these bio-based aldehydes and acid monomers required for high performance polymer synthesis from cardanol is under progress and will be reported separately.

4.5 Experimental and supporting information

4.5.1 ^{1}H NMR characterization
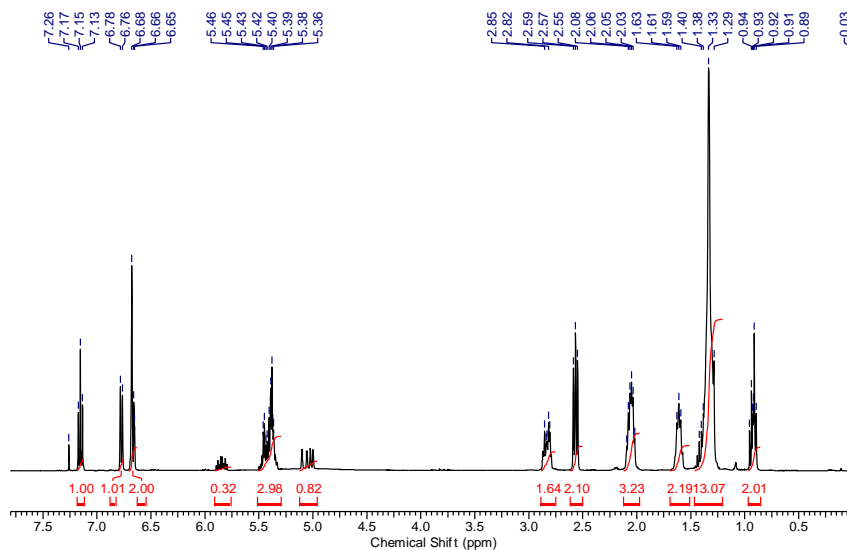
Figure 4.12 ^{1}H NMR of standard cardanol
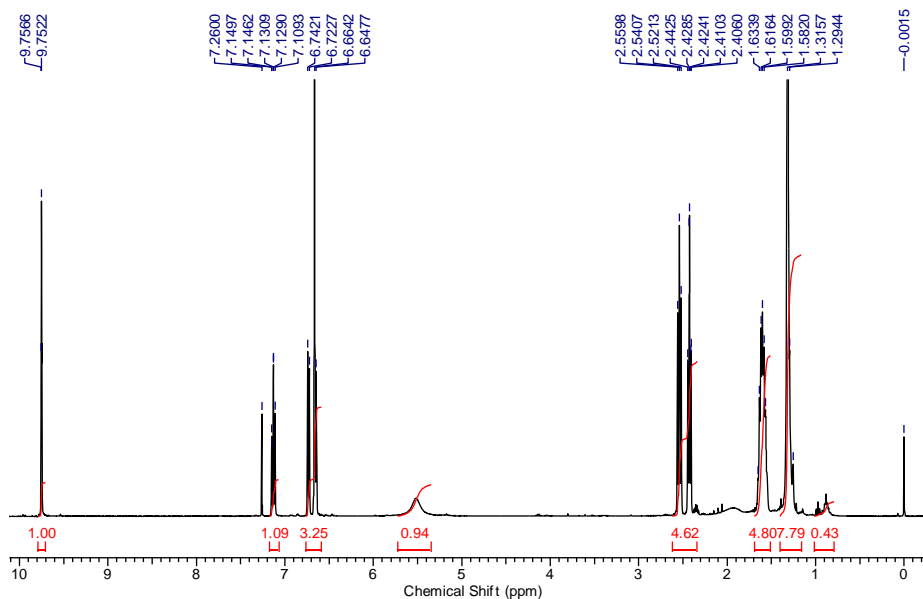
Figure 4.13 ^{1}H NMR of 8-(3-hydroxyphenyl)octanal (isolated from semi-batch)
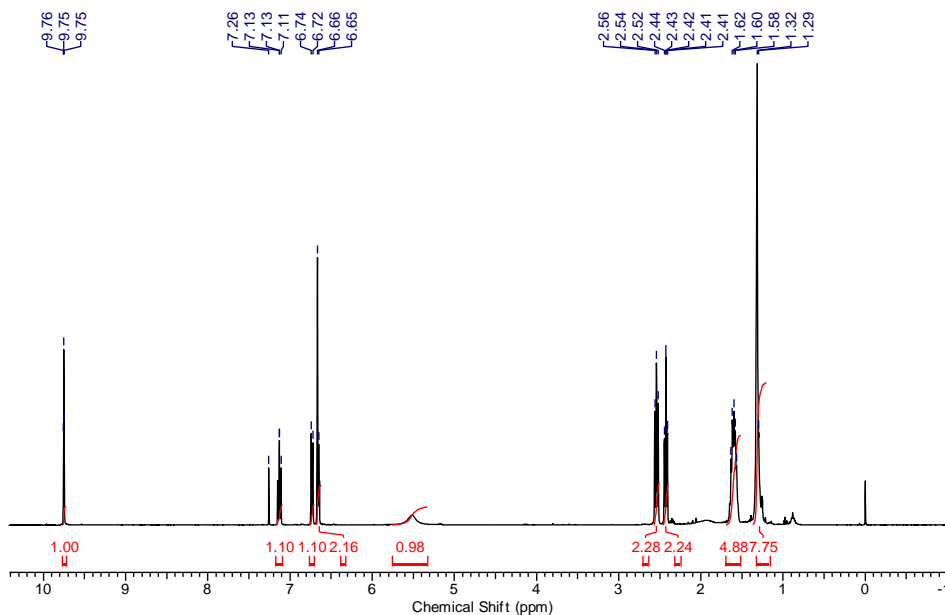
Figure 4.14 ^{1}H NMR of 8-(3-hydroxyphenyl) octanal (isolated from continuous flow synthesis)
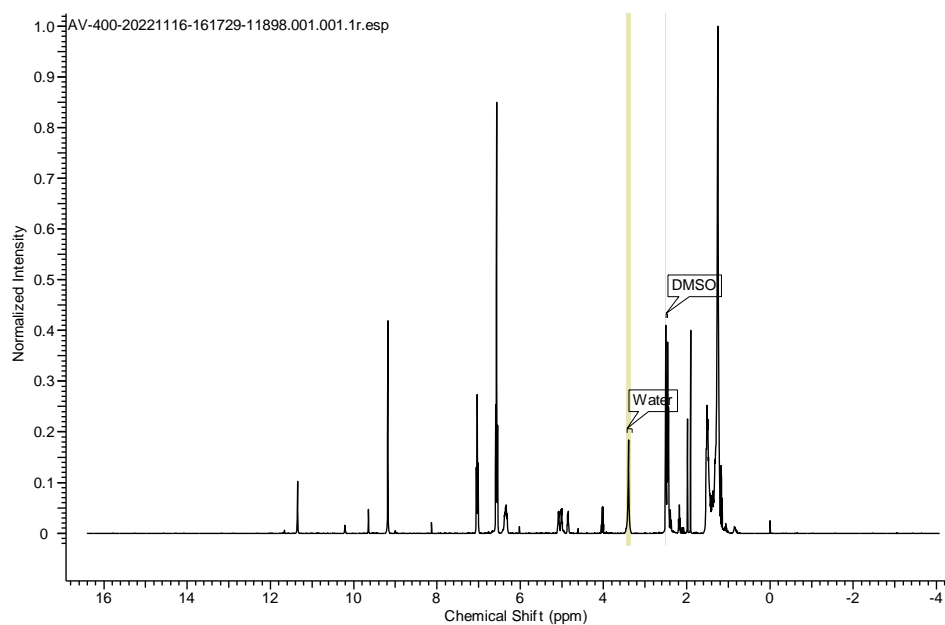
Figure 4.15 ^{1}H NMR of reaction mixture confirming presence of acid, aldehydes and other products

4.5.2 Actual photograph of reaction mixture
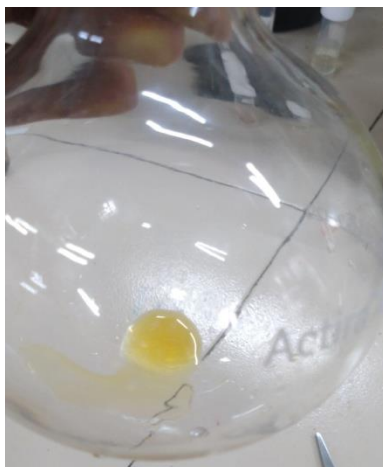
Figure 4.16 Actual photograph of reaction mixture

4.5.3 Gas Chromatography-Mass Spectrometric analysis
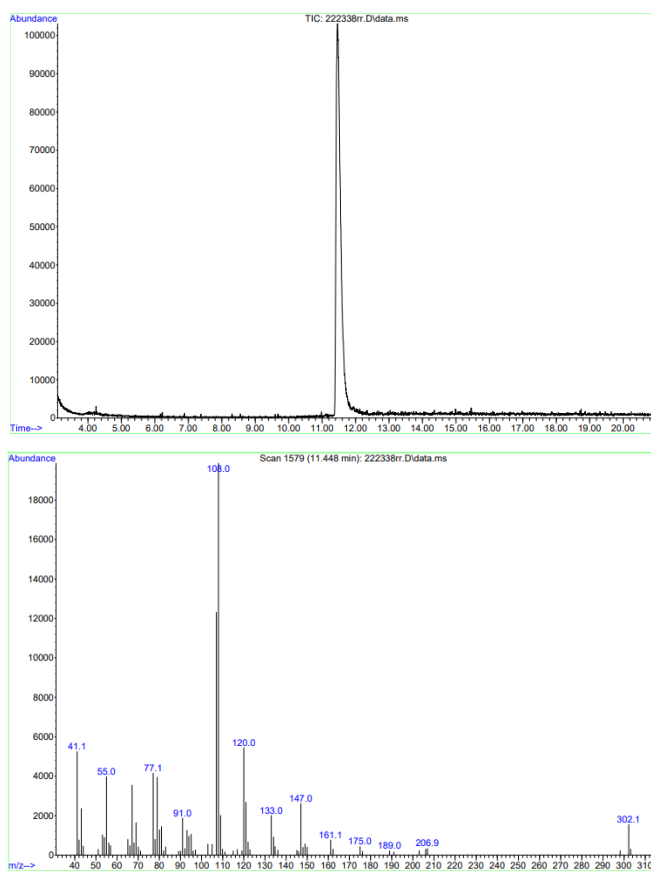
Figure 4.17 GC-MS spectra of standard cardanol (molecular weight 302 g/mol)
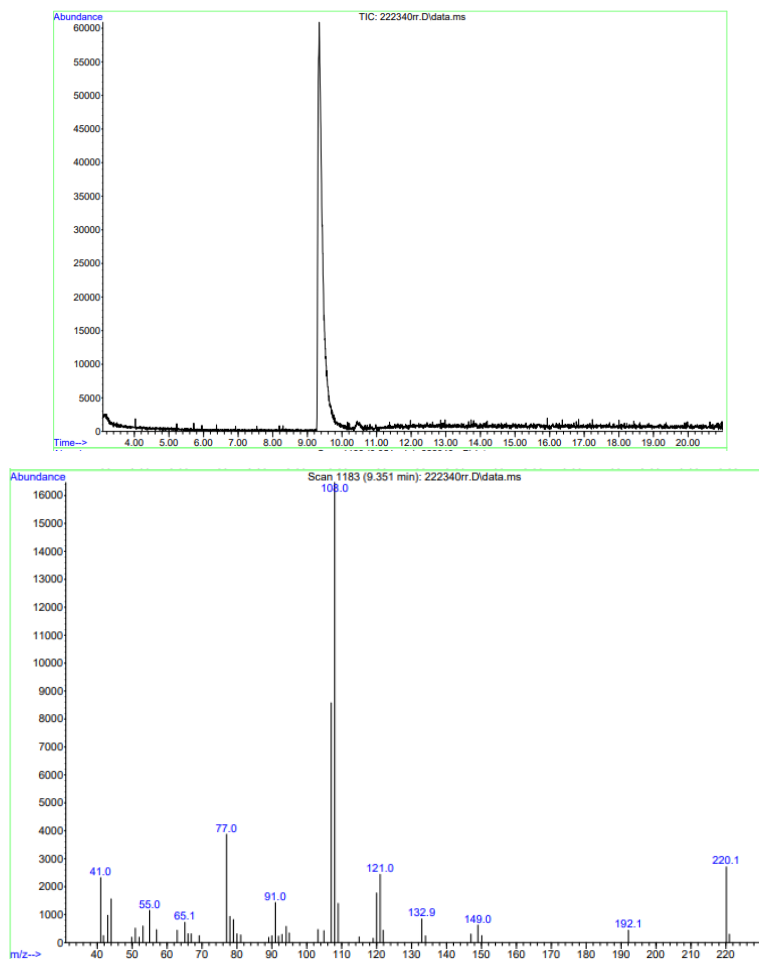
Figure 4.18 GC-MS of isolated 8-(3-hydroxyphenyl)octanal (molecular weight 220 g/mol)
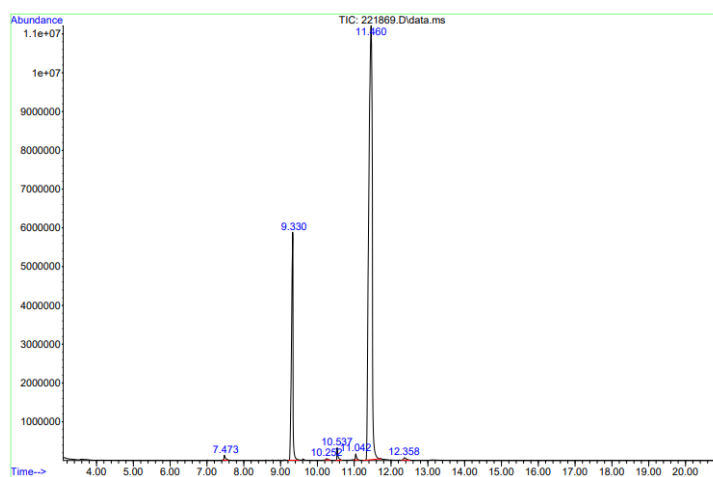
Figure 4.19 Chromatogram of reaction mixture (Ozone to Cardanol molar flow ratio: 2)
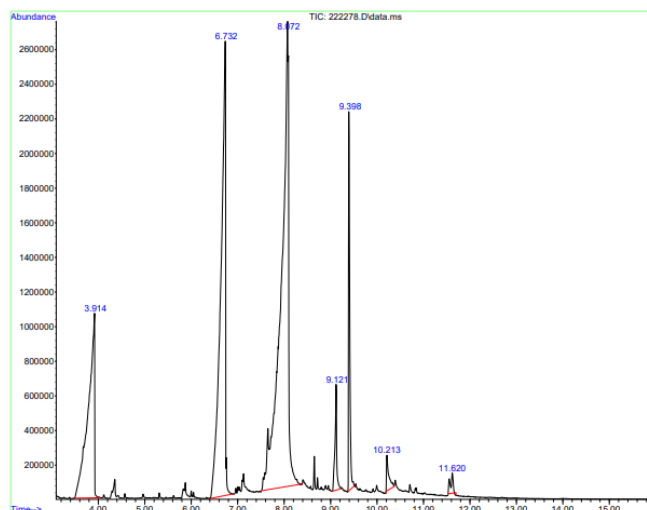
Figure 4.20 Chromatogram of reaction mixture (Ozone to Cardanol molar flow ratio: 12)
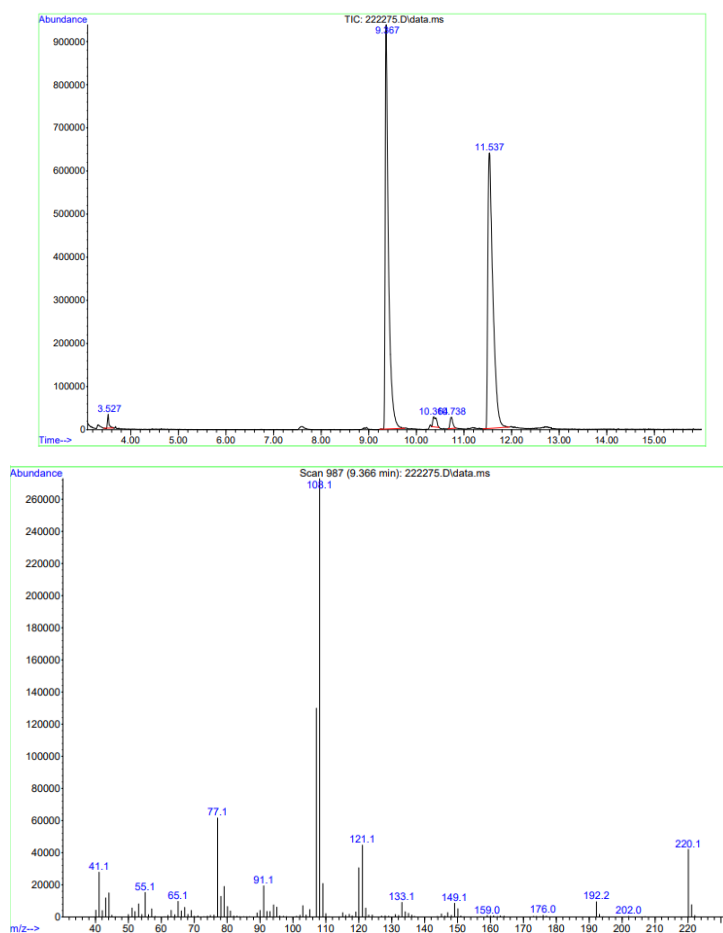
Figure 4.21 GC MS of reaction mixture (HPOA)

4.5.4 Estimation of gas-liquid mass transfer coefficient

The liquid side volumetric mass transfer coefficient (MTC) were determined by method given in 4.2.6.
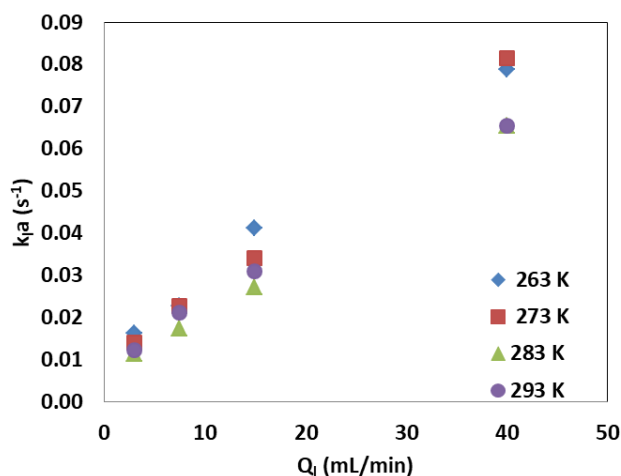
Figure 4.22 Effect of liquid flow rates on mass transfer coefficient

4.5.5. RTD analysis

RTD of gas-liquid flow was determined by tracer method. The obtained c-curves were converted to E-curve considering the Gaussian distribution of c-curve. Mean residence time and peclet number were calculated from E-curve from mean and variance.

4.6 References

1. Feldman, D. Polymer history. *Des. Monomers Polym.* **11**, 1–15 (2008).

2. Ghori, S. W., Siakeng, R., Rasheed, M., Saba, N. & Jawaid, M. *The role of advanced polymer materials in aerospace*. *Sustainable Composites for Aerospace Applications* (Elsevier Ltd, 2018). doi:10.1016/B978-0-08-102131-6.00002-5

3. Yang, Z., Peng, H., Wang, W. & Liu, T. Crystallization behavior of poly(ε-caprolactone)/layered double hydroxide nanocomposites. *J. Appl. Polym. Sci.* **116**, 2658–2667 (2010).

4. Briou, B., Caillol, S., Robin, J. J. & Lapinte, V. Cardanol-Based and Formaldehyde-Free Flexible Phenolic Networks. *Eur. J. Lipid Sci. Technol.* **120**, (2018).

5. Caillol, S. Cardanol: A promising building block for biobased polymers and additives. *Curr. Opin. Green Sustain. Chem.* **14**, 26–32 (2018).

6. Deutsch, J. & Köckritz, A. Synthesis of novel chemicals from cardanol as a product of cashew nutshell processing. *Food Sci. Nutr.* **8**, 3081–3088 (2020).

7. Voirin, C. *et al.* Functionalization of cardanol: Towards biobased polymers and additives. *Polym. Chem.* **5**, 3142–3162 (2014).

8. Jaffe, M. Applications of liquid crystal polymers. *J. Stat. Phys.* **62**, 985–995 (1991).

9. C. K. S. Pillai, D. C. S. and A. S. Therrnotropic liquid crystalline copolyester based on 8-(3-hydroxyphenyl) octanoic acid and p-hydroxybenzoic acid C. *Polym. Commun. Guildf.* **27**, 2–5 (1986).

10. Veena Vihaynathan, V.S. Prasd, C. K. S. P. Synthesis and Thermal Behavior of Thermotropic Terpolymers Based on 8-(3-Hydroxyphenyl)octanoic Acid, 2,6-Naphthalenedicarboxylic Acid, and Substituted Hydroquinones. *J. Appl. Polym. Sci.* **82**, 941–947 (2001).

11. Mitra, S. & Pillai, C. K. S. Semiflexible random thermotropic copolymers from 8-(3-hydroxy phenyl) octanoic acid and 3-chloro-4-hydroxy benzoic acid/3,5-dibromo-4-hydroxy benzoic acid. *J. Appl. Polym. Sci.* **107**, 778–783 (2008).

12. Graham, M. B. & Tyman, J. H. P. Ozonization of phenols from Anacardium occidentale (cashew). *JAOCS, J. Am. Oil Chem. Soc.* **79**, 725–732 (2002).

13. Michael D. Lundin, Andrew M. Danby, and Geoffrey R. Akien, Padmesh Venkitasubramanian and Kevin J. Martin, Daryle H. Busch, B. S. Intensified and Safe

Ozonolysis of Fatty Acid Methyl Esters in Liquid CO2 in a Continuous Reactor. *AIChE J.* **63**, 215–228 (2017).

14. Danby, A. M., Lundin, M. D. & Subramaniam, B. Valorization of Grass Lignins: Swift and Selective Recovery of Pendant Aromatic Groups with Ozone. *ACS Sustain. Chem. Eng.* **6**, 71–76 (2018).

15. Steffan Green, Thomas Binder, Erik Hagberg, and B. S. Correlation between Lignin−Carbohydrate Complex Content in Grass Lignins and Phenolic Aldehyde Production by Rapid Spray Ozonolysis. *ACS Eng. Au* (2022).

16. Subramaniam, B., Danby, A. M. & Lundin, M. D. Continuous process for the ozonolysis of lignin to yield aromatic monomers. *World Intellectual Property Organization* (2018).

17. Franco, C. & Olmsted, J. Photochemical determination of the solubility of oxygen in various media. *Talanta* **37**, 905–909 (1990).

18. Criegee, R. Mechanism of Ozonolysis. *Anyew. Chem. inrernal. Ed.* **14**, (1975).

19. Trabelsi, F. *et al.* Oxidation of phenol in wastewater by sonoelectrochemistry. *Chem. Eng. Sci.* **51**, 1857–1865 (1996).

20. Schiaffo, C. E. & Dussault, P. H. Ozonolysis in solvent/water mixtures: Direct conversion of alkenes to aldehydes and ketones. *J. Org. Chem.* **73**, 4688–4690 (2008).

21. Sikula, I. & Markoš, J. Modeling of enzymatic reaction in an airlift reactor using an axial dispersion model. *Chem. Pap.* **62**, 10–17 (2008).

22. Charles, G. *et al.* Determination of kinetic constants of a photocatalytic reaction in micro-channel reactors in the presence of mass-transfer limitation and axial dispersion. *J. Photochem. Photobiol. A Chem.* **223**, 202–211 (2011).

Chapter 5

Challenges, Conclusions and Future Outlook

In this chapter, the operational challenges pertaining to the investigation of hydrothermal processing and ozonolysis are discussed. The primary aim is to make readers aware about what needs to be carefully handled during such experiments and what one must avoid. It was also realized that some of the experiments could be done more efficiently had it was planned that way. An algorithm for such possible planning of successful experiments is also given at the end.

5.1 Challenges associated with NAG hydrolysis by subcritical and supercritical water

While developing insights of the transformations using reaction engineering, several challenges were faced that limited the development of technology in the given timeline. Nevertheless, the current insights pave the ways to the developments further and forms basis for further studies. In this chapter, the challenges encountered during Ph.D. work and their solutions are discussed.

5.1.1 Myriad product formation and selective synthesis during sub/supercritical water hydrolysis

Hydrothermal processing of any biomass results in myriad product formation. During NAG hydrolysis, there were several peaks in the chromatogram. Initially, method development by HPLC using aminex column was carried out. Sugars glucose, fructose, etc. could be quantitated using the method. However, this method was misleading as the accountability (accounted mass of products / total mass of product) done using number of compounds (peaks) and their yields was as low as 10-20 %. Hence, around 80 % of mass of NAG was unidentifiable. Hence, few more analytical techniques had to be used. Various protocols of GC, HPLC with different column and detectors were used to increase the accountability of the reaction. Finally, four different analysis methods GC (Carbowax and HP-5 column) and HPLC (C18 and aminex) were used to reach to a 60 % accountability of the products. The chromatogram of the reaction mixture obtained by all these methods is given below.
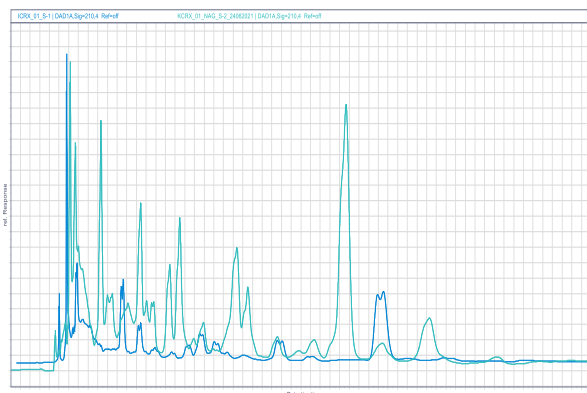
Figure 5.1 HPLC chromatograms of NAG hydrolysis reactions in subcritical and supercritical water at 25 MPa; residence time 10 s; initial conc. 5 % (w/w) a)Light blue: 400 ^{o}C b)Dark blue: 250°C (C18 column and UV detector)
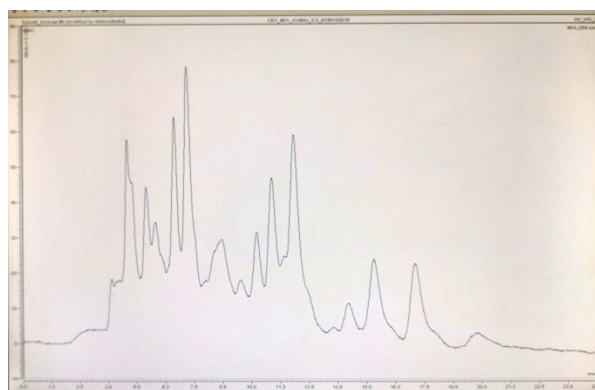
Figure 5.2 HPLC chromatogram of NAG hydrolysis reactions in subcritical water at 250 ^{o}C; 25 MPa; residence time 10 s; initial conc. 5 % (w/w) (Shodex Aminex-NH2 column and RI detector)

Non catalytic degradation of NAG in subcritical and supercritical water in continuous flow reactor actually produced many compounds, at 400 ^{o}C and 25 MPa some identified compounds are given in table 5.1, where the accountability on mass basis is around 40 %.

The yield of any of these compounds was not higher than 25 %; hence, it was difficult to have a selective synthesis of any compound. Such problem is similar to pyrolysis.[125]
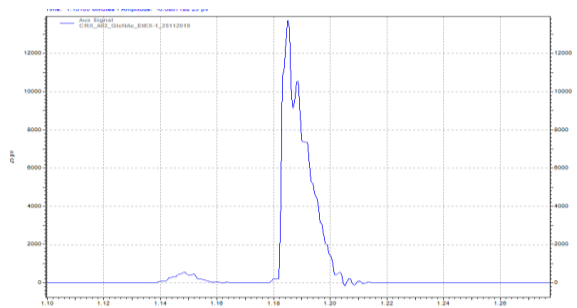
Figure 5.3 GC chromatogram of NAG hydrolysis reactions in subcritical water at 250 $^{\circ}$C; 25 MPa; residence time 10 s; Initial conc. 5 % (w/w) (HP-5 column and FID detector)

Table 5.1 Yield of products

Products	Yield % (mass basis)
Glycolic acid	20.62
Formic acid	7.06
Acetic acid	4.87
5-Hydroxymethylfurfural	0.20
Furfural	0.20
Acetamide	6.51
Pyrazole	0.37
1-Methyl pyrrolidine	0.00
3-Pyridine carboxyldehyde	0.28
2-Acetyl pyrazine	1.21

Hence, instead of selective synthesis, hydrothermal processing of biomass can be targeted for bio-oil production, wherein, the value of the product mixture is estimated based on calorific value estimated by accounting carbon, nitrogen, hydrogen and oxygen in the mixture irrespective of the number and nature of the compounds.

The usage of the in-line measurement of reaction progress using in-line analytical techniques such as an in-line NMR / IR or LCMS is highly recommended as it provides the real time data which can be used to track the instantaneous transformations and optimize process accordingly by cutting down the analysis time from hours to minutes. In general, while understanding NAG hydrolysis by sub/supercritical water the total time required for one complete experiment involving unsteady state and steady state was around 4-5 h while the analysis of complete reaction mass for coming to 60 % accountability was took around 2-3 days owing to longer retention times in HPLC (60-

120 min) and GC (30 min). While the added challenge was the degradation of reaction samples. The reaction samples contained a mixture of products including acids and amines, solids, it was seen that the reaction samples degraded rapidly, sometimes even before complete analysis. A graph of reactions resulted in generating actual output and total reactions is shown below.
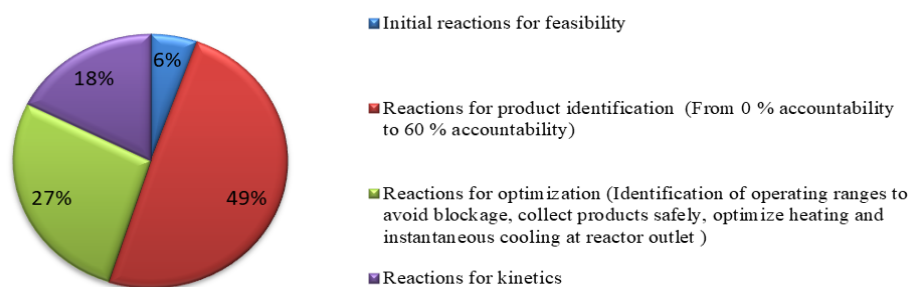
Figure 5.4 Statistics of experiments for complete investigation of NAG hydrolysis
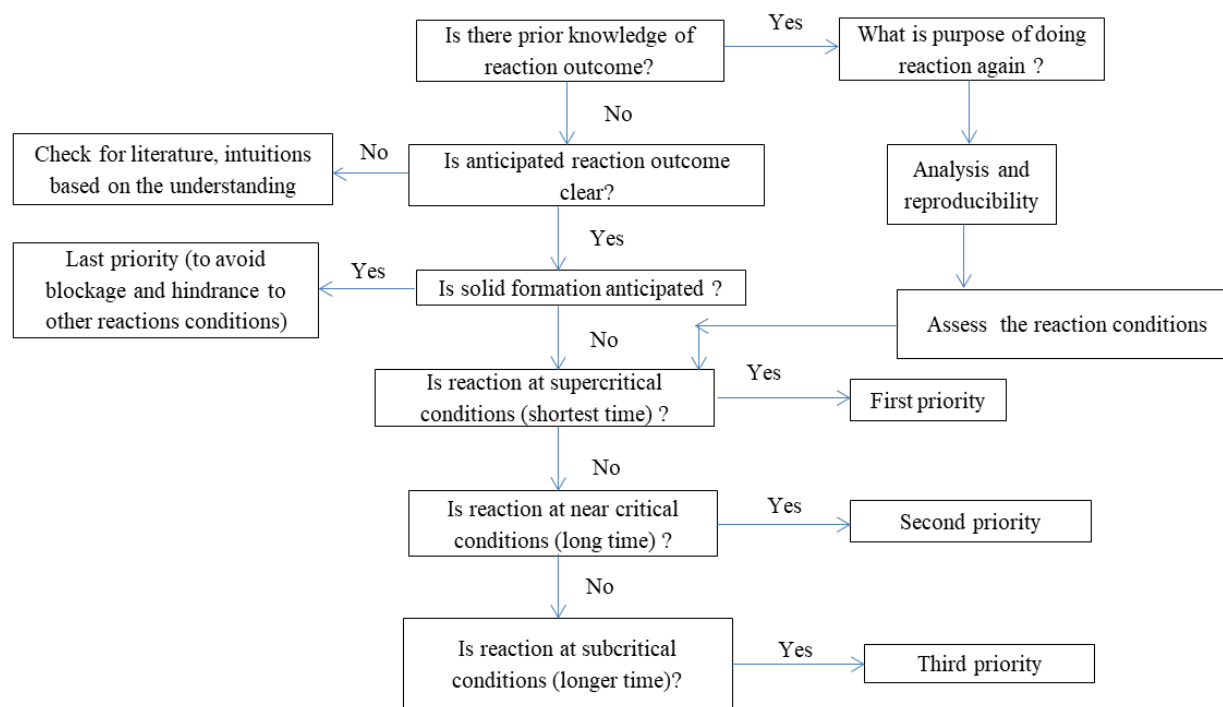
Figure 5.5 Algorithm for design of continuous flow experiments for sub/supercritical water hydrolysis of NAG

5.1.2 Unavailability of standards of the reaction products and product identification

Many of the products obtained during NAG hydrolysis were scarcely available. While most of the compounds were similar to that of products produced during glucose hydrolysis, the nitrogen containing compounds were new and had to be prepared in the laboratory based on the methods reported in the literature. 3-acetamideo-5-acetyl furan was one of products with importance in medical applications was quite commonly reported product, however, is not commercially available in several countries including India. In such problems, hydrothermal processing waste biomass may generate unknown products. Thus, product identification is bottleneck in such cases and developing a proper analytical protocol was a challenge. The typical organic chemistry practice of separating compounds by column chromatography was attempted to separate the compounds with both polar (silica) and non-polar (charcoal-celite) stationary phases. The major challenge is low concentration and highly similar nature (polar) of compounds resulting in no clear separation of products. Instead, the more efforts can be dedicated for fractionation of products and separation by distillation or extraction and development of analytical methods using HPLC, GC, IR e.g. development of a combination of two separating columns with two or more detectors.

5.1.4 Operating conditions and reactor selection

Since, subcritical and supercritical water are states of water achieved by maintaining specific temperature and pressure conditions, a slight change in these properties resulted in unsteady state. As water plays key role of oxidant, catalyst and solvent, the corresponding changes in the physicochemical properties resulted in change in product distribution drastically. Some products formed at particular conditions, while the major products disappeared as phase changes.

Moreover, the reactions at such elevated temperature and pressure are fast with reaction time in the range of milliseconds.[54] Maintaining reaction conditions and achieving reaction times is a key challenge as the heat transfer rate from external electrical heater to the reactor was slower than the reaction rate. The critical mass required to carry the heat was varying with reaction temperature as the specific heat capacity of water goes through maxima, with maximum at pseudo-critical point.[150] Reactor selection for supercritical

water processes has been an independent topic of research as the reaction time is in milliseconds requiring smaller reactor volumes posing challenges for achieving process conditions such as high temperature and pressure.

A detailed modelling of the heat transfer of a supercritical system will help know the real temperature profiles in the reactor. Which such simulations are possible, the assumptions regarding the physico-chemical properties of reaction mass will pose restrictions in becoming realistic.

5.1.5 Limited feasible range of operating conditions

The product distribution obtained during NAG hydrolysis included solids, liquids and gaseous products which varied with phase of water as discussed in chapter 3. Hence, at subcritical conditions excessive solid formation blocked the reactor. This blockage along with high pressure resulted in the severe sudden pressure increase and pump failures. Hence, a careful design of experimental conditions was done to avoid this scenario. It should be noted that the desired product distribution could be obtained at the designed experimental conditions. For larger scales, it is imperative to take into account these challenges.

5.1.6 Need for data generation on fundamental physical properties of compounds for software databases

Biomass conversion processes utilizing supercritical water involve many compounds new to the software databases including NIST. Few Aspen simulations were attempted to simulate the supercritical water hydrolysis process for NAG valorisation as shown in figure 5.2. However, due to non-availability of the fundamental properties of the compounds produced during NAG hydrolysis, a simple mass balance was not achieved.[151–153] A simple Rgibbs model was used to predict the yields of the products by providing inputs based on the experimentally identified products. Rgibbs model® uses Gibbs energy minimization strategy to estimate the output. Since, the basic binary interaction parameters and physicochemical properties of several compounds including Pyrazole, Pyrazine, Pyridine, Pyrrolidine, and etc. derivatives were not available in the databanks provided in the aspen. The solution is to calculate and regress properties by various group contribution methods.
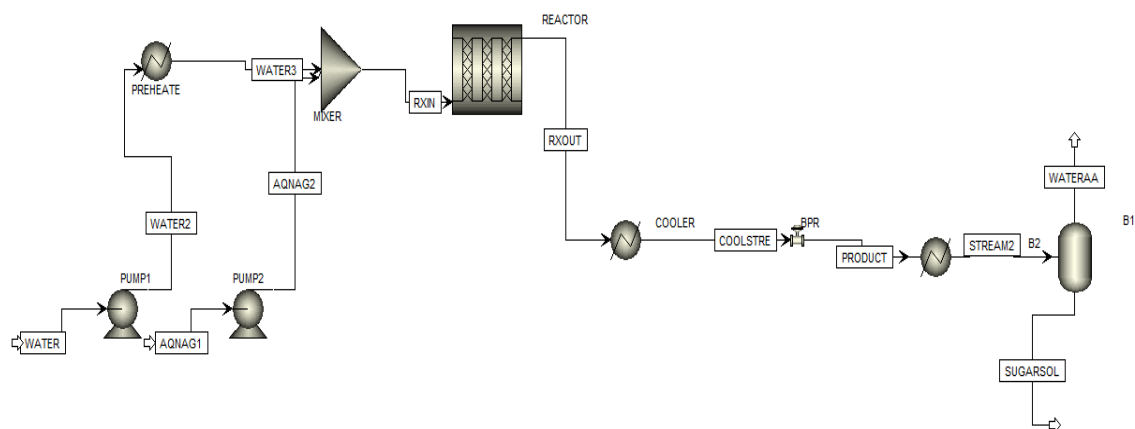
Figure 5.6 Aspen simulations for supercritical water hydrolysis of NAG

The reactor models those could be employed for describing the process were Rgibbs and RYield as no kinetic data was available. Nevertheless, the kinetic model developed using continuous flow reactor, as discussed in chapter 3, is now a fundamental study and the kinetic parameters estimated can be accurately used to simulate process using other reactor models RPlug, RCSTR, etc.

5.1.7 Reactor design for hydrolysis of chitin

Since NAG was a representative of chitin, inspired by the developed understanding of NAG hydrolysis, few experiments for direct hydrolysis of chitin were carried out. The reactor used was a flow through reactor in which the solid powder of chitin (<5 μm) was filled inside the reactor through which water preheated to supercritical conditions was passed. The obtained reaction mixture had similar composition to that of NAG hydrolysis. However, it also blocked the reactor as the powder was converted to complete black solid melt within few minutes. Thus, it could be seen that the chitin can be hydrolysed with only water at supercritical conditions provided a reactor should enable short reaction times and faster residence times.

5.2 Challenges associated with cardanol ozonolysis and technology development

5.2.1 Safety

First and foremost challenge associated with any ozonolysis reaction is the safety associated with the handling of the ozone and ozonides. As ozone is inherently hazardous chemical causing the shortness of breath and wheezing and coughing if inhaled by the personal working. The ozonides are highly unstable oxygenated compounds which can cause explosion if accumulated.[154]

During development of continuous flow method for cardanol, the set up was designed such that the ozone exposure was minimum. The ozonides were quenched in situ by water in the solvent mixture and were not accumulated inside the reactor as the flow was continuous through the reactor.

5.2.2 Downstream processing and selective production of monomers

The ozonolysis of cardanol resulted in the mixture of oxygenated compounds including aldehydes, acids, etc. Developing a separation protocol for this reaction mixture is critical for efficient production and commercial use of 8-hydroxyphenyl octanal a potential monomer for liquid crystal polymer synthesis. Micro distillation is the simplest method that can separate these products, coupling micro distillation with flow reactor is a potentially efficient technology for synthesis of functional monomers.

5.3 Summary and conclusions

With the emergence of the concept of circular bio-economy, the efficient utilization of wastes and residues has gained immense importance. Seafood waste and plant oils are abundant waste biomass resources generated in several million tons every year, however, surprisingly remain under explored compared to lignocellulosic biomass. The conversion of such materials to value-added chemicals can solve issues of the disposal of these wastes and bring back the material to carbon chain, thus, promoting the bio-economy cycle. In this thesis, the valorization of two waste biomass-derived chemicals viz. *N*-acetyl-D-glucosamine (NAG) and cardanol have been investigated via sub- and supercritical water hydrolysis and continuous flow ozonolysis, respectively.

The **chapter 1** of the thesis discusses the necessity to valorize waste biomass and compares various approaches, including thermochemical, chemical, and biological ones. This chapter

specifically describes the goals, difficulties, and necessity of two experiments that were conducted, namely the continuous flow ozonolysis of cardanol and supercritical water hydrolysis of NAG.

In the **chapter 2**, it is examined whether or not N-acetyl-D-glucosamine (NAG), a monomer of the abundant renewable marine biopolymer chitin, may be hydrolyzed in subcritical water to produce value-added compounds. Acetic acid and humins were the main byproducts of non-catalytic hydrolysis, with quantities of formic acid, lactic acid, glucose, fructose, 5-hydroxymethylfurfural (5-HMF), etc. Enough acidity is produced by the increased ionization of water at subcritical temperatures (200 °C; 5-10 MPa) to allow for the deacetylation of NAG. The considerable humin production shows that 5-HMF polymerization and self-condensation are encouraged in water at subcritical circumstances. The acid catalyst was used, and process parameters were optimized using Box-Behnken design coupled with the maximum yield of 27.13 1% and 53.46 1% of 5-HMF and LA, respectively using response surface methodology.

In **chapter 3**, a thorough investigation of the kinetics of NAG hydrolysis in a continuous flow reactor under sub-critical conditions has been conducted. Using a continuous flow reactor, experiments were conducted by varying the temperature (250-400 ^{o}C), pressure (5-25 MPa), and residence time (2-60 s). The reactions produced a diverse range of products, including sub- or supercritical water-sensitive solid, liquid, and gaseous chemicals. The main products in the liquid fraction were acetamide, glycolic acid, formic acid, acetic acid, and acetic acid. Several oxidation, reduction, and secondary processes take place during the hydrolysis of NAG in subcritical and supercritical water, followed by the immediate deacetylation of NAG. Acetic acid, glycolic acid, and formic acid yields are predicted using a kinetic model. The network of reactions showed specifc deviations than conventional understanding.

The development of a continuous flow ozonolysis technique for the valorization of cardanol through the synthesis of 8-(3-hydroxyphenyl) octanal (HPOA), a functional monomer utilized in the production of liquid crystal polymers is covered in the **chapter 4**. For effective ozone utilization and controlled oxidation, ozonolysis was performed in continuous flow utilizing a helical coil reactor, following batch optimization and product analysis by NMR. The two main products that had been identified were HPOA and heptanal. A significant yield of HPOA was

obtained at 50 % conversion of Cardanol in very short time, along with their acid derivatives. Owing to high mass transfer rates, a simple kinetic model incorporating residence time distribution was developed by considering reactions in liquid phase only. The predicted yields of aldehydes and cardanol conversion at various temperatures are in good agreement with the experimental results.

5.4 Future outlook

1. Use of software like Rings for network generation and detailed kinetics of the NAG hydrolysis using water at subcritical and supercritical water

2. Use of machine learning for optimization and process parameters prediction coupled with kinetics. While there is lack of information available for hydrothermal processing of chitin and NAG, a data involving transformations of identified intermediates at similar conditions can be considered for generating database. However, the difficulties in experimentation and analysis also imply that the data reported must be scrutinized for reliability.

3. Reactor design- Reactor design for an efficient and high throughput process for value-up gradation of biomass using sub-/supercritical water is critical due to 1. Constantly fluctuating properties of water at such conditions; 2. Solid raw material to be fed at high pressures and solid flow; 3. Formation of solid products humins during reactions. A careful heat and mass coupled modelling of reactor is crucial for understanding and optimizing the reactor performance. Reactors with high surface area at small volumes are required in particular as the residence times falls to seconds at supercritical conditions. However, it is always recommended to have the simplest reactor configuration like a plug flow reactor for safe and easy handling of reactions at such high temperature and pressure.

4. Optimization of hydrolysis process- The process optimization is a key to study the process; however, carrying out numerous experiments is problematic, especially, at such high pressure and temperature conditions. Hence, new techniques as employed in chapter 2, must be adapted. However, those should be linked with prior experimental understanding to come up with the right operating ranges.

5. Development of hydrothermal process for chitinous biomass

6. Reactor design and optimization for selective synthesis of monomers

7. Development of continuous separation method for purification of aldehyde monomers

ABSTRACT

Name of the Student: Sphurti Prakash Kulkarni   **Registration No.:** 20EE18J26016

Faculty of Study: Engineering Sciences   **Year of Submission:** 2023

AcSIR academic centre/CSIR Lab: CSIR-National Chemical Laboratory, Pune

Name of the Supervisor(s): Dr. Amol A. Kulkarni and Dr. Sunil S. Joshi

Title of the thesis: "Valorization of waste biomass derived chemicals via supercritical water hydrolysis and continuous flow ozonolysis"

Seafood waste and plant oils are abundant waste biomass resources generated in several million tons every year, however, surprisingly remain under explored compared to lignocellulosic biomass. The conversion of such materials to value-added chemicals can solve issues of the disposal of these wastes and bring back the material to carbon chain, thus, promoting the bio-economy cycle. In this thesis, the valorization of two waste biomass-derived chemicals viz. N-acetyl-D-glucosamine (NAG) and caradnol have been investigated via sub- and supercritical water hydrolysis and continuous flow ozonolysis, respectively.

In the first chapter of the thesis the need for valorization of waste biomass is discussed along with the comparison of various techniques including thermochemical, chemical and biological methods. Specifically, this chapter discusses the objectives, challenges and need of two investigations undertaken i.e. supercritical water hydrolysis of NAG and continuous flow ozonolysis of Cardanol.In the second chapter, the subcritical water hydrolysis of N-acetyl-D-glucosamine (NAG), a monomer of abundant renewable marine biopolymer chitin, for production of value-added chemicals in presence and absence of a catalyst is investigated. During non-catalytic hydrolysis, the major products identified were acetic acid and humins along with traces of formic acid, lactic acid, glucose, fructose, 5- hydroxymethylfurfural (5-HMF),etc. The enhanced ionization of water at subcritical conditions (200 ◦C; 5-10 MPa), provides enough acidity for deacetylation of NAG. The significant humin formation indicates that the self-condensation and polymerisation of 5-HMF is favored in water at subcritical conditions. The maximum yield of 27.13 ± 1% and 53.46 ± 1% of 5-HMF and LA, respectively, was obtained by employing the acid catalyst, at process conditions optimized using Box-Behnken design coupled with response surface methodology. A detailed invetigation of immddiate transformations and kinetics of NAG hydrolysis in sub-critical using continuous flow reactor has been studied in detail, in third chapter. Experiments were carried out using a continuous flow reactor by varying temperature (250-400 °C), pressure (5-25 MPa) and residence time (2 - 60 s). A wide product distribution was obtained during the reactions including solid, liquid and gaseous compunds, sensitive to the state of water sub- or supercritical. The prominent products present in liquid fraction were glycolic acid, acetic acid, formic acid , 5-HMF and acetamide. Followed by instantaneous deacetylation of NAG, several oxidation, reduction and secondary reactions occur during hydrolysis of NAG in subcritical and supercritical water. A kinetic model for prediction of yields of acetic acid, glycolic acid and formic acid is developed. The network of reactions showed specifc deviations than conventional understanding.

In the fourth chapter, the development of continuous flow ozonolysis process for valorization of Cardanol by synthesizing 8-(3-hydroxyphenyl)octanal (HPOA) (a functional monomer used for synthesis of liquid crystal polymers) is dicsussed. Followed by batch optimization and product characterization by NMR, ozonolysis was carried out in continuous flow using a helical coil reactor for efficient utilization of ozone and controlled oxidation. A significant yield of HPOA was obtained at 50 % conversion of Cardanol in very short time, along with their acid derivatives. Mass transfer and mixing in the reactor were systematically characterized; kinetics of cardanol consumption was evaluated by incorporating non-ideal behavior in the axial dispersion model to predict the conversion of cardanol. The predictions show good agreement with the experimental yields of aldehydes and cardanol conversion at various temperatures. In the last chapter the major challenges, insights generated and future directions are discussed.

Erratum

List of publications

1. **Kulkarni, S. P.**, Dure, S. N., Joshi, S. S., Pandare, K. V., & Mali, N. A. Subcritical water hydrolysis of N-acetyl-D-glucosamine: Hydrolysis mechanism, reaction pathways and optimization for selective production of 5-HMF and levulinic acid. (2022) Carbohydrate Research, 516, 108560.

2. **Kulkarni, S. P.**, Joshi, S. S., & Kulkarni, A. A. Reaction pathways and kinetics of N-acetyl-D-glucosamine hydrolysis in sub-and supercritical water. (2023) React. Chem. Eng., Advance Article

3. **Kulkarni, S. P.**, and Kulkarni, A. A. Ozonolysis of cardanol in a continuous flow tubular reactor (Manuscript under revision)

4. **Kulkarni, S. P.**, Joshi, S. S., & Kulkarni, A. A. Cellulose hydrolysis by sub- and supercritical water-A minireview, (Manuscript under revision)

5. **Kulkarni, S. P.**, and Kulkarni, A. A. Continuous flow ozonolysis of biomass: A review (Manuscript under revision)

List of conferences

1.   Oral presentation in 4th NCL-RF Annual Students Conference 2022 at CSIR-NCL, Pune, India, Nov-2022

Exploring reaction pathways and kinetics of hydrolysis of *N*-acetyl-D-glucosamine in sub-and supercritical water using a compact flow reactor

Abstract

N-acetyl-D-Glucosamine (NAG), a basic building block of biopolymer chitin, is the most important model compound of chitinuous seafood waste biomass, generated in several million tonnes annually. On the other hand, Water, at subcritical (SubCW; $100^{\circ}C<T<374^{\circ}C$ and 25 MPa) and supercritical conditions (SCW; $T>374^{\circ}C$ and 25 MPa), offers excellent advantages as a reaction medium enabling sustainable and greener processing of biomass. In this study, the hydrolysis of NAG in SubCW and SCW to produce valuable chemicals is investigated using a batch and a compact tubular reactor. A tubular flow reactor, developed considering the dynamicity of transport properties of SubCW and SCW, provided high heating rates and very short residence times (8-24 s) required to understand the fast reactions involved in NAG hydrolysis at prevailing conditions. A wide product distribution was obtained during NAG hydrolysis including solid, liquid and gaseous compounds, sensitive to the state of water sub- or supercritical. SubCW promoted the excessive formation of solid compounds, while no solids but gaseous products predominantly formed in SCW. Interestingly, the nitrogen containing heterocyclic compounds i.e. derivatives of Pyrazole, Pyrazine and pyrrolidine were obtained only during SCW hydrolysis, whereas the valuable acids viz. Glycolic acid, Acetic acid and Formic acid were the major products in the liquid fraction at all conditions. Screening various reaction pathways and kinetic modeling approaches, a comprehensive kinetic model for prediction of acid yields is provided. Though the overall NAG decomposition reaction followed Arrhenius behavior, few individual reactions deviated

from Arrhenius behavior indicating the peculiar effect of the phase of water on the mechanism of hydrolysis of NAG in SubCW and SCW. The finding of this study is essential in the development of the shell bio-refinery to produce value- added chemicals from chitinous biomass.

2.   Poster presentation in 26th International Symposium on Chemical Reaction Engineering (ISCRE 26), India, Nov-2021

Tunable transformations of *N*-acetyl-D-glucosamine in subcritical and supercritical water

Abstract

Water in the subcritical and supercritical state is a fascinating reaction medium for clean, safe and environmentally benign organic reactions, as it exhibits some unique chemical and physical properties. The dielectric constant decreases whereas the ionic product of water increases towards critical point (T_c=374°Cand P_c=22MPa).With low viscosity, high dispersion and extremely small surface tension, the subcritical and supercritical water may offer several advantages for mass transfer limited reactions1 . The tunability of these properties with temperature and pressure can provide the control over reaction selectivity by avoiding the byproduct formation. The combination of above factors with often considerable water content of biomass makes the subcritical and supercritical water a potential medium for biomass processing. Chitin is world's second most abundant biopolymer after cellulose, is also derived from seafood waste. *N*-Acetyl-D-Glucosamine (GlcNAc), being monomer of chitin, is a strong candidate for mass production of platform chemicals from seafood waste. The present work discusses the non-catalytic reactions of GlcNAc in subcritical, near critical and supercritical water, in the temperature range of 200-400 ^{o}C and pressure range of 10-25 MPa. The effect of phase of water on product distribution is studied. A kinetic model for reaction network using lumping scheme is developed and values of activation energies and pre-exponential factors are estimated.

Methodology: A reactor set up was designed for high temperature and pressure reactions with precise pressure control and high heating rate. The reactions were carried out at temperature between 200-400 ^{o}C and pressure between 10-25 MPa. The effect of phase of reaction medium was studied by varying operating conditions from subcritical to supercritical conditions. For the complete analysis of the reaction products, different analytical tools were used including HPLC, GC and Mass Spectroscopy. The detailed reaction mechanism is devised based on the identified products. The reaction network is reduced to a lumped model for developing the kinetic model. The kinetic parameters were estimated on the basis of nonlinear regression and the differential equations were solved using MATLAB software.

Results: The products of non-catalytic conversion of GlcNAc in subcritical and supercritical included the solid, liquid and gaseous products. The major liquid soluble products were simple organic acids, amides

and heterocyclic compounds. The unprecedented formation of some distinct heterocyclic compounds could be achieved at supercritical conditions. The solid formation at subcritical conditions could be avoided completely at supercritical conditions, as predominating reaction mechanism shifts from ionic to free radical. The transformations of GlcNAc in water are very fast reactions at such high temperature and pressure. The reaction network devised from the mechanism of such fast transformations could be reduced using lumping scheme. The lumped kinetic model showed excellent agreement with experimental data.

Key Conclusion: The phase of reaction medium has a profound effect on the reaction mechanism as diverse nature and numbers of products are obtained in different operating zones. The product distribution of conversion of *N*-acetyl-D-Glucosamine could be tuned with operating conditions and kinetic model using lumping scheme could fairly describe the kinetic structure of transformations.

3.   Oral presentation in Advances in Chemistry and Chem. Eng. 2021(ACCE-2021), SVNIT, Surat, India, Aug-2021

Non-catalytic reactions of Chitin monomer, *N*-acetyl-D-glucosamine, in Sub and Supercritical Water

Abstract

Water, near or above critical point (374 ^{o}C, 22 MPa), is a fascinating reaction medium as an environmental innocuous medium for new reactions. The solvent and transport properties of water change dramatically and can be tuned by varying temperature and pressure. Recent reports on biomass conversions to value-added chemicals highlighted Supercritical Water as a potential reaction medium. Application of Sub or Supercritical water for biomass processing incorporates many principles of green chemical engineering. N-acetyl-D-glucosamine (GlcNAc) is a basic unit of the second most abundant biopolymer, Chitin. The conversion of Chitin to value-added chemicals is intermediated by its monomer GlcNAc. However, very limited information is available on the conversions of GlcNAc at such high temperatures and pressures. The present work discusses the non-catalytic reactions of GlcNAc in the water at subcritical, near critical and supercritical conditions, the optimization of process conditions at the temperatures in the range of 200-400 ^{o}C and pressure in the range of 10-25 MPa. The reactions were carried out in a reactor setup developed for carrying out non-catalytic or homogenous catalytic reactions at high temperature and high pressure. The water was preheated and then mixed with an aqueous solution of GlcNAc in a tubular reactor maintained at the required reaction temperature and pressure and quickly quenched to avoid the decomposition of products due to longer reaction times. The analysis of the

reaction samples was done by using HPLC, GC and Mass Spectrometry. The investigation showed that the major product distribution varied with the process conditions. In the case of the temperature, at a lower temperature, the major products formed were acetic acid and N-containing compounds like amino sugar derivatives, whereas, high temperature facilitated the breakage of C-N bond resulting in dehydration compounds, sugar derivatives, and more gaseous products. The change in the product distribution with the change in conditions (sub, near critical and supercritical) attributed to the effect of the phase of the reaction medium on the reaction mechanism (ionic reactions at near-critical water and radical reactions in supercritical water). The reactions are found to be very fast, as the reaction times required for almost 90 % conversion of GlcNAc was as low as 4-5 s at high temperatures. The major products have resulted from a combination of series and parallel reactions of GlcNAc and secondary decomposition reactions of initially formed unstable products of GlcNAc in the sub and supercritical conditions.

4.   Poster presentation in Advances in Chemical Engineering-2020 (AdCHE-2020), UPES, Dehradun, India, Feb-2020

An investigation of non-catalytic reactions of *N*-acetyl-D-glucosamine in sub and supercritical water

Abstract

Water, near or above critical point (374 °C, 22 MPa), has attracted the attention of researchers in recent years as an environmental innocuous medium for new reactions. The solvent and transport properties of water change dramatically and can be tuned by varying temperature and pressure. Recent reports on biomass conversions to value-added chemicals highlighted Supercritical Water as a potential reaction medium. In the review, Lachos-Perez et. al. concluded that the application of Sub or Supercritical water for biomass processing incorporates many principles of green chemical engineering. *N*-acetyl-D-glucosamine(GlcNAc) is a basic unit of the second most abundant biopolymer, Chitin. The conversion of Chitin to value-added chemicals is intermediated by its monomer GlcNAc. However, very limited information is available on the conversions of GlcNAc at such high temperatures and pressures. The present work discusses the non-catalytic reactions of GlcNAc in the water at subcritical, near critical and supercritical conditions, the optimization of process conditions with kinetic studies of the reactions at the temperatures in the range of 200-400°C and pressure in the range of 10-25 MPa. The reactions were carried out in a continuous flow reactor, developed for carrying out non-catalytic or homogenous catalytic reactions at high temperature and high pressure. The water was preheated and then mixed with an aqueous solution of GlcNAc in a tubular reactor maintained at the required reaction temperature and

pressure and quickly quenched to avoid the decomposition of products due to longer reaction times. The analysis of the reaction samples was done by using HPLC, GC and Mass Spectrometry. The investigation showed that the major product distribution varied with the process conditions. In the case of the temperature, at a lower temperature, the major products formed were acetic acid and N-containing compounds like amino sugar derivatives, whereas, high temperature facilitated the breakage of C-N bond resulting in dehydration compounds, sugar derivatives, and more gaseous products. The change in the product distribution with the change in conditions (sub, near critical and supercritical) attributed to the effect of the phase of the reaction medium on the reaction mechanism (ionic reactions at near-critical water and radical reactions in supercritical water). The reactions are found to be very fast, as the reaction times required for almost 90 % conversion of GlcNAc was as low as 4-5 s at high temperatures. The rate of conversion of GlcNAc was found to follow first-order kinetics. The major products have resulted from a combination of series and parallel reactions of GlcNAc and decomposition reactions of initially formed unstable products of GlcNAc in the sub and supercritical conditions.

Awards

1. First runner up prize for poster presentation at Advances in Chemical Engineering-2020 (AdCHE-2020), UPES, Dehradun, India, Feb-2020

Subcritical water hydrolysis of N-acetyl-D-glucosamine: Hydrolysis mechanism, reaction pathways and optimization for selective production of 5-HMF and levulinic acid

Sphurti Prakash Kulkarni [a,b], Shital N. Dure [a], Sunil S. Joshi [a,b,*], Kiran V. Pandare [c], Nilesh A. Mali [a,b]

[a] Chemical Engineering and Process Development Division, CSIR-National Chemical Laboratory, Dr. Homi Bhabha Road, Pune, 411008, India
[b] Academy of Scientific and Innovative Research (AcSIR), Ghaziabad, 201002, India
[c] Polymer Science and Engineering Division, CSIR-National Chemical Laboratory, Dr. Homi Bhabha Road, Pune, 411008, India

A B S T R A C T

In this study, the subcritical water hydrolysis of N-acetyl-D-glucosamine (NAG), a monomer of abundant renewable marine biopolymer chitin, for production of value-added chemicals is investigated. The enhanced ionization of water at subcritical conditions (200 °C; 50–100 bar), provides enough acidity for deacetylation of NAG resulting in 80% yield of acetic acid along with traces of formic acid, lactic acid, glucose, fructose, 5-hydroxymethylfurfural (5-HMF),etc. The significant humin formation indicates that the self-condensation and polymerisation of 5-HMF is favored in water at subcritical conditions. A catalyst p-toluenesulfonic acid (p-TsOH) was employed to selectively convert NAG to levulinic acid (LA) via ring opening of 5-HMF previously formed during hydrolysis. The maximum yield of $27.13 \pm 1\%$ and $53.46 \pm 1\%$ of 5-HMF and LA, respectively, was obtained at process conditions optimized using Box-Behnken design coupled with response surface methodology. Subcritical water enables greener conversion of NAG to platform chemicals wherein the selective production can be achieved by tuning the process conditions.

1. Introduction

With the emergence of the concept of circular bio-economy, the efficient utilisation of wastes and residues has gained immense importance. The conversion of waste biomass, in particular, is an inherent part of circular bio-economy strategies [1,2]. Around 6–8 million tons of seafood waste is generated annually [3]. The properties of these materials such as high thermal and mechanical stability help marine animals sustain the harsh environmental conditions while alive. On the other hand, these properties pose serious disposal problems when discarded as seafood waste [4]. The conversion of such materials to value-added chemicals can solve issue of the disposal of waste and bring back the material to carbon chain, thus, promoting the bio-economy cycle. Chitin is one of the major constituents (20–50%) of the seafood waste, representing almost 50% of the total marine biomass. Chitin is a polysaccharide composed of monosaccharide viz. N-acetyl-D-glucosamine (NAG). Any process that converts chitin biopolymer to chemicals proceeds *via* depolymerisation followed by conversion of NAG to the chemicals. On the other hand, NAG is efficiently obtained by acid or enzymatic hydrolysis of chitin [5–7]. Hence, NAG has become a strong candidate for production of valuable chemicals alongside glucose.

Chitin and NAG have been investigated previously to produce organic acids like acetic acid, formic acid, glyceric acid and lactic acid using oxidative reagents in the presence of water. Qi and co-workers reported that around 33% and 30% of acetic acid is produced from NAG and chitin, respectively using V_2O_5 as catalyst under 5 bar pressure of oxygen at 200 °C in 2–3 h [8]. Various organic acids were synthesized from chitin and NAG using base catalysts, among which $Ba(OH)_2$ showed best results at moderate oxygen pressure by Wu and co-workers. Though the total yield of organic acids was 53.1%, the yield of acetic acid obtained was as low as 16% [9].

The platform chemicals namely 5-hydroxymethylfurfural (5-HMF) and levulinic acid (LA) are listed as the top ten molecules with versatility and ability to bridge the gap between petroleum-based processes and

bio-based processes [10]. Recently, the metal salt catalysts such as $FeCl_2$, $ZnCl_2$ etc. have been explored for the production of 5-HMF and LA from NAG or chitin using various volatile organic solvents [11]. Among all the studied metal catalysts, the higher yields of 5-HMF from chitin (19.3%) and NAG (37.9%) were obtained in the presence of $FeCl_2.4H_2O$ at 180 °C for a longer reaction time of 5 h. Among the various combinations of different dipolar aprotic solvents with water, DMSO-water favored the formation of 5-HMF wherein DMSO promoted the breaking of intra-molecular hydrogen bonding of water molecules and thus pushing reaction towards formation of 5-HMF as reported by Yu et al. [12]. Wang et al. [11] utilized aqueous solution of $ZnCl_2$ for conversion of chitin to 5-HMF along with the co-catalysts. Chitin was dissolved after swelling in a 67% aqueous $ZnCl_2$ solution in 48 h, still the yields obtained from chitin and its monomer NAG were very low (<10 and 2.8%) which was accounted to the weak interaction of –NHAc with Zn^{2+} arising from the steric hindrance of –Ac group. However, a large amount of humins were also formed. Recently, Hou and co-workers [13] reported the production of LA from chitin using ionic liquids. At 180 °C, 56.7% yield of LA was obtained from chitin using ($[C_3SO_3Hmim]HSO_4$) in 5 h. LA yield increased with the acidity of ionic liquid (IL), therefore, acid catalyst has critical role in the formation of LA from chitin. The mechanism of chitin hydrolysis differs from that of cellulose and chitosan as –N acetyl group restricts the access of acid catalysts to glycosidic linkage by forming strong inter- and intra-molecular hydrogen bonding. Recently, Zang et al. [14] showed that IL [Hmim][HSO_4] effectively catalyzed the conversion of NAG to 5-HMF in a DMSO-water mixture. The cation [Hmim] promotes the NAG conversion whereas the anion [HSO_4] selectively catalyses the conversion to 5-HMF. At atmospheric pressure, the yield of 5-HMF was low ~3% which increased to 44% under hydrothermal conditions, suggesting the critical role of pressure in converting NAG to 5-HMF. Though the ILs gave promising yields, their intricate and expensive synthesis procedures are main challenges for the practical use of ILs for large scale [15]. Szabolcs and co-workers [16] employed microwave activation for conversion of simple carbohydrates to LA. Microwave heating reduced the time of conversion of NAG to LA and resulted in LA yield of 22.1% in the presence of HCl and 20.6% in the presence of H_2SO_4 in 10 min. However, the extensive humin formation could not be avoided which is generally known to occur in strong acidic environment by self-condensation of 5-HMF. The methods reported so far use volatile solvents and toxic catalysts for the synthesis of valuable chemicals from NAG which hinders the development of a green process. Only replacing the feedstock does not ensure the ecological process but the process itself should consider the greener solvents and catalysts for a sustainable production.

Subcritical water, that is, water at a temperature above its boiling point and at a pressure enough high to maintain the liquid state, has emerged as a green solvent due to its unique solvent properties. The ionic product of water at subcritical conditions i.e. at 150–250 °C and 10–100 bar, increases from 10^{-14} to 10^{-11}, indicating higher concentration of H^+ and OH^- ions at subcritical conditions than that of normal conditions, as shown in Table 1 [17]. Therefore, subcritical water as a solvent can bring out the reactions by eliminating the need of acid-base catalyst. Moreover, the solubility of carbohydrates is higher in water than in any other volatile solvent, water can solubilize highest amount of NAG than any other solvent, which further can be enhanced by increasing the temperature [18].

In the study reported by Rongchuna and co-workers, the degradation of both D-glucosamine and NAG in subcritical water was investigated,

wherein the kinetics of the degradation of both D-glucosamine and NAG was reported. It was found that D-glucosamine forms minute quantities of 5-HMF, however, no details concerning the products obtained from NAG were provided [19]. Considering the interactions, between NAG molecule and subcritical water, it is imperative to form some organic acids like acetic acid. However, to best of our knowledge, no previous study has reported the non-catalytic synthesis of acetic acid from NAG. There is limited information available on product distribution of NAG at such hydrothermal conditions, which is necessary for developing a process using chitinous feedstock.

In the present study, the transformations NAG undergoes during noncatalytic and catalytic subcritical water hydrolysis are investigated. Herein, for the first time, a detailed insight of the non-catalytic efficient deacetylation of NAG to acetic acid using only subcritical water without any external oxidative reagent is reported which is supported by the detailed product distribution and reaction mechanism study. Encouraged by the findings, a combination of catalyst p-toluenesulfonic acid (p-TsOH) with subcritical water was explored for greener selective production of platform chemicals viz. 5-HMF and LA [20,21]. A multi response optimization based on Box-Behnken Design is carried out for estimating the optimum process conditions for maximizing yields of 5-HMF and LA during p-TsOH catalyzed subcritical water hydrolysis of NAG. The influence of process variables and their interactions on the yields is studied using response surface methodology. The models are developed by regression analysis of experimental data for predicting yield of both 5-HMF and LA during hydrolysis.

2. Materials and methods

2.1. Chemicals

N-Acetyl-D-glucosamine (purity >99%) was purchased from HiMedia Laboratories, Mumbai, India. 5-Hydroxymethylfurfural (purity >99%) and levulinic acid (purity 98%) were purchased from Sigma Aldrich. Acetic acid (purity >99%) and p-toluenesulfonic acid monohydrate (purity 98%) were obtained from Loba Chemie Pvt.Ltd.. Formic Acid (purity >98%) and lactic Acid (purity >90%) were purchased from Avra Chemicals and Merck Specialities, respectively. All chemicals were used as received. The deionized water obtained from LabQ apparatus was used in all the experiments.

2.2. Subcritical water hydrolysis

In a typical experiment, the reactor was loaded with the reaction mixture and filled with inert gas followed by heating to the required temperature at a constant stirring speed of 600 rpm, maintaining the operating conditions for the stipulated time, followed by quick cooling to stop the reaction. The reactant NAG (1–5 g) and catalyst p-TsOH (0–5 g) were added to deionized water (90–95 g) in a batch autoclave of volume 300 mL (Hast C, Parr Instruments, Moline, IL, USA), designed for maximum operating pressure of 2500 psi. The pressure in the reactor (50 bar) was maintained by using argon. The initial pressure was estimated considering the expansion of argon gas with reaction temperature. The reactor was heated to the required temperature (170–250 °C) using the electrical heating mantle. The temperature and stirring speed of 600 rpm were maintained by using a PID controller. After the stipulated time (30–90 min), the reactor was quickly cooled down to the room temperature by passing cold water through dip U tube placed inside the reactor. In case of the solid formation during the reaction, the

Table 1
Physical and chemical properties of reaction medium [17].

Reaction medium	Temperature (°C)	Pressure (bar)	State	Density (g/mL)	Ionic Product (k_w)	Dielectric Constant (ε)
Ambient Water	0–100	1	Liquid	0.99(25 °C)	10^{-14}	78.5
Subcritical Water	170–250	50	Hot Compressed Liquid	0.90(170 °C)-0.80(250 °C)	10^{-12} to 10^{-11}	27.1 (250 °C and 50 bar)

solid and liquid products were separated by vacuum filtration and analysed without any further treatment.

2.3. Qualitative and quantitative analysis of products

The filtered aqueous reaction mixture was further diluted and analysed using HPLC and Mass Spectroscopy. The identification of the products was done by LC-MS and HR-MS (Figs. S1–S3) and also by injecting standard compounds for confirmation to HPLC. For quantitative analysis of products, the aqueous reaction mixture obtained by filtration was analysed using HPLC. The black coloured solid residue was dried in a vacuum oven at 75 °C/25 mmHg for 3 h and vacuum and analysed using ATR-FTIR (Fig. S7).

The aqueous product mixture obtained in the reaction was analysed using HPLC equipped with the Aminex-87H column (Bio-Rad, USA) and Shodex Refractive Index detector. The analysis of sample was done using 5 mM sulfuric acid as mobile phase at a flow rate of 0.6 mL/min while keeping column at a constant temperature of 50 °C. The samples were filtered using 0.22 μm filter before injecting for the analysis; the chromatograms are shown in Figs. S4–S6. The calibration curves for each compound were generated for quantification using HPLC.

The conversion of NAG and yield of 5-HMF and LA are calculated using following equations

$$Conversion\ of\ NAG(\%) = \frac{(Initial\ moles\ of\ NAG - Moles\ of\ NAG\ after\ the\ reaction)}{Initial\ moles\ of\ NAG} * 100$$

$$Yield\ of\ Product(\%) = \frac{Moles\ of\ Product}{Initial\ Moles\ of\ NAG} * 100$$

2.4. Design of experiments

The Box Behnken Design (BBD) method is an efficient method for design of experiments in order to find out the optimum operating conditions and the effect of interactions of the reaction variables on the reaction yield as it uses fewer experiments for predicting the results. Recently, BBD has been extensively used to optimize for complex reactions like biomass processing where systematic optimization becomes difficult as the number of influential operating parameters is almost always higher than two [22,23]. The preliminary reactions of NAG in presence of p-TsOH in subcritical water were conducted to determine the key variables and their ranges affecting yield of 5-HMF and LA. Further, the catalytic reactions of NAG were designed using BBD method for determining the optimum operating conditions. A method comprising three levels and four factors that is total 27 experiments was designed using the software Design Expert 13.0 (Stat-Ease, Inc., Minneapolis, MN, USA). In this study, four variables x_1 -Temperature (170–250 °C), x_2

-Time (30–90 min), x_3 -NAG concentration (1–5% w/w) and x_4 -p-TsOH loading (1–5% w/w) were varied in the specified ranges for optimizing yield of y_1-HMF and y_2- LA, as given in Table 2.

The empirical models for the yield of 5-HMF and yield of LA were developed by fitting the experimental data for the value of the regression coefficient of approximately 1. Further, the quality of model was assessed by analysis of variance (ANOVA).

3. Results and discussion

3.1. Non-catalytic subcritical water hydrolysis of NAG

The subcritical water hydrolysis of NAG was studied initially by varying temperature in the range of 70–200 °C, reaction time in the range of 60–180 min and pressure in the range of 10–150 bar. There was practically no conversion of NAG at temperatures less than 170 °C; on the contrary NAG was almost always consumed 100% at all temperatures higher than 170 °C irrespective of the reaction time. Hence, the hydrolysis of NAG is instantaneous and controlled by the temperature. It was interesting to see the formation of some products identified to be lactic acid, formic acid, acetic acid, glucose, fructose and solids characterized as humins during non-catalytic hydrolysis of NAG, as the formation of these products requires either acid or base catalysts. Based on moles, 80% yield (20% on mass) of acetic acid was obtained at almost all operating conditions of temperature higher than 170 °C. Thus, it can be stated that NAG undergoes almost complete deacetylation forming acetic acid and glucosamine. Glucosamine was not detectable using HPLC method mentioned in 2.3, however, the formation of the other compounds like glucose, fructose and large amount of humins indicates that the glucosamine undergoes deamination which further gets converted to glucose followed by formation of fructose and lactic acid. The only plausible pathway for formation of lactic acid is by the conversion of glucose which requires a basic catalyst. The presence of traces of lactic acid and formic acid in product mixture of non-catalytic subcritical hydrolysis of NAG confirms that water at subcritical conditions acts as an acid-base catalyst. However, the concentration of dissociated water ions catalyzing reaction is not enough for selective formation of the particular acid. A reaction pathway of NAG hydrolysis in subcritical water is shown in Fig. 1.

Table 3 summarizes the product distribution of non-catalytic hydrolysis of NAG in water at various subcritical temperatures and pressures. The previously reported TGA-DSC analysis of NAG shows that it starts decomposing at temperatures near 180 °C, as the mass of NAG drastically drops even before NAG melts completely [18]. Simultaneously, the neutral reaction medium becomes acidic as the value of ionization constant of water drops from 14 at 25 °C to 11.2 at 170 °C at constant 100 bar, indicating the increased concentration of H^+ and OH^- ions at the higher temperature [24]. This temperature conditional behavior of NAG deacetylation can be attributed to the combined effect of thermal instability of NAG and properties of subcritical water. The subcritical temperature provides the activation energy while the dissociated ions of water catalyze the transformation; hence, NAG undergoes efficient and instantaneous deacetylation at 170 °C. There was less pronounced effect of pressure on the product yields of NAG hydrolysis in the operating pressure range (50–100 bar) at a temperature of 200 °C and time of 60 min. The value of the ionic product of water is in the range of 11.2–11.5 at tested temperature and pressure combinations;

Table 2
Range and levels of key parameters selected for optimization using BBD method.

Factor	Reaction Parameters	Unit	Range and Level		
			Minimum (-1)	Middle (0)	Maximum (+1)
x_1	Temperature	°C	170	210	250
x_2	Time	min	30	60	90
x_3	NAG Loading	% (w/w)	1	3	5
x_4	p-TsOH Loading	% (w/w)	1	3	5
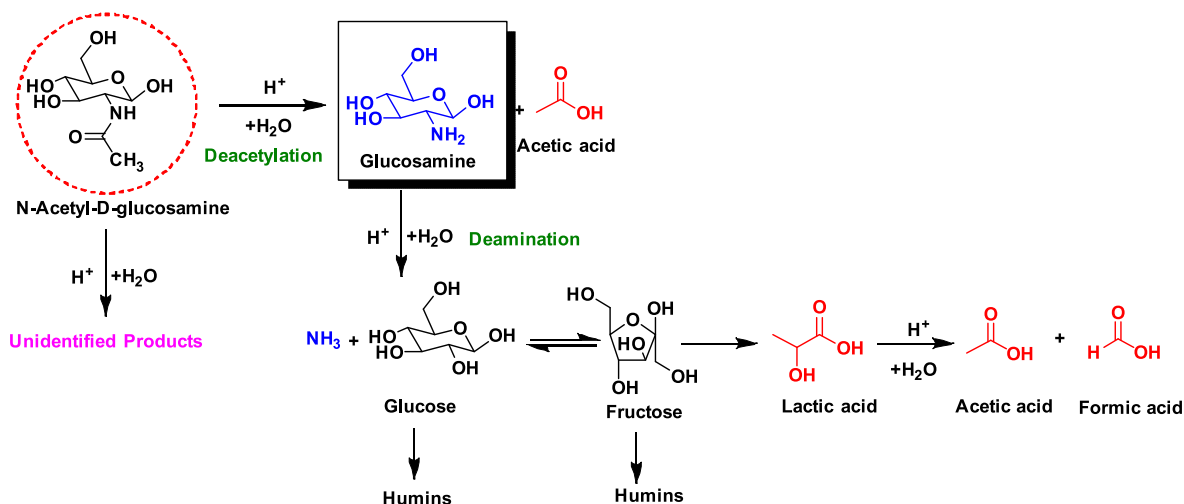
Fig. 1. Reaction pathway for hydrolysis of NAG in subcritical water in absence of external catalyst.

Table 3
Product distribution of non-catalytic subcritical water hydrolysis of NAG (based on identified products).

Experiment	Temperature ($^{\circ}$C)	Pressure (bar)	Time (min)	Initial NAG Concentration (%)	Conversion of NAG (%)	Product Distribution (weight of product/weight of NAG) *100						
						Glucose	Fructose	Lactic acid	Formic acid	Acetic acid	Humins	Accountability# (%)
1	70	100	60	5.0	0	0	0	0	0	0	0	100
2	170	100	60	5.0	91.00	0.0	0.30	0.14	0.35	5.85	33.64	40.28
3	200	100	60	5.0	99.64	0.12	0.40	0.35	1.16	15.82	29.61	47.46
4	200	15	60	5.0	98.60	0.12	0.33	0.42	1.13	18.17	39.60	59.78
5	200	50	60	5.0	99.62	0.14	0.55	0.89	5.57	15.72	31.50	49.30
6	200	100	120	5.0	100	0.10	0.00	0.04	0.80	15.94	29.91	46.71
7	200	100	180	5.0	100	0.37	0.14	0.34	0.95	21.47	38.90	62.18

#**(Total weight of identified products/Initial weight of NAG) *100.**

increasing pressure from 20 to 150 bar does not change ionic product significantly, hence, the product distribution is least affected by the pressure in the tested pressure range at subcritical temperature [24]. The product distribution was significantly influenced by the reaction time during the subcritical water hydrolysis of NAG. At 200 °C and 100 bar, the yield of acetic acid and humins increased with time from 60 to 180 min, however, the variation in the yields of other products was insignificant. As against previously reported systems [8,9], the comparable or even higher yield of acetic acid was obtained at shorter reaction time and even in the absence of catalyst or oxidative reagents such as oxygen.

Acetic acid, the deacetylation product of NAG, was one of the major products amongst all identified compounds with almost 80% yield on mol basis and maximum 20% on weight basis. As per the previous reports, the deacetylation of NAG is an acid-catalyzed reaction, which requires strong mineral acids such as HCl, H_2SO_4 etc. [25]. Recently, solid acid catalysts such as the cation exchange resins are used for deacetylation [26]. Recent studies have also showed that the role of oxidative reagent, oxygen gas in particular, is crucial in facilitating breakage of acetamide bond which is least affected by the presence of catalyst or temperature [8,9]. We report for the first time that the highly efficient deacetylation of NAG can be achieved using water at subcritical
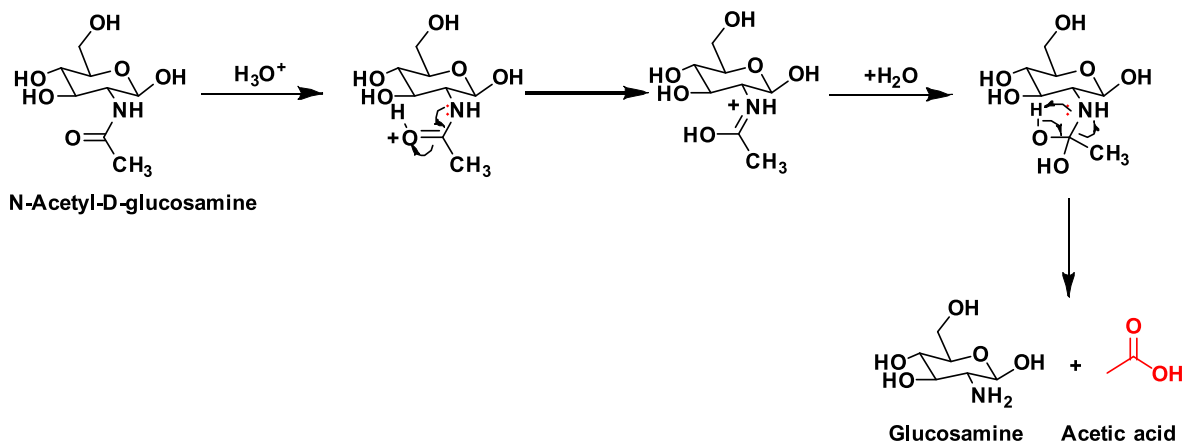
Fig. 2. Plausible mechanism of NAG deacetylation in subcritical water in absence of any external catalyst.

conditions in the absence of any external catalyst and/or an oxidative reagent.

Water at the temperature and pressure ranges maintained here becomes acidic as the ionic product of water drops to 11.2–11.5, engendering the formation of hydronium ion responsible for deacetylation of NAG. A plausible mechanism is shown in Fig. 2. The protonation of oxygen of carbonyl group by hydronium ion present in subcritical water forms a carbocation. The carbocation is then attacked by the nucleophilic water molecule forming an oxonium intermediate. Another attack of hydroxyl ion results in the addition of one water molecule and removal of the acetic acid from glucosamine ring followed by the regeneration of another water molecule [25].

3.2. p-TsOH-catalyzed subcritical water hydrolysis of NAG

The previous results of non-catalytic hydrolysis show that after deacetylation some of the transformations of NAG proceed *via* formation of glucose. A stronger catalyst is required to further convert the glucose to 5-HMF and LA by avoiding the formation of solid humin products. An acid catalyst viz. *p*-TsOH was employed to produce 5-HMF and LA from NAG. The preliminary reactions were carried out to investigate the catalytic performance of *p*-TsOH towards selectively converting NAG to LA in subcritical water. The temperature and time varied in the range of 170–250 °C and 5–180 min, respectively for a constant pressure of 50 bar. The pressure of 50 bar was selected to maintain acidity of water at all temperatures, as the ionic product varies from 11.2 to 10.90 at 170–250 °C at 50 bar [24].

The major products of the reactions were LA, acetic acid, formic acid along with traces of 5-HMF, lactic acid, glucose, etc. A remarkable yield of 57 mol % of LA was obtained from 5% (w/w) NAG at 250 °C and 50 bar in 60 min using *p*-TsOH 5% (w/w) in subcritical water. The yield of LA was even higher (~53.46%) than that obtained from glucosamine (~49.9%) using methanesulfonic acid at 200 °C in 30 min [27]. The yield of humins was drastically dropped than that observed in non-catalytic reactions. During *p*-TsOH-catalyzed hydrolysis of NAG the yield of solids was less than 10% whereas during non-catalytic hydrolysis the yield of humins was almost always more than 20% at all subcritical operating conditions. As shown in Fig. S7, FT-IR analysis of the solids formed during *p*-TsOH-catalyzed hydrolysis showed that there may be structural difference between the solids formed during non-catalytic and catalytic hydrolysis of NAG subcritical water. The solids formed in presence of *p*-TsOH might constitute sulfonated products as has been reported previously [28].However, the detailed structural analysis of humins was not undertaken in the present study. Nevertheless, it was confirmed that *p*-TsOH shows a significant catalytic activity by suppressing solid humin formation and selectively transforming NAG to LA which is discussed in 3.3.

The sensitive range of operating conditions was identified based on the results of the preliminary experiments carried out to optimize 5-HMF and LA yield using BBD method.As observed in non-catalytic reactions, the minimum temperature required for conversion of NAG is 170 °C at which low yield of LA (~5%) was obtained even in the presence of *p*-TsOH (Fig. 3a). It was found that the yield of LA was increased with increasing temperature at lower reaction time of 60 min. For longer reaction times, the yield of LA and formic acid was highest at 210 °C and was lowest at 170 °C. However, the yield of LA was highest at 210 °C than that at temperatures of 170 °C and 250 °C. The yield of acetic acid was least affected by the operating temperature and time, as shown in Fig. 3b, however, on comparison with non-catalytic reaction, the complete deacetylation of NAG with 100% yield of acetic acid was observed in the presence of *p*-TsOH.
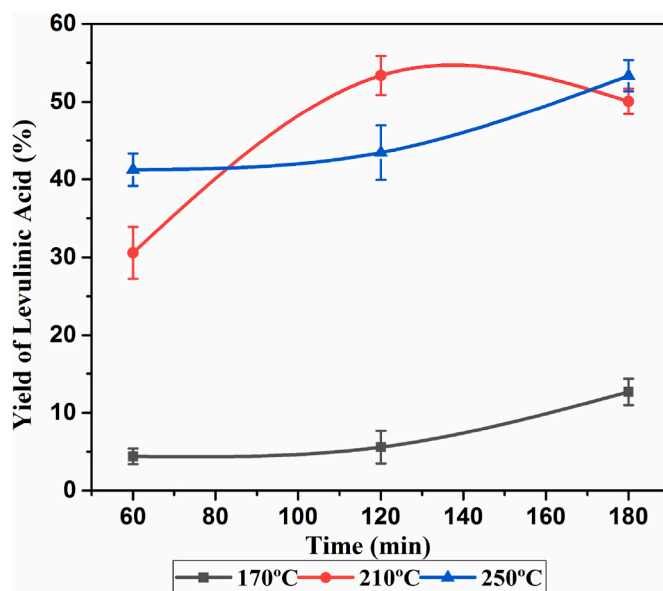
Fig. 3a. Effect of temperature and time on yield of LA [NAG aqueous concentration 1% (w/w); pressure-50 bar; *p*-TsOH:NAG-5:1(w/w))].
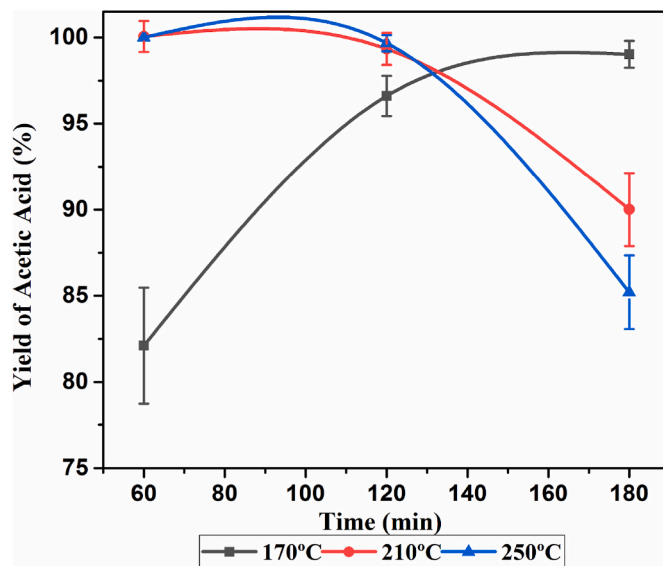
Fig. 3b. Effect of temperature and time on yield of acetic acid [NAG aqueous concentration 1% (w/w); pressure-50 bar; *p*-TsOH:NAG-5:1(w/w)].

As shown in Fig. 3c, though small but the yield of 5-HMF was favored by short reaction time at low temperature (170 °C) and by longer reaction time at 210 °C. The presence of minute quantity of 5-HMF and its response to the changes in the operating conditions show that even 5-HMF can be obtained in significant amount during same process. However, it is imperative to find out the suitable conditions. In order to find out if the lower or higher reaction time favors yield of LA and 5-HMF at low and high temperatures at different concentrations of *p*-TsOH catalyst and initial NAG, a multi response optimization study was
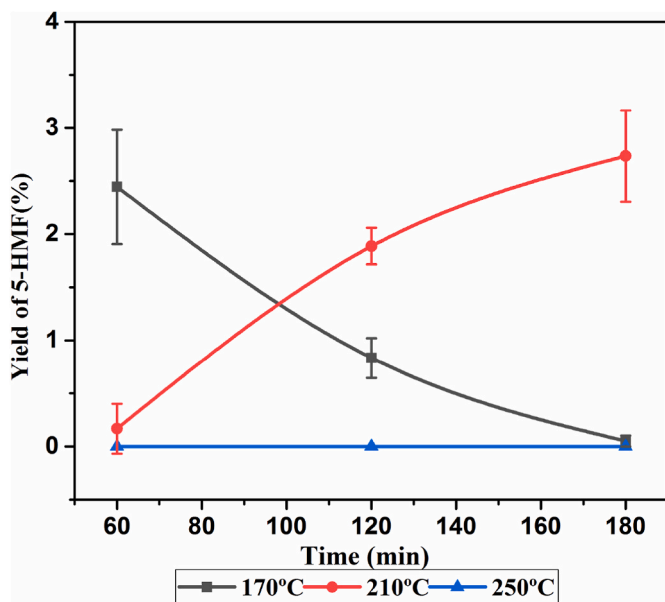
Fig. 3c. Effect of temperature and time on yield of 5-HMF [NAG aqueous concentration 1% (w/w); pressure-50 bar; *p*-TsOH: NAG-5:1(w/w))].

carried out along with a detailed analysis of the response surfaces of yields of compounds obatined by response surface methodology (RSM). The initial ranges of factors for optimization were fixed based on preliminary observations and the range of studied temperature, time, *p*-TsOH loading and NAG concentration are shown in Table 2.

3.3. Reaction pathway and catalytic mechanism of LA formation

The reaction pathway for the formation of LA is proposed based on the product distribution of *p*-TsOH-catalyzed conversion of NAG in subcritical water. Similar to the non-catalytic reactions, the subcritical water facilitates the deacetylation of NAG to form glucosamine and acetic acid as the equal moles of acetic acid were obtained from initial moles of NAG in both the cases (Fig. 4a). Glucosamine undergoes deamination forming glucose and ammonia. The isomerization of
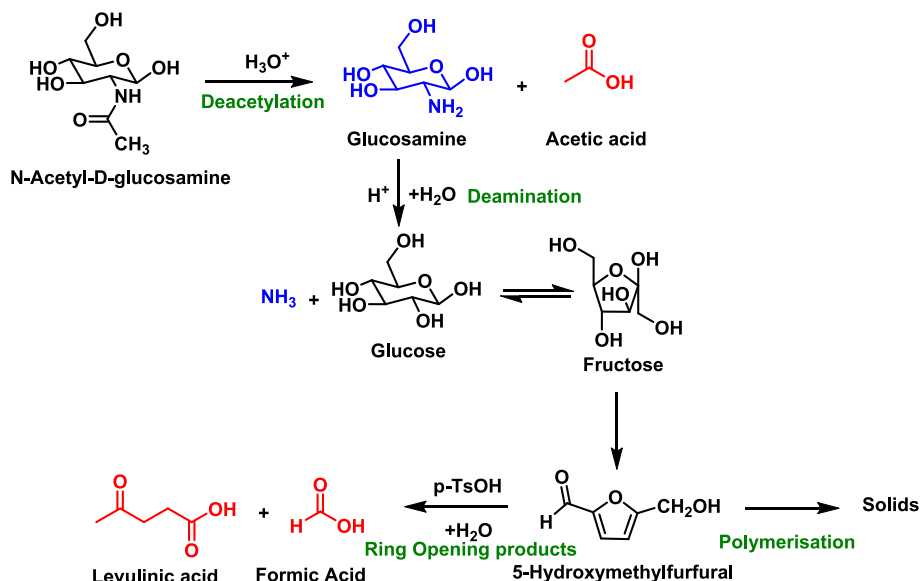
glucose to fructose is accelerated in presence of *p*-TsOH. Further, *p*-TsOH catalyses the dehydration of fructose to form 5-HMF, upon rehydration 5-HMF forms LA along with formic acid as by-product. The mechanism of formation of 5-HMF is presumed to be similar to that of conversion of fructose to 5-HMF as reported previously [29].

The solid products are characterised to be humins, having similar functional groups to that of products reported previously in subcritical water(Fig. S7). The solids are a polymerisation product of the compounds formed during subcritical water hydrolysis of 5-HMF and glucose [30].Hence, the formation of solids during NAG hydrolysis was accounted to 5-HMF. In the absence of any strong acid, 5-HMF undergoes self-condensation wherein it's own nucleophilic oxygen of hydroxyl group attacks aldehyde group removing water and forming polymers, which may further combine with glucose and undergo polymerisation to produce solid humins.On the contrary, in presence of *p*-TsOH, alcoholic oxygen of 5-HMF acts as a base instead of nucleophile which leads to ring opening by protonation rather than self-condensation. Hence, the solid formation is avoided, causing the ring opening followed by the formation of LA and formic acid, as shown in Fig. 4b. A quantitative comparison of catalytic and non-catalytic subcritical water hydrolysis of NAG was done by carrying out reactions under similar operating conditions with and without *p*-TsOH. The results summarised in Table 7 supports the mechanism proposed above, as around 60% (mass basis) of solids were formed during non-catalytic reactions from NAG at similar temperature, pressure and reaction time, whereas, only 8.4% (mass basis) of solids were obatined in *p*-TsOH-catalyzed reaction with highest LA yield.

4. Response surface methodology (RSM) study for 5-HMF and LA production from NAG

4.1. Model analysis

The results of the various experiments designed according to the BBD (27 runs) for studying the effect of four variables viz. temperature, time, feed concentration and catalyst loading on yield of two important compounds 5-HMF and LA obtained by *p*-TsOH-catalyzed subcritical water hydrolysis of NAG are shown in Table 4. The linear, 2 FI, quadratic and cubic polynomial models were inadequate for predicting the response of the yield of 5-HMF and LA, indicated either by high p-values

Fig. 4a. Proposed reaction pathway of *p*-TsOH-catalyzed subcritical water hydrolysis of NAG.
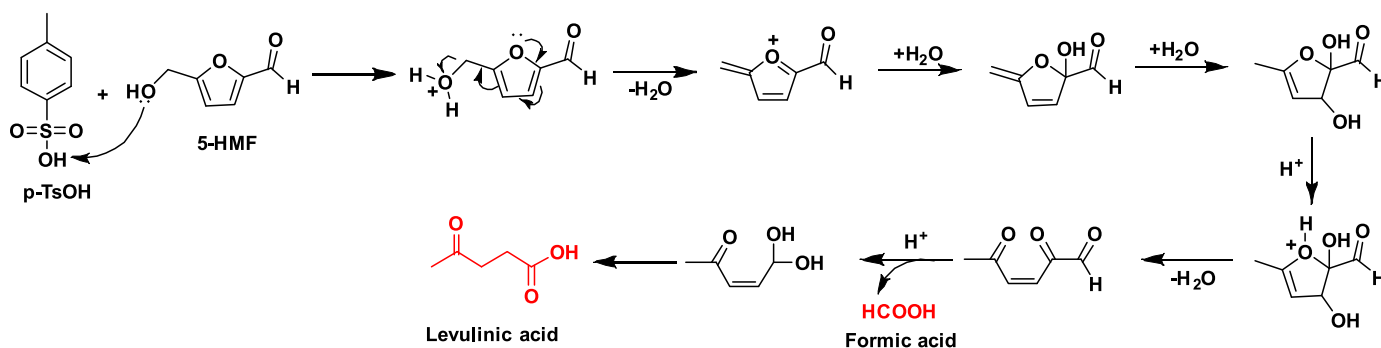
Fig. 4b. Proposed reaction mechanism of *p*-TsOH-catalyzed formation of LA during subcritical water hydrolysis of NAG.

Table 4
Box-Behnken Design reaction matrix with actual response of yield of 5-HMF and LA.

Run	A: Temperature (°C)	B: Time (min)	C:NAG Concentration (w/w)%	D:p-TsOH Loading (w/w)%	Yield of 5-HMF (% on mol basis)	Yield of LA (% on mol basis)
	x_1	x_2	x_3	x_4	y_1	y_2
1	210	90	1	3	1.69	38.69
2	170	60	1	3	3.01	3.64
3	170	60	5	3	7.26	2.98
4	250	60	3	5	0.49	42.45
5	250	30	3	3	0.45	33.95
6	170	60	3	5	3.03	3.47
7	170	90	3	3	6.83	3.19
8	210	60	5	1	13.05	3.82
9	210	30	1	3	5.17	19.84
10	210	30	3	5	3.61	17.61
11	210	30	3	1	21.79	4.58
12	210	90	3	1	19.89	1.69
13	250	60	3	1	8.04	0.08
14	210	90	5	3	22.15	9.14
15	170	60	3	1	12.16	7.54
16	250	60	1	3	0.00	46.07
17	210	60	5	5	2.40	24.16
18	250	60	5	3	1.39	8.64
19	210	60	3	3	7.38	22.82
20	210	60	3	3	7.38	22.82
21	170	30	3	3	3.89	3.41
22	210	60	1	1	23.70	13.46
23	210	30	5	3	27.14	2.88
24	210	90	3	5	1.37	34.66
25	210	60	3	3	7.38	22.19
26	210	60	1	5	2.60	36.14
27	250	90	3	3	0.00	32.97

Where x_1, x_2, x_3 and x_4 are reaction temperature (°C), reaction time (min), NAG concentration (% w/w) and catalyst *p*-TsOH loading (% w/w) respectively. The value of R^2 for 5-HMF model and LA model were 0.9999 and 0.9998, respectively, that is very close to 1 which indicates that the models can adequately predict the response of the experiments in the prescribed range of operating conditions. Tables 5 and 6 describe the analysis of variance (ANOVA) for the models with F-values and p-Values. Both the models were significant with small p-values (<0.05) and high F-values. For 5-HMF yield the analysis revealed that the all the model terms except the interaction model terms x_1x_4, x_2x_3 and x_2x_4 were highly significant, as the p-values of these terms x_1x_4, x_2x_3, and x_2x_4 were higher than 0.05 the yield of 5-HMF has least effect of interaction between temperature and catalyst loading, time and feed concentration and time, catalyst loading, etc. On the other hand, the interaction terms of LA model x_1x_2, x_3x_4, quadratic terms x_1^2, x_3^2 were insignificant with p-values higher than 0.05, indicating the less significance of interaction between temperature-time, feed loading-catalyst loading and the increase in the temperature and feed loading itself on LA yield, all other model terms were highly significant. The parity plots (Figs. S8 and S9) of both the models demonstrated the competence of both the models developed for predicting the yield of 5-HMF and LA in the investigated range of operating conditions.

4.2. Response surface analysis of 5-HMF yield

The effect of interaction of four factors is more complex as the yield is governed by both the formation and consumption of 5-HMF. Therefore, it is essential to study the interaction carefully to obtain the optimum yield of 5-HMF. The contour plots 5a-f represents the effect of the parameters on yield of 5-HMF within the limited range of operating conditions that is temperature from 170 to 250 °C, reaction time from 30 to 90 min, NAG concentration 1–5% (w/w) and *p*-TsOH loading 1–5% (w/w) at zero levels of the constant parameters.

As shown in Fig. 5a, 5-HMF yield does not vary with the proportion of change in temperature and time, a certain combination of these parameters must be maintained to get the high yield of 5-HMF. The

or by small R^2 or F-values. Therefore, it was imperative to employ the reduced quartic models for prediction of both, the yield of 5-HMF and the yield of LA, as in eqs. (1) and (2).

$Y_{5\text{-}HMF} = 368.705 - 2.7356x_1 - 0.5732x_2 - 142.134x_3 - 186.093x_4 - 0.0007x_1x_2 + 1.1984x_1x_3 + 1.4424x_1x_4 + 0.1307x_2x_3 + 0.0814x_2x_4 + 6.6896x_3x_4 + 0.0065x_1^2 + 0.0036x_2^2 + 0.9956x_3^2 + 41.4959x_4^2 - 0.0028x_1^2x_3 - 0.0034x_1^2x_4 - 0.3490x_1x_4^2 - 0.0228x_2x_3^2 - 0.0138x_2x_4^2 + 0.6590x_3^2x_4 - 1.1606x_3x_4^2 + 0.0008x_1^2x_4^2 - 0.0840598x_3^2x_4^2$.… … … … ….. eq.1

$Y_{LA} = -506.849 + 4.9137x_1 - 5.4509x_2 + 356.763x_3 + 182.09x_4 + 0.0574x_1x_2 - 3.3504x_1x_3 - 2.040x_1x_4 - 0.0524x_2x_3 + 0.2200x_2x_4 - 4.8128x_3x_4 - 0.0123x_1^2 - 0.0054x_2^2 - 49.804x_3^2 - 38.8256x_4^2 - 0.0001x_1^2x_2 + 0.0079x_1^2x_3 + 0.00584x_1^2x_4 + 0.4931x_1x_3^2 + 0.3981x_1x_4^2 - 0.02282x_2x_4^2 + 0.7777x_3x_4^2 - 0.00121x_1^2x_3^2 - 0.00105x_1^2x_4^2$.… … … … ….. eq.2

Table 5
ANOVA for the regression model of yield of 5-HMF.

Source	Sum of Squares	Df	Mean Square	F-value	p-value	
Yield of 5-HMF						
Model	1713.24	23	74.49	923.47	<0.0001	Significant
A:Temperature (°C)	45.83	1	45.83	568.22	0.0002	
B:Time (min)	1.55	1	1.55	19.16	0.0221	
C:NAG Concentration (% w/w)	450.16	1	450.16	5580.85	<0.0001	
D:p-TsOH Loading (% w/w)	336.78	1	336.78	4175.27	<0.0001	
AB	2.87	1	2.87	35.59	0.0094	
AC	2.05	1	2.05	25.4	0.0151	
AD	0.6237	1	0.6237	7.73	0.0689	
BC	0.5622	1	0.5622	6.97	0.0777	
BD	0.0291	1	0.0291	0.3612	0.5902	
CD	27.33	1	27.33	338.83	0.0003	
A^2	227.98	1	227.98	2826.31	<0.0001	
B^2	39.38	1	39.38	488.24	0.0002	
C^2	42.34	1	42.34	524.91	0.0002	
D^2	1.96	1	1.96	24.35	0.016	
A^2C	169.24	1	169.24	2098.15	<0.0001	
A^2D	50.12	1	50.12	621.38	0.0001	
AD^2	1.42	1	1.42	17.66	0.0246	
BC^2	15.01	1	15.01	186.03	0.0009	
BD^2	5.49	1	5.49	68.1	0.0037	
C^2D	3.06	1	3.06	37.96	0.0086	
CD^2	354.87	1	354.87	4399.44	<0.0001	
A^2D^2	29.04	1	29.04	360.07	0.0003	
C^2D^2	1.81	1	1.81	22.43	0.0179	
Residual	0.242	3	0.0807			
Cor Total	1713.48	26				
R^2	0.9999					

Table 6
ANOVA for the regression model of yield of LA.

Source	Sum of Squares	Df	Mean Square	F-value	p-value	
Yield of LA						
Model	5551.28	23	241.36	526.83	0.0001	Significant
A:Temperature (°C)	909.52	1	909.52	1985.28	<0.0001	
B:Time (min)	157.68	1	157.68	344.17	0.0003	
C:NAG Concentration (% w/w)	540.78	1	540.78	1180.4	<0.0001	
D:p-TsOH Loading (% w/w)	990.72	1	990.72	2162.52	<0.0001	
AB	0.146	1	0.146	0.3186	0.6119	
AC	338.23	1	338.23	738.27	0.0001	
AD	538.92	1	538.92	1176.34	<0.0001	
BC	39.64	1	39.64	86.52	0.0026	
BD	99.35	1	99.35	216.87	0.0007	
CD	1.37	1	1.37	2.99	0.182	
A^2	0.7825	1	0.7825	1.71	0.2824	
B^2	87.43	1	87.43	190.84	0.0008	
C^2	0.0421	1	0.0421	0.0919	0.7816	
D^2	35.66	1	35.66	77.83	0.0031	
A^2B	86.59	1	86.59	189	0.0008	
A^2C	8.87	1	8.87	19.37	0.0218	
A^2D	6.44	1	6.44	14.05	0.0331	
AC^2	18.69	1	18.69	40.79	0.0078	
AD^2	103.62	1	103.62	226.19	0.0006	
BD^2	15.01	1	15.01	32.76	0.0106	
CD^2	77.42	1	77.42	169	0.001	
A^2C^2	60.94	1	60.94	133.01	0.0014	
A^2D^2	45.6	1	45.6	99.54	0.0021	
Residual	1.37	3	0.4581			
Cor Total	5552.65	26				
R^2	0.9998					

temperature around 210 °C and time either short 30 min or high 90 min resulted in higher yield of 5-HMF. As discussed in the previous sections, 5-HMF undergoes rehydration to form LA and formic acid. Low temperature does not suffice the energy of formation of 5-HMF and that at 210 °C the energy is just sufficient for formation of 5-HMF. On the other hand, longer reaction time allows degradation of 5-HMF to other compounds explaining the high yield of 5-HMF at medium temperature and low time. When the interaction between the temperature and NAG concentration is considered, as shown in Fig. 5b, similar to the previous

discussion moderate temperature and a high NAG loading resulted in the high yield of 5-HMF at 3% p-TsOH loading. The effect of feed concentration on yield gives an idea about the order of the reaction that the reaction rate is not first order unlike the reaction of glucose to 5-HMF.

The circular nature of contour plot 5c showed that the maximum yield is obtained near 210 °C and 1% (w/w) p-TsOH loading. Any further increase in temperature and p-TsOH concentration leads to further reactions like rehydration which consumes 5-HMF resulting in lower yields of 5-HMF. There was strong interaction between NAG loading and

Table 7
Optimized conditions for 5-HMF and LA yield-prediction and validation.

Experiment	Reaction Temperature (ºC)	Reaction Pressure (bar)	Reaction Time (min)	NAG concentrations (%)	*p*-TsOH Loading (%)	Yield % (mol basis)		Error[a]	Solid Yield (% w/w of NAG)
						Predicted	Obtained		
5-HMF yield optimization	210	50	30	5	3	27.02	27.13	0.40	9.7
LA yield optimization	238	50	83	1	4.09	53.21	53.46	0.46	8.4
Non-catalytic reaction	238	50	90	1	-	-	-	NA	60

[a] Error = [(Experimental value – Predicted value)/Predicted value] *100.

Fig. 5. Response surfaces of 5-HMF yield.

time, as in Fig. 5d, where the yield was highest at maximum NAG loading obtained in time shorter than 30 min, at 210 °C and 3% *p*-TsOH loading. The yield of 5-HMF increases by decreasing time than 30 min and maintaining 3% *p*-TsOH loading, as shown in Fig. 5e, clearly increasing *p*-TsOH loading alone does not improve 5-HMF yield. According to the contour plot 5f, low *p*-TsOH to NAG ratios favored the formation of 5-HMF. In general, the yield of 5-HMF can be maximized by using high NAG loading and low *p*-TsOH concentration at temperature 210 °C in time shorter than 30 min.

4.3. Response surface analysis of LA yield

The four reaction variables viz. reaction temperature, time, NAG loading and *p*-TsOH concentration has conspicuous effect on the yield of LA in the investigated region of the variables. Fig. 6a–f shows the interaction effects of variables on LA yield at subcritical pressure of 50 bar when remaining variables are maintained at the zero levels. The elliptical nature of contours in Fig. 6a indicates that the temperature and time have significant interaction on LA yield, where, the temperature dominates the yield; as the yield of LA is high at high temperature irrespective of the time at 1:1 ratio of NAG and *p*-TsOH. Fig. 6b shows that the low NAG concentration favours the formation of LA from 5-HMF at sufficient *p*-TsOH loading of 3% (w/w) in an hour at higher temperatures around 250 °C. The increase in the initial concentration of NAG is

probably introducing mass transfer limitations causing the drop in the yield and conversion. High *p*-TsOH loading favours the formation of LA from 5-HMF, as discussed in reaction pathway section, *p*-TsOH catalyses both fructose to 5-HMF conversion and 5-HMF to LA conversion, hence, for obtaining high yields of LA, high concentration of *p*-TsOH is required, as shown in Fig. 6c. The nature of 6d plot indicates that time and NAG loading have less interaction and to achieve the maximum LA yield for the longer reaction times are required at low NAG loading, which can further increase when NAG concentration in increased. Fig. 6e, shows that the interaction between time and catalyst loading is moderately significant due to the elliptical curvature, increasing both the *p*-TsOH concentration and time simultaneously can improve the yield of LA. Unlike the case 5-HMF, higher *p*-TsOH to NAG ratio would favour the formation of LA. The surface plot 6f shows increasing both concentrations of *p*-TsOH and NAG leads to poor yield of LA. However at low NAG concentration of 1% (w/w) high LA yield upto 46% was obtained at *p*-TsOH loading of 4% (w/w). It is interesting to note that the further increase in the *p*-TsOH loading could not improve LA yield which could be ascribed to the side reactions leading to the formation of humins. In nutshell, for maximizing the yield of LA, higher temperatures and high *p*-TsOH to NAG ratios should be employed for sufficiently longer reaction times.
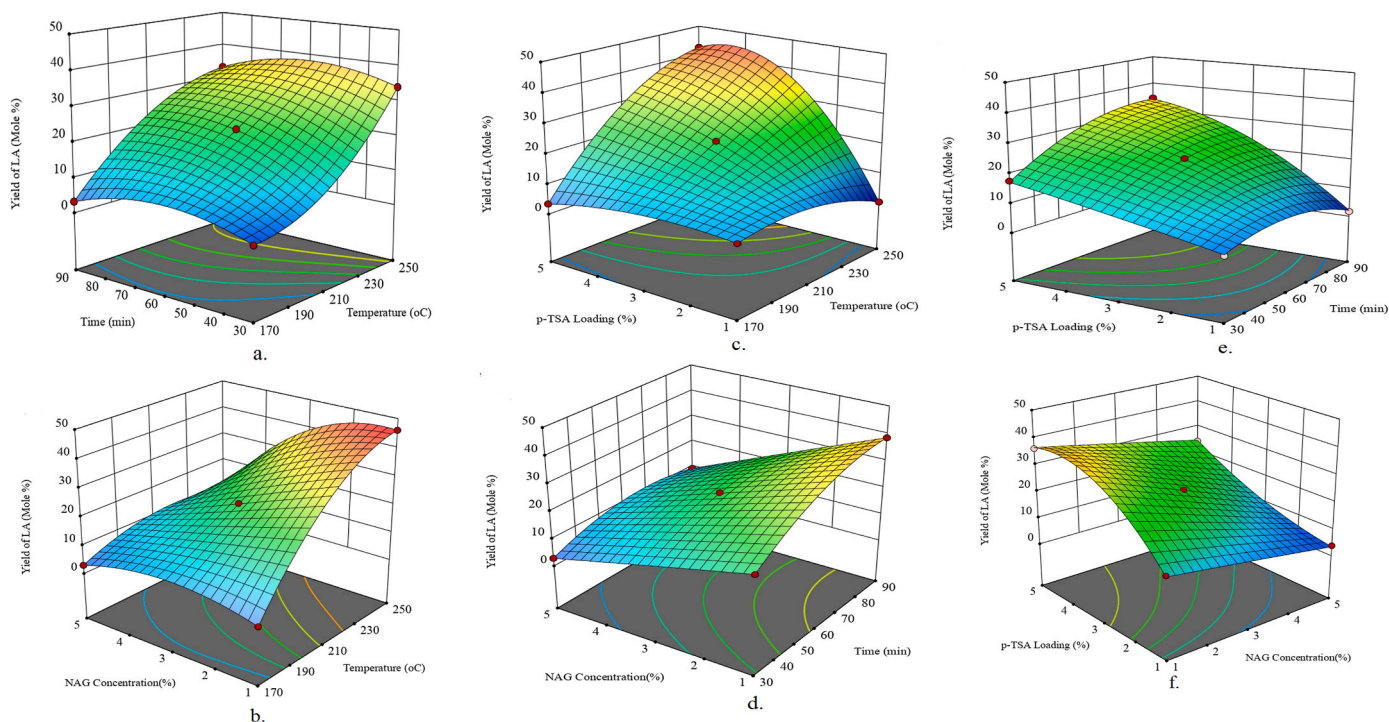
Fig. 6. Response surfaces of LA yield.

4.4. Optimization study

The operating conditions for obtaining highest yield of 5-HMF and LA using *p*-TsOH- catalyzed subcritical water hydrolysis were identified. A numerical optimization based on the model and the analysis of response surfaces were performed using design expert 13 where the criteria for 5-HMF yield was maximization of 5-HMF and minimization of LA and that in case of LA yield was the minimization of 5-HMF and maximization of LA. The maximum yield of 5-HMF was obtained by subcritical water hydrolysis of NAG at 210 °C for 30 min with 5% (w/w) NAG concentration and 3% (w/w) *p*-TsOH loading with desirability of 1, The maximum yield of LA could be achieved from hydrolysis at 238 °C, 1%(w/w) NAG concentration, 4% (w/w) *p*-TsOH loading in 83 min with desirability of 0.971, where desirability describes the closeness of response to ideal value based on desirability function analysis available in software. The solid yield of the reaction carried out at optimum temperature, time and pressure without catalyst was 60% unlike 8.4% to that of catalytic showing significant suppression of humin formation by *p*-TsOH.

The yield of 5-HMF and LA obtained by performing the reactions at the predicted optimum conditions were 27.13 and 53.21% with error less than 1% and is within 5% significance level, as shown in Table 7 The obtained yields of LA are comparable to that of obtained from glucose [31].

5. Conclusion

The efficient deacetylation of NAG to produce acetic acid could be achieved by using water at subcritical conditions in the absence of any external catalyst or oxidative reagent. Further, a catalytic activity of subcritical water was observed which was confirmed by presence of lactic acid and formic acid in product mixture. However, the humin formation by self-aldol condensation of 5-HMF followed by polymerisation was the dominating reaction during hydrolysis of NAG. The overall reactions occurring during hydrolysis of NAG at subcritical conditions are complex, instantaneous and temperature dependent, as NAG was always completely consumed as the temperature reached minimum 170 °C which was unaffected by the presence of catalyst.

LA was selectively produced by employing *p*-TsOH as a catalyst during hydrolysis of NAG in subcritical water. *p*-TsOH significantly supressed humin formation by favouring the ring opening of 5-HMF. The process conditions viz. temperature, reaction time, NAG concentration and *p*-TsOH loading were optimized using BBD coupled with RSM. A maximum 27.02% yield of 5-HMF was obtained at 210 °C for a NAG to *p*-TsOH ratio of 5:3 in 30 min whereas maximum 53.21% yield of LA was achieved at 238 °C for a 1:4 ratio of NAG to *p*-TsOH in 83 min, at constant 50 bar, with desirability of 0.97 and 1, respectively. The control over selectivity of 5-HMF and LA can be achieved by tuning the process conditions during subcritical water hydrolysis of NAG ascertained by multi-response optimization technique.

Declaration of competing interest

The authors declare that they have no known competing financial interests or personal relationships that could have appeared to influence the work reported in this paper.

Appendix A. Supplementary data

Supplementary data to this article can be found online at https://doi.org/10.1016/j.carres.2022.108560.

Appendix-Abbreviations

NAG	N-acetyl-D-glucosamine
5-HMF	5-hydroxymethylfurfural
LA	Levulinic Acid
p-TsOH	*p*-toluenesulfonic acid
BBD	Box-Behnken Design
RSM	Response Surface Methodology

References

[1] P. Stegmann, M. Londo, M. Junginger, The circular bioeconomy: its elements and role in European bioeconomy clusters, Resour. Conserv. Recycl. X. 6 (2020) 100029, https://doi.org/10.1016/j.rcrx.2019.100029.

[2] Y. Li, S.S. Bhagwat, Y.R. Cortés-Penã, D. Ki, C.V. Rao, Y.S. Jin, J.S. Guest, Sustainable lactic acid production from lignocellulosic biomass, ACS Sustain. Chem. Eng. 9 (2021) 1341–1351, https://doi.org/10.1021/acssuschemeng.0c08055.

[3] N. Yan, X. Chen, Don't waste seafood waste: turning cast-off shells into nitrogen-rich chemicals would benefit economies and the environment, Nature 524 (2015) 155–157.

[4] S. Islam, M.A.R. Bhuiyan, M.N. Islam, Chitin and chitosan: structure, properties and applications in biomedical engineering, J. Polym. Environ. 25 (2017) 854–866, https://doi.org/10.1007/s10924-016-0865-5.

[5] D.N. Poshina, S.V. Raik, A.N. Poshin, Y.A. Skorik, Accessibility of chitin and chitosan in enzymatic hydrolysis: a review, Polym. Degrad. Stabil. 156 (2018) 269–278, https://doi.org/10.1016/j.polymdegradstab.2018.09.005.

[6] V.Y. Novikov, Acid hydrolysis of chitin and chitosan, Russ. J. Appl. Chem. 77 (2004) 490–493.

[7] A. Zhang, G. Wei, X. Mo, N. Zhou, K. Chen, P. Ouyang, Enzymatic hydrolysis of chitin pretreated by bacterial fermentation to obtain pure: N -acetyl-d-glucosamine, Green Chem. 20 (2018) 2320–2327, https://doi.org/10.1039/c8gc00265g.

[8] M. Qi, X. Chen, H. Zhong, J. Wu, F. Jin, Base-free, vanadium-catalyzed conversion of chitin into acetic acid under low oxygen pressure, ACS Sustain. Chem. Eng. 8 (2020) 18661–18670, https://doi.org/10.1021/acssuschemeng.0c07147.

[9] J. Wu, M. Qi, G. Gozaydln, N. Yan, Y. Gao, X. Chen, Selectivity-switchable conversion of chitin-derived N-acetyl- d -glucosamine into commodity organic acids at room temperature, Ind. Eng. Chem. Res. 60 (2021) 3239–3248, https://doi.org/10.1021/acs.iecr.0c05805.

[10] T. Werpy, G. Petersen, Top Value Added Chemicals from Biomass Volume I, Us Nrel, 2004, p. 76, https://doi.org/10.2172/15008859. Medium: ED; Size.

[11] Y. Wang, C.M. Pedersen, T. Deng, Y. Qiao, X. Hou, Direct conversion of chitin biomass to 5-hydroxymethylfurfural in concentrated ZnCl2 aqueous solution, Bioresour. Technol. (2013), https://doi.org/10.1016/j.biortech.2013.06.024.

[12] S. Yu, H. Zang, S. Chen, Y. Jiang, B. Yan, B. Cheng, Efficient conversion of chitin biomass into 5-hydroxymethylfurfural over metal salts catalysts in dimethyl sulfoxide -water mixture under hydrothermal conditions, Polym. Degrad. Stabil. 134 (2016) 105–114, https://doi.org/10.1016/j.polymdegradstab.2016.09.035.

[13] W. Hou, Q. Zhao, L. Liu, Selective conversion of chitin to levulinic acid catalyzed by ionic liquids: distinctive effect of: N-acetyl groups, Green Chem. 22 (2020) 62–70, https://doi.org/10.1039/c9gc02669j.

[14] H. Zang, S. Yu, P. Yu, H. Ding, Y. Du, Y. Yang, Y. Zhang, Hydrothermal conversion of N-acetyl-D-glucosamine to 5-hydroxymethylfurfural using ionic liquid as a

recycled catalyst in a water-dimethyl sulfoxide mixture, Carbohydr. Res. 442 (2017) 1–8, https://doi.org/10.1016/j.carres.2017.02.002.

[15] G. Cevasco, C. Chiappe, Are ionic liquids a proper solution to current environmental challenges? Green Chem. 16 (2014) 2375–2385, https://doi.org/10.1039/c3gc42096e.

[16] Á. Szabolcs, M. Molnár, G. Dibó, L.T. Mika, Microwave-assisted conversion of carbohydrates to levulinic acid: an essential step in biomass conversion, Green Chem. 15 (2013) 439–445, https://doi.org/10.1039/c2gc36682g.

[17] M. Möller, P. Nilges, F. Harnisch, U. Schröder, Subcritical water as reaction environment: fundamentals of hydrothermal biomass transformation, ChemSusChem 4 (2011) 566–579, https://doi.org/10.1002/cssc.201000341.

[18] W. Fang, K. Chen, L. Ji, J. Zhu, B. Wu, Y. Wu, Solubility and thermodynamic properties of N-acetylglucosamine in mono-solvents and binary solvents at different temperatures, Phys. Chem. Liq. 57 (2019) 587–599, https://doi.org/10.1080/00319104.2018.1506921.

[19] W. Rongchun, K. Takashi, A. Shuji, Degradation of N -Acetyl- d -glucosamine and d -glucosamine in subcritical water and properties of the degradation, Products 17 (2011) 273–278.

[20] N. Azizi, A.K. Amiri, R. Baghi, M. Bolourtchian, M.M. Hashemi, PTSA catalyzed simple and green synthesis of benzothiazole derivatives in water, Monatshefte Fur Chemie 140 (2009) 1471–1473, https://doi.org/10.1007/s00706-009-0209-4.

[21] B. Baghernejad, Application of P -toluenesulfonic Acid (PTSA) in Organic Synthesis, 2011, pp. 3091–3097.

[22] N.A.S. Ramli, N.A.S. Amin, Optimization of biomass conversion to levulinic acid in acidic ionic liquid and upgrading of levulinic acid to ethyl levulinate, Bioenergy Res. 10 (2017) 50–63, https://doi.org/10.1007/s12155-016-9778-3.

[23] S. Varala, B. Dharanija, B. Satyavathi, V.V. Basava Rao, R. Parthasarathy, New biosorbent based on deoiled karanja seed cake in biosorption studies of Zr(IV): optimization using Box-Behnken method in response surface methodology with desirability approach, Chem. Eng. J. 302 (2016) 786–800, https://doi.org/10.1016/j.cej.2016.05.088.

[24] A.V. Bandura, S.N. Lvov, The ionization constant of water over wide ranges of temperature and density, J. Phys. Chem. Ref. Data 35 (2006) 15–30, https://doi.org/10.1063/1.1928231.

[25] N. V Dolgopyatova, V.Y. Novikov, I.N. Konovalova, N.M. Putintsev, Mechanism of acid hydrolysis of N-acetyl-D-glucosamine, Russ. J. Appl. Chem. 86 (2013) 986–991, https://doi.org/10.1134/S1070427213070070.

[26] A.D. Grund, A. Thomas, Jerrell JR., Deacetylation of N-acetylglucosamine, 2005.

[27] M.R. Park, H.S. Kim, S.K. Kim, G.T. Jeong, Thermo-chemical conversion for production of levulinic and formic acids from glucosamine, Fuel Process, Technol. 172 (2018) 115–124, https://doi.org/10.1016/j.fuproc.2017.12.016.

[28] S. Kang, G. Zhang, X. Yang, H. Yin, X. Fu, J. Liao, J. Tu, X. Huang, F.G.F. Qin, Y. Xu, Effects of p-toluenesulfonic acid in the conversion of glucose for levulinic acid and sulfonated carbon production, Energy Fuel. 31 (2017) 2847–2854, https://doi.org/10.1021/acs.energyfuels.6b02675.

[29] H. Pawar, A. Lali, Microwave assisted organocatalytic synthesis of 5-hydroxy-methyl furfural in a monophasic green solvent system, RSC Adv. 4 (2014) 26714–26720, https://doi.org/10.1039/c4ra03137g.

[30] A. Chuntanapum, Y. Matsumura, Formation of tarry material from 5-HMF in subcritical and supercritical water, Ind. Eng. Chem. Res. 48 (2009) 9837–9846, https://doi.org/10.1021/ie900423g.

[31] K.S. Lau, S.X. Chin, S.N.S. Jaafar, C.H. Chia, Conversion of glucose into levulinic acid in continuous segmented turbulent flow with enhanced chemical reaction, Tetrahedron Lett. 80 (2021) 153330, https://doi.org/10.1016/j.tetlet.2021.153330.

Reaction Chemistry & Engineering

PAPER

Check for updates

Reaction pathways and kinetics of *N*-acetyl-D-glucosamine hydrolysis in sub- and supercritical water†

Sphurti P. Kulkarni, [iD] [ab] Sunil S. Joshi [iD] [ab] and Amol A. Kulkarni [iD] *[ab]

Subcritical and supercritical water hydrolysis of *N*-acetyl-D-glucosamine (NAG) to value-added chemicals has been studied in detail. Experiments were carried out using a continuous flow reactor by varying temperature (250–400 °C), pressure (5–25 MPa) and residence time (2–60 s). A wide product distribution was obtained during the reactions, including solid, liquid and gaseous compounds, sensitive to the state of water: sub- or supercritical. Subcritical conditions promoted the formation of solid compounds, whereas gasification was favored in supercritical water. The prominent products present in the liquid fraction were glycolic acid, acetic acid, formic acid, 5-HMF and acetamide. The formation of a few distinct nitrogen-containing heterocyclic compounds was observed only in supercritical water. Following instantaneous deacetylation of NAG, several oxidation, reduction and secondary reactions occur during hydrolysis of NAG in subcritical and supercritical water. A kinetic model for the prediction of yields of acetic acid, glycolic acid and formic acid is developed. The network of reactions showed specifc deviations from conventional understanding. The current findings show that it is possible to develop a suitable process to make a set of value-added chemicals from chitinous biomass.

1 Introduction

With rapid depletion of fossil fuels and increased global demand for energy, the need for the development of a sustainable circular bio-economy has arisen. The efficient utilization of wastes and residues is a crucial step in the development of a circular bio-economy.[1] With around 6–8 million tonnes of global annual production, seafood waste is an abundant and cost-effective resource of carbon- and nitrogen-rich material and energy. Given the fact that it does not compete with the food chain, chitinous seafood waste has emerged as a potential feedstock to produce various chemicals and bring the carbon and nitrogen from oceanic biomass waste back into the energy cycle.[2] Along with protein and calcium carbonate, chitin is a major component representing almost 40% of seafood shell waste. Chitin is a biopolymer composed of linear chains of monomer *N*-acetyl-D-glucosamine (NAG). The direct conversion of chitin to value-added chemicals is inherently a two-step reaction involving depolymerisation of chitin to NAG followed by conversion of

NAG to various compounds. Hence, NAG has a pivotal role in chitin chemistry and the valorisation of chitinous biomass. Structurally, NAG is an amide derivative of glucose, but unlike glucose NAG is still understudied, specifically due to the complexity introduced by the nitrogen atom, and the amide linkage. Owing to the presence of natural nitrogen in the molecule, NAG could be a natural resource for the greener production of N-containing heterocyclic compounds. NAG has previously been explored for the synthesis of various compounds, such as organic acids (*viz.* acetic acid, formic acid, levulinic acid, *etc.*) and platform chemicals (*viz.* 5-hydroxymethylfurfural (5-HMF), 3-acetamido-5-acetylfuran (3A5AF), and nitrogen-containing heterocyclic compounds like pyrrole, pyrrolidine, *etc.*)[3]

Omari and co-workers[4] have reported the one-pot synthesis of 3A5AF from NAG using boric acid (B(OH)$_3$) and sodium chloride (NaCl) in dimethyl acetamide. Under microwave irradiation, around 62% 3A5AF was obtained in 15 min at 220 °C from NAG. The use of mineral acids, especially sodium and chloride ions, needs to be eliminated in order to develop an environmentally benign process. Drover and co-workers[5] employed ionic liquids (ILs) along with boric acid replacing NaCl to synthesize 3A5AF, and 60% yield of 3A5AF was obtained in a short time of 3 min under microwave irradiation. In another study, Chen and co-workers[6] found that the presence of chloride ions is essential in ILs to produce high yields of 3A5AF. At 180 °C, along with

[a] Academy of Scientific and Innovative Research (AcSIR), Ghaziabad-201002, India
[b] Chem. Eng. and Process Dev. Div, CSIR-National Chemical Laboratory, Dr. Homi Bhabha Road, Pune, 411008, India. E-mail: aa.kulkarni@ncl.res.in

† Electronic supplementary information (ESI) available. See DOI: https://doi.org/10.1039/d3re00046j

the additives boric acid and hydrochloric acid (HCl), the IL 1-butyl-3-methylimidazolium chloride ([BMIm]Cl) resulted in the highest yield under the prevailing conditions. However, the overall reported yield was lower for ILs than for organic solvents and was in general lower than for other reported processes. Wang et al.[7] used a greener IL system based on amino acids and obtained ~53% yield of 3A5AF in 10 min from NAG without using boron-based catalysts. The higher yield is attributed to the introduction of chloride ions in the form of $CaCl_2$. Padovan et al.[8] showed that comparable yields of 3A5AF could be achieved in a relatively simple process by employing $AlCl_3.6H_2O$, wherein a 30% yield was obtained at 120 °C in N,N-dimethylformamide (DMF) solvent in 30 min. Zang et al.[9] employed a pyridinium salt based IL for converting NAG to 3A5AF; however, the need for additives B_2O_3 and $CaCl_2$ along with IL 1-carboxymethyl pyridinium chloride could not be avoided, to achieve a higher 67% yield of 3A5AF at 180 °C in 20 min. Another platform chemical 5-HMF was synthesized from NAG using N-methylimidazolium hydrogen sulfate ([Hmim][HSO_4]) in a solvent mixture of water/dimethyl sulfoxide wherein a 64% yield of 5-HMF was obtained at 180 °C; however, it required a longer reaction time of 6 h.[10] Some organic acids, viz. acetic acid, formic acid and glyceric acid, were produced from NAG at room temperature using NaOH as a catalyst in the presence of oxidative reagents like hydrogen peroxide.[11] Though the obtained yields of formic acid (57%), acetic acid and glyceric acid (total 42%) were higher when compared under the milder conditions reported so far, the use of oxidants and sodium hydroxide poses various challenges for the development of a completely green process. Thus, the methods reported so far for the conversion of NAG to a variety of products use ILs or metal salts and organic volatile solvents. The intricate and expensive synthesis of ILs, problems of disposing of waste containing metal and chloride and the use of organic volatile solvents pose various environmental challenges. There is a need for the development of newer and greener methods to convert NAG to more valuable compounds, which not only eliminate the usage of these compounds but also reduce the number of steps and are universal for both monomer NAG and polymer chitin.

Subcritical (SubCW) and supercritical water (SCW) are being extensively explored as potential green reaction media for a number of reactions.[12–15] Thermodynamically, SubCW refers to a state of water at temperatures higher than its boiling point but below its critical temperature (100 °C < T < 374 °C) at a pressure high enough to maintain a compressed liquid state. On the other hand, supercritical water (SCW) is a distinct state of water (T > T_c = 374 °C; P > P_c = 22 MPa) wherein the distinction between liquid and vapour disappears and water becomes non-polar. The thermo-physical properties of water under such hydrothermal conditions can be tuned by varying temperature and pressure conditions. SCW is a more suitable medium for processing a chitin biopolymer as it can overcome the challenges

associated with chitin, such as solubility and crystallinity.[16] SCW hydrolysis has already been reported to be an effective pre-treatment for the enzymatic depolymerisation of chitin, wherein the hydrolysis efficiency was significantly increased as the crystallinity of chitin was significantly reduced in SCW.[16–18] During our previous study we found that NAG undergoes instantaneous reactions in SubCW.[19] Hence, during the hydrothermal pre-treatment of chitin if even a small quantity of NAG is formed, its exposure to such conditions even for a fraction of time may produce undesirable products. The presence of such compounds can even affect the enzymatic depolymerisation of chitin if not separated. Thus, it is imperative to investigate the reactions of NAG under such conditions in order to develop processes using chitin and NAG. Osada et al. reported that NAG undergoes dehydration to form chromogen I and III which further form 3A5AF in water under subcritical conditions.[20,21] Adachi and co-researchers[22] reported the degradation behaviour of NAG in SubCW; but the product distribution in SCW was not investigated. In our previous study, it was demonstrated that NAG forms organic acids, such as acetic acid, formic acid and lactic acid, in SubCW; however, longer reaction times and lower heating rates resulted in the excessive formation of solids.[19]

This study attempts to provide more insights into the hydrolysis of the chitin model compound, NAG, in SubCW and SCW. Detailed analysis of the conversion of NAG to various compounds was done to understand the underlying mechanism and the kinetics of acid formation are elucidated using a compact continuous flow reactor enabling short residence times and high heating rates. This paper reports for the first time the synthesis of valuable chemicals from NAG via SubCW and SCW hydrolysis without using any external catalyst or oxidant.

2 Experimental

2.1 Hydrolysis of NAG in SubCW and SCW using a continuous flow reactor

NAG was purchased from HiMedia Laboratories (India). Glycolic acid and acetamide were obtained from Merck Specialities. Acetic acid and formic acid were purchased from Loba Chemie Pvt. Ltd. and Avra Chemicals Pvt. Ltd., respectively. The standards for 5-HMF, 3-pyridine carboxyldehyde, piperidine, pyrrole, N-methyl pyrrolidine, pyridine, and 2-acetyl pyrazine were obtained from Sigma Aldrich. Deionized water (LabQ) was used in all the experiments. Analytical grade solvents were used for the purposes of analysis.

Experiments were carried out using an experimental set-up designed for operation of continuous-flow high-pressure and high-temperature reactions (Fig. 1). In a typical continuous hydrolysis experiment, water was pumped using pump 1 (Gilson 305) to a helical coil pre-heater at flow rates in the range of 8 to 25 mL min^{-1}, where the water was heated to temperatures (250 to 420 °C) higher than desired in the
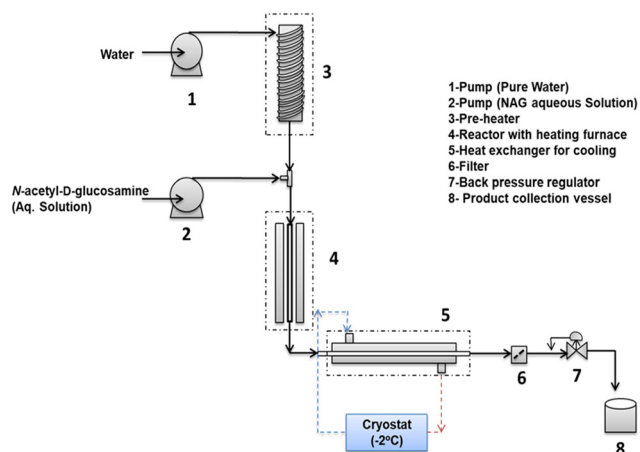
Fig. 1 Schematic of the experimental set-up used for hydrolysis of NAG in subcritical and supercritical water.

reactor using an electrical heater (1 kW, Yog Electronics, India) placed inside the brass rod around which the pre-heater helical coil is wrapped, as shown in Fig. S1.† An aqueous solution of NAG (1–10%) was fed to the tee mixer using pump 2 (Gilson, 305) at a flow rate of 0.8 to 2.5 mL min^{-1}, where it was instantly mixed with SubCW or SCW, which further entered a 5.5 mL tubular reactor (SS 316) tube (Sandvik 3R60; OD = 6.35 mm and thickness = 1.24 mm). The reactor was heated to the reaction temperatures of 250 °C to 400 °C using an electrical furnace (500 W). Temperature was monitored using thermocouples at the inlet and outlet of the reactor and a PID controller (KLB Instruments). The reaction mixture was quickly cooled to room temperature using a sequence of heat exchangers placed at the immediate exit of the reactor using an external cooling jacket through which coolants are passed using a chilling unit (Thermo HAAKE DC 30). All the experiments were carried out at a constant pressure of 25 MPa maintained by using a back pressure regulator (Tescom, model 26) placed after the heat exchanger and a filter of 7 microns mounted inline to avoid the flow of any solids to the regulator. A range of operating conditions was selected, as given in Table 1. The residence time (τ) was calculated considering the variation in the density with temperature and pressure, using following formula,

$$\tau = \frac{V}{[F \times (\rho_I/\rho_{R \times T})]}$$

where V is the volume of the reactor, F is the total flow rate, and ρ_I and $\rho_{R \times T}$ are densities of pure water at room

temperature and at reaction temperature, respectively. Since the reaction mixture was a dilute aqueous solution of NAG (<1% (w/w)), the influence of density variation on residence time is calculated by considering the density of pure water (99% (w/w)), similar to the approach adopted by several researchers previously.[21,26–29] Corresponding values of densities were obtained from National Institute of Standard and Technology (NIST) database.

2.2 Design of reaction set-up and reaction matrix for flow of SubCW and SCW

Unlike the constant property flow of fluids, the design of the flow reaction set-up and reaction matrix for SubCW and SCW is not straightforward, as the governing thermo-physical properties vary continuously with variation in temperature and pressure. In particular, the maximum achievable temperature and minimum residence time for this particular reactor set-up were dependent on i) the minimum/critical mass for achieving higher temperature and ii) heat transfer limitations and the minimum residence time. The specific heat capacity of water goes through maxima with the highest value at the pseudo-critical point (76 J g^{-1} K^{-1} at 385 °C and 25 MPa and 13.2 J g^{-1} K^{-1} at 400 °C and 25 MPa); hence, the flow rate required to achieve a particular temperature using a pre-heater (1 kW) was different at different temperatures. Thermodynamically, SubCW is a hot compressed state, whereas SCW does not undergo a phase change; hence no latent heat was considered. The approximate flow rates were calculated simply from a sensible heat balance across the pre-heater,

$$Q = \dot{m} C_{pR \times T}[T_{R \times T} - T_I]$$

where Q is the heat provided by the external heater, $\dot{m}$ is the mass flow-rate, $T_{R \times T}$ is the desired reaction temperature, T_I is the reactor inlet temperature (25 °C) and $C_{pR \times T}$ corresponds to the specific heat capacity of water at temperature $T_{R \times T}$. It should be noted that $C_{pR \times T}$ is a function of temperature; however, for a generic idea of flow ranges, the maximum value at the reaction temperature was considered. Shorter residence times were required to analyse the primary products of NAG hydrolysis. One way to achieve short residence times was by using high flow-rates; however, heat transfer limitations posed challenges in achieving shorter times (<2 s). The minimum residence time (*i.e.* maximum mass flow rate) was estimated by considering the transient state unidirectional heat transfer from the reactor wall to the

Table 1 Reaction conditions and properties of reaction medium[23–25]

Reaction medium	State	Temperature °C	Pressure MPa	Time s	Density of water kg m^{-3}	pk_w	Dielectric constant (ε)
Subcritical water	Hot compressed liquid	250	25	1–60	820	−11.05	~78.5
Near critical water	Hot compressed liquid	350	25	1–60	620	−11.55	~15
Supercritical water	Supercritical state	400	25	1–15	160	−16.57	~5.9

fluid. The major problem with this method is the unknown values of h, the heat transfer coefficient, at SubCW and SCW. There are several modified correlations, which consider the continuous change in density, viscosity, thermal conductivity and overall thermal diffusivity, but to date no accurate correlation has been proposed.[30] Nevertheless, from experimental observation and theoretical calculations, it was understood that in order to have a practical reactor configuration for reactions with a flow of SCW providing required shorter reaction times (s), the reactor should be designed to provide a maximum heat transfer coefficient by means of either high heat transfer area and low volume or by improving heat transfer by mixing during the flow. In this study, the reactor configuration described in section 2.1 is used; a small tubular reactor with a helical coil pre-heater of almost double volume was used to achieve a high temperatures at 25 MPa. NAG hydrolysis was explored in the range of the shortest possible residence times achieved by the current reaction set-up.

2.3 Hydrolysis of NAG in SubCW and SCW using a batch reactor

Initially, batch reactions were carried out in a batch autoclave of volume 300 mL (Hast C, Parr Instruments, Moline, IL, USA), designed for a maximum operating pressure of 17.5 MPa (2500 psi). In a typical experiment, the reactor was loaded with the aqueous reaction mixture of NAG (0.1 to 5% w/w). Pressure in the reactor was maintained at 5 MPa under argon. The initial pressure was estimated by considering the expansion of argon gas with reaction temperature. The reactor was heated to the required temperature (170 to 250 °C) using an electrical heating mantle. The temperature and stirring speed of 600 rpm were maintained by using a PID controller. After the stipulated time (30–90 min), the reactor was quickly cooled to room temperature by passing cold water through a dip U tube placed inside the reactor. In case of solid formation during the reaction, the solid and liquid products were separated by vacuum filtration and analysed without any further treatment.

2.4 Analytical techniques

Qualitative analysis of the products is done by using high resolution mass spectrometry (HR-MS) (Q Exactive Orbitap spectrometer; Thermo Scientific Acela 1250 Pump) equipped with ODS C18 (Hypersil™ ODS C18) and an electrospray ionisation mass spectrometry (ESI) detector and high-performance liquid chromatography (HPLC) (Agilent 1260 Infinity II). The solids formed during the reaction were filtered and analysed using attenuated total reflection-Fourier transform infrared spectroscopy (ATR-FTIR) (PerkinElmer Spectrum 65). The quantitative analysis of NAG, glycolic acid, formic acid, acetic acid, and acetamide was done using HPLC equipped with an Aminex-87H column (Bio-Rad, USA) and Shodex refractive index detector. A mobile phase of 5 mM sulfuric acid was passed at a flow rate of 0.6 mL min^{-1}

through the column maintained at 50 °C. The calibration curves for each compound were generated for quantification using HPLC. In another method, HPLC (Agilent 1260 Infinity II) equipped with an ODS C18 (Hypersil™ ODS C18) column and UV detector was used to qualitatively investigate the products of the reaction mixture. A mobile phase of 90:10 water:methanol was used to separate the products passed through the column at a flow rate of 0.5 mL min^{-1}.

Based on previous reports on the products of NAG hydrolysis and pyrolysis, the number of products were compared and analyzed. There were several unknown peaks in the chromatogram and the identified peaks were confirmed by comparing the retention times with standard compounds and/or by spiking standard compounds with the samples. Solids were analyzed using ATR-FTIR.

Owing to the very small formation of non-condensable gaseous products at particular reaction conditions, no gaseous products were analysed. Total reactant conversion, product selectivity and product yields are estimated on the basis of mass balance and mole balance.

3 Results and discussion

3.1 Product distribution and reaction pathways of NAG hydrolysis in SubCW and SCW

The conversion of NAG in SubCW and SCW was instantaneous, as NAG was almost always consumed completely at all temperatures (200 to 400 °C) even at the lowest reaction time of 2 s. Products of diverse nature were obtained during, hydrolysis of NAG under the tested hydrothermal conditions including solids, gases and mainly aqueous compounds, as given in Table 2. As liquid products were always the dominant fractions with minute amounts of solids or gases (<1%), no attempts were made to quantify solid and gaseous products. The most commonly identified products of NAG hydrolysis in water at both subcritical (250 to 350 °C) and supercritical temperatures (400 °C) were glycolic acid, formic acid, acetic acid, 5-HMF and acetamide. Other identified products were furfural, pyrazole, 3-pyrdine carboxyldehyde, piperidine, 1-methyl pyrrolidine, pyridine, 2-acetyl pyrazine, piperidine, pyrrole. These products were found to be present in the reaction product mixture under supercritical conditions, but were not seen over the entire range of reaction temperature and residence time. There were several other unidentified products in the product mixture indicated by the unknown peaks in the chromatogram, as shown in Fig. S2(a–e),† which are suspected to be nitrogen-containing compounds, which are predominantly heterocyclic, and a few compounds were identified by HR-MS, as shown in Fig. S3(a–g).†

Fig. 2 shows the plausible reaction pathways for the formation of the identified compounds from NAG in SubCW and SCW. The presence of a wide range of products of diverse nature confirmed that during SubCW or SCW hydrolysis of NAG, it undergoes rapid decomposition forming several compounds which undergo further secondary degradation.

Table 2 Product distribution of continuous flow hydrolysis of NAG in SubCW and SCW (% yield for various products: (1) glycolic acid, (2) formic acid, (3) acetic acid, (4) 5-HMF, (5) furfural, (6) acetamide, (7) pyrazole, (8) 1-methyl pyrrolidine, (9) 3-pyridine carboxyldehyde, and (10) 2-acetyl pyrazine)

Temperature (°C)	Pressure (MPa)	Residence time (s)	Initial NAG[b] (% w/w)	% yield										Accountability[a] %
				1	2	3	4	5	6	7	8	9	10	
400	25	3–10	0.7–0.9	20.64 (±1.99)	3.68 (±2.12)	5.43 (±2.0)	0.142 (±0.07)	0.124 (±0.1)	7.29 (±0.95)	0.29 (±0.16)	4.86 (±0.09)	0.36 (±0.08)	0.76 (±0.32)	40.58 (±2.09)
250	25	24–30.5	0.9–1	11.97 (±2.13)	1.19 (±0.07)	5.34 (±0.26)	0.733 (±0.38)	0.1 (±0.01)	3.25 (±0.29)	0	0	0	0	22.59 (±1.61)

[a] Accountability = (weight of total identified products × 100/initial weight of NAG). [b] Concentration of NAG after mixing with hot water at reactor inlet.

The products identified from such a sequence of reactions are the most stable compounds under the tested hydrothermal conditions. NAG first undergoes deacetylation to form acetic acid and glucosamine, which is an acid-catalysed reaction and/or requires an oxidative reagent.[31] The pk_w of water decreases from 14 under ambient conditions to 11.2 under subcritical and/or supercritical conditions, providing enough acidity for the reaction medium to catalyse the NAG deacetylation; see Table 1.

Moreover, the dissociation of water is an endothermic reaction; hence, with an increase in temperature greater dissociation of water molecules occurs, which can also provide an oxidative environment under these conditions. Under these conditions water can act as both a mild catalyst and an oxidant. However, the phase of water, subcritical or supercritical, has a significant effect, dominating the reaction mechanism. A few products, such as nitrogen-containing heterocyclic compounds identified as pyrazole, 3-pyrdine carboxyldehyde, piperidine, 1-methyl pyrrolidine, pyridine, 2-acetyl pyrazine, piperidine, and pyrrole, were detected only in SCW at 400 °C and 25 MPa. This can happen if glucosamine further reacts in two competing ways; (i) either it undergoes deamination forming glucose or (ii) it gets protonated to form ammonium salt, which undergoes further cyclization to form distinct cyclic products. The only pathway to form glycolic acid and formic acid is by oxidation of glucose, which was also previously reported to happen at the hydrothermal liquefaction of cellulose.[32,33] Hence, the reaction medium favours both oxidation and reduction. Another important compound 5-HMF was believed to be formed by the dehydration of glucose. The presence of acetamide indicated that acetic acid undergoes amidation by reacting with the ammonia formed by deamination of glucosamine. There may be other pathways by which amides can be generated as decomposition products.[34] The phase of the reaction medium has a significant influence on product composition, which is discussed in detail in section 3.2.

3.2 Effect of the state of water or reaction temperature

Water is a unique reaction medium owing to its tunable thermo-physical properties, which can be tuned by varying temperature and pressure. Water in the subcritical state exists as a hot compressed liquid. Under these conditions, the dissociation of water molecules is highest, as indicated by highest ionization constant value 10^{-11} (at 200 to 350 °C); hence, water turns acidic under subcritical conditions.[25]

As shown in Fig. 3, the phase of water had an influence on the nature of the products. In SubCW at 250 °C and 25 MPa, among the products identified were glycolic acid, formic acid, acetic acid, 5-HMF, furfural and acetamide. Glycolic acid was the major product with a yield of 13% based on mass along with a 3 to 7% yield of acetic acid and acetamide along with traces of formic acid, 5-HMF and furfural. Under these conditions, the flow reactor often choked due to excessive formation of solids and it is not easy to remove the charred
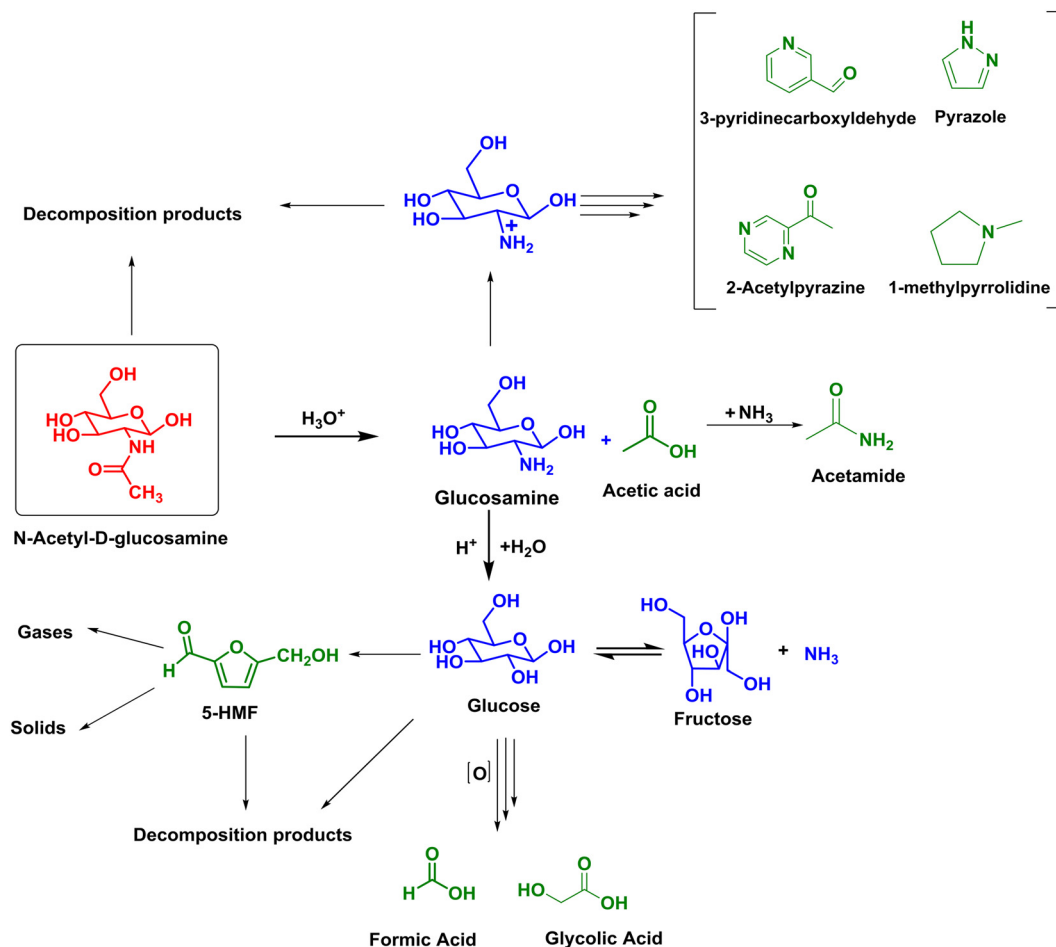
Fig. 2 Plausible reaction pathways of product formation during SubCW/SCW hydrolysis of NAG.

products that get stuck to the reactor wall. FTIR characterization of solids revealed that the solids are humins and have structural similarity to the solids formed during batch reactions of NAG in subcritical water (Fig. S5†). Solids, in the absence of any other strong catalyst, are formed by self-aldol condensation and the polymerization of glucose and 5-HMF.[35] Hence, it could be concluded that NAG undergoes immediate deacetylation followed by deamination and several other degradation

Fig. 3 Effect of state of water on product distribution during NAG hydrolysis in sub- and supercritical water.

reactions, leading to the formation of solids by polymerization of 5-HMF and other degradation products.

In contrast, no solids were formed during the hydrolysis of NAG in SCW, *i.e.* at 400 °C and 25 MPa. Nevertheless, the presence of foam and bubbles coming from the outlet indicated the gasification of products. The reactions in SCW were carried out smoothly in the flow reactor without choking. Under these conditions, the maximum yield of glycolic acid *i.e.* 23.2% on the basis of mass was obtained along with 5.4% acetic acid and 3.6% formic acid. No 5-HMF or furfural were detected under these conditions. Interestingly, some distinct heterocyclic compounds, *viz.* pyrazole, 3-pyrdine carboxyldehyde, piperidine, 1-methyl pyrrolidine, pyridine, 2-acetyl pyrazine, were identified in the product mixture of SCW hydrolysis of NAG. While not all the heterocyclic products could be quantified using our analysis method, the total yield of pyrazole, 1-methyl pyrrolidine, 3-pyridine carboxyldehyde and 2-acetyl pyrazine was around 6% (w/w of NAG). The formation of exactly these compounds was not observed during SubCW hydrolysis of NAG; however, the chromatogram had several peaks near the retention time of these compounds. Hence, there is a possibility that some other similar heterocyclic products are formed during the hydrolysis of NAG
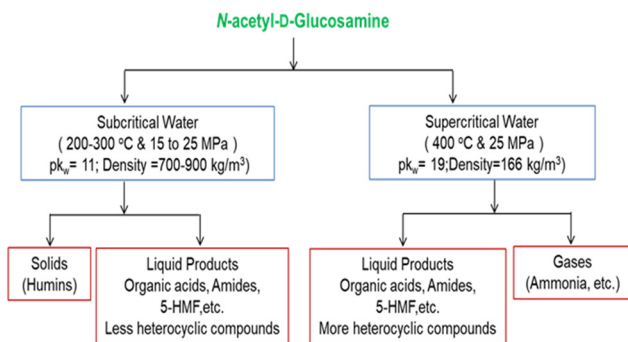
in both SubCW and SCW. Water under subcritical conditions is in a hot-compressed liquid state with higher acidity ($pk_w \sim$ 11.05) which is a favourable reaction medium for ionic reactions. On the other hand, under supercritical conditions, water, with a density of 160 kg m^{-3}, lower dielectric constant and ionic product values, loses its liquid-like characteristics and behaves as a gas-like fluid promoting free radical reactions.[36] Therefore, such a change in product distribution observed during the hydrolysis of NAG can be attributed to the change in the phase of water and consequently the properties of the reaction medium. This dramatic change in solvent properties and consequently in the product distribution can act as a control factor for tuning the product distribution, especially beneficial in the case of molecules containing nitrogen like NAG, as distinct N-heterocyclic compounds, *viz.* pyrazole, 3-pyrdine carboxyldehyde, piperidine, 1-methyl pyrrolidine, pyridine, 2-acetyl pyrazine, and pyrrole, are formed under supercritical conditions.[37]

3.3 Effect of pressure

There was no significant effect of pressure on the composition of aqueous products in the range of pressure investigated here; however, the pressure had a role in suppressing gas formation during SCW hydrolysis and solid suppression during SubCW hydrolysis. Due to the very low concentration of gaseous and solid products, the effect of pressure could not be quantitated. Fig. S4† shows the visual changes observed during NAG hydrolysis in SubCW at 250 °C at 5 MPa, 12.5 MPa and 25 MPa, respectively. The reaction mixture was found to be cloudy at 5 MPa, turned dark at 12.5 MPa and turned clear brown at 25 MPa, indicating the compositional change.

3.4 Effect of residence time

Due to the excessive formation of solids in SubCW (250 °C and 350 °C) resulting in the blockage of the reactor, the influence of residence time was explored mainly in SCW at 400 °C and 25 MPa, where more products were identified and no solids were formed. The effect of time was studied by varying the flow rates of pure water and aqueous NAG solution in a constant ratio. The residence time was varied in the range of 3 to 10 s. Above 10 s, there was almost no change in the product yields. The yields of glycolic acid and 3-pyridine carboxyldehyde were seen to be higher at 5 s and decreased further, which can be attributed to their further degradation to other compounds. In contrast, 1-methyl pyrrolidine formed only after 5 s, whereas the yield of formic acid decreased with residence time. The yields of all other products identified were less influenced by residence time in this time range, as shown in Fig. 4.

3.5 Effect of heating rate

The heating rate was observed to have a significant effect on the product distribution of hydrolysis of NAG. In general, the heating rate of the batch reactor was around 2.5 °C min^{-1},
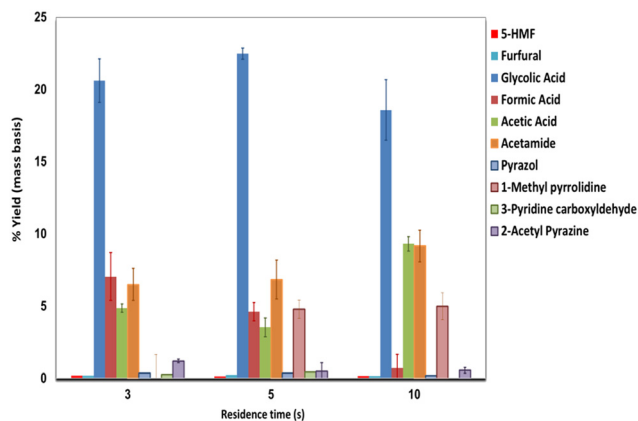

Fig. 4 Effect of residence time on yields of the products at a NAG concentration of 1% (w/w); 400 °C; 25 MPa.

which means that at least 58 min were required to achieve 170 °C from the room temperature of 25 °C.

A few batch reactions were carried out to understand the effect of time during the heating period, by allowing the reaction mixture to achieve the temperature and then cooling it quickly. It was observed that the major products formed during the heating period were solids, which were similar to the compounds obtained in batch reactions carried out under various subcritical conditions. The yield of solids obtained during the batch experimentation in SubCW was not much affected by the changes in the operating temperature and pressure, but it increased with an increase in the reaction time. Another experiment was carried out to check the minimum time required for the complete conversion of NAG. It was observed that the NAG was completely converted during the heating period alone. Hence, it was evident that higher heating rates are required for an investigation of the immediate transformations NAG is undergoing in SubCW and SCW. Higher heating rates of around 150–190 °C s^{-1} were obtained using a continuous reaction set-up, developed as shown in Fig. 1, wherein the desired temperature is reached in <1 to 8 s depending on the temperature set point (due to density variation, as discussed previously).

3.6 Kinetics of formation of organic acids

A wide product distribution is obtained during NAG hydrolysis in SubCW and SCW. In particular, the oxidation products carboxylic acids, *viz.* acetic acid (AA), glycolic acid (GA) and formic acid (FA), are key platform chemicals finding wide applications.[38–40] The formation of myriad compounds and complex reactions complicate the understanding of the mechanism and kinetics of NAG hydrolysis. Similar complexity in developing kinetic models in the cases of hydrothermal liquefaction, pyrolysis or gasification of biomass, have been simplified by adopting a lumping approach.[41]

Herein, a simplified kinetic model is developed to predict the yields of AA, GA and FA, as shown in Fig. 5. While
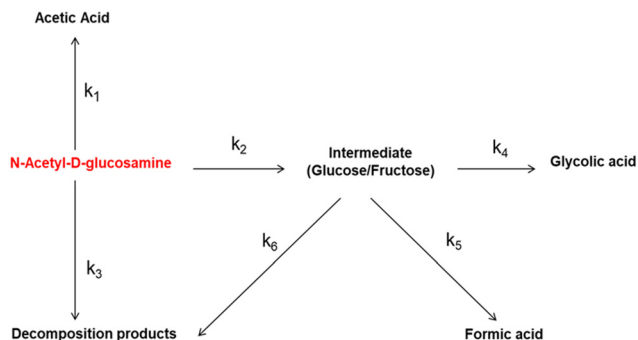
Fig. 5 Proposed model for estimation of the kinetics of acid formation during hydrolysis of NAG in SubCW and SCW.

developing the scheme, it was assumed that the AA is directly formed from NAG in the first step during deacetylation. An intermediate 'I' was introduced representing the lumping of all the products involved in the formation of GA and FA, such as glucose, fructose, glycolaldehyde, erythrose, and pyruvaldehyde. The formation of GA, FA and unknown compounds termed as decomposition products (DP) is intermediated by 'I'. As 'I' hypothetically represented glucose and similar compounds, it was considered to form and react instantaneously as there were no traces of glucose in the product mixture, as discussed previously. As the total yield of identified N-containing products including cyclic products is less than 10%, it is proposed that DP mostly represents the polymerization products, *i.e.* solids and few other secondary products.

The model equations to estimate the rate parameters of the reactions involved in acid formation during SubCW and SCW hydrolysis of NAG are given below. All the reactions were assumed to be pseudo-first order with reference to individual components, as the water was always in excess. The temperature and density were assumed to be constant along the length of the reactor.

The reaction was considered homogenous and the mass transfer limitations were neglected. The intermediate 'I' was considered to be the instantaneous reaction intermediate forming and disappearing in a fraction of time; hence, the net rate of 'I' was considered to be zero. The net rate equations for other molecules were developed considering the quantitative concentration of the compounds. The expression for the concentration of 'I' was determined from eqn (1)–(3) and inserted in the final differential eqn (4)–(8),

$$\frac{d[I]}{dt} = k_2[NAG] - (k_4 + k_5 + k_6)[I] \tag{1}$$

$$r_I = \frac{d[I]}{dt} = 0 \tag{2}$$

$$[I] = k_2[NAG]/(k_4 + k_5 + k_6)[I] \tag{3}$$

$$\frac{d[NAG]}{dt} = -(k_1 + k_2 + k_3)[NAG] \tag{4}$$

$$\frac{d[AA]}{dt} = k_1[NAG] \tag{5}$$

$$\frac{d[GA]}{dt} = k_4[I] \tag{6}$$

$$\frac{d[FA]}{dt} = k_5[I] \tag{7}$$

$$\frac{d[DP]}{dt} = k_3[NAG] + k_6[I] \tag{8}$$

where [NAG], [I], [AA], [GA], [FA] and [DP] are the concentrations of NAG, intermediates, acetic acid, glycolic acid, formic acid and decomposition products, respectively. The rate constants of individual steps, calculated by solving ODEs (eqn (4)–(8)) using MATLAB ODE45 solver and the *fminsearch* method, are given in Table 3. Fig. 6(a–c) compare the experimental data with model predictions at three temperatures 250 °C, 350 °C and 400 °C at 25 MPa. The plots on a normal scale are shown in Fig. S6.† The model can accurately predict the concentrations of NAG and other products, evident from the 0.85–0.99 values of R^2 estimated by comparing model predictions and experimental yields at the same residence times. It could be seen that the time required to completely consume NAG and formation of the products is far less (<0.1 s) than the minimum experimental reaction time (2.5 s). The consumption of NAG itself is instantaneous under those conditions (time shorter than 0.1 s at 400 °C and 25 MPa).

This simplified model accurately predicts the different product concentrations obtained at different temperatures (250 °C, 350 °C and 400 °C) at a constant pressure of 25 MPa. Though the rate constants for the reactions involved in the NAG hydrolysis were influenced by the temperature, the rates do not necessarily increase with temperature. The complexity of the reaction network and the number of possible reaction paths under highly ionic conditions make this process extremely fast, which does not allow monitoring of the reaction under real conditions at such small time scales. The model helps to understand the mechanism and kinetics to some extent in a systematic manner. The rates of both AA and GA formation increased with temperature under subcritical conditions (250 and 350 °C) but dropped in SCW at 400 °C. As previously reported, the formation of AA by deacetylation is an acid-catalyzed reaction whereas GA is an oxidation product.[42] The ions formed by dissociation of water, *i.e.* H^+ and OH^-, catalyze these reactions during hydrolysis using only water. The ionic product of water increases under subcritical conditions but drops in SCW, resulting in reduced ion concentration. The reduction in the rate of formation of AA and GA was presumably caused by this reduction in the concentration of the ions H^+ and OH^- while shifting from subcritical to supercritical conditions.[25,43]

Table 3 Rate constants obtained from the model for NAG hydrolysis in SubCW and SCW

Temperature (°C)	k_1 (s^{-1}) NAG[a] to acetic acid	k_2 (s^{-1}) NAG to intermediates	k_3 (s^{-1}) NAG to DP[a]	k_4 (s^{-1}) Glycolic acid formation	k_5 (s^{-1}) Formic acid formation	k_6 (s^{-1}) Intermediates to DP
250	15.9	64.9	180.1	124.1	9.8	139.2
350	22.0	81.2	162.9	130.3	18.5	129.0
400	14.8	99.7	152.3	126.1	48.5	118.6

[a] [NAG]: *N*-acetyl-D-glucosamine; [DP]: decomposition products.
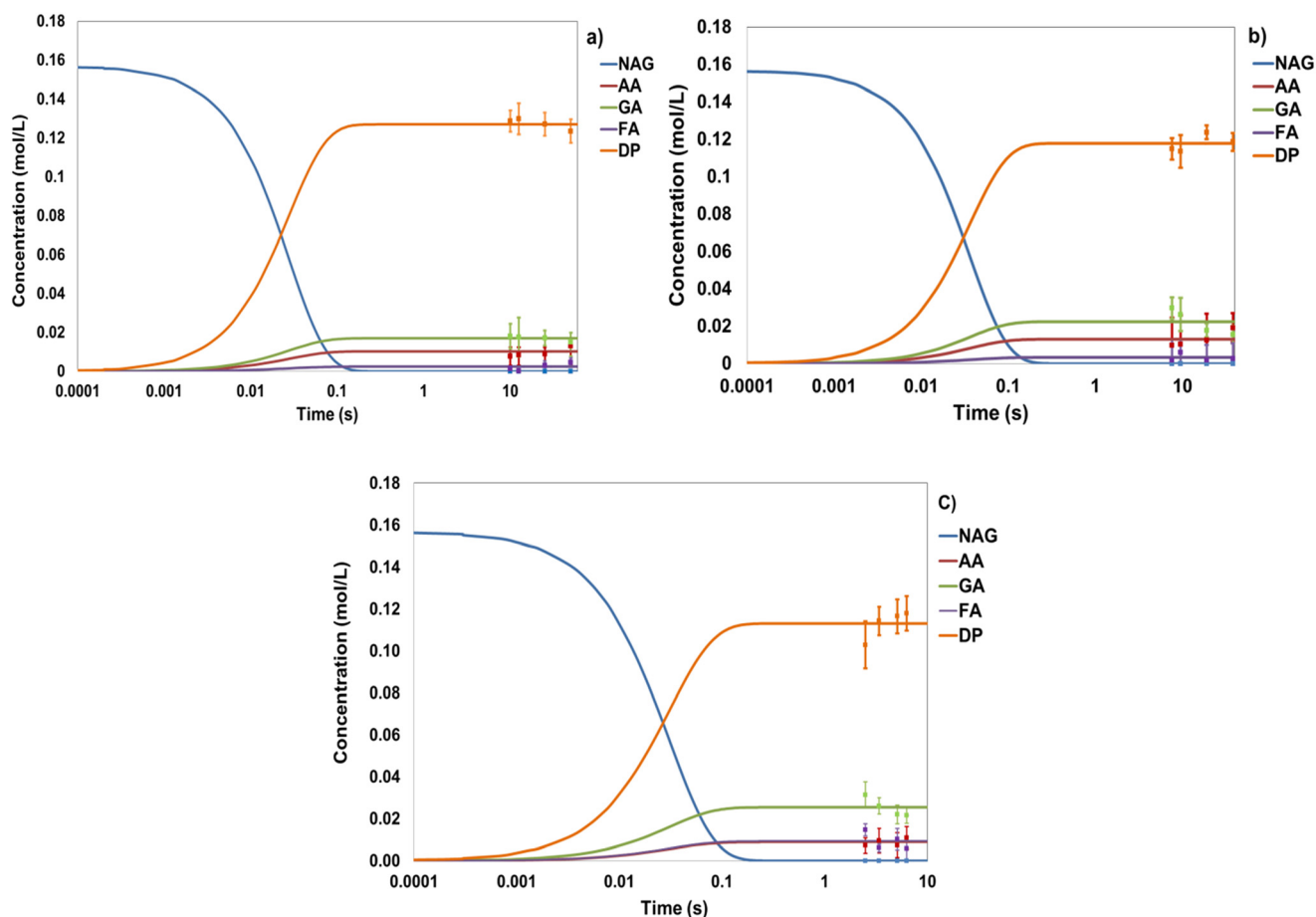
Fig. 6 Kinetics of NAG hydrolysis in sub- and supercritical water: concentration of compounds with reaction time (a) 250 °C, (b) 350 °C and (c) 400 °C at 25 MPa; NAG: *N*-acetyl-D-glucosamine; AA: acetic acid; GA: glycolic acid; FA: formic acid; DP: decomposition products.

The rates of formation of FA and intermediates increased with temperature; in contrast, the formation of DP from both, directly from NAG and from other intermediates, decreased with an increase in temperature. This can be explained by correlating this behaviour with experimental observations. As discussed previously, during the experiments it was observed that solid formation under subcritical conditions was unavoidable and it blocked the reactor; in contrast, the hydrolysis of NAG in SCW could be carried out smoothly with almost no formation of solids. As previously reported, solids are formed by polymerization of 5-HMF and other furfurals.

Promdej *et al.*[25] and a few other researchers[44] reported that the decomposition of 5-HMF to such solids in water suddenly decreases in SCW and a similar negative temperature effect is a classic observation in such cases. Referring to our definition of DP (solids and a few other secondary degradation products), the reduction in rate of formation of DP with temperature is attributed to the change in reaction environment, that is from ionic in SubCW to radical in SCW, causing the change in solid formation. The decomposition of NAG to 'I' leading to acid formation follows Arrhenius behaviour with an activation energy of 7.3
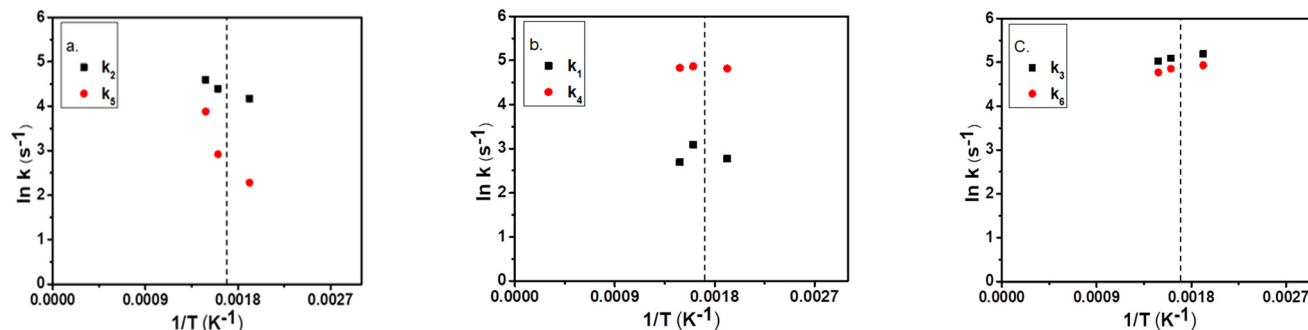
Fig. 7 Arrhenius plots of rate constants of reactions during NAG hydrolysis in SubCW and SCW (a) NAG to I (k_2) and Formation of FA (k_5) (b) NAG to AA (k_1) and GA formation (k_4) (c) NAG to DP (k_3) and I to DP (k_6); NAG: *N*-acetyl-D-glucosamine, I: intermediates, FA: formic acid, AA: acetic acid, GA: glycolic acid, DP: decomposition products.

kJ mol^{-1} and pre-exponential factor of 394.17 s^{-1}. The Arrhenius plots of the rate constants are shown in Fig. 7(a–c). The formation of AA and GA showed Arrhenius behaviour in SubCW; however, overall, it could not be described by the Arrhenius law, as shown in Fig. 7b.

It is speculated that this behaviour is observed due to the influence of water properties on the unknown pathways of AA and GA formation. On the other hand, FA formation showed a positive temperature effect (Fig. 7a). It is suggested that FA forms mainly by C–C cleavage of glucose, as reported earlier, and by oxidation of glucose.[32] The formation of DP from both reactions showed non-Arrhenius behaviour. As the lumped terms 'I' and 'DP' take into account the combined unknown reactions occurring during NAG hydrolysis, deviation from ideal Arrhenius behaviour also suggests that a few of these reactions could be reversible.[45] The results agree with well-known observations of sugar degradation in SubCW and SCW and with our experimental observations.[44]

The overall rate constant for the disappearance of NAG takes into account three reactions NAG to acetic acid, NAG to intermediates and NAG to DP. These three reactions show different temperature dependence, which is attributed to the change in the reaction medium properties. As the temperature effect is compensated by the change in the mechanism of the three individual reactions, the apparent change in overall rate constant is not significant. However, there is an effect of temperature on the mechanism of NAG disappearance, higher temperature results in more intermediate products and less DP, whereas the rate of acetic acid formation from NAG increases in SubCW and comparatively drops in SCW. Unlike a single-step reaction, the temperature effect on overall NAG hydrolysis can be explained by using apparent activation energy, which can be estimated in different ways by considering all the elementary steps. Detailed discussion on apparent activation energy is given by Mao *et al.*[46]

The present approach assists in understanding the acid formation mechanism and kinetics during NAG hydrolysis in SubCW and SCW. A lumped kinetic model for predicting overall product distribution can be developed from a quantitative understanding of the complete product distribution. Owing to very rapid reactions occurring during

the hydrolysis of NAG, to carry out a detailed study, a reactor that is able to provide a short residence time (*i.e.* low volumes) with sufficient heating and mixing should be employed. Monitoring of the reaction using inline measurement can assist in studying the kinetics; however, the process temperature and pressure should be considered when designing the system. Nevertheless, the present model accurately predicts the yields of AA, GA and FA produced by NAG hydrolysis during SubCW and SCW hydrolysis, which can be used to design a system for the selective production of these key chemicals from NAG.

4 Conclusions

The hydrolysis of NAG, a monomer of the abundant biopolymer chitin, in water under sub- and supercritical conditions (250 to 400 °C; 25 MPa; 2–60 s) was investigated using a continuous flow tubular reactor. The product distribution was varied with reaction conditions. The liquid products along with solids were the main products formed during hydrolysis of NAG in SubCW, whereas liquid and gaseous products were obtained in SCW. The main identified products present in the liquid fractions were glycolic acid (10–23%), acetic acid (5–10%), formic acid (2–7%), 5-HMF (0.1–2%), and acetamide (3–8%), *etc.* For the first time it has been reported that acetic acid, glycolic acid and formic acid can be obtained by SubCW/SCW of NAG without addition of any external catalyst or oxidant. The distinct nitrogen-containing heterocyclic compounds (*viz.* pyrazole, 3-pyridine carboxyldehyde, piperidine, 1-methyl pyrrolidine, pyridine, 2-acetyl pyrazine, piperidine, pyrrole) were also observed, however, with significantly lower yields. The excessive solid formation from NAG hydrolysis in SubCW could be overcome in the SCW conditions.

A first-order kinetic model based on the reaction network of NAG conversions in SubCW and SCW was used to estimate the rate constants of the reactions. The overall hydrolysis reactions of NAG followed Arrhenius behaviour; however, individual reactions largely deviated from Arrhenius behaviour. These reactions are believed to lead to the formation of solids in SubCW and gases in SCW; the shift in

product distribution was attributed to a change in the dominant reaction mechanism from ionic in SubCW to radical in SCW, accelerating and suppressing known or unknown reactions during NAG hydrolysis.

The obtained product distribution and results of kinetic modelling of NAG hydrolysis demonstrate that sub- and supercritical water are excellent reaction media for the production of valuable chemicals from chitinous biomass. This needs extremely accurate temperature and residence time conditions to be maintained. Not using any organic solvents makes this approach greener. The downstream processing of these products and greater efforts in that direction are in progress and will be reported separately as a larger quantity of materials needs to be processed under SC conditions.

Conflicts of interest

There are no conflicts to declare.

Acknowledgements

References

1 P. Stegmann, M. Londo and M. Junginger, *Resour. Conserv. Recycl.: X*, 2020, **6**, 100029.

2 N. Yan and X. Chen, *Nature*, 2015, **524**, 155–157.

3 S. Cao, Y. Liu, L. Shi, W. Zhu and H. Wang, *Green Chem.*, 2022, **24**, 493–509.

4 K. W. Omari, L. Dodot and F. M. Kerton, *ChemSusChem*, 2012, **5**, 1767–1772.

5 M. W. Drover, K. W. Omari, J. N. Murphy and F. M. Kerton, *RSC Adv.*, 2012, **2**, 4642–4644.

6 X. Chen, Y. Liu, F. M. Kerton and N. Yan, *RSC Adv.*, 2015, **5**, 20073–20080.

7 J. Wang, H. Zang, S. Jiao, K. Wang, Z. Shang, H. Li and J. Lou, *Sci. Total Environ.*, 2020, **710**, 136293.

8 D. Padovan, H. Kobayashi and A. Fukuoka, *ChemSusChem*, 2020, **13**, 3594–3598.

9 H. Zang, J. Lou, S. Jiao, H. Li, Y. Du and J. Wang, *J. Mol. Liq.*, 2021, **330**, 115667.

10 H. Zang, S. Yu, P. Yu, H. Ding, Y. Du and Y. Yang, *Carbohydr. Res.*, 2017, **442**, 1–8.

11 J. Wu, M. Qi, G. Gozaydln, N. Yan, Y. Gao and X. Chen, *Ind. Eng. Chem. Res.*, 2021, **60**, 3239–3248.

12 P. E. Savage, *Chem. Rev.*, 1999, **99**, 603–622.

13 W. Wahyudiono, S. Machmudah and M. Goto, *Eng. J.*, 2013, **17**, 1–12.

14 D. A. Cantero, M. Dolores Bermejo and M. José Cocero, *J. Supercrit. Fluids*, 2015, **96**, 21–35.

15 P. E. Savage, S. Gopalan, T. I. Mizan, C. J. Martino and E. E. Brock, *AIChE J.*, 1995, **41**, 1723–1778.

16 T. Michael, K. Oshima, C. Abe, R. Maruta, M. Iguchi, M. Watanabe and R. L. Smith, *Carbohydr. Polym.*, 2014, **106**, 172–178.

17 M. Osada, C. Miura, Y. S. Nakagawa, M. Kaihara, M. Nikaido and K. Totani, *Carbohydr. Polym.*, 2013, **92**, 1573–1578.

18 M. Osada, C. Miura, Y. S. Nakagawa, M. Kaihara, M. Nikaido and K. Totani, *Carbohydr. Polym.*, 2015, **134**, 718–725.

19 S. P. Kulkarni, S. N. Dure, S. S. Joshi, K. V. Pandare and N. A. Mali, *Carbohydr. Res.*, 2022, **516**, 108560.

20 M. Osada, S. Shoji, S. Suenaga and M. Ogata, *Fuel Process. Technol.*, 2019, **195**, 106154.

21 M. Osada, K. Kikuta, K. Yoshida, K. Totani, M. Ogata and T. Usui, *Green Chem.*, 2013, **15**, 2960–2966.

22 R. Wang, T. Kobayashi and S. Adachi, *Food Sci. Technol. Res.*, 2011, **17**, 273–278.

23 M. Möller, P. Nilges, F. Harnisch and U. Schröder, *ChemSusChem*, 2011, **4**, 566–579.

24 H. Yoshida, S. Izhar, E. Nishio, Y. Utsumi, N. Kakimori and S. A. Feridoun, *Detritus*, 2018, **4**, 98–103.

25 A. V. Bandura and S. N. Lvov, *J. Phys. Chem. Ref. Data*, 2006, **35**, 15–30.

26 B. M. Kabyemela, T. Adschiri, R. M. Malaluan and K. Arai, *Ind. Eng. Chem. Res.*, 1997, **36**, 1552–1558.

27 S. Kumar and R. B. Gupta, *Ind. Eng. Chem. Res.*, 2008, **47**(23), 9321–9329.

28 T. Noguchi, K. Matsui, N. M. Islam, Y. Hakuta and H. Hayashi, *J. Supercrit. Fluids*, 2008, **46**(2), 129–136.

29 C. Yan, J. Fraga-Dubreuil, E. Garcia-Verdugo, P. A. Hamley, M. Poliakoff, I. Pearson and A. S. Coote, *Green Chem.*, 2008, **10**(1), 98–103.

30 E. Shitsi, S. K. Debrah, V. Y. Agbodemegbe and E. Ampomah-Amoako, *World J. Eng. Technol.*, 2018, **06**, 241–267.

31 N. V. Dolgopyatova, V. Y. Novikov, I. N. Konovalova and N. M. Putintsev, *Russ. J. Appl. Chem.*, 2013, **86**, 986–991.

32 R. He, T. Ma, J. Cheng, B. Jin and J. Xu, *ACS Omega*, 2021, **6**, 11260–11265.

33 N. Shimizu, B. Zeng and K. Kushima, *SN Appl. Sci.*, 2021, **3**, 1–15.

34 J. Chen, M. Wang and C. T. Ho, *J. Agric. Food Chem.*, 1998, **46**, 3207–3209.

35 Z. Xu, Y. Yang, P. Yan, Z. Xia, X. Liu and Z. C. Zhang, *RSC Adv.*, 2020, **10**, 34732–34737.

36 M. J. Antal Jr., A. Brittain, C. DeAlmeida, S. Ramayya and J. C. Roy, *ACS Symposium Series*, 1987, 77–86.

37 C. A. Eckert, C. L. Liotta, D. Bush, J. S. Brown and J. P. Hallett, *J. Phys. Chem. B*, 2004, **108**(47), 18108–18118.

38 C. Cotellessa, K. Peris and S. Chimenti, *J. Eur. Acad. Dermatol. Venereol.*, 1995, **5**, 215–217.

39 K. Shah and S. Consultant, *Indian Petrochem Conf.*, 2014, pp. 1–23.

40 X. Liu, S. Li, Y. Liu and Y. Cao, *Chin. J. Catal.*, 2015, **36**, 1461–1475.

41 R. Kumar, *Energy Nexus*, 2022, **5**, 100042.

42 N. V. Dolgopyatova, V. Y. Novikov, I. N. Konovalova and N. M. Putintsev, *Russ. J. Appl. Chem.*, 2013, **86**, 986–991.

43 D. A. Cantero, M. D. Bermejo and M. J. Cocero, *ChemSusChem*, 2015, **8**, 1026–1033.

44 A. Chuntanapum, T. L. K. Yong, S. Miyake and Y. Matsumura, *Ind. Eng. Chem. Res.*, 2008, **47**, 2956–2962.

45 L. E. Revell and B. E. Williamson, *J. Chem. Educ.*, 2013, **90**, 1024–1027.

46 Z. Mao and C. T. Campbell, *ACS Catal.*, 2019, **9**, 9465–9473.